Investigating the biological role of human NEIL3

Thomas ROEDL

Biomedical Research Centre, School of Environment & Life Sciences

University of Salford, Salford, UK

Submitted in partial fulfilment of the requirements of the Degree of

Doctor of Philosophy, June 2013

Acknowledgements

First of all I would like to thank my supervisor Dr Rhoderick H. Elder for giving me the opportunity to work on this project, for his belief in my skills, advice and challenge, patience and guidance, encouragement and steady support.

I thank the University of Salford for the opportunity to finance my PhD via a GTA studentship.

The work in the first year of my PhD could not have been possible without laboratory space during the refurbishment period at the University of Salford. Therefore, I would like to thank Prof Roger Bisby for giving me a place to work at the University of Salford and Dr's Ian and Lynne Hampson for giving me space to work in their lab at the University of Manchester. In addition, I greatly thank Dr's Ian and Lynne Hampson and especially Dr Anthony Oliver for their support, motivation and the feedback they gave me on the Y2H system throughout my studies.

For supplying me with various reagents and giving me the opportunity to use their lab equipment, my thanks go to Dr Belgees Boufana and Dr Jackie Hughes at the University of Salford. For their limitless help in various situations regarding my lab life at the University of Salford I want to give special thanks to Dr Natalie Ferry, Helen Bradshaw and Ray Ogden.

I also thank Roman Lagoutte for his great support and long scientific discussions, which played a big part in my successful application for a graduate teaching assistantship (GTA) at the University of Salford. Ryan Joynson, Patrick Killoran and

many other colleagues and friends I met during my studies and who I want to thank for their support and the entertaining nights out.

Special thanks go to Kathrin Maria Scherer, a PhD student who started the same time as me and who always was an exceptional supportive and motivating friend who gave me objective and constructive feedback throughout my time in Salford and therefore the opportunity to reflect on my work.

Furthermore, I would like to thank many undergraduate and postgraduate students that I have worked with in the lab. Thanks for giving me all the positive feedback regarding my teaching skills and trusting my lead during your lab project work.

Special thanks and all the love I can give go to my parents and grandparents who, for a long time, were the only people in my life who always believed in my chosen educational path. Steady motivation, through some hard times helped me to successfully finish this PhD project.

Finally, I thank my beloved fiancée Carolin Clausen for all her love and trust that she put into my work and me as a person. Very often during my studies only her motivating words and her faithful and solid character gave me the motivation and the inner force to fulfil the expectations that lecturers and my supervisor had for my work. - My heart felt your warmth with no pause. The fact that we had to live more than 1000 km apart from each other for four years made us even stronger. I love you and I thank you for all the faith you always had and still have in me and our united future.

Abstract

Oxidised bases in DNA are removed by a number of DNA glycosylases in the first step of base excision repair. These include 8-oxoguanine DNA glycosylase (OGG1), endonuclease III-like 1 (NTH1) and the Nei-like proteins, NEIL1, NEIL2 and NEIL3. While NEIL1 and NEIL2 are relatively well characterized, the function of NEIL3 is still not fully understood. Although all three proteins show homology to the *Escherichia coli* Fpg/Nei family, NEIL3 is the largest member with an extended C-terminal domain and contains a valine instead of the highly conserved proline residue at amino acid position two. While it has been reported that recombinant murine NEIL3 shows DNA glycosylase and AP lyase activities *in vitro*, its biological role remains unclear. Therefore, to gain an insight into the function of NEIL3 *in vivo*, the full-length human NEIL3 cDNA has been expressed in *Saccharomyces cerevisae* as a prelude to undertake a yeast 2-hybrid screen to determine specific protein-protein interactions. To date, cDNA library screenings for potential hNEIL3 interactors have been completed and clones expressing potential interactors have been isolated, sequenced and analysed. This data, along with the results of other confirmatory experiments are presented in this thesis. Furthermore, clones of *Pichia pastoris* harbouring an expression cassette with full-length human NEIL3 or mouse NEIL1 or truncated versions of hNEIL3 with amino acid length 1-394 and 1-502 cDNA have been generated in preparation for its overexpression in a eukaryotic system. It is envisaged that the expression of 6XHis tagged hNEIL3 in *P. pastoris* will enable the purification of hNEIL3 protein that can be used in enzyme assays and for further *in vitro* investigations of putative protein interactions discovered by yeast two-hybrid (Y2H) screen.

Table of Contents

Acknowledgements ..... **i**

Abstract ..... **iii**

Table of Contents ..... **iv**

1 Abbreviations ..... **ix**

2 Introduction **1**

2.1 DNA damage **2**

2.1.1 Oxidation of DNA bases *4*

2.1.2 Spontaneous DNA damage formation *9*

2.1.3 UV damage *9*

2.1.4 Lipid peroxidation *11*

2.1.5 Alkylation DNA damage *15*

2.1.6 DNA strand breaks *16*

2.2 Antioxidants: the first instance of DNA protection **16**

2.3 DNA repair pathways **17**

2.3.1 Direct reversal (DR) *18*

2.3.2 Mismatch repair (MMR) *19*

2.3.3 Nucleotide excision repair (NER) *20*

2.3.4 Homologous recombination (HR), Non-homologous end-joining (NHEJ) *21*

2.3.5 Base excision repair (BER) *22*

2.3.6 Reported protein interactions with mammalian BER proteins *50*

2.4 Theoretical background to methods used in this thesis **52**

2.4.1 Yeast Two-Hybrid assay *52*

2.4.2 Protein overexpression in Pichia pastoris *54*

3 Materials **56**

3.1 Media preparation for bacterial methods **56**

3.2 X-Gal and IPTG Preparation **56**

3.3 Ethylenediaminetetraacetic acid (EDTA) stock solution **57**

3.4 TE-Buffer (Tris-EDTA-Buffer) **57**

3.5 5X TBE **57**

3.6 Loading buffer for agarose gel electrophoresis (Loading dye) **57**

3.7 Buffers for SDS-PAGE 57
3.7.1 Acrylamide stock solution 57
3.7.2 "Lower Tris" (4x stock solution) 58
3.7.3 "Upper Tris" (4x stock solution) 58
3.7.4 Separating gel (10 %) 58
3.7.5 Stacking gel (5 %) 58
3.7.6 SDS-Running buffer (10x stock solution) 59
3.7.7 SDS-Running buffer (1x) – Bio-Rad 59
3.7.8 SDS-PAGE sample buffer (5x stock solution) 59
3.7.9 Coomassie blue staining solution 59
3.7.10 Destain solution 59
3.8 Buffers for Western Blotting 60
3.8.1 Western blot transfer buffer 60
3.8.2 10x TBS 60
3.8.3 TBS(T) 60
3.8.4 5% blocking buffer 60
3.8.5 Antibody dilution buffer 60
3.9 Buffers and solutions for Y2H 61
3.9.1 10X TE 61
3.9.2 10X LiOAc (Lithium acetate) 61
3.9.3 50% PEG-3350 61
3.9.4 1x TE/LiOAc/H_2O 61
3.9.5 1x TE/LiOAc/PEG-3350 61
3.9.6 Glucose/galactose/raffinose 62
3.9.7 Amino acid (and pyrimidine) solutions 62
3.9.8 YPD broth/agar plates 62
3.9.9 YNB broth/agar plates 62
3.9.10 YNB selective liquid cultures 63
3.9.11 YNB selective plate preparation 63
3.9.12 LB-medium 64
3.9.13 LB-(ampicillin)-medium (LBA) 64
3.9.14 LB-(kanamycin)-medium (LBK) 64
3.9.15 Trp^- bacterial minimum medium for electroporation 64
3.9.16 X-Gal plates for blue/white screening 65
3.10 Buffers and solutions for overexpression in *P. pastoris* 65
3.10.1 YPD(S) broth/agar plates (Zeocin selection) 65
4 Methods 66
4.1 Transformation into NovaBlue cells 66

4.2 -80°C stock preparation of yeast and bacterial cultures 66
4.2.1 Yeast -80°C stocks 66
4.2.2 Bacterial -80°C stocks 66
4.2.3 KC8 -80°C stock preparation 67
4.3 Plasmid DNA extraction 67
4.4 Quantification of DNA 68
4.5 Digestion with restriction endonucleases 68
4.6 Agarose gel electrophoresis 68
4.7 Polymerase chain reaction 69
4.8 DNA Ligation 69
4.8.1 Insert:Vector molar ratio calculation 69
4.8.2 Ligation of hNEIL3 into pGEM-T vector (Promega) 69
4.8.3 Ligation of hNEIL3 into pJET1.2/blunt vector (Fermentas) 69
4.9 DNA sequencing 70
4.10 Bradford assay 71
4.10.1 Protein extraction for Bradford assay 71
4.10.2 BSA standard dilutions 72
4.10.3 Bradford reagent assay method 72
4.11 SDS-PAGE 73
4.11.1 Protein extraction from yeast for direct SDS gel loading 73
4.11.2 Casting of SDS-PAGE gels 73
4.11.3 SDS gel loading 74
4.11.4 Coomassie blue staining dye 75
4.12 Western blot 75
4.12.1 Blotting 75
4.12.2 Western blotting 76
4.13 Yeast two-hybrid 77
4.13.1 Small scale transformation 77
4.13.2 Large scale transformation of library cDNA 78
4.13.3 Library cDNA screening (placental cDNA library) 80
4.13.4 Library plasmid DNA extraction of potential positives 81
4.13.5 Mating assay to confirm potential interaction partners for hNEIL3 84
4.13.6 Interaction studies with LigIIIα and Polβ 84
***4.14* Overexpression in *Pichia pastoris* 86**
4.14.1 Electroporation of pGAPZαA constructs into P. pastoris 86
4.14.2 Extraction of chromosomal DNA from P. pastoris using LiOAc-SDS 87
4.14.3 PCR of incorporated pGAPZαA inserts extracted from P. pastoris 88
4.14.4 Overexpression conditions 89

5 Results 90
5.1 Y2H Summary 90
5.2 Y2H bait vector preparation 90
5.2.1 Preparation of hNEIL3 cDNA insert 90
5.2.2 Preparation of pEG202 and pEG202-NLS vectors 94
5.2.3 Cloning of hNEIL3 (A_2) into pEG202 and pEG202-NLS 95
5.2.4 DNA sequencing 96
5.2.5 PCR of pCMV6-AC/hNEIL3 (Phusion) 99
5.2.6 DNA sequencing of pEG202(-NLS)-N3 (Phusion) 101
5.3 Small scale transformation of pEG202(-NLS)-N3 into EGY48 102
5.4 Autoactivation tests and repression assay 104
5.4.1 Autoactivation test of Leu2 expression by hNEIL3-LexA 105
5.4.2 Autoactivation test of LacZ expression by hNEIL3-LexA 106
5.4.3 Repression assay 107
5.5 Western blot of hNEIL3-LexA expression 108
5.6 Y2H screening with a human placental cDNA library 109
5.6.1 Large scale transformation of library cDNA 109
5.6.2 Screening of transformants for potential positive interactors 110
5.6.3 Galactose/Glucose tests with potential positive clones 111
5.6.4 X-Gal test of potential positive interactors 113
5.6.5 Library plasmid DNA identification – "Modified" standard method 116
5.6.6 Library plasmid DNA identification – "PCR Method" 117
5.6.7 DNA sequencing of potential clones 121
5.6.8 Mating Assay 122
5.7 Y2H screening with a Jurkat T-Cell cDNA library 126
5.7.1 Galactose/Glucose test of potential positive interactors 127
5.7.2 X-Gal test of potential positive interactors 127
5.7.3 DNA sequencing of potential positive clones 130
5.8 Interaction studies of human LigIIIα and Polβ with hNEIL3-LexA 131
5.8.1 Preparation of library vectors containing either LigIIIα or Polβ 131
5.8.2 Preparation of library vector pJG4-5 for blunt end cloning 133
5.8.3 Ligation of LigIIIα and Polβ into linearized pJG4-5 133
5.8.4 Confirmation of correct integration of LigIIIα and Polβ into pJG4-5 134
5.8.5 Small scale transformation of pJG4-5-LigIIIα and pJG4-5-Polβ into EGY48 138
5.8.6 Testing LacZ and Leu2 gene expression for LigIIIα/hNEIL3 clone 138
***5.9* Overexpression of hNEIL3 and mNEIL1 in *Pichia pastoris* 140**
5.9.1 Confirmation of pGAPZαA clones obtained from bacterial stocks 141
5.9.2 Linearization of pGAPZαA clones hN3-394, hN3-502 and mNEIL1 142

5.9.3 Electroporation of pGAPZαA clones into P. pastoris 143
5.9.4 PCR of chromosomal DNA extractions from P. pastoris 144
5.9.5 SDS-PAGE of cell lysates 145
6 Discussion 147
6.1 Yeast two-hybrid results 147
6.1.1 Potential positive interactors 148
6.1.2 Reasons for false positive results 150
6.2 Overexpression in *P. pastoris* 154
6.3 Future outlook 157
6.4 Overall discussion 159
7 References 171
8 Appendix 209
8.1 Vector maps 209
8.2 NEIL3 origin sequence included in the pCMV6-AC vector from OriGene 215
8.3 Motif sequences in hNEIL3 (OriGene) 216
8.4 SNPs in hNEIL3 DNA 218
8.5 PCR product quality from EGY48 yeast extractions 220
8.6 Complete sequencing (BLAST) results of Y2H screenings 222
8.6.1 Complete sequencing (BLAST) results of placental cDNA library screen 222
8.6.2 Complete sequencing (BLAST) results of Jurkat T-cell cDNA library screen 227
8.7 Additional pictures 229

1 Abbreviations

3′P	3′-phosphate
3′PUA	3′-phospho α,β-unsaturated aldehyde
5′dRP	5′-deoxyribonucleotide phosphate
5′P	5′-phosphate
5-OH-U	5-hydroxyuracil
5-OH-C	5-hydroxycytosine
6XHis	polyhistidine tag
2-oxoA	2-oxo-1,2-dihydroadenine
8-oxoA	8-oxo-7,8-dihydroadenine
8-oxoG	8-oxo-7,8-dihydroguanine
ADH	alcohol dehydrogenase
AP	apurinic/apyrimidinic
APE1	apurinic/apyrimidinic (abasic) endonuclease
APE2	apurinic/apyrimidinic (abasic) endonuclease 2
APNG	alkylpurine DNA-*N*-glycosylase
APS	ammonium persulphate
APTX	forkhead-associated domain histidine triad-like protein
AmpR	ampicillin resistance sequence
ATM	ataxia telangiectasia mutated
ATR	ATM and Rad3-related
BER	base excision repair
BLAST	basic local alignment search tool
bp	base pair(s)
cDNA	complementary DNA
cfu	colony forming unit(s)
conc.	concentration
DDR	DNA-damage response
DSB(s)	DNA double strand break(s)
DHT	dihydrothymine
DHU	dihydrouracil
DNA-BD	DNA binding domain
DMSO	dimethylsulfoxide
DR	direct reversal
dRPase	deoxyribophosphodiesterase
dsDNA	double-stranded DNA

FapyA	4,6-diamino-5-formamidopyrimidine
FapyG	2,6-diamino-4-hydoxy-5-formamidopyrimidine
FEN1	Flap endonuclease 1
GAPDH	glyceraldehyde-3-phosphate dehydrogenase
Gh	guanidinohydantoin
H2TH motif	helix-two turn-helix motif
HDAC1	histone deacetylase-1
HhH motif	helix-hairpin-helix motif
HR	homologous recombination
HRP	horseradish peroxidase
hN3-394	truncated version of human NEIL3, amino acids 1-394
hN3-502	truncated version of human NEIL3, amino acids 1-502
hNEIL3	human NEIL3
IPTG	isopropyl-β-D-thiogalactopyranoside
LacZ	*LacZ* gene
LB-Carb	Lysogeny broth - agar plate with carbenicillin
LB-Carb-broth	Lysogeny broth with carbenicillin
Leu2	leucine coding gene (*Leu2*)
LexA	LexA – repressor
LigI	DNA ligase I
LigIIIα	DNA ligase III alpha
M1dG	pirymido-[1,2 α]purine-10(3H)-one-2′-deoxyribose
M2H	mammalian two-hybrid
Me-FapyG	2,6-diamino-4-hydroxy-5-N-methylformamidopyrimidine
MGMT	O^6-methylguanine-DNA methyltransferase
mNEIL3	mouse NEIL3
mNTH1	mouse NTH1
MMEJ	microhomology-mediated end joining
MMR	mismatch repair
MOLT4	human acute lymphoblastic leukaemia cells
MutS, MutL, MutH	methyl-directed mismatch repair proteins
NaOAc	sodium acetate
NEIL/Neil	nei-like
NER	nucleotide excision repair
NHEJ	non-homologous end joining
NLS	nuclear localization sequence
NTH1	endonuclease III-like 1

OGG1	8-oxoguanine DNA glycosylase
PARP-1	Poly (ADP-ribose) polymerase 1
PCR	polymerase chain reaction
pEG202	bait vector used in yeast two-hybrid
pEG202-N3	pEG202 containing hNEIL3 cDNA
pEG202(-NLS)	pEG202 and pEG202-NLS
pEG202(-NLS)-N3	pEG202 and pEG202-NLS containing hNEIL3 cDNA
PNK	polynucleotide kinase
Pro2	proline at amino acid position two (N-terminal)
Polβ	DNA polymerase β
Polδ	DNA polymerase δ
Polε	DNA polymerase ε
ROS	reactive oxygen species
SDS-PAGE	sodium dodecyl sulphate polyacrylamide gel electrophoresis
SMUG1	single-strand selective monofunctional uracil DNA glycosylase
SNP	single nucleotide polymorphism
SOD	superoxide dismutase
Sp	spiroiminodihydantoin
SSB(s)	DNA single-strand breaks
ssDNA	single-stranded DNA
TDG	thymine DNA glycosylase
Tg	thymine glycol
TEMED	tetramethylethylendiamine
TopoIIIα	DNA topoisomerase IIIα
UAS	upstream activation sequence
UDG/UNG	uracil-DNA glycosylase
UvrD	DNA helicase II
Val2	valine at amino acid position two
vDNA	viral DNA
X-gal	bromo-chloro-indolyl-galactopyranoside
Y2H	yeast two-hybrid

2 Introduction

DNA damage in aerobic cells is mainly caused by reactive oxygen species (ROS). ROS are formed as by-products of electron transport in mitochondria or by exposure to environmental agents. At low concentrations ROS are mediators of specific physiological processes such as cell proliferation and inflammatory responses. However, if the concentrations become too high, the negative effects of these oxidants are increased including DNA damage which can cause various changes in the chemistry of bases, sugars and phosphates resulting in mutagenesis or cell death (Nakabeppu *et al.*, 2004; Uchida, 2003; Winczura *et al.*, 2012). One of several DNA repair mechanisms, base excision repair (BER) is a major pathway that can recognize and replace damaged DNA bases (David & Williams, 1998). BER is initiated by DNA glycosylases. The oxidative damage-specific DNA glycosylases in bacteria have been extensively studied and in *Escherichia coli,* formamidopyrimidine [fapy]-DNA glycosylase (Fpg), endonuclease VIII (Nei), and endonuclease III (Nth) act on overlapping sets of modified DNA bases (Wallace, 2002). Nth and the mammalian homologues 8-oxoguanine DNA glycosylase (OGG1) and nth endonuclease III-like 1 (NTH1) have an internal lysine (Lys) residue at the active site, while Fpg and Nei use an N-terminal proline (Pro) residue. Nth and Nei in *E. coli* act as DNA glycosylases that remove oxidized pyrimidines, including free radical - damaged thymines and cytosines. Fpg, also known as MutM, can recognize and repair oxidized purines such as 8-oxo-7,8-dihydroguanine (8-oxoG) and 2,6-diamino-4-hydroxy-5-formamidopyrimidine (FapyG) (Tchou *et al.,* 1994; Hazra *et al.,* 2002a; Wallace, 2002). NEIL1, NEIL2 and NEIL3 are mammalian proteins of the Nei-like (NEIL) family. Nei-like is designated in this way, because Nei, encoded by the *nei* gene of *E. coli*, is homologous to NEIL1, NEIL2 and NEIL3. However, NEIL2 is the only protein of these three which recognizes oxidized pyrimidines exclusively while

NEIL1 is a functional hybrid of Fpg and Nei as it can repair oxidized purines and pyrimidines. NEIL3 has recently been shown to act on oxidized purines such as FapyG, 4,6-diamino-5-formamidopyrimidine (FapyA), and the hydantoin lesions guanidinohydantoin (Gh) and spiroiminodihydantoin (Sp), preferentially on single-stranded DNA (ssDNA) (Liu *et al.,* 2013).

2.1 DNA damage

Under aerobic conditions, a cell of any origin has the potential to be under oxidative stress, the level of which can vary dramatically depending on different factors such as environmental stress levels (*e.g.* radiation or heat exposure). Oxidative stress is the imbalance between oxidants and antioxidants in favour of the oxidants that can lead to cell damage and death. Such oxidants can either enter a cell exogenously in the form of oxidising agents or are produced endogenously as by-products from mitochondria during oxidative phosphorylation (Devasagayam *et al.*, 2004). Oxidants and radiation can lead to various types of DNA damage which include single- and double-strand DNA breaks, DNA inter-, intra-strand and protein cross-links, DNA adduction and oxidation, covalent dimer formation and spontaneous hydrolysis of a base leaving an abasic, an apurinic/apyrimidinic (AP) site (Bernstein *et al.*, 2002; Drablos *et al.*, 2004).

One major reason for DNA damage caused by oxidants are ROS, chemically reactive molecules containing oxygen that are formed as a natural by-product during aerobic respiration (Devasagayam *et al.*, 2004). ROS can attack and alter the chemical nature of cellular components. However, over time cells have developed an incredible diversity of defence mechanisms to either neutralize such threats before any damage has occurred or to recognize and repair or replace cellular

macromolecules (Pierce, 2012; Izumi *et al.,* 2003). In particular the maintenance of genomic integrity plays a crucial role for the survival of any organism. A loss of genomic stability often leads to an increased risk of genetic diseases, premature aging and the formation of malignant diseases. The integrity of the genome is ensured by a strictly coordinated regulation of different cellular processes such as DNA replication, DNA repair, senescence and apoptosis. These processes are controlled and coordinated by DNA damage checkpoints (Shiotani & Zou, 2009).

The activation of checkpoint signals can lead to an arrest of the cell cycle in G_1 thus preventing DNA replication. This process allows the cell to remove lesions from its genomic DNA, and therefore hinders the rise of mutations or the collapse of the replication fork. The latter can lead to the formation of DNA double-strand breaks (DSBs) which can result in chromosomal damage and cell death. In many cases, checkpoint-signals stimulate the cellular DNA repair machinery and therefore greatly contribute to minimize the toxic effects of DNA damage (Li & Zou, 2005).

Cell-cycle progression, DNA repair, DNA replication, transcription and apoptosis are coordinated by the DNA-damage response (DDR). Studies on genes involved in DDR have revealed that their deletion can lead to lethality, premature aging syndromes, cancer and neurodegenerative disorders (Nam & Cortez, 2011). Although to date the mechanism of DNA damage sensing within a cell remains unclear, it has been proposed that Rad1, Rad9 and Hus1, all fission yeast proteins, form a trimeric protein complex, a damage sensor clamp known to interact with DNA polymerase β (Polβ) and increasing its efficiency in DNA repair (Toueille *et al.*, 2004). The structure of this complex is similar to the conformation of the eukaryotic DNA sliding clamp proliferating cell nuclear antigen (PCNA) a cofactor for DNA polymerase δ (Polδ). Therefore, PCNA is likely to have a similar function to that of

the Rad9/Rad1/Hus1 complex and thus increases the processivity of DNA replication in eukaryotes (Lowndes & Murguia, 2000; Venclovas & Thelen, 2000).

If the integrity of the genome in mammalian cells is compromised, the activation of DDR is coordinated by three major protein kinases, ataxia telangiectasia mutated (ATM), DNA-dependent protein kinase (DNA-PK) and ataxia telangiectasia and Rad3-related (ATR) (Brown & Baltimore, 2003; Nam & Cortez, 2011). These serine/threonine-specific protein kinases belong to the phospho-inositol-3-kinase-like protein kinase family and share similar domain structures. However, while ATM and DNA-PK are activated primarily by DSBs, ATR can additionally be activated by a much wider spectrum of DNA lesions such as base adducts, stalled replication forks and DNA cross-links (Nam & Cortez, 2011). When activated, ATR phosphorylates the kinase Chk1 and this way initiates a signal transduction cascade that leads to G_1 cell cycle arrest that gives the cell time to repair the DNA damage before DNA replication is restarted (Brown & Baltimore, 2003). The tumour suppressor p53 is also regulated by the DDR and is one of the most important proteins involved in the maintenance of genomic integrity. In the cell, p53 plays an essential role in the regulation of cell cycle progression, apoptosis and DNA repair in response to various stress signals resulting from oxidative stress (Harris & Levine, 2005).

2.1.1 Oxidation of DNA bases

ROS are generated as by-products of the mitochondrial electron transport chain, such as superoxide ($O_2^{\bullet -}$), hydrogen peroxide (H_2O_2) and the highly reactive hydroxyl radical ($^{\bullet}OH$) (Figure 1).

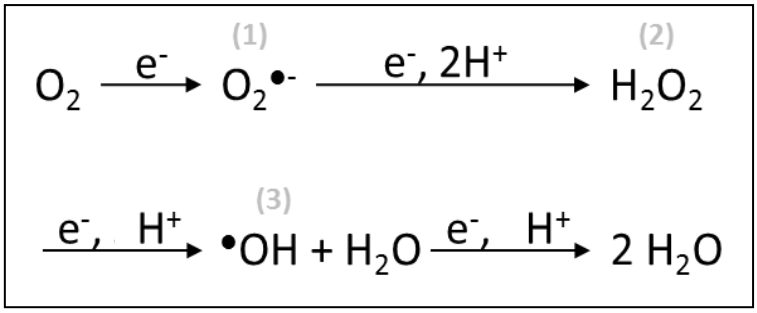

Figure 1: Example for ROS formed during aerobic metabolism. The unpaired orbits of dioxygen can accept single electrons to form the superoxide radical (1) which then can accept more electrons to form hydrogen peroxide (2) and further reduction leads to the highly reactive hydroxyl radical (3).

The most abundant oxidized DNA purine base, 8-oxoG, is generated by ROS and ionizing radiation where an additional oxygen is added to the C8 position of guanine (Figure 2). Furthermore, the frequency of 8-oxoG generation is increased in organisms with a higher metabolic rate and in mitochondrial DNA rather than in nuclear DNA (Beckman & Ames, 1998). Because of its abundant nature 8-oxoG is often used as an indicator for oxidative stress in a cell. 8-oxoG can lead to G → T transversions and is therefore highly mutagenic. Guanine can also be oxidized to FapyG (Figure 2) another abundant form of abnormal guanine that can lead to G → T base transversions and other base mutations (Jena & Mishra, 2012; Krwawicz *et al.*, 2007; Izumi *et al.,* 2003; Morland *et al.,* 2002). The levels of FapyG lesions in cells is significantly (6.5 fold) higher than the levels of 8-oxoG and FapyA and therefore new methods using FapyG to quantify the oxidative stress level have been developed (Hu *et al.,* 2005). However, the best way to measure cellular oxidative stress might be to include several types of DNA lesions in such assays as the type of base oxidation varies depending on the type of oxidative stress the cell undergoes (Kanvah *et al.*, 2010).

Me-FapyG, the methylated analogue of FapyG, is the result of alkylation of guanine in DNA with subsequent oxidative attack or UV radiation (Figure 3) (Asagoshi *et al.*,

2002). Furthermore, Me-FapyG is able to significantly block DNA synthesis in *E. coli* (Hu *et al.,* 2005). Due to the fact that Me-FapyG is chemically distinct from FapyG, extrapolating results obtained with Me-FapyG to FapyG must be interpreted with care, although it is commonly done by several groups (*e.g.* Asagoshi *et al.,* 2002; Graziewicz *et al.,* 2000).

Further oxidation of 8-oxoG caused by various oxidizing agents results in the hydantoin lesions Sp or Gh respectively while the pyrimidine ring of guanine is opened in Gh and closed in Sp (Figure 2) (Niles *et al.*, 2004; Jena & Mishra, 2012).

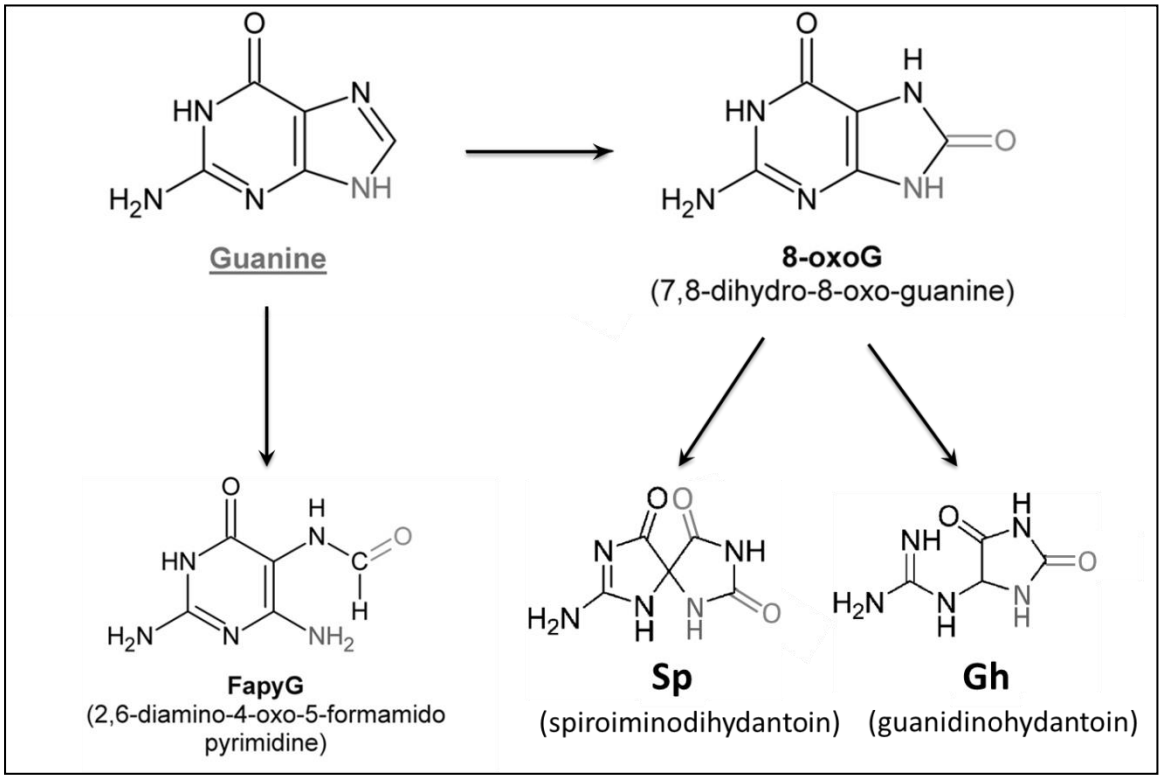

Figure 2: Examples of oxidations of guanine. O in grey is the oxidized site. N in grey is the β-*N*-glycosidic binding site.

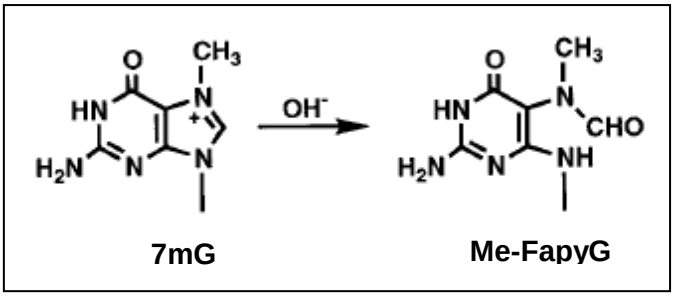

Figure 3: Oxidation of 7-methyl guanine (7mG) forms Me-FapyG. (Image taken from Asagoshi *et al.,* 2002).

Like 8-oxoG and FapyG, FapyA (Figure 4) is another very abundant oxidised base lesion generated by ionizing radiation or ROS. FapyA can be a toxic lesion due its ability to block DNA synthesis (Graziewicz *et al.,* 2000). The oxidized adenine residue 8-oxo-7,8-dihydroadenine (8-oxoA) causes no mutagenic incorporation, does not block DNA synthesis by the *E. coli* DNA polymerase I and the DNA duplex conformation stays intact which implies that 8-oxoA has limited or no biological effect on DNA replication (Guschlbauer *et al.*, 1991; Figure 4). However, a more recent study showed that 8-oxoA in mammalian cells can induce A→C transversions and A→G transitions at a rate comparable to that of 8-oxoG (Kamiya *et al.,* 1995a). However, as other research showed that the A→C transversion rate caused by 8-oxoA is at least four times lower than for 8-oxoG, the real biological significance of 8-oxoA remains to be determined (Tan *et al.*, 1999). The C2 position in adenine is also prone for oxidation via ionizing radiation and various ROS resulting in 2-oxo-1,2-dihydroadenine (2-oxoA; Figure 4). Although, 2-oxoA generally still pairs with thymine it can also pair with cytosine resulting in an A→G transition (Hori *et al*., 2010; Kamiya & Kasai, 1995b). The 2-oxo-dATP nucleotide can be misincorporated opposite G during DNA synthesis resulting in a G→T transversion (Inoue *et al.*, 1998).

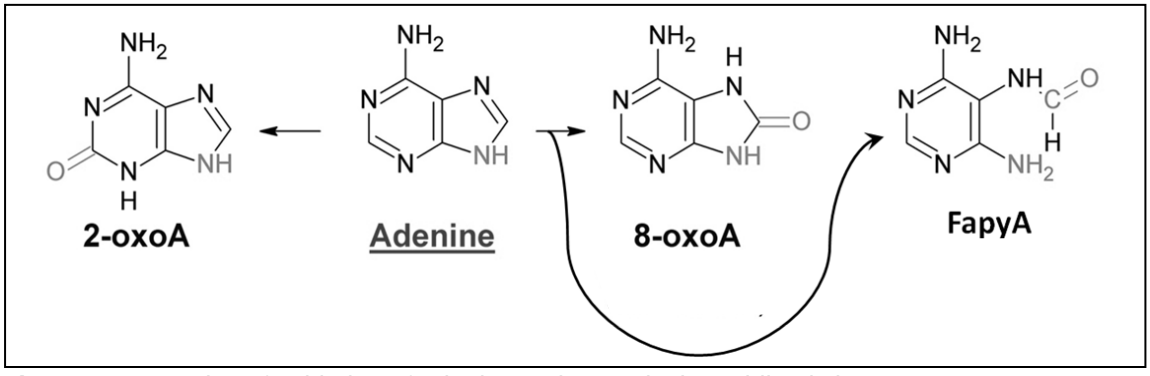

Figure 4: Examples of oxidation of adenine. O in grey is the oxidized site.

Cytosine can be oxidized to 5-hydroxycytosine (5-OH-C; Figure 5) which has a weak C → T mutagenic activity. However, 5-OH-C can be deaminated to 5-hydroxyuracil (5-OH-U; Figure 6) which is a highly mutagenic lesion and responsible for C → T transition mutations (Kreutzer & Essigmann, 1998).

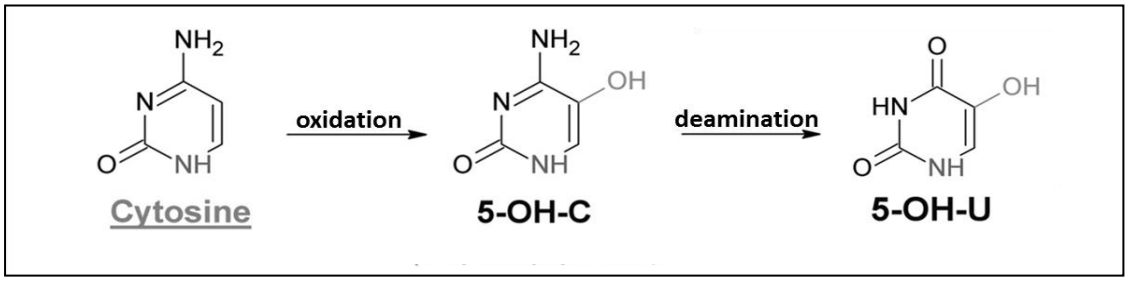

Figure 5: Examples of oxidation and further deamination of cytosine. NH in grey is the deoxyribose binding site. OH in grey is the oxidized site.

As a result of ionizing radiation and oxidative stress thymine can be transformed to thymine glycol (Tg; Figure 6) an abundant DNA lesion known to block DNA replication and also to form a Tg:G mismatch resulting in a T→C transition (Krwawicz *et al.,* 2007; Kusumoto *et al.*, 2002; Yoon *et al.*, 2003).

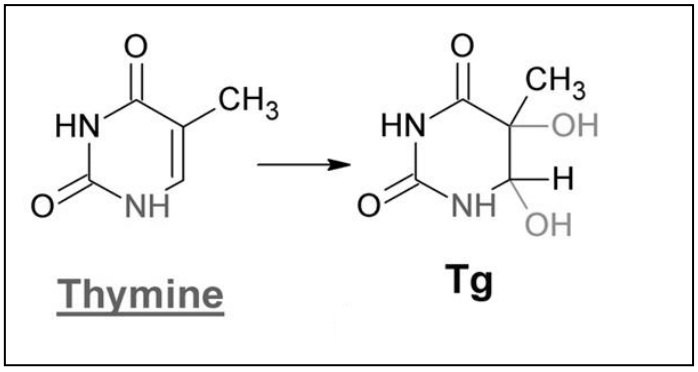

Figure 6: An example of the oxidation of thymine. OH in grey is oxidized site.

2.1.2 Spontaneous DNA damage formation

Two major forms of spontaneous DNA damage exist, deamination of bases and depurination. Depurination is the spontaneous DNA hydrolysis of the purines adenine and guanine at the β-*N*-glycosidic bond resulting in an AP site that can block DNA synthesis and is therefore cytotoxic (Breen & Murphy, 1995). It has been estimated that every day, between 2,000 – 10,000 DNA purine bases are lost due to depurination in a human cell (Lindahl, 1993).

Base deamination, is the hydrolytic removal of an amine group from cytosine, adenine or guanine. Deamination of cytosine results in uracil that can lead to C→T transition as uracil pairs with adenine during DNA replication (Figure 7).

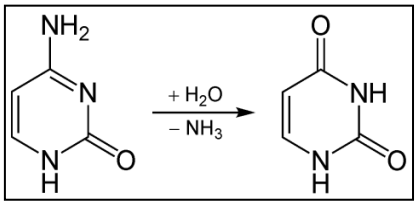

Figure 7: Deamination of cytosine (left) to uracil (right).

2.1.3 UV damage

The ultraviolet (UV) light spectrum includes the wavelengths in the range 100-380 nm. This area is subdivided into UV-A (315-380 nm), UV-B (280-315 nm) and UV-C (100-280 nm). UV-B is the most mutagenic component of the UV spectrum that can lead to bipyrimidine photoproducts such as the toxic and mutagenic cyclobutane-pyrimidine dimers (Figure 8) and 6-4-photoproducts that are formed at 5′-T-C-3′, 5′-C-C-3′, 5′-T-T-3′ DNA sequences (Figure 9) (Sinha & Häder, 2002; Cadet *et al.*, 2005).

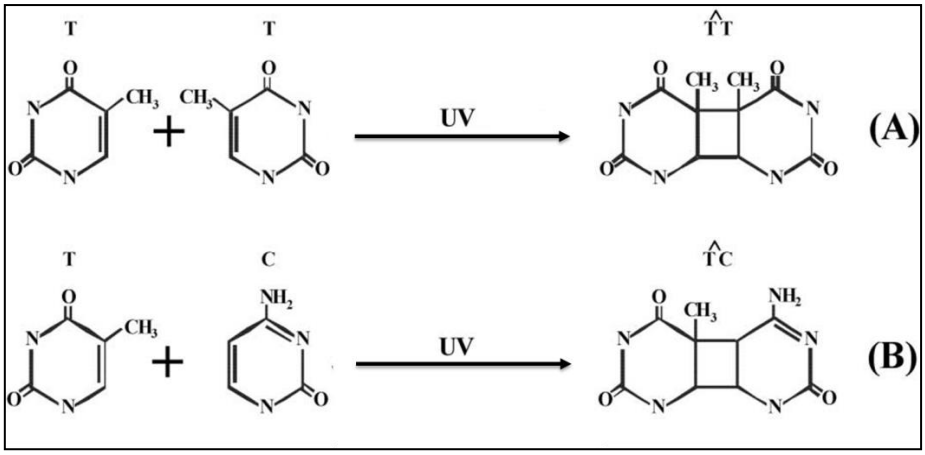

Figure 8: Formation of cyclobutane-pyrimidine dimers: thymine-thymine dimer (A) and thymine-cytosine dimer (B). (Image adapted from Sinha and Häder, 2002).

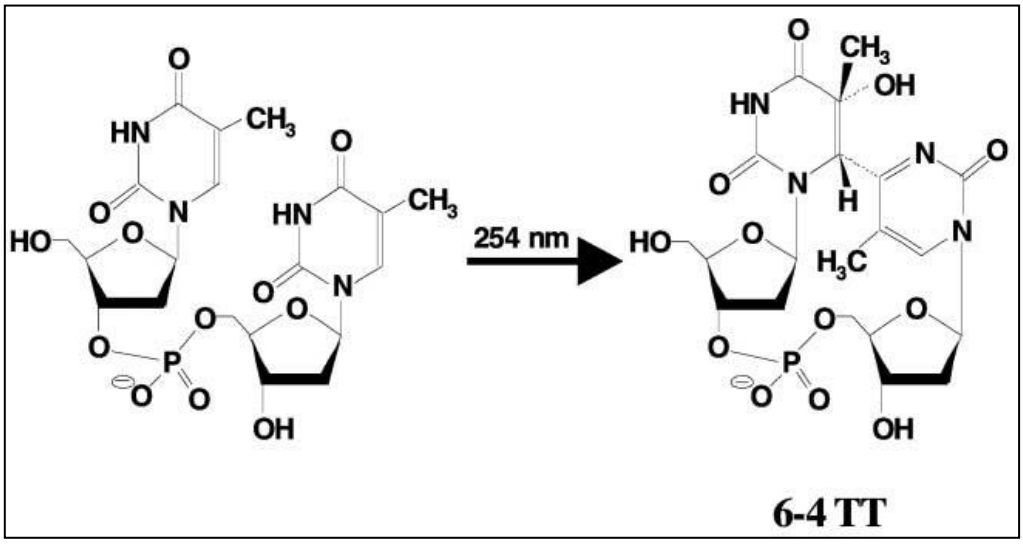

Figure 9: Formation of a 6-4 photoproduct, in this case 6-4 TT from 5′-T-T-3′. (Image adapted from Sinha and Häder, 2002).

If these DNA lesions are not removed from DNA they can affect genomic integrity which subsequently can affect cell and tissue homeostasis and cause mutations in oncogenes and tumour-suppressor genes leading to carcinogenesis or apoptosis of the cell (Cadet *et al.*, 2005).

2.1.4 Lipid peroxidation

There is evidence that many damaging effects on cellular components under oxidative stress are caused by the products of lipid degradation. This process of peroxidative degradation of polyunsaturated fatty acids is called lipid peroxidation and is a result of a free radical chain reaction (Uchida, 2003). Lipid peroxidation includes three steps, the initiation, propagation and the termination step. The oxidative chain reaction is initiated by ROS such as $^{\bullet}OH$ attacking the double bonds of the polyunsaturated fatty acids which then leads to a lipid radical that reacts with O_2 producing a lipid peroxyl radical (1 in Figure 10). This lipid peroxyl radical is highly reactive oxidizing further lipids and propagating a chain reaction (2 in Figure 10). This chain reaction carries on until a lipid radical reacts with another lipid radical or an antioxidant such as γ-tocopherol (vitamin E) terminates the process by transferring a hydrogen atom that renders the lipid peroxyl radical into a lipid peroxide that can be further processed either enzymatically or spontaneously into an inert hydroxy fatty acid or other stable products (4 in Figure 10) (Uchida, 2003; Sattler *et al.*, 2006; Winczura *et al.*, 2012).

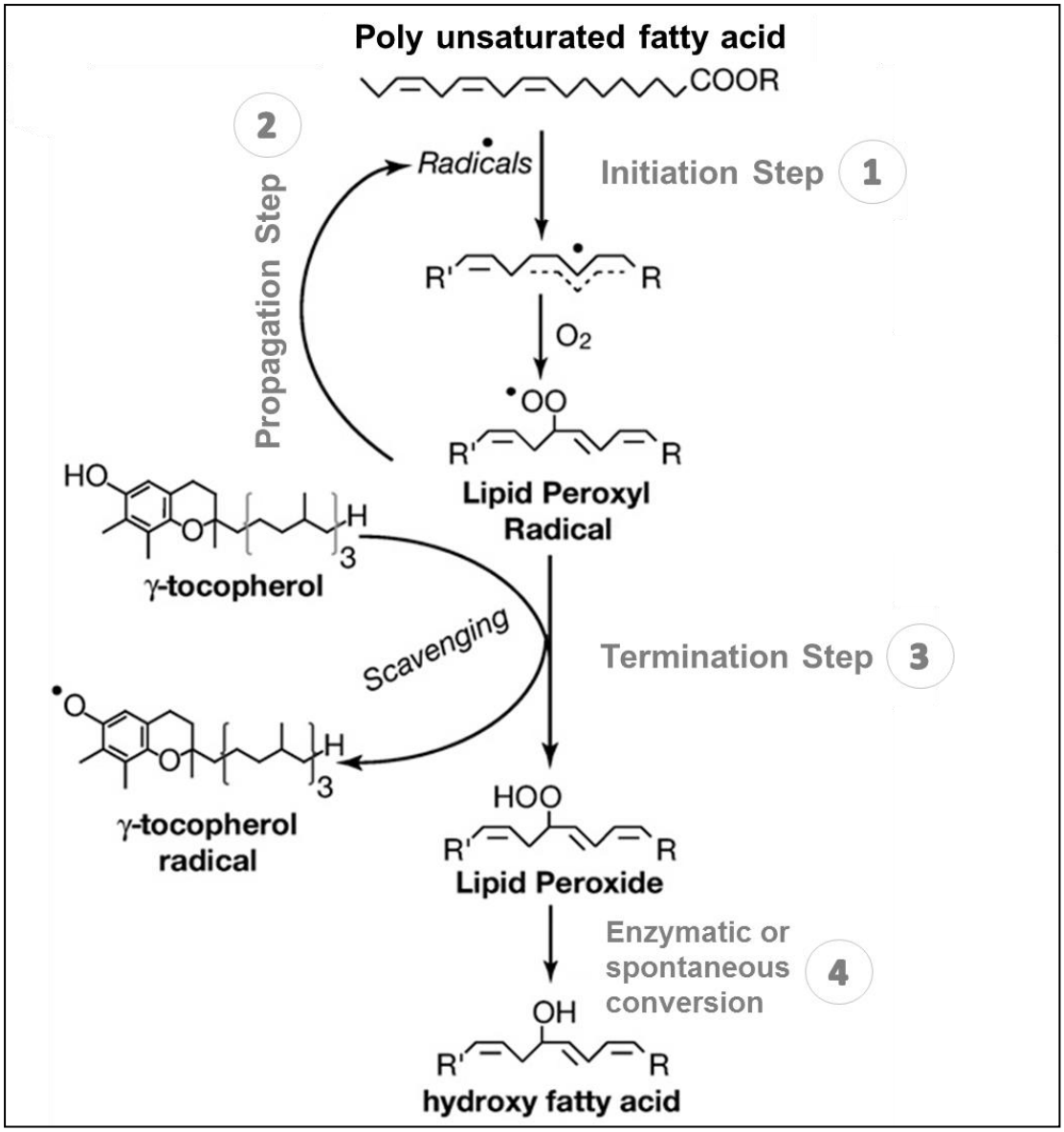

Figure 10: The three steps of the lipid peroxidation chain reaction. Initiation step (1) renders a polyunsaturated fatty acid into a lipid peroxyl radical. This radical can react with further polyunsaturated fatty acids in the propagation step (2). Only if neutralized by an antioxidant such as γ-tocopherol or another lipid peroxyl radical is the chain reaction terminated (3). Further enzymatic or spontaneous conversion changes the lipid peroxide into a more stable product such as hydroxy fatty acid (4). (Image adapted from Sattler *et al.,* 2006).

The lipid peroxyl radical can cyclize and subsequently be further oxidized by O_2 to form an isoprostane (Figure 11) (Winczura *et al.*, 2012). The so formed isoprostane is highly unstable and either spontaneously rearranges to form other types of isoprostanes or it decays into fragments, releasing malondialdehyde (MDA; Figure 11) (Sattler *et al.*, 2006; Winczura *et al.*, 2012).

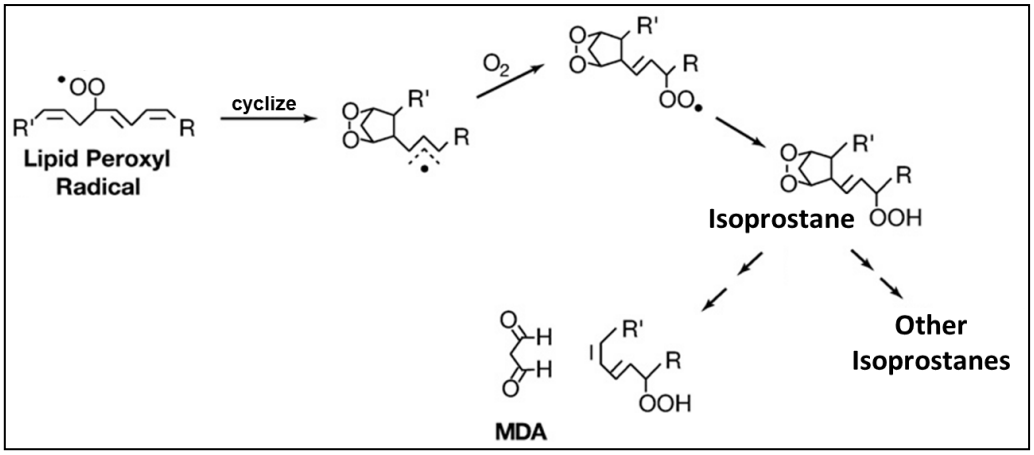

Figure 11: Formation of Isoprostane and MDA. (Image adapted from Sattler *et al.,* 2006).

In DNA, MDA reacts with guanine, adenine and cytosine to form several pre-mutagenic adducts. The major adduct is the cyclic pirymido-[1,2 α]purine-10(3H)-one-2′-deoxyribose (M1dG; Figure 12) which can induce G→T transversions or G→A transitions at a similar frequency to 8-oxoG (Valko *et al.*, 2006).

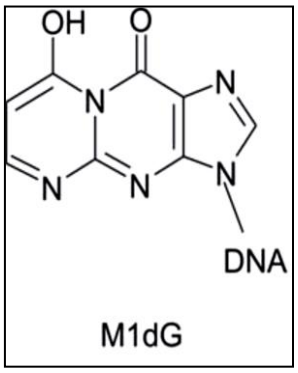

Figure 12: Chemical structure of M1dG. (Image adapted from Winczura *et al.,* 2012).

Further DNA lesions caused by lipid peroxidation products, but also by exposure to carcinogens such as vinyl chloride, are etheno adducts where a five membered exocyclic ring is attached to DNA bases leading to 1,N^2-ethenoguanine (1,N^2-εG), N^2,3-ethenoguanine (N^2,3-εG), 3,N^4-ethenocytosine (3,N^4-εC) and 1,N^6-ethenoadenine (1,N^6-εA). How the formation of etheno adducts exactly occur *in vivo* is not fully understood to date and remains to be determined (Winczura *et al.*

2012). However, exocyclic bases can be mutagenic. After DNA replication, 1,N^2-εG can lead to G→T and G→C transversions (Langouet *et al.*, 1997) and N^2,3-εG is prone to base pair with cytosine and thymine leading to G→A transitions if the latter (Cheng *et al*., 1991). 3,N^4-εC can mismatch with thymine and adenine resulting in C→A transversions and C→T transitions (Moriya *et al.*, 1994). If paired with adenine or cytosine, 1,N^6-εA can lead to A→T tranversions or A→G transitions respectively (Pandya & Moriya, 1996).

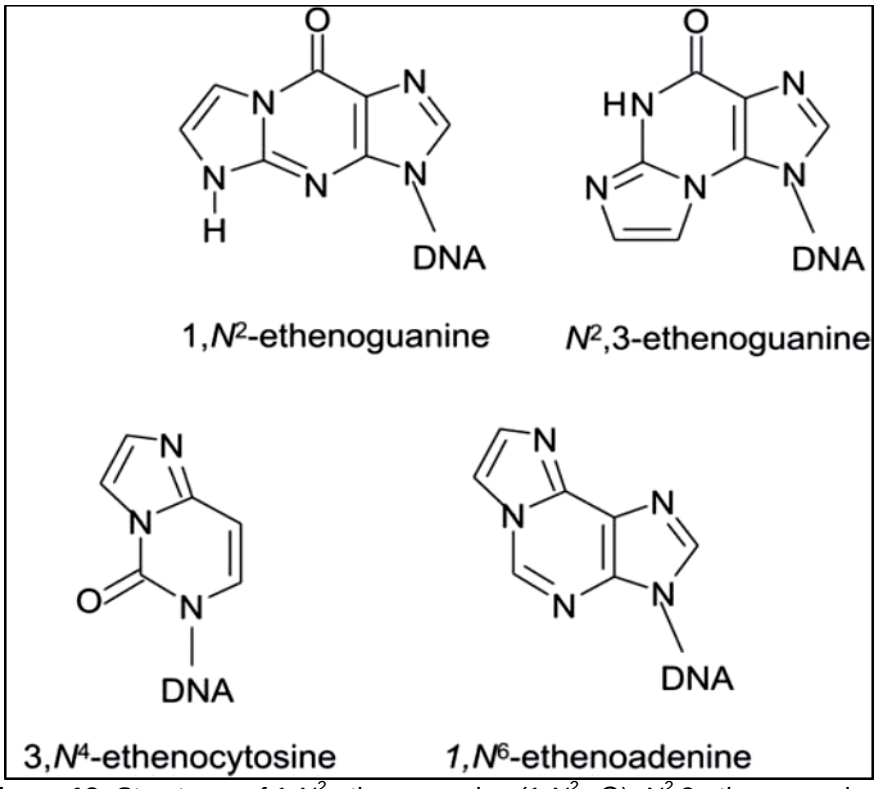

Figure 13: Structures of 1,N^2-ethenoguanine (1,N^2-εG), N^2,3-ethenoguanine (N^2,3-εG), 3,N^4-ethenocytosine (3,N^4-εC), 1,N^6-ethenoadenine (1,N^6-εA). (Image adapted from Winczura *et al.,* 2012).

2.1.5 Alkylation DNA damage

A very common form of alkylation is the methylation of DNA. Depending on the position of the methyl group, the nucleotide can be rendered pre-mutagenic or toxic. However, methylation of cytosine on C5 that forms 5-methylcytosine (5meC) is crucial for several functions within a cell such as regulation of gene expression and chromatin modification in eukaryotic cells (Jair *et al.*, 2013).

Figure 14 shows a summary of positions that are susceptible to methylation and alkylation in general whereas the different positions either cause toxicity, mutagenesis or spontaneous depurination.

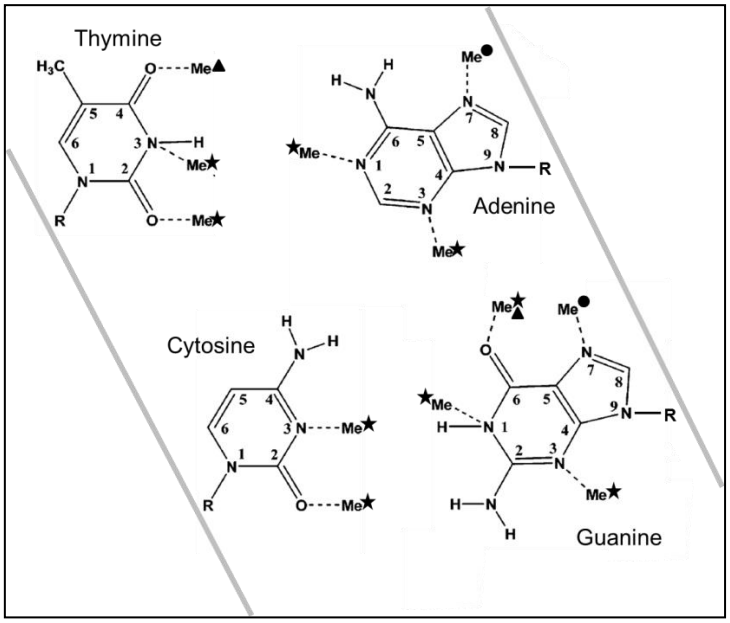

Figure 14: Summary of positions prone to methylation (Me) in thymine, adenine, cytosine and guanine. Me with a star represents toxic lesions, with a triangle pre-mutagenic lesions and with a circle lesions that are susceptible to spontaneous depurination. (Image adapted from Wyatt and Pittman, 2006).

Commonly known agents that can cause DNA alkylation are cytotoxic anti-cancer drugs, *N*-nitroso compounds found in tobacco, methane gas released from industry and *N*-nitrosamines that are consumed with smoked meat (Hecht, 1999; Lijinsky, 1999).

2.1.6 DNA strand breaks

Double-strand breaks can be generated by blocking lesions that stop DNA replication and can lead to a collapse of the replication fork. Such blocking lesions are generally generated, either directly or indirectly by radiation, ROS or other chemical agents that cause oxidative damage to C1 or C4 of the deoxyribose in the phosphate backbone of DNA. Although, DSBs are essential for meiotic recombination they also can be indirectly lethal to cells by inducing mutations, deletions or translocations to the chromosomal DNA that can lead to apoptosis or cancer whereas apoptosis is controlled by the ATM-ATR signalling pathway that arrests cell cycle in G1 phase allowing DSBs repair mechanisms to resolve DNA damage (Kaina, 2003). Ionising radiation and ROS generate single-strand breaks (SSBs) and if these breaks lie in close proximity on opposite strand this will result in in double-stranded DNA (dsDNA) breaks (DSB). If unrepaired, DSBs can trigger apoptosis (Demple & DeMott, 2002).

2.2 Antioxidants: the first instance of DNA protection

Antioxidants are molecules and enzymes that can prevent other molecules from being oxidised and either are taken up from the environment (e.g. certain essential vitamins) or produced in the cell itself. One example is the enzyme superoxide dismutase (SOD) that can dismutate the radical superoxide (O_2^-) to oxygen (O_2) and hydrogen peroxide (H_2O_2) (Peter *et al.*, 2006). Superoxide is a highly reactive ROS that is generated as a by-product of the mitochondrial respiration pathway. If not neutralized by antioxidants such as SOD it can lead to chain-reactions that oxidise cellular macromolecules such as DNA (Keyer & Imlay, 1996).

2.3 DNA repair pathways

To maintain genomic integrity, living organisms have developed several DNA repair pathways that include, direct reversal (DR), mismatch repair (MMR), nucleotide excision repair (NER), BER, homologous recombination (HR), and non-homologous end joining (NHEJ) (Hakem, 2008; Figure 15).

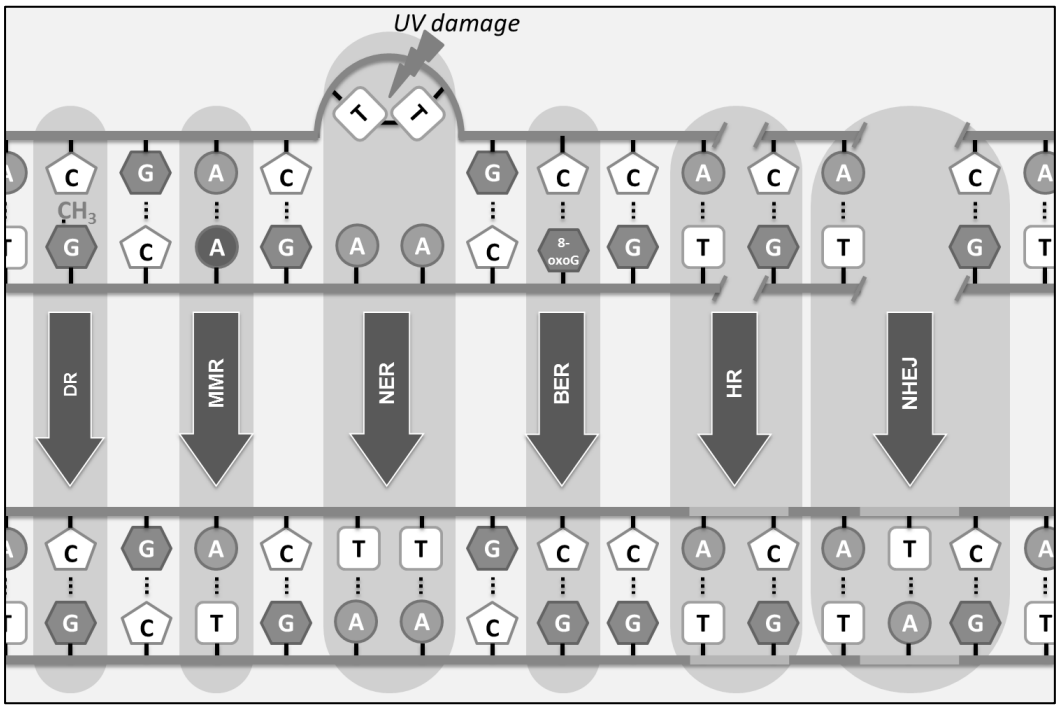

Figure 15: Overview of DNA-repair pathways for different DNA lesions. DR = Direct reversal; MMR = mismatch repair; NER = nucleotide excision repair; BER = base excision repair; HR = homologous recombination; NHEJ = non-homologous end joining (examples for DNA damage shown in this picture are O^6-methylation of guanine (DR pathway), A/A mismatch (MMR pathway), UV light damage produced pyrimidine dimers (NER pathway), oxidation of guanine to 8-oxoG (BER pathway).

2.3.1 Direct reversal (DR)

The DR pathway repairs DNA base alterations such as pyrimidine dimers induced by UV radiation (Section 2.1.1) or O^6-methylguanine produced by alkylating agents that transfer methyl- or other alkyl-groups to DNA bases (Section 2.1.5). Pyrimidine dimers are a type of intrastrand crosslink whereby either two thymines or cytosines that are next to each other on the same DNA strand are linked by covalent bonds. In many species including bacteria, fungi and non-placental animals, these lesions can be repaired by the enzyme photolyase in a process known as photoreactivation (Sancar *et al.*, 2006). The O^6-alkyl adduct O^6-methylguanine (Figure 16), on the other hand, is repaired in *E. coli* by the enzymes Ada and Ogt and in mammalian cells by O^6-methylguanine-DNA methyltransferase (MGMT).

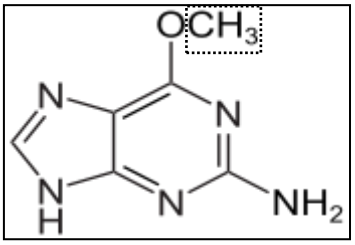

Figure 16: The guanine derivative O^6-methylguanine bears a methyl group on its oxygen (dotted box).

Instead of replacing damaged bases DR changes them back into their original state. Therefore, unlike BER it is a one-step pathway which does not require the excision of the damaged base. However, because MGMT repairs O^6-methylguanine-DNA by transferring the alkyl group from the oxygen in the DNA to its own amino acid residue cysteine in its active site, it can only be used once before it becomes inactivated and subsequently degraded by the proteasome (Pierce, 2012; Hakem, 2003).

2.3.2 Mismatch repair (MMR)

If, after DNA replication an incorrect base was incorporated and not corrected by the proofreading activity of the replicating DNA polymerase, the base mismatch is repaired by the MMR complex. It is known that in bacteria the subsequent methylation of a GATC sequence in the newly replicated strand is delayed and therefore the methyl group on the parental strand can be recognised and identified by the MMR proteins. Then the complementary strand is nicked before the guanine in the GATC sequence. This allows the MMR complex to bend the DNA and to bring the mismatched bases close to the methylated CTAG sequence. Subsequently exonucleases remove nucleotides from the new strand just before the 5′ guanine of the GATC sequence and the 3′ end of the nucleotide just after the mismatched base pair. Finally DNA polymerase closes the gap with bases complementary to the parental strand and nicks in the deoxyribose-phosphate backbone are sealed by DNA ligase (Pierce, 2012). Several enzymes are known that are involved in the MMR complex. In *E. coli* it is the homodimer MutS that binds to a mismatched base, while MutL recognises the binding and identifies the new DNA strand by binding to the methyl group on the CTAG sequence in the old strand. Then MutH nicks the nascent strand, the helicase II (UvrD) separates the double-stranded DNA, exonucleases remove the oligonucleotide that contains the DNA lesion and finally polymerase III resynthesizes the excised DNA (Iyer *et al.*, 2006).

Although several proposals have been made about the function of MMR in eukaryotic cells, the mechanism of recognition of a mismatched base remains unclear (Hsieh & Yamane, 2008; Iyer *et al.*, 2006; Jiricny, 2006). However, it is known that different types of base mismatch specific homologs of the methyl-directed mismatch repair proteins in *E. coli* exist in eukaryotes. MutSα binds to single base-base mismatches and 1-2 base insertion/deletion. If more than two bases are inserted/deleted then

MutSβ will recognize it instead of MutSα. The three eukaryotic heterodimers MutLα, MutLβ and MutLγ have a similar function to that of MutL in *E. coli*, but in addition, MutLα and MutLβ have an endonuclease activity and therefore can nick the dsDNA (the role performed by MutH in *E. coli*). Pluciennik *et al.,* (2010) discovered that interaction of PCNA with MutLα orientates this endonuclease in the direction on the dsDNA that is needed for correct incision on the oligonucleotide that contains the DNA lesion.

Beside its exonuclease activity, necessary for the final excision of this oligonucleotide, Exo1 can carry out the prior separation of the dsDNA and therefore no helicase such as the UvrD in *E. coli* is needed. The resulting gap is then closed by DNA Polδ (Larrea *et al.*, 2010; Iyer *et al.,* 2006).

2.3.3 Nucleotide excision repair (NER)

NER removes bulky DNA lesions such as UV radiation-induced thymine dimers and 6-4-photoproducts, inter- and intra-strand crosslinks formed by DNA reactive substances, large-volume adducts and ring systems such as benzo[*a*]pyrene and aflatoxin residues (Friedberg, 2001; Hoeijmakers *et al.,* 1990). Like in MMR, in NER an oligonucleotide containing the lesion is removed and replaced by DNA synthesis. Due to the change of conformation of the DNA structure (helix distortion) caused by the DNA lesion the NER enzyme complex is able to recognize the DNA damage. Subsequently, the double-stranded DNA is separated and the single strands are stabilized by single-strand binding proteins. Then, in eukaryotic NER, the strand that carries the lesion is cleaved and as oligonucleotide of 25-30 nucleotides removed, the gap filled by a DNA polymerase and the phosphodiester bond sealed by a DNA ligase (Pierce, 2012; Hakem, 2008). Two sub-pathways of NER exist, global genome

NER (GG-NER) and transcription-coupled NER (TC-NER). GG-NER guards the whole genome while TC-NER repairs actively transcribed genes. However, except from different proteins involved in the recognition of the damaged DNA the repair pathways are the same (Hakem, 2008).

2.3.4 Homologous recombination (HR), Non-homologous end-joining (NHEJ)

In order to repair DSBs, cells have two major pathways, homologous recombination (HR) and non-homologous end-joining (NHEJ). All proteins involved in this repair process are closely linked to the ATM-ATR signalling pathway described in Section 2.1 (Shrivastav *et al.*, 2008). NHEJ ligates the break ends directly and uses short homologous DNA sequences that are present in ss overhangs on the ends of DSBs. Only if the overhangs are compatible, will NHEJ repair the DSB without loss of DNA sequence (Moore, & Haber, 1996). Incorrect NHEJ can lead to carcinogenesis due to translocations and telomere fusion (Espejel *et al*., 2002). HR on the other hand needs a second, homologous DNA molecule that can act as a template for the repair process and is therefore much more precise than the NHEJ pathway. Furthermore, HR uses the homologous DNA from the sister chromatid and therefore incorporates new genetic information into a chromosome during mitosis (Moynahan & Jasin, 2010).

2.3.5 Base excision repair (BER)

The BER is a highly conserved pathway from bacteria to mammals that combats oxidative and alkylation damage occurring in the DNA molecule. Substrates include chemically modified bases, AP sites generated by spontaneous depurination and SSBs. Two types of BER exist, short patch (SP-) and long patch (LP-) BER. In SP-BER a DNA glycosylase, specific for the type of base lesion, flips the base outside the DNA helix and releases the damaged base from the β-*N*-glycosidic bond resulting in an AP site (Figure 17, Figure 18 and Figure 19). The DNA glycosylases involved in BER fall into two main groups, monofunctional and bifunctional, regarding their mechanisms of action.

Bifunctional DNA glycosylases such as NTH1 and OGG1 have an AP-lyase (DNA-(apurinic or apyrimidinic site) lyase) activity and can perform β-elemination which cuts at the C-O-P bond 3′ to the AP-site resulting in a 3′-phosphate unsaturated aldehyde (3′PUA; Figure 17, **2** in Figure 18). The 3′PUA will then be removed by apurinic endonuclease 1 (APE1; Figure 17, **2** in Figure 18) which results in a 3′OH and a 5′P site. The NEIL proteins on the other hand are bifunctional DNA glycosylases that can perform β,δ-elimination and therefore cut the AP-site also on its 5′ site leaving a 3′-phosphate (3′P). This phosphate group will then be further processed by the polynucleotide kinase (PNK) forming a 3′OH site (Figure 17, **3** in Figure 18). The resulting gap with 5′P and 3′OH overhangs is ready to be filled with the correct base by Polβ that uses the opposite DNA strand as template (Date *et al.*, 1992; Sandigursky & Franklin, 1992). The final step in SP-BER is ligation by DNA ligase III α (LigIIIα) which joins the 3′OH end to the 5′P (Figure 17) (Brown, 2002).

Monofunctional DNA glycosylases on the other hand are not able to process the resulting AP site after release of the damaged base. Therefore, APE1 is needed

which can due to its endonuclease activity cut the AP site resulting in a 3′OH and a deoxyribose phosphate (5′dRP) overhang (Figure 17, **1** in Figure 18). Because of the high affinity of poly(ADP-ribose)polymerase-1 (PARP-1) for DNA SSBs it binds to this SSB intermediate generated by APE1 before any other downstream protein can bind. This way PARP-1 regulates DNA repair activity by binding to DNA strand breaks allowing other repair enzymes such as Polβ and LigIIIα to act on the lesion while XRCC1 acts as a scaffold for these proteins (Parsons *et al.*, 2005; Woodhouse *et al.*, 2008). The 5′dRP is released by Polβ resulting in a 3′OH and 5′P gap that can be filled by the DNA polymerase activity of Polβ and sealed by LigIIIα (Figure 17).

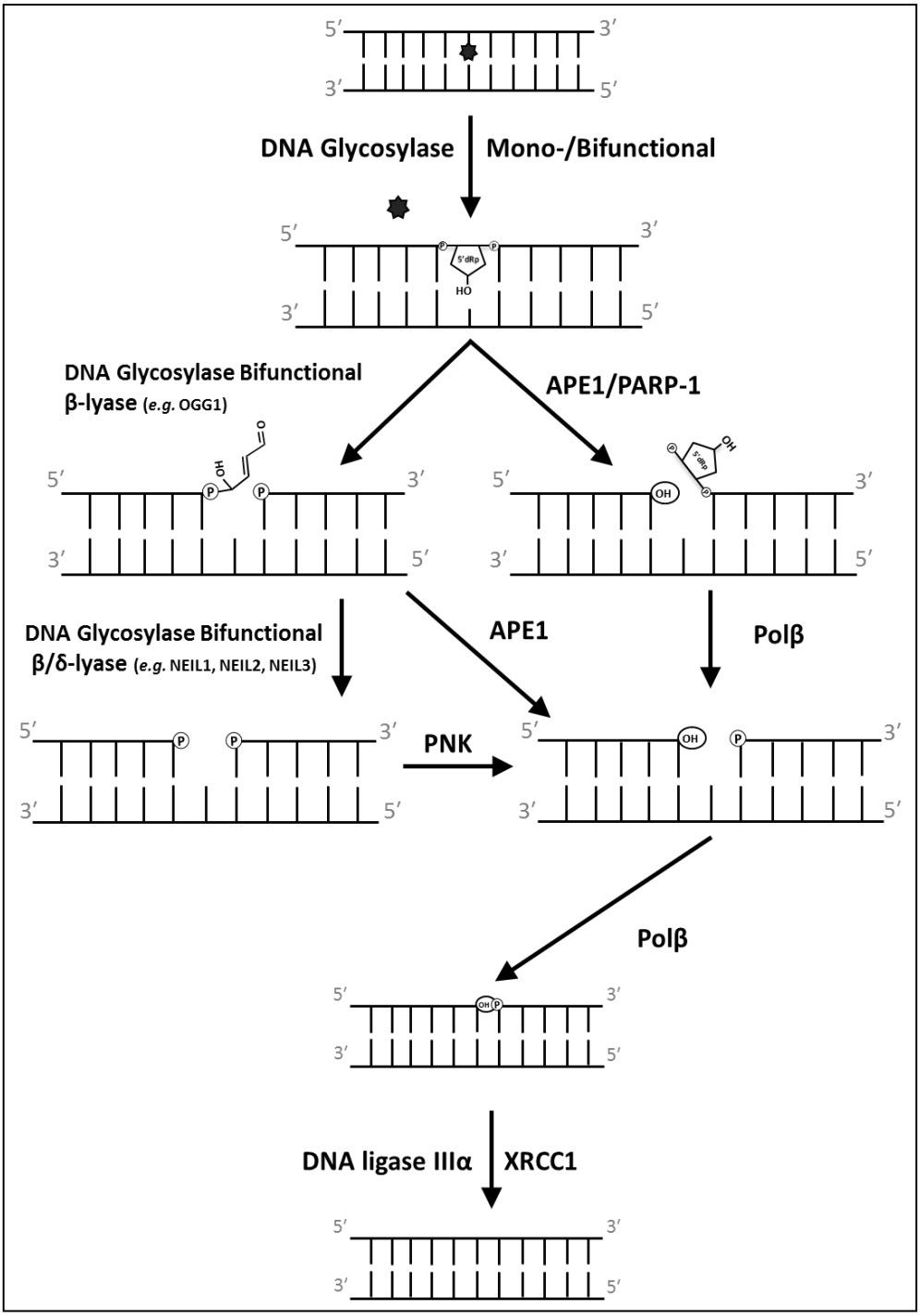

Figure 17: Scheme for the mammalian short patch (SP) BER.

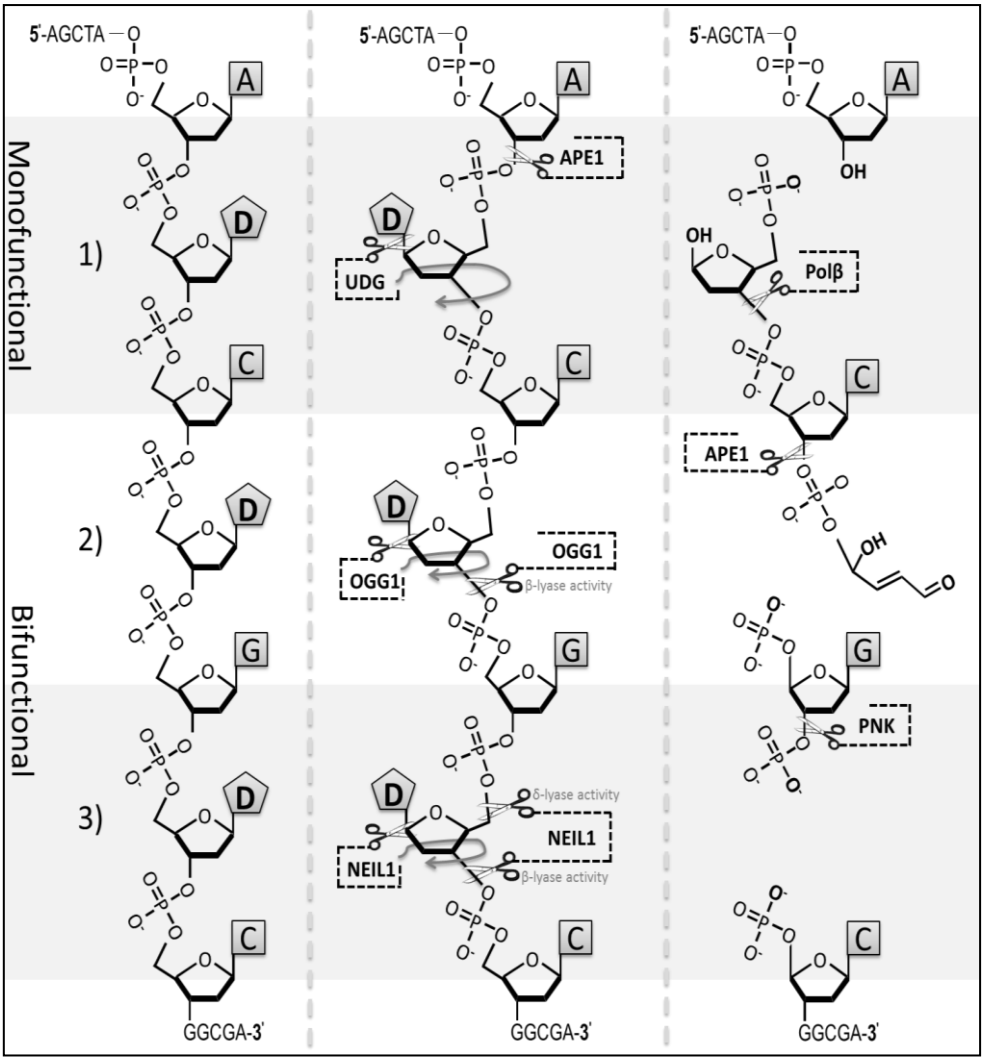

Figure 18: A comparison of reactions catalysed by monofunctional and bifunctional DNA glycosylases. In the first step, DNA glycosylases recognise, bind to and then flip the damaged base lesion out of the DNA helix. Monofunctional DNA glycosylases such as uracil DNA glycosylase (UDG; **1**) catalyse an one-step removal of the damaged base leaving an AP site which is then further processed by APE1 and Polβ. Bifunctional DNA glycosylases, such as OGG1 (**2**) and NEIL1 (**3**) are able to attach to the AP site by their nucleophilic active site residue and cleave either at 3′ via their β-lyase activity (OGG1; **2**), or at 3′ and 5′ via their β,δ-lyase activity (NEIL1; **3**) which results in a DNA single-strand break for OGG1 and a gap for NEIL1. The unsaturated aldehyde produced by OGG1 is further processed by APE1 and the 3′-phosphate produced by NEIL1 is excised by PNK.

The LP-BER pathway on the other hand shares enzymes that are involved in DNA replication such as Polδ, DNA polymerase ε (Polε), Flap endonuclease 1 (FEN1), PCNA and DNA ligase I (LigI) (Izumi *et al*., 2003). LP-BER removes and resynthesizes a patch of 2 – 15 nucleotides. Interestingly there are overlapping

substrates within the SP- and LP-BER which might increases the overall protection of the genome against oxidative damage (Figure 19) (Hegde *et al.*, 2008b).

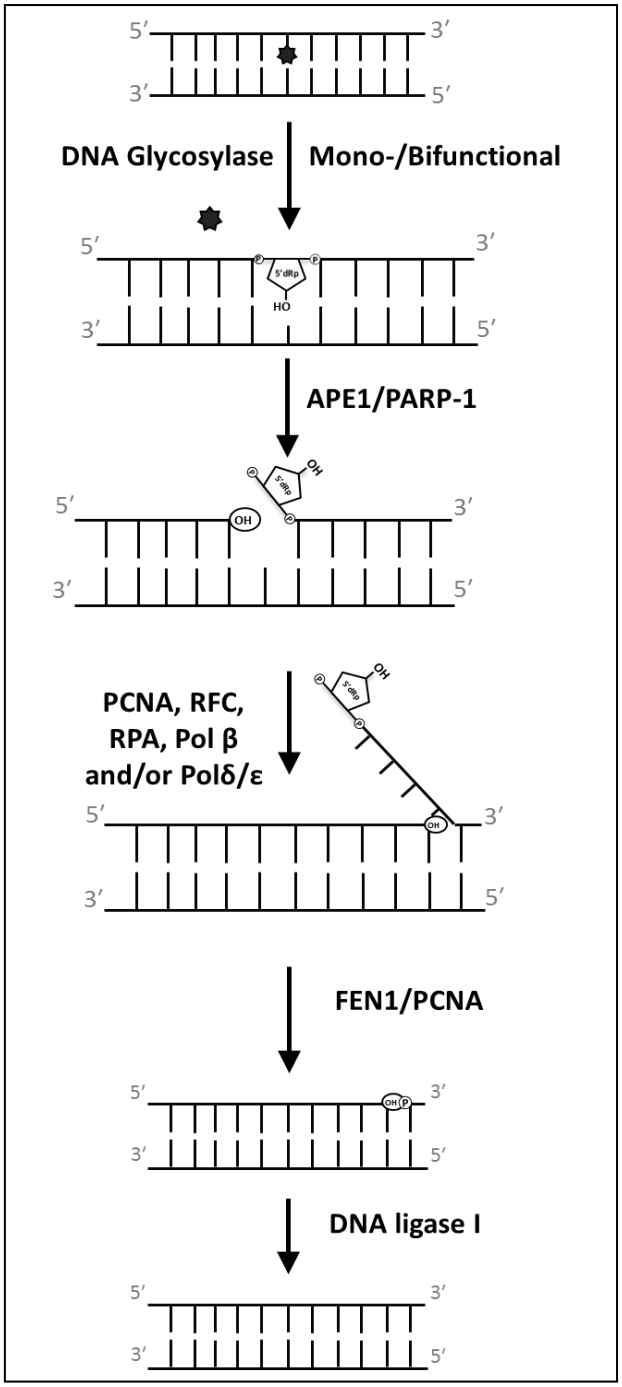

Figure 19: Scheme for the mammalian long patch (LP) BER.

Due to the fact that in each step of BER a potential toxic lesion is generated such as an AP site, it is suggested that proteins work tightly together in big complexes during the BER process where they “hand over” each product until the resynthesized DNA strand is ligated (Campalans *et al.*, 2005).

2.3.5.1 DNA glycosylases in E. coli

Due to their overlapping substrate specificity it is difficult to identify new DNA glycosylases on the basis of their activity in cell extracts. Hence, most of the human DNA glycosylases where cloned on the basis of functional complementation or sequence homology with *E. coli* or yeast homologs already discovered (Hazra *et al.*, 2003).

In *E. coli* the enzyme Fpg is essential for the repair of oxidized purines, such as 8-oxoG, FapyA (Wiederholt *et al.*, 2002) and FapyG (Wiederholt *et al.*, 2003). Fpg is a bifunctional DNA-glycosylase with a β/δ AP lyase activity leading to a 3′P blocking residue and a 5′P site at the DNA strand break (Zharkov *et al.*, 2003). The activity of Fpg is accomplished by the amino acid residue proline at amino acid position two (Pro2). This N-terminal residue of the Fpg/Nei family acts as a nucleophile in the DNA-glycosylase/AP lyase reaction (Saparbaev *et al.,* 2002).

Nei encoded by the *nei* gene in *E. coli* excises various oxidized pyrimidines such as 5-OH-C and 5-OH-U and the oxidized purine FapyA (Wallace *et al.*, 2003). Like Fpg, the active residue Pro2 plays a major role as a nucleophile in its activity as a DNA glycosylase (Saparbaev *et al.,* 2002). However, although its sequence is similar to that of Fpg its function is homologous to that of Nth (described underneath). Furthermore, it has been shown by site directed mutagenesis studies that the removal of the Glu3 and Glu174 residues in Nei resulted in a loss of activity on 5-OH-U substrates indicating that these residues are essential for the function of the DNA glycosylase domain in Nei (Burgess *et al.*, 2002).

Nth encoded by the *nth* gene in *E. coli* is a DNA glycosylase essential for the removal of Tg (Alanazi *et al.*, 1997). This bifunctional DNA glycosylase contains an internal Lys residue crucial for its β-lyase activity.

The monofunctional adenine glycosylase MutY is expressed in *E. coli* and excises adenine that is mispaired with 8-oxoG, guanine or cytosine. If MutY excises A mispaired with 8-oxoG the following DNA replication cycle may result in an 8-oxoG:C DNA base pair that can then be repaired by Fpg/MutM (Krokan *et al.*, 1997, Williams & David, 1998), or it may result in another 8-oxoG:A mispair.

2.3.5.2 DNA glycosylases in mammalian cells

Like the *E. coli* Fpg, OGG1 releases oxidized purines such as 8-oxoG and FapyG from dsDNA (Hazra *et al.,* 2002a; Takao *et al.,* 2002; Hitomi, Iwai, & Tainer, 2007). OGG1 is a bifunctional DNA glycosylase belonging to the *E. coli* Nth type that contains, like NTH1, an internal Lys residue at its active site (amino acid position 249; Hazra *et al.,* 2002b). Its expression is cell cycle independent (Dhenaut *et al.*, 2000).

The localization of OGG1 depends on the isoform and the level of oxidative stress present in the cell. Isoform 1a is known to be located to the nucleus because of its NLS at the C-terminus and isoform 2a which has a unique C-terminus and a mitochondrial targeting signal is located in the mitochondria (Nishioka *et al.,* 1999; Campalans *et al.*, 2007). OGG1 belongs to the *E. coli* Nth family that features a conserved helix-hairpin-helix (HhH) motif. This protein structure is required for interaction with phosphate and oxygen atoms of the DNA backbone and is essential for DNA binding in these enzymes (Huffman *et al.*, 2005).

After OGG1 removes 8-oxoG it remains bound to the resulting AP site until APE1 releases it from the 5′P (Hill *et al.*, 2001). Recent studies have also revealed that NEIL1 can stimulate OGG1 activity similar to APE1 (Mokkapati *et al.*, 2004).

NTH1, the human ortholog to *E. coli* endonuclease III, is like OGG1 a bifunctional DNA glycosylase that contains a Lys residue at its active site (amino acid position 220) and a HhH motif for DNA interaction. Its β AP lyase activity results in a 3′PUA residue that has to be further processed by APE1. However, unlike OGG1, instead of oxidized purines, it can release pyrimidine lesions such as dihydrouracil (DHU), 5-OH-U and Tg from dsDNA (Hazra *et al.,* 2002a; Takao *et al.,* 2002). Mouse NTH1 (mNTH1) was shown to be active in the nucleus and mitochondria and contains transport signals for both organelles in its N-terminal region (Takao *et al.*, 1998).

MUTYH, also known as hMYH, is the human ortholog of the *E. coli* MutY DNA-glycosylase and is localised in the nucleus and mitochondria (Takao *et al.,* 1998). hMYH removes misincorporated adenine or 2-oxoA from 8-oxoG or G prior to DNA replication (Ohtsubo *et al.,* 2000; Ushijima *et al.,* 2005). There is evidence that the resulting AP site is then processed by proteins involved in LP-BER as hMYH interacts with APE1, PCNA and RPA (Parker *et al.,* 2001).

To investigate their biological significance, NTH1 and OGG1 genes have been knocked out in mice. However, because no obvious phenotype such as cancer caused by unrepaired DNA lesions has been observed in these mice the assumption arose that there must be a backup pathway or enzyme(s) that is/are able to recognize and neutralize DNA lesions that are usually substrates for NTH1 and OGG1. This was confirmed when the Nei-like proteins NEIL1, NEIL2 and NEIL3 were discovered. Like Fpg, Nei contains a helix-two turns-helix (H2TH) DNA binding motif that is also found in all three NEIL proteins. Similarly, the substrate specificities of

NEIL1, NEIL2 and NEIL3 overlap with that of Fpg and Nei (Hazra *et al*., 2003). Furthermore, although the NEIL proteins are different to NTH1 and OGG1 in both domain structure and reaction mechanism, they act on many of the same substrates which confirmed the assumption that at least NEIL1 and NEIL2 act as backup proteins in NTH1/OGG1 knockout mice (Das *et al.,* 2007a).

2.3.5.2.1 *NEIL1*

Extracts from NTH1 knockout mice were still able to repair Tg lesions after exposure to 8 Gy X-Ray radiation. As mNTH1 is known to be a major DNA glycosylase in the repair of Tg lesions it was suggested that another protein, NEIL1, acts as backup DNA glycosylase thus having a complementary function to that of NTH1 (Takao *et al.,* 2002).

NEIL1 is mainly expressed during the S-phase of the cell cycle and is a bifunctional DNA glycosylase with a β/δ AP lyase activity and is a functional hybrid of Fpg and Nei. It excises oxidized purines as well as pyrimidines from single-stranded (ss) DNA and dsDNA such as 8-oxoG, FapyA, FapyG, Tg and 5-OH-U (Dou *et al.*, 2003). Unlike Fpg, NEIL1 shows nearly no activity against 8-oxoG in dsDNA when paired to cytosine. However, it can stimulate the enzyme activity of OGG1 and catalyses the incision of resulting AP site with its β/δ AP lyase activity (Mokkapati *et al.,* 2004).

Furthermore, although NEIL1 is not as efficient as OGG1 in the removal of the 8-oxoG, the excision of the 8-oxoG derivatives Gh and Sp is more than 100-fold faster than that of Tg and 5-OHC, especially if paired with T, G or C. Hence, these hydantoin lesions are the most preferred substrates for NEIL1 *in vitro* (Krishnamurthy *et al.*, 2008).

Structural comparison of NEIL1 with Fpg and Nei reveals that in total, the amino acid sequence is more homologous to Nei than Fpg, but the conserved H2TH domain shows a higher correlation to Fpg than to Nei. In addition, a “zinc-less finger” also known to be a DNA binding motif is found uniquely in NEIL1 in place of the highly conserved zinc finger motif found in Fpg (Doublié *et al.*, 2004). However, while Fpg and Nei feature a C-terminal zinc finger motif needed to stabilize DNA binding, NEIL1 does not. Therefore, the extended C-terminal of NEIL1 features its own unique DNA binding motif (Doublié *et al.,* 2004). Unlike NEIL2 and NEIL3, NEIL1 has a lysine residue at amino acid position 54 that is highly conserved in Fpg and Nei and essential for their function together with Pro2 (Rosenquist *et al.,* 2003; Takao *et al.,* 2002).

Furthermore, NEIL1 has been shown to interact through its C-terminal residue (amino acid position 288-349) with the Werner syndrome protein (WRN) a DNA helicase (Das *et al.,* 2007a). This interaction is enhanced when intracellular oxidative stress is increased. NEIL1 is active in a BER protein complex that involves several proteins such as Polβ, LigIIIα, PNK and x-ray repair cross-complementing 1 protein (XRCC1) (Dou *et al.,* 2003).

Interestingly, NEIL1$^{-/-}$ mice cells show a significant accumulation of (5′R) – and (5′S)-8,5′-cyclo-2′-deoxyadenosine DNA lesions, which was not observed in OGG1$^{-/-}$ mice cells used as control. As this kind of DNA damage is normally removed by NER rather than by BER it might be an indicator that NEIL1 is also involved in NER (Jaruga *et al.*, 2010).

2.3.5.2.2 NEIL2

Like NEIL1, NEIL2 has a Pro2 as the active site to fulfil its function as a DNA glycosylase. Interestingly, except for a few conserved domains such as the DNA glycosylase and H2TH domains, NEIL1 and NEIL2 show no other significant homology and whereas NEIL1 is cell cycle dependent NEIL2 is not. However, both act as bifunctional DNA glycosylases with βδ AP lyase activity and excise various oxidized pyrimidines such as 5-OH-U and 5-OH-C with preference for a DNA bubble structure (Dou *et al.,* 2003). NEIL2 in its function as a DNA glycosylase excises 5-OH-U and other oxidized derivatives of cytosine that are similar to substrates for NTH1. Compared to NEIL1, only weak excision activity of NEIL2 on dsDNA was observed. The preferred substrate of NEIL2 is ssDNA (Bandaru *et al.*, 2007). However, in complex with the Y box-binding (YB-1) protein its activity on dsDNA was increased by 7-fold (Das *et al.,* 2007b).

2.3.5.2.3 NEIL3

The nucleophile Pro2 residue present in *E. coli* Fpg and Nei is only preserved in NEIL1 and NEIL2 (Section 2.3.5.2.1 and 2.3.5.2.2). Instead, NEIL3 has a valine residue at amino acid position 2 (Val2) which, nevertheless, acts in the same way as Pro2 in the DNA glycosylase reaction by forming a Schiff base intermediate with the C1 atom of the damaged DNA (Liu *et al.* 2010). Site-directed mutagenesis studies on Pro2 in NEIL1 and NEIL2 showed the functional importance of this residue for the activity of these proteins (Bandaru *et al.,* 2002). Because of problems to recover active full-length NEIL3, the possible biological functions of NEIL3 remain unclear and thus are the focus of this project.

Conserved domains of hNEIL3

Several parts of the NEIL3 protein have been characterized as they are highly conserved in other proteins such as in *E. coli* Fpg/Nei and NEIL1/NEIL2. This structural information can be seen in Figure 20, Figure 27 and Figure 105 and have been assembled via the use of the basic local alignment search tool (BLAST), InterPro and publications from Morland *et al.* (2002), Torisu *et al.* (2005), Liu *et al.* (2010) and Krokeide *et al.* (2009) as described in detail below.

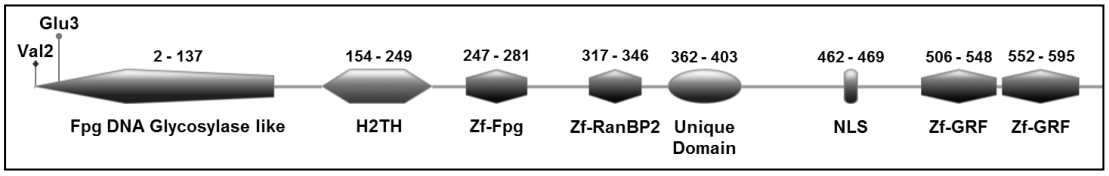

Figure 20: Summary of conserved domains in human NEIL3 and their positions within the protein.

As mentioned above, NEIL3 has a Val2 residue at the active side in place of the Pro2 residue more commonly found in homologs. However, Liu *et al.* (2010) recently showed that the N-terminal Val2 residue in mNEIL3, like Pro2, also forms an imine intermediate (Schiff base) by using a borohydride-dependent “trapping assay” which can reduce the transient Schiff base intermediate to a covalent protein-DNA complex (Figure 21).

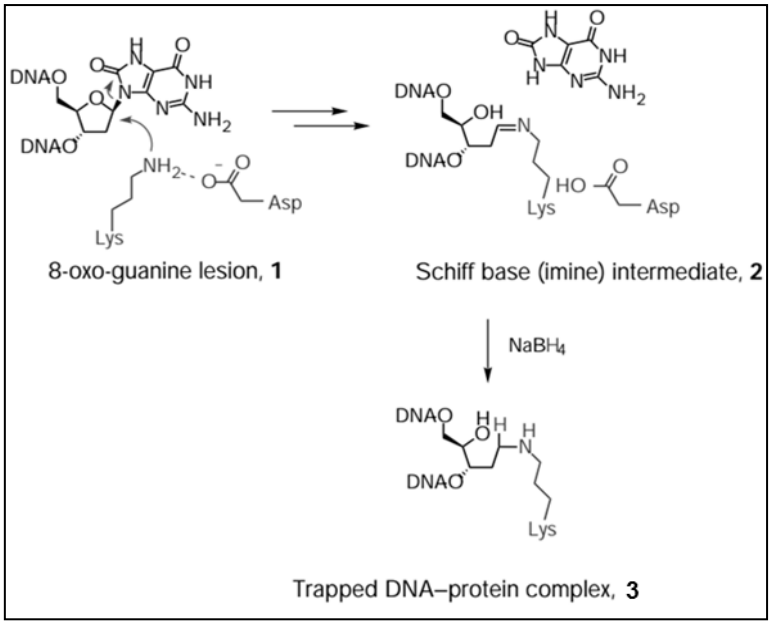

Figure 21: An example of a Schiff base intermediate and the chemical reaction of borohydride-dependent "trapping assay" that Liu *et al.* (2010) used to produce a covalent bond between the DNA backbone and the protein. OGG1 forms a Schiff base intermediate during processing an 8-oxoG lesion (**1**). If borohydride is added once the Schiff base intermediate is formed (**2**) then an irreversible cross-linking (trapping) of the enzyme to the DNA will result (**3**). (Image adapted from Bruner *et al.,* 1998).

Torisu et al. (2005; Figure 105) and BLAST studies carried out in this project with the hNEIL3 protein sequence compared with the human proteome (Figure 22) show, that the C-terminus of NEIL3 has homology with the C-terminus of AP-endonuclease 2 (APE2) and the C-terminus of DNA topoisomerase IIIα (TopoIIIα). The N-terminal region (amino acids 1-313) of APE2 is homologous to the *Xth*-like AP endonuclease family that includes APE1 (Tsuchimoto *et al.,* 2001). Like APE1, APE2 has the ability to recognize and bind specifically to AP DNA (Hadi & Wilson, 2000). Furthermore, the C-terminal domain of APE2 is homologous to a region in human TopoIIIα (Zumstein *et al.,* 1986). This C-terminal sequence (amino acids 314-518) is conserved in many proteins which are involved in nucleic acid metabolism. This gives an indication that NEIL3 is also acting in nucleic acid metabolism. Recent studies have shown that NEIL3 excises DNA lesions preferentially from ssDNA (Liu *et al.,* 2012; Liu *et al.*, 2013). However, because only truncated versions of NEIL3 were

used in these studies, it might be the case that the additional GRF zinc fingers at the C-terminal end also found in other DNA binding proteins, might affect the affinity of NEIL3 for different DNA structures including ssDNA and dsDNA.

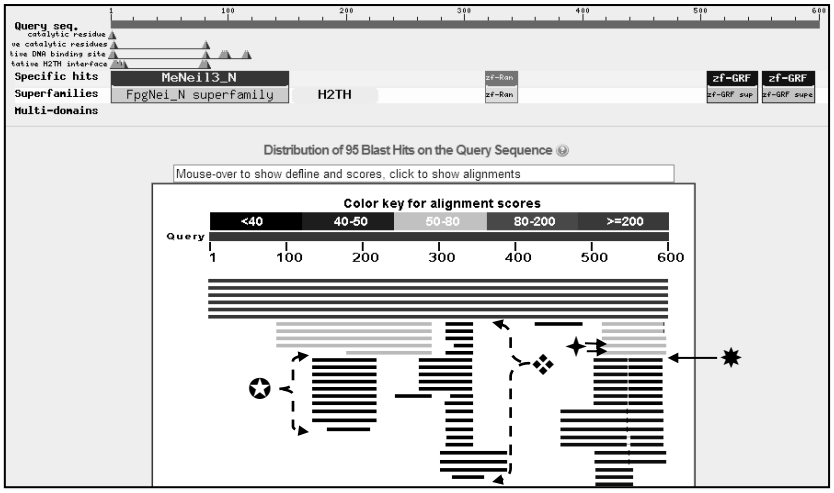

Figure 22: BLAST result of the amino acid sequence of hNEIL3 compared with the human proteome. Correlations of hNEIL3 sequence to other proteins are shown as followed: ✪ = ATP binding cassette (unknown domain); ❖ = RanBP binding protein (or RanBP binding domain); ✦ = TopoIIIα (GRF zinc finger domain); ✸ = APE2 (GRF zinc finger domain).

In addition to the BLAST results an InterProScan revealed an FPG zinc finger at amino acid position 247-281 (highlighted in Figure 23) in addition to the already known domains.

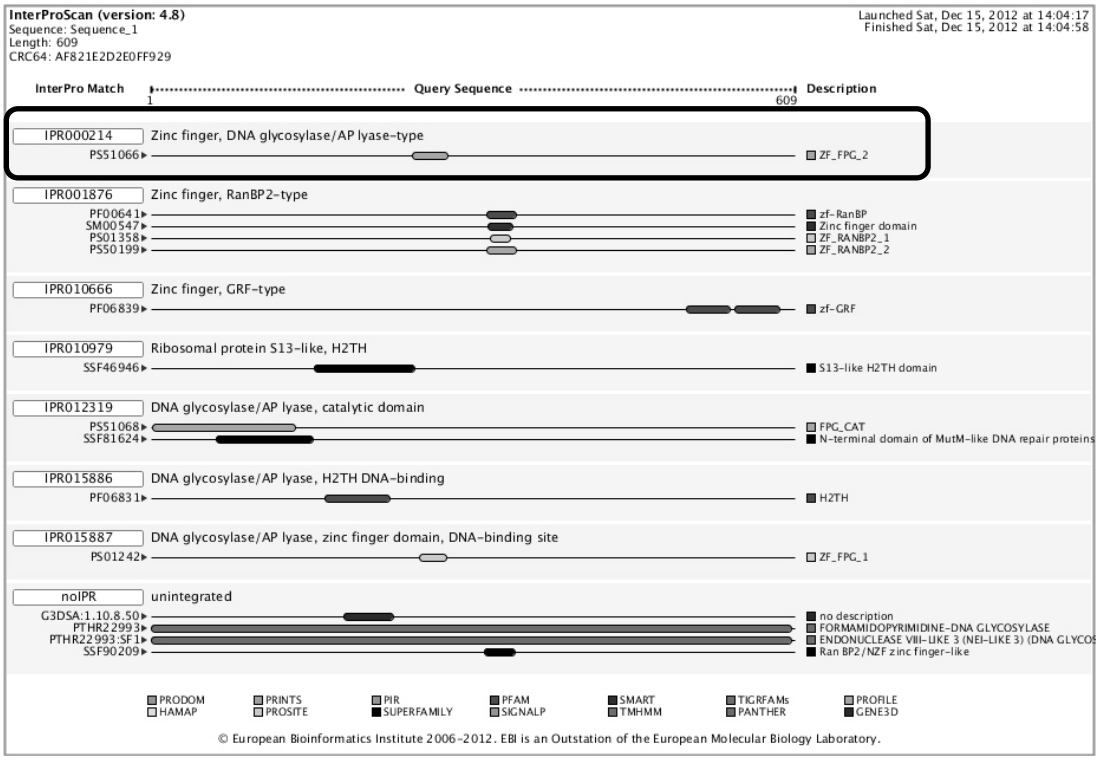

Figure 23: InterPro signature analysis for human NEIL3 protein sequence.

NLS motif

The location and existence of a putative NLS in hNEIL3 has been a matter of debate. For example, Morland *et al.* (2002), Torisu *et al.* (2005), Takao *et al.* (2009) and Liu *et al.* (2010 and 2012) stated that human NEIL3 has a putative nuclear localization signal (NLS) motif. However, Liu *et al.* (2010 and 2012) and Takao *et al.* (2009) did not mention any exact amino acid position while Torisu *et al.* (2005) only mention the position between amino acids 463 and 470 (Figure 27) but without stating a reference. Furthermore, the existence of an NLS could not be confirmed; neither via BLAST (NCBI; Figure 22) nor by further bioinformatical research via the European Bioinformatics Institute webpage (http://www.ebi.ac.uk; Figure 23) nor GeneCards (http://www.genecards.org) nor UniPort (http://www.uniprot.org/). However, the NLS in hNEIL3 was initially shown on NCBI – Conserved domains in 2008 (personal observation). Furthermore, Morland *et al.* (2002) did show via fluorescence experiments in living HeLa S3 cells that NEIL3 is located to nuclei after translation

and that NEIL3 contains a putative NLS at amino acid position 462-469 predicted by the PSORTII algorithm.

GRF-zinc finger motifs in NEIL3

Zinc finger (Znf) domains are relatively small protein motifs that allow the protein to bind DNA, RNA, other proteins or lipid substrates (Hall 2005; Matthews & Sunde 2002). How the protein binds to a particular sequence of DNA depends on the amino acid sequence of the Znf motif. The Znf domains can be present in clusters, where the Znf can have different binding specificities. Because of the many different types of Znf motifs with different sequences resulting in different structures, the functions also vary. For example, they can function in zinc sensing, chromatin remodelling, gene transcription and protein folding (Laity *et al.,* 2001). Although there is no recent study which characterizes the zinc finger domains in NEIL3, another study by Das *et al.* (2004) confirmed that NEIL2 has a zinc finger domain crucial for its structure and enzyme activity. This information about zinc finger domains, leads to the conclusion, that it is necessary to express NEIL3 in full-length to obtain its correct structural integrity and enzyme activity. This is confirmed by the recent study of Liu *et al.* (2010) who showed that full-length mouse NEIL3 has a DNA glycosylase activity *in vitro* while other groups expressed NEIL3 to a maximum amino acid length of 300 and were not able to detect DNA glycosylase activity (Krokeide *et al.,* 2009; Takao *et al.,* 2009). NEIL3 contains two additional zinc finger motifs at the C-terminal end which were not expressed in the truncated versions of Krokeide *et al.* (2009) and Takao *et al.* (2009) and are not present in other Nei/Fpg homologs, but could be essential for NEIL3 to interact with the correct DNA substrates or with other proteins (Figure 27; Figure 105).

A BLAST analysis to search for conserved domains in hNEIL3 revealed conservation of these domains in the C-terminus of hNEIL3 between amino acid position 813 and 943 (Figure 22). The duplicated GRF-zinc finger motif in NEIL3 (Figure 27 and Figure 105) is also conserved in the human APE2 and TopoIIIα.

TopoIIIα contains two GRF zinc finger domains, one at amino acid position 811-852 and one at amino acid position 895-939 (Figure 24). Further BLAST results showed a correlation between the hNEIL3 C-terminus and APE2 at amino acid position 242-291, which includes a putative AP binding site, and amino acid position 466-515 which includes a GRF zinc finger domain (Figure 25).

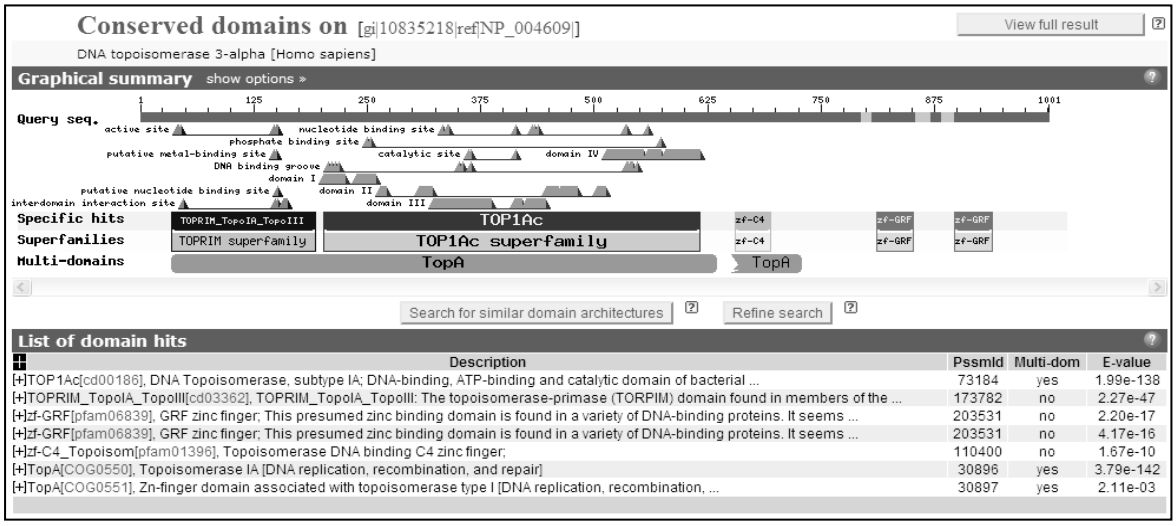

Figure 24: Conserved domains in human TopoIIIα.

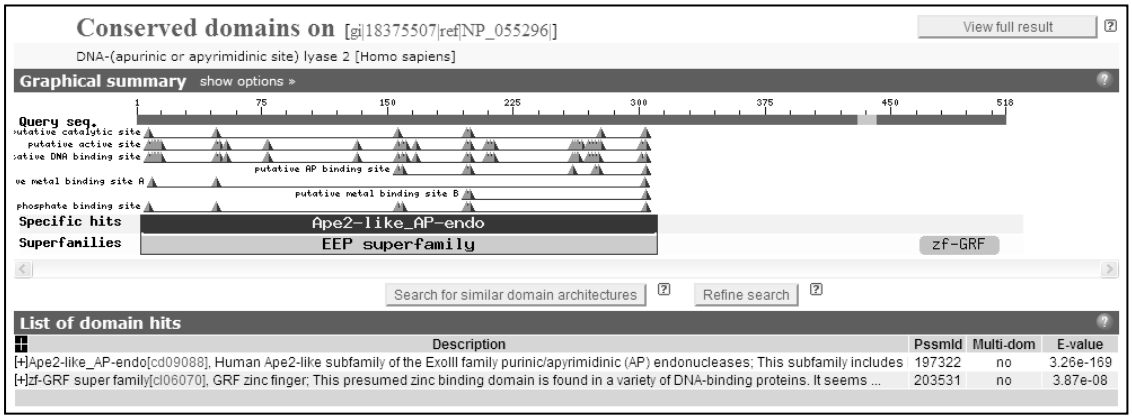

Figure 25: Conserved domains in human APE2.

RanBP zinc finger motif

Between amino acid position 317 and 345 is a conserved, putative Ras-related nuclear protein binding protein (RanBP) zinc finger motif, in this case from RanBP2 (also known as Nup-358). RanBP1 can diffuse into the nucleus due to its small size (23 kDa) and as it also carries an N-terminal nuclear export sequence it is actively transported back to the cytoplasm (Seewald *et al.,* 2003). RanBP2 on the other hand, is a large protein (358 kDa) that is located in the nuclear pore complex and is known to interact with various protein partners. However, its zinc fingers are known to bind to RanGDP, another protein that is needed for an active transport of cargo into the nucleus where it is transformed to RanGTP that acts as a nuclear export protein. Thus, as already suggested by Morland *et al.* (2002) this conserved RanBP zinc finger motif in NEIL3 might play a role in its nuclear transport.

Fpg-like zinc finger motif

There is a highly conserved Fpg-like zinc finger domain at amino acid position 247 – 281 (KVYKRPNCGQCHCRITVCRFGDNNRMTYFCPHCQK; Figure 23). This zinc finger motif acts in Fpg as a DNA binding motif and might also play an important role in the ability of NEIL3 to interact correctly with DNA structures to fulfil its specific biological functions (Tchou *et al.*, 1993).

Unique domain in hNEIL3

All NEIL3 proteins identified so far contain a highly conserved domain at amino acid position 362 - 403 (LMKYPCNTFGKPHTEVKINRKTAFGTTTLVLTDFSNKSSTL) (Figure 26). However, to date no biological role has been linked to this domain and it is not found in any other of the Nei homologs (Krokeide *et al.,* 2009).

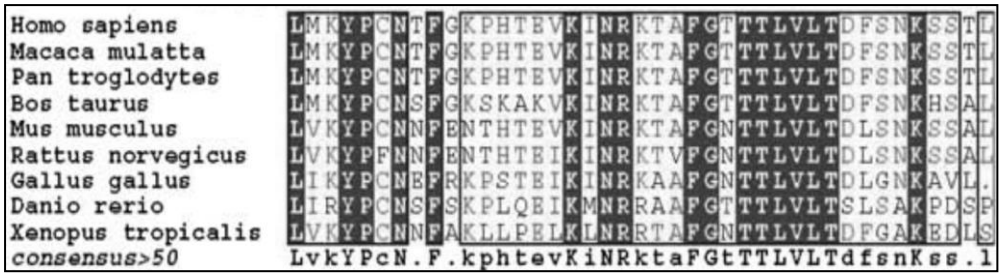

Figure 26: Unique motif on NEIL3 found to be highly conserved amongst several species. (Image taken from Krokeide *et al.,* 2009).

Conserved moieties in NEIL proteins

The Glu3 moiety, essential for the DNA glycosylase activity of the *E. coli* Nei and Fpg (Burgess *et al.,* 2002, Lavrukhin *et al.,* 2000), is conserved in all three NEIL proteins. Furthermore, site directed mutagenesis studies have shown that the Glu3 residue plays an important role in the activity of NEIL1 and NEIL2 (Bandaru *et al.,* 2002). All three NEIL proteins also contain a lysine residue (Lys55 in NEIL1, Lys51 in NEIL2, Lys82 in NEIL3) that corresponds to the Lys52 and Lys56 residues in Nei and Fpg, respectively. These motifs in Nei and Fpg are necessary to coordinate the 5′P group of the damaged deoxynucleotide (Zharkov *et al.,* 2003). Gly4 is preserved in all NEIL proteins and in *E. coli* Nei but not in Fpg where leucine is substituted. The Gly4 residues in the NEIL proteins and Nei and the Leu4 residue in Fpg are thought to be part of the active site (Pro2 and Glu3) of these proteins (Zharkov & Grollman, 2002).

Predicted structure of NEIL3

NEIL3 contains a H2TH domain which is a typical motif for all proteins from the Fpg/Nei superfamily including all NEIL proteins. Liu *et al.* (2013) was the first group to solve the crystal structure of a truncated version of mouse NEIL3 (N-terminus with 324 amino acids). They discovered that unlike the bacterial Fpg, NEIL3 has no αF-β9/10 loop that can hold 8-oxoG. This would explain why, to date, no excision activity on 8oxo-G for NEIL3 has been observed. Furthermore, NEIL3 not only lacks

two of three motifs essential for the stabilisation of the DNA strand opposite the base damage, but even contains negatively charged residues that do not allow proper binding of the phosphate backbone of the undamaged, template strand. This fact correlates well with the discovery that NEIL3 prefers ssDNA substrates (Liu *et al.* 2010, 2012 and 2013).

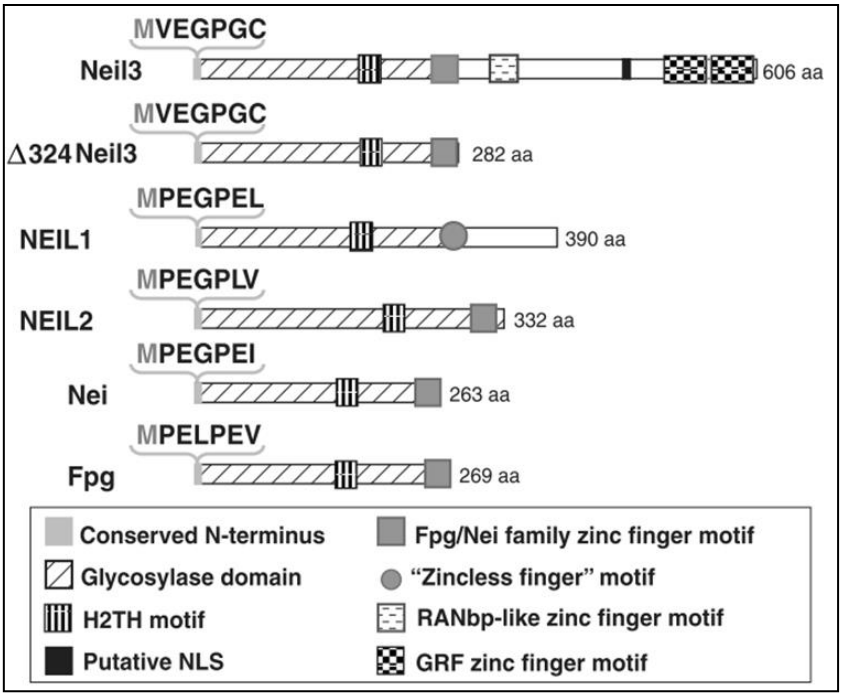

Figure 27: Neil3: full-length mNEIL3; Δ324Neil3: truncated version of mNEIL3 containing the conserved DNA glycosylase domain; NEIL1: human NEIL1; NEIL2: human NEIL2; Nei: *E. coli* Nei (endonuclease VIII); Fpg: *E. coli* Fpg (MutM). The schematic representation of mouse NEIL3 in this diagram is the same as for human NEIL3 including the first amino acids shown above the N-terminal end (Figure 105). (Image adapted from Liu *et al.*, 2010).

Expression patterns of NEIL3

NEIL3 is mainly expressed in haematopoietic tissues, thymus and testes (Morland *et al.,* 2002; Torisu *et al.,* 2005; Takao *et al.,* 2009; Figure 28). Although Takao *et al*. (2009) did not find expression of NEIL3 in adult mouse brain cells, Hildestrand *et al.* (2009) found expression during embryonic mouse brain development where expression levels were highest during the E12.5 stage (Figure 29).

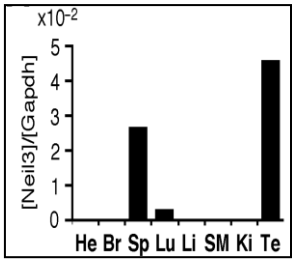

Figure 28: Tissue expression patterns of human NEIL3 relative to GAPDH. He, heart; Br, brain; Sp, spleen; Lu, lung; Li, liver; SM, skeletal muscle; Ki, kidney; Te, testis. (Image taken from Takao *et al.,* 2009).

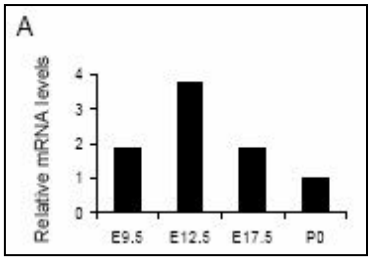

Figure 29: Quantified mRNA levels of NEIL3 normalized to GAPDH. The mRNA was obtained from mouse brain extracts at four different developmental stages. (Image taken from Hildestrand *et al.*, 2009).

Further expression patterns have been published in several tumour and healthy tissues and in macrophages and activated T-lymphocytes where the highest expression levels were found in activated CD4-positive T-lymphocytes (Zhou *et al.,* 2008, Figure 30).

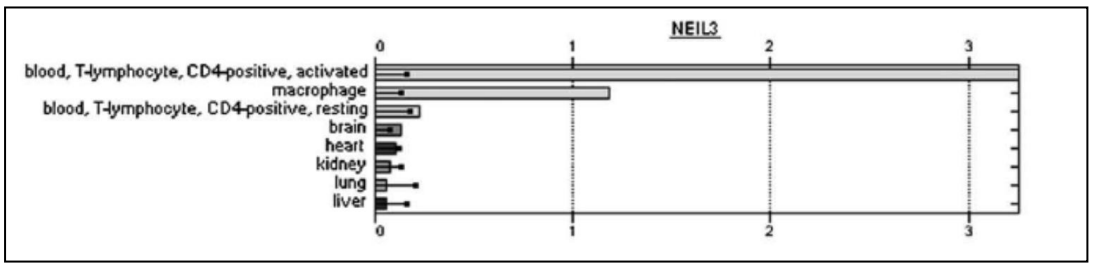

Figure 30: Cell and tissue expression patterns of human NEIL3. (Image taken from Zhou *et al.*, 2008).

Furthermore, it has been shown that the expression levels of NEIL3 are cell cycle dependent. The expression of NEIL3 is upregulated in cells that leave the G_0 phase

and start dividing. This, and the fact that the expression pattern of NEIL3 is related to that of FEN1, a protein active on replication forks during S phase, which might be an indicator for the activity of NEIL3 in replication associated DNA repair (Neurauter *et al.,* 2012). Metastatic cancer cells also show a high level of NEIL3 expression, although this is not the only protein involved in BER to be upregulated (Figure 31) (Kauffmann *et al.*, 2008).

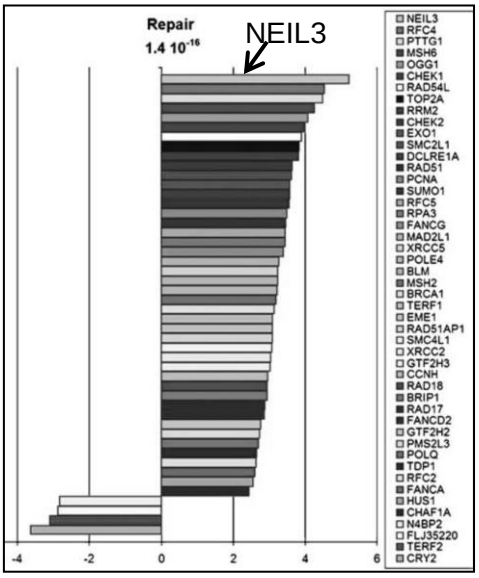

Figure 31: Standardized mean differences of log(ratio) between tumours that will metastzie within 4 years and tumours that will not for genes involved in DNA repair. (Image taken from Kauffmann *et al.*, 2008).

In general it can be said that expression levels of NEIL3 are elevated in tumour cells compared to normal cells except for testes (Figure 32) (Hildestrand *et al.*, 2009).

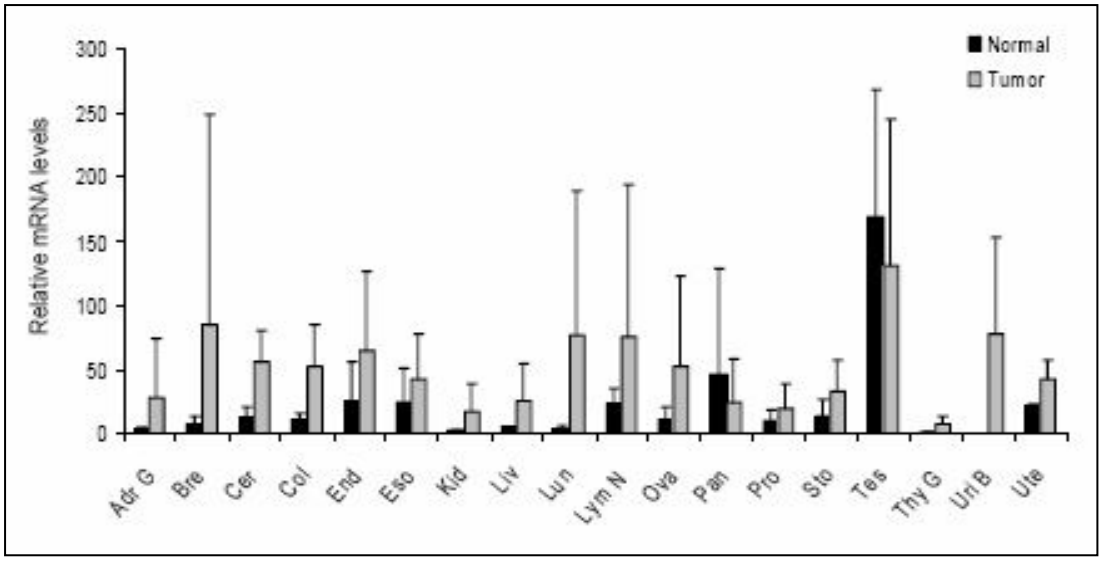

Figure 32: This image of a transcript profile of mNEIL3 was taken from Hildestrand *et al*. (2009). Amounts were normalized to β-actin and mNEIL3 mRNA levels are shown relative to the stomach cancer sample which showed the lowest expression level of mNEIL3 Abbreviations: Adr G, adrenal gland; Bre, breast; Cer, cervix; Col, colon; End, endometrium; Eso, esophagus, Kid, kidney; Liv, liver; Lun, lung; Lym N, lymph node; Ova, ovary; Pan, pancreas; Pro, prostate; Sto, stomach; Tes, testis; Thy G, thyroid gland; Uri B, urinary bladder; Ute, uterus.

DNA glycosylase activity of NEIL3

The ability of NEIL3 to act as a DNA glycosylase has now been confirmed by several groups. The first indication came from Morland *et al.* (2002) who observed the removal of Me-FapyG lesions from [^{3}H]-methyl-faPy-poly(dG:dC) by full-length mouse NEIL3 expressed in a baculovirus Sf9 insect cell system. However, no active NEIL3 was recovered from expression in *E. coli* or in a cell-free system. Hence, the group assumed that posttranslational modifications might be necessary for the DNA glycosylase activity of NEIL3 and this could be one explanation for activity only being observed in mammalian and insect cells Morland *et al.* (2002). Further evidence in support of this is indicated from the work of Takao *et al.* (2009) who could not confirm a DNA glycosylase activity of NEIL3 expressed in *E. coli*. On the other hand Krokeide *et al*. (2009) had no problem expressing full-length NEIL3 in a cell-free system in the presence of [^{35}S] methionine. However, although the translated protein was confirmed via western blotting no activity on 8-oxoG or Me-Fapy lesions could be

detected. Furthermore, they tried to express full-length NEIL3 in and a truncated version in *E. coli* and although expression was successful no activity on dsDNA and ssDNA containing 8-oxoG, 5-ohU, Me-Fapy or abasic sites was observed. However, more recently both full length mNEIL3 and a truncated version of hNEIL3 have been found to act as DNA glycosylases on oxidized purines such as Sp, Gh, FapyA, FapyG and the oxidized pyrimidine Tg on ssDNA and dsDNA (Liu *et al.*, 2010, 2012). Subsequently it was shown that overall DNA glycosylase activity in NEIL3$^{-/-}$ mouse tissue extracts from brain, heart, thymus and spleen tissues was nearly 2 fold lower on Sp or Gh ssDNA substrates compared to dsDNA substrates and to extracts from NEIL3$^{+/+}$. This suggests that NEIL3 is the main DNA glycosylase in mammalian cells for the excision of Sp and Gh from ssDNA (Rolseth *et al*., 2013). Thus, in general the activity of mNEIL3 might be more similar to that of NEIL1 as it repairs oxidized purines and pyrimidines, preferentially from ssDNA.

Liu *et al.* (2010) expressed the DNA glycosylase domain of a truncated version of mNEIL3 in an *E. coli* mutant. This mutant lacked Fpg, Nei, and MutY glycosylase activities and interestingly, the truncated version of mNEIL3 decreased the level of FapyG lesions about two fold more than a control expressing NEIL1. The fact that Liu *et al.* (2010) found that mNEIL3 prefers lesions in single-stranded DNA, fork and bubble substrates, might be an indicator that mNEIL3 is active during DNA replication similar to NEIL1.

AP lyase activity of NEIL3

Takao *et al.* (2009) reported that mNEIL3 has an AP lyase activity which is specific for ssDNA. This group used a truncated version of mNEIL3 (amino acids 1-290) that only contained the conserved DNA glycosylase domain and expressed it in *E. coli*. Therefore, they concluded that the C-terminal domain could be responsible for the

regulation of enzyme activity or function to direct the appropriate repair *in vivo* via interactions with other proteins (Takao *et al.,* 2009). Subsequently, Liu *et al.* (2010) determined that mNEIL3 acts as bifunctional DNA glycosylase under *in vitro* conditions.

NEIL3 and its role in human immunodeficiency virus integration

Recent siRNA studies have revealed that BER proteins play an important role in retroviral integration into the host genome (Espeseth *et al.*, 2011a; Yoder *et al.,* 2011; Zhou *et al.,* 2008). Zhou *et al.* (2008) used a siRNA screen to identify six genes coding for essential host factors for HIV DNA integration: AKT, PRKAA1, CD97, BMP2K, SERPINB6 and NEIL3. The protein kinases AKT1 and PRKAA1 are important proteins involved in many cellular processes including glucose transport, glycolysis, fatty acid and protein synthesis. They might support HIV replication and integration by their capability of inhibiting cell apoptosis. Like SERPINB6 and NEIL3 the protein kinase BMP2K, involved in the regulation of bone mineralization, is also able to aid HIV replication and integration although their functional role remains unclear and is under investigation. CD97 on the other hand seems to play a role after HIV was integrated which needs to be determined (Zhou *et al.,* 2008).

Espeseth *et al.* (2011a) made additional screens using siRNA targeting other essential BER proteins and discovered that knockdown of NEIL3 decreased HIV infection efficiency by 70%. After reverse transcription, the viral DNA is located to the nucleus and integrated into the chromosomal DNA. While HIV reverse transcription and the localization into the nucleus seem to be unaffected in cells lacking BER proteins, the integration into the host chromosome is significantly decreased (Yoder *et al.,* 2011). Furthermore, Espeseth *et al.* (2011a) showed that HeLa P4/P5 cells

transfected with siRNAs targeting MUTYH, NTH1 or Polβ also decreased HIV integration up to 70% compared to control cells transfected with luciferase siRNA.

Before Zhou *et al.* (2008) published their results instead of BER it was NHEJ that was frequently linked to HIV replication (Daniel *et al.,* 2004, Kilzer *et al.,* 2003, Li *et al.,* 2001). However, only one of the proteins found in the siRNA screening carried out by Espeseth *et al.* (2011a) was related to NHEJ while 23% of the hits were linked to BER. Furthermore, other groups have already shown, that the HIV-1 transactivator of transcription (Tat) protein which is responsible for efficient viral transcription (Debaisieux *et al.*, 2012), induces expression of BER proteins such as Polβ (Srivastava *et al.,* 2001) and OGG1 (Imai *et al.,* 2005). As large protein complexes are very important for the efficiency of BER, it is likely that the knockdown of essential proteins involved in BER such as the scaffold protein XRCC1, decreases the integration efficiency of HIV due the loss of functionality of other proteins that rely on XRCC1.

NEIL3 and the brain

While NEIL1, NEIL2, OGG1 and NTH1 have been found to show similar expression levels regardless of the age of the brain, NEIL3 protein was only observed during embryonal brain development and then only in regions that contain stem cells such the subventricular zone, the rostral migratory stream, and the hilar region of the hippocampal formation (Rolseth *et al.,* 2008). Sejersted *et al.* (2011) confirmed these findings from another perspective. They investigated the expression levels of NEIL3 in damaged mouse brains and examined an increase in NEIL3 during regeneration of damaged brain regions leading to the conclusion that expression of NEIL3 is triggered in rapidly proliferating cells.

Regnell *et al.* (2012) demonstrated that in neural/progenitor stem cells lacking NEIL3, the proliferation rate was reduced resulting in learning and memory deficits of the tested mice as well as decreased anxiety-like behaviour. Although there was no obvious difference between brain phenotypes of $Neil3^{+/+}$ and $Neil3^{-/-}$ mice, Rolseth *et al.* (2013) confirmed the results by Regnell *et al.* 2012. They found a reduced self-renewal capacity of neural/progenitor stem cells in $Neil3^{-/-}$ mice while the differentiation capacity was not affected.

Other proteins involved in BER

APE1 is the mammalian ortholog of *E. coli* Xth (exonuclease III) and plays a role as a transcriptional co-factor, as a suppressor of ROS via a redox site and in DNA repair where it incises AP sites (Tell *et al.*, 2005). More recently it was found that APE1 also plays a major role in neuroprotection when its expression is induced by PACAP and its downstream mediators CREB and ATF2 (Stetler *et al.,* 2010). The AP site substrates for APE1 are generated spontaneously or by monofunctional DNA glycosylases. APE1 cuts the deoxyribose backbone which results in a 3′OH and a 5′dRP moiety. Due to their β AP-lyase activity, OGG1 and NTH1 leave a 3′ PUA group after they cut an AP site. This blocking residue is removed by the 3′ phosodiesterase activity of APE1 in preparation for the next step in BER, the gap filling by Polβ. In addition, APE1 acts as a stimulator for OGG1 by releasing it from the AP site and therefore increasing its turnover (Hill *et al.,* 2001).

It is known that XRCC1 is an important protein involved in the repair of indirect SSBs (caused by BER) and direct SSBs (caused by DNA damaging agents). Although it has no enzymatic activity itself, it is an important scaffold protein for other DNA repair proteins. It stabilizes protein complexes involved in BER and is usually found in

complex with DNA ligase III (Vidal *et al.*, 2001b). Which proteins these are and how XRCC1 interacts will be discussed in Section 2.3.6 in more detail.

PNK is a downstream protein for bifunctional DNA glycosylases with β/δ AP lyase activity such as NEIL1 and NEIL2. After excising an oxidized base from DNA bifunctional DNA glycosylases cut the resulting AP site which leaves a 3′P blocking residue. This phosphate is then removed by PNK generating a 3′OH group that enables Polβ to fill the resulting gap.

FEN1 is active during DNA replication where it processes the 5′ ends of the Okazaki fragments via its ribonuclease activity on displaced RNA-DNA primers generated during discontinuous DNA replication on the lagging DNA strand (Neurauter *et al.*, 2012; Turchi *et al.*, 1994; Bambara *et al.*, 1997). FEN1 is also essential for the repair of reduced AP sites that cannot be processed by β-elemination or occurred during long-patch BER (Klungland *et al.,* 1997).

PCNA plays an important role as a sliding clamp in DNA replication and repair. In long patch BER, PCNA acts as a DNA polymerase processivity factor for Polδ which thereby stays attached to DNA (McConnell *et al.*, 1993). Interestingly, its structure resembles that of the 9-1-1 complex, containing Rad9, Rad1 and Hus1 which is involved in the ATR-mediated detection of DNA damage in yeast (Section 2.1) (Li & Zou, 2005; Dou, *et al.,* 2008).

Poly(ADP-ribose)polymerase 1 (PARP-1) is involved in SSB repair and catalyses the attachment of poly(ADP-ribose) polymers to itself as well as to histones, nuclear proteins, DNA repair proteins, transcription factors and chromatin modulators using NAD^+ as a donor of ADP-ribose units (Hooten *et al.*, 2011).

Polβ is an essential protein in SP BER where it can process the 3′dRP overhangs produced by APE1 and then resynthesizes the missing nucleoside. Polδ/ε on the other hand are involved in DNA synthesis of the repair products of NER but also of the LP BER pathway.

RPA stimulates LP BER. It can enhance functionality of FEN1 and unwinds dsDNA in preparation for BER (DeMott *et al*., 1998). LigIIIα seals the phosphate backbone by synthesising the phosphodiester bonds between the 3′OH and 5′P groups of the repaired DNA in the last step of SP and LigI in LP BER (Section 2.3.5) (Lehman, 1974; Chen *et al.,* 1995).

2.3.6 Reported protein interactions with mammalian BER proteins

Table 1 and Figure 33 summarize proteins related to BER known to interact with each other during different stages of the pathway. It has been shown that PARP-1 binds directly to BER proteins such as OGG1 (Hooten *et al.,* 2011) and NEIL1 (Hooten *et al.,* 2012) through its BRCA1 C-terminal domain. This domain is comprised of around 100 amino acids and is conserved in several proteins that play a role in DNA repair, recombination and cell cycle control. The BRCA1 C-terminal domain is known to be essential for various protein-protein interactions and as a phospho-protein binding domain (Zhang *et al.,* 1998, Yu *et al.*, 2003).

XRCC1 interacts with the DNA glycosylases OGG1 (Marsin *et al.,* 2003), NEIL1 (Wiederhold *et al.,* 2004) and NEIL2 (Das *et al.,* 2006) but also with other BER proteins including APE1 (Vidal *et al.,* 2001b), LigIIIα and Polβ (Caldecott *et al.*, 1995; Whitehouse *et al.,* 2001), PARP-1 (Leppard *et al.*, 2003; Caldecott, Aoufouchi, Johnson, & Shall, 1996), PNK (Whitehouse *et al.,* 2001, Wiederhold *et al.,* 2004) and

PCNA (Fan *et al.*, 2004). The interaction with PARP-1 and DNA glycosylases indicates the involvement of XRCC1 in the SSB repair process and BER pathway. However, PARP-1 might also play a role in BER in searching for indirect SSBs caused by DNA glycosylases. Once PARP-1 recognized a SSB it binds to XRCC1. XRCC1 on the other hand acts as a stabilizing protein for LigIIIα necessary to seal the SSB. In addition XRCC1 can recruit further proteins such as PNK, Polβ and APE1 in order to prepare the gap for ligation (Leppard *et al.,* 2003).

Table 1: Summary of known protein interactions of important BER proteins.

DNA-Glycosylases											
NTH1					APE[3]					YB1[24]	
OGG1				XRCC1[27]	APE[1, 19]			PARP-1[31]		PKC[28]	
NEIL1	LIG3α[20]	Polβ[20]	PNK[20]	XRCC1[20]	CSB[25]	PCNA[22]	FEN-1[17]	PARP-1[30]	OGG1[18]	WRN[26]	
NEIL2	LIG3α[21]	Polβ[21]	PNK[21]	XRCC1[21]						YB1[23]	
MUTYH					APE[2,4,13]	PCNA[13]				RPA[13]	
UNG						PCNA[14]				RPA[14]	
Other BER proteins											
XRCC1	LIG3α[7,9,16]	NEIL1 [20]	NEIL2[21]	PNK[9, 20]	APE[8]	PCNA[15]	FEN-1[12]	PARP-1[11,16]	OGG1[27]	Polβ[9]	APTX[10]
LIG3α		NEIL1[22]	NEIL2[21]	XRCC1[7,9]				PARP-1[11]			
Polβ		NEIL1[22]	NEIL2[21]	XRCC1[9]							
PARP-1	LIG3α[11]	NEIL1[30]		XRCC1[11, 16]					OGG1[31]		
PCNA		NEIL1[22]		XRCC1[15]							
PNK		NEIL1[22]	NEIL2[21]	XRCC1[9, 20]							

APE1= apurinic/apyrimidinic (abasic) endonuclease; **YB1**= Y box binding protein 1; **PKC**= protein kinase C; **XRCC1**= X-ray repair complementing defective repair in Chinese hamster cells 1; **APTX**= aprataxin, forkhead-associated domain histidine triad-like protein; **PNK**= polynucleotide kinase 3′-phosphatase; **Polβ**= human DNA polymerase β; **LIG3α**= human ligase 3 alpha; **FEN-1**= flap structure-specific endonuclease; **PCNA**= proliferating cell nuclear antigen; **WRN**= Werner syndrome ATP-dependent helicase; **CSB**= Cockayne syndrome B protein; **RPA**= replication protein A; **NTH1**= endonuclease III-like 1 (E. coli); **OGG1**= 8-oxoguanine DNA glycosylase; **NEIL1**= nei endonuclease VIII-like 1 (E. coli); **NEIL2**= nei endonuclease VIII-like 2 (E. coli); **MUTYH**= mutY homolog (E. coli); **UNG**= uracil-DNA glycosylase; **PARP-1**= poly(ADP-ribose) polymerase 1.

[1] Vidal *et al.* (2001a); [2] Yang *et al.*(2001); [3] Marenstein *et al.* (2003); [4] Xia *et al.* (2005); [5] Kavli *et al.*(2002); [7] Caldecott *et al.* (1995); [8] Vidal *et al.* (2001b); [9] Whitehouse *et al.* (2001); [10] Clements *et al.* (2004); [11] Leppard *et al.* (2003); [12] Klungland & Lindahl, (1997); [13] Parker *et al.* (2001); [14] Otterlei *et al.* (1999); [15] Fan *et al.* (2004); [16] Caldecott *et al.* (1996); [17] Hegde *et al.* (2008a); [18] Mokkapati *et al.* (2004); [19] Sidorenkoa *et al.* (2008); [20] Wiederhold *et al.* (2004); [21] Das *et al.* (2006); [22] Dou *et al.* (2008); [23] Das *et al.* (2007a); [24] Marenstein *et al.* (2001); [25] Muftuoglu *et al.* (2009); [26] Das *et al.* (2007b); [27] Marsin *et al.* (2003); [28] Dantzer *et al.* (2002); [29] Hazra *et al.* (2002a); [30]Hooten *et al.* (2012); [31]Hooten *et al.* (2011).

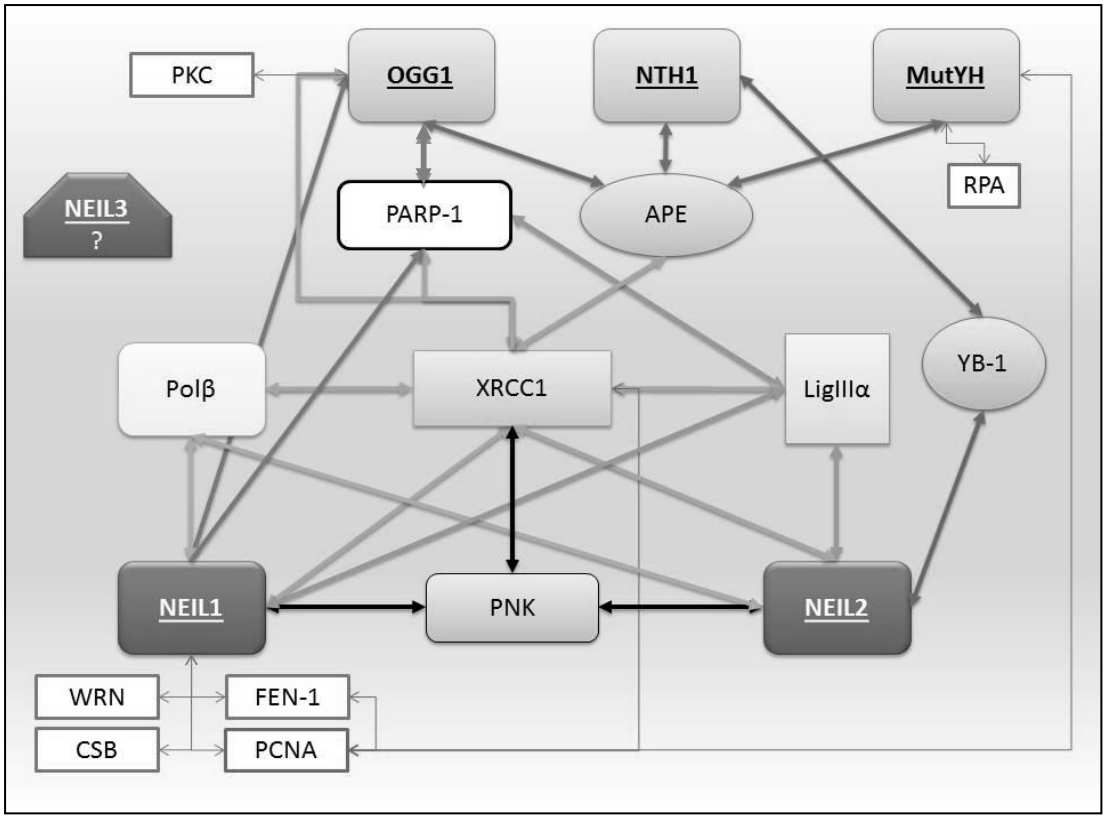

Figure 33: Known interactions between several BER proteins (references see Table 1).

2.4 Theoretical background to methods used in this thesis

2.4.1 Yeast Two-Hybrid assay

To investigate the biological role of hNEIL3 a yeast two-hybrid (Y2H) assay, a system that allows the examination of protein-protein interactions was carried out. In Y2H, the chosen 'bait' protein (hNEIL3) is expressed in the *Saccharomyces cerevisae* strain EGY48 fused to the DNA-binding domain of a bipartite transcription factor (LexA; Figure 34), while the second protein (the prey) is expressed from a cDNA library, bound to the activation domain (B42; Figure 34) which, in combination with LexA activates transcription. Neither LexA nor B42 alone are able to activate the transcription; only if they are in close proximity due to interaction of the bait protein with a prey protein, will transcription of a downstream reporter gene occur. In this project the LexA-operator is responsible for the expression of two genes; *Leu2*, which

is involved in leucine biosynthesis and *LacZ* (Figure 34). The use of two reporter systems allows a double selection, which decreases the number of false negatives (Muelhardt, 2009).

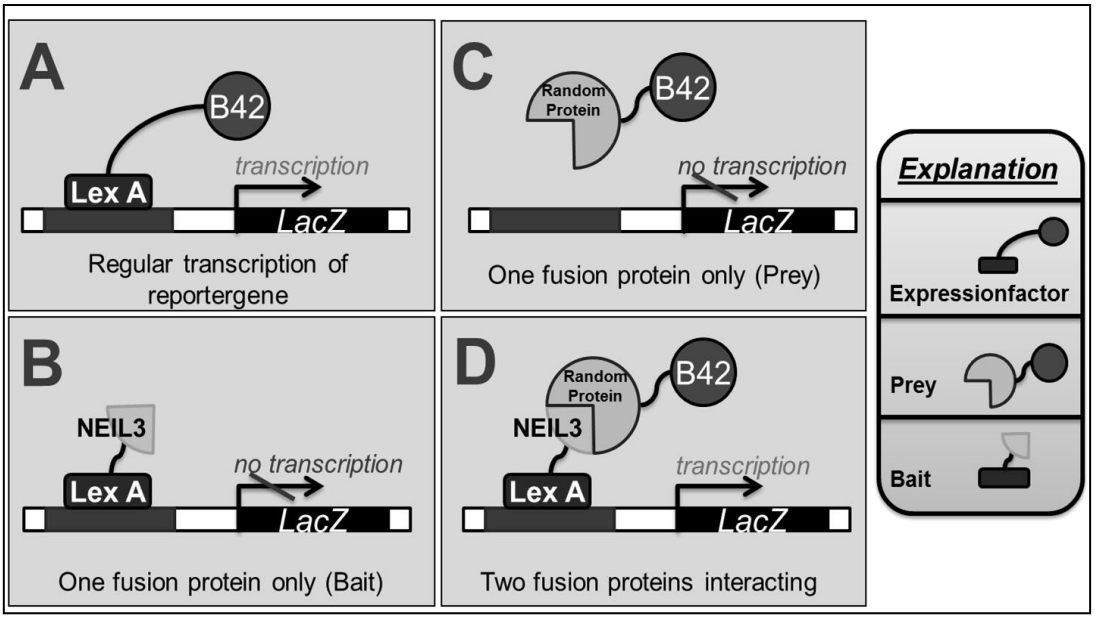

Figure 34: Theory of the yeast two-hybrid assay used in this project. Here *LacZ* is shown as an example for a reporter gene.

Molecular cloning of hNEIL3 cDNA into two bait vectors, pEG202 and pEG202-NLS (Appendix, Figure 98 and Figure 99) was necessary to carry out the Y2H assay. The vectors contain an ampicillin resistance gene (AmpR) and there is a LexA region before the multiple cloning site. This region allows expression of a fusion protein featuring LexA as the DNA-binding domain and hNEIL3 as the bait protein (Bait in Figure 34; Lewis *et al.*, 1994). The expression of this fusion protein is controlled by the alcohol dehydrogenase (ADH) promoter and ADH terminator region (Appendix Figure 98 and Figure 99) which starts and stops the transcription in yeast. Furthermore, Figure 99 shows that pEG202-NLS contains a NLS in the multiple cloning site that ensures the expressed bait fusion protein will be located into the nucleus.

As recent protein interaction studies with NEIL1 and NEIL2 carried out by Wiederhold *et al.* (2004) and Das *et al.*, (2006) showed that there are genuine interactions with both human Polβ and LigIIIα the Y2H assay was also used to estimate if LigIIIα and Polβ is also interacting with NEIL3. The fact that nothing was published regarding interaction studies with NEIL3 might be due to problems in expressing NEIL3 in full length. However, as it was possible in this project to express full length NEIL3 fused to LexA in the Y2H system it was also tested for interaction with these two proteins using Y2H.

2.4.2 Protein overexpression in Pichia pastoris

Although *E. coli* is a commonly used expression system, overexpression of recombinant full length hNEIL3 in *E. coli* has not been successful (Section 2.3.5.2.3). Therefore, it was decided to use methylotrophic yeast, *P. pastoris*, which are commonly used for the expression of recombinant proteins (Daly & Hearn, 2005) and thus is more likely to process the nascent polypeptide chain of hNEIL3 correctly following translation. Posttranslational modifications may be essential to study the role of NEIL3 *in vivo*. Furthermore, higher yields of protein can be obtained than with other yeast strains such as *S. cerevisae* and *P. pastoris* is amenable for use in large scale fermentation. In this project pGAPZαA (Invitrogen) was the overexpression vector of choice. This vector is designed for high-level protein expression in *P. Pastoris* and employs a glyceraldehyde-3-phosphate dehydrogenase (GAPDH) promoter for constitutive expression of the protein of interest and therefore no manual induction of gene expression is needed by adding methanol. Furthermore, this vector contains an α-factor secretion signal sequence that is fused to the N-terminal of the expressed protein. A *myc* epitope and a polyhistidine tag (6XHis) are fused to the C-terminal end of the expressed protein, which simplifies protein

purification and identification with tag-specific antibodies. Following site-specific linearization with *Avr*II and electroporation into *P. pastoris*, the plasmid DNA integrates into the yeast genome via homologous recombination at the GAPDH promoter locus. In this project cloning of the hNEIL3 cDNA sequence and truncated versions into the pGAPZαA vector and subsequent integration it into the yeast genome was successfully performed.

3 Materials

3.1 Media preparation for bacterial methods

Lysogeny broth (LB)-broth was prepared at a concentration of 8 g LB-broth powder (Sigma-Aldrich) in 400 ml dH_2O and used for liquid cultures. LB-agar was prepared by adding 14 g of LB-agar powder (Sigma-Aldrich) to 400 ml dH_2O. The mixtures were autoclaved at 121°C for 20 min to dissolve the powder and sterilise the medium. After the LB-agar had cooled to ~50°C, carbenicillin or kanamycin sulphate was added to obtain an antibiotic concentration of 50 µg/ml and plates were poured and allowed solidify before use, or stored at 4°C. For liquid cultures, carbenicillin or kanamycin sulphate was added to LB-broth to a final conc. 50 µg/ml just before inoculation.

3.2 X-Gal and IPTG Preparation

X-Gal stock solution:

50 mg/ml X-Gal: 25 mg X-Gal powder was dissolved in 500 µl of N,N′-dimethylformamide and stored at -20°C.

IPTG stock solution:

100 mM IPTG: 12 mg of IPTG powder was dissolved in 500 µl dH_2O, filter sterilized and stored at -20°C.

Treatment of LB-Agar plates (Carb.) with X-Gal/IPTG:

100 µl (100 mM) IPTG and 20 µl X-Gal (50 mg/ml) were spread evenly on each LB-agar plate.

3.3 Ethylenediaminetetraacetic acid (EDTA) stock solution

To obtain a 0.5 M ethylenediaminetetraacetic acid (EDTA) stock solution, 18.61 g EDTA-disodium-salt was dissolved in 70 ml of dH_2O and the pH adjusted to pH 8.0 by adding NaOH and adjusted with dH_2O to a total volume of 100 ml.

3.4 TE-Buffer (Tris-EDTA-Buffer)

To prepare Tris/EDTA (TE) buffer, 10 ml of 1 M Tris-HCl pH 7.5 and 2 ml of 500 mM EDTA were mixed and pH was adjusted to 8.0 with NaOH.

3.5 5X TBE

5X Tris/Borate/EDTA (TBE) stock solution: 54 g of Tris base (Trizma base, Sigma-Aldrich) and 27.5 g of boric acid was dissolved in 900 ml of dH_2O. 20 ml of 0.5 M (4.65 g) EDTA was added and the solution was adjusted with dH_2O to a final volume of 1 L.

3.6 Loading buffer for agarose gel electrophoresis (Loading dye)

Twenty-five milligrams of bromophenol blue, 4 g sucrose and 2.4 ml of 0.5 M EDTA were mixed and made up to 10 ml with dH_2O.

3.7 Buffers for SDS-PAGE

3.7.1 Acrylamide stock solution

The premade acrylamide stock solution (Protogel, National Diagnostics) contained 30% acrylamide and 0.8% bis-acrylamide.

3.7.2 "Lower Tris" (4x stock solution)

To prepare 4x stock solution of lower Tris buffer, 1.5 M Tris-HCl pH 8.8, 0.4% (w/v) SDS, 18.17 g Tris base and 2 ml of 20% (w/v) SDS were added to 80 ml of dH_2O. Then, the pH was adjusted with HCl until pH 8.8 and dH_2O added to bring the solution up to 100 ml.

3.7.3 "Upper Tris" (4x stock solution)

To prepare 4x stock solution of upper Tris buffer, 0.5 M Tris-HCl pH 6.8, 0.4% (w/v) SDS, 6.06 g Tris base, 2 ml of 20% (w/v) SDS were added to 80 ml of dH_2O. Then, the pH was adjusted with HCl until pH 6.8 and dH_2O added to bring the solution up to 100 ml.

3.7.4 Separating gel (10 %)

For 12 ml of separating gel mix (enough for two mini gels, Labnet), 4 ml of Protogel (30% acryl, 0.8% bis), 3 ml of 4x Lower Tris (Section 3.7.2) and 5 ml of dH_2O were mixed. Just before pouring, 80 µl of 10% (w/v) APS (ammonium persulphate) and 8 µl TEMED (tetramethylethylendiamine, 0.10%) were added to catalyse polymerisation.

3.7.5 Stacking gel (5 %)

For 6 ml of stacking gel mix (enough for two mini gels, Labnet), 1 ml of Protogel (30% acryl, 0.8% bis), 1.5 ml of 4x Upper Tris (Section 3.7.3) and 3.5 ml of dH_2O were mixed. Just before pouring, 80 µl of 10% (w/v) APS and 8 µl TEMED (0.13%) were added to catalyse polymerisation.

3.7.6 SDS-running buffer (10x stock solution)

To prepare a 10x stock solution of SDS-running buffer, 15 g Tris base (final conc. 250 mM), 72 g glycine (final conc. 1.92 M), 5 g SDS (or 50 ml of 10% (w/v) SDS) were dissolved in a final volume of 500 ml of dH_2O.

3.7.7 SDS-running buffer (1x) – Bio-Rad

To prepare a 1x stock solution of SDS-running buffer, 50 ml of 10x Tris/glycine stock solution (Bio-Rad), 5 ml of 10% (w/v) SDS (0.1% (w/v) final conc.) and 445 ml dH_2O were mixed (enough to fill the Labnet tank) to give a final conc. of 25 mM Tris and 192 mM glycine.

3.7.8 SDS-PAGE sample buffer (5x stock solution)

Two millilitres of 100% glycerol (20% final conc.), 3ml of 1 M Tris-HCl pH 6.8 (300 mM final conc.), 5 ml of 20% (w/v) SDS (10% (w/v) final conc.), 0.386 g of DTT (0.25 M final conc.) and 5 mg bromophenol blue (0.05% (w/v) final conc.) were mixed together to obtain a 5x stock solution of SDS-PAGE Sample Buffer.

3.7.9 Coomassie blue staining solution

The stain was prepared by mixing 1.25 g Coomassie blue R250 (0.25% (w/v) final conc.), 200 ml methanol (40% (v/v) final conc.), 50 ml acetic acid (glacial, 10% (v/v) final conc.) and 250 ml dH_2O to obtain a final volume of 500 ml. The Coomassie stain was reused several times.

3.7.10 Destain solution

The destain solution was prepared by mixing 100 ml of methanol (20% (v/v) final conc.), 25 ml of acetic acid (glacial, 5% (v/v) final conc.) and 375 ml of dH_2O to obtain a final volume of 500 ml.

3.8 Buffers for Western Blotting

3.8.1 Western blot transfer buffer

The transfer buffer contained 6.05 g Tris base (25 mM final conc.), 28.8 g glycine (final conc. 192 mM), 400 ml methanol (20% (v/v) final conc.) and 1600 ml dH_2O and was stored at 4°C.

3.8.2 10x TBS

To prepare 500 ml of 10X TBS buffer, 30.25 g of Tris base and 43.8 g of NaCl was added to 450 ml of dH_2O. The pH adjusted to pH 7.5 with conc. HCl (~15 ml), made up to 500 ml with dH_2O and stored at 4°C.

3.8.3 TBS(T)

To prepare 500 ml of TBS(T), 50 ml of 10x TBS (50 mM Tris-HCl final conc.; 150 mM NaCl, Section 3.8.2) and 0.5 ml Tween-20 (0.1% (v/v) final conc.) was mixed, the volume made up to 500 ml with dH_2O and stored at room temperature.

3.8.4 5% blocking buffer

To prepare blocking buffer, 5% (w/v) non-fat milk (Marvel) was mixed with TBS(T) (Section 3.8.3).

3.8.5 Antibody dilution buffer

To prepare 0.5% blocking buffer, used as dilution buffer for antibodies, the 5% Blocking Buffer (Section 3.8.4) was diluted 1:10 with TBS(T) (Section 3.8.3).

3.9 Buffers and solutions for Y2H

3.9.1 10X TE

To prepare 10X TE, 50 ml of 1 M Tris-HCl pH 7.5 and 10 ml of 0.5 M EDTA pH 8.0 were added to 440 ml dH_2O, mixed and autoclaved.

3.9.2 10X LiOAc (Lithium acetate)

Fifty-one grams of lithium acetate (1 M final conc.) was made up to a total volume of 500 ml with dH_2O, mixed until dissolved and autoclaved.

3.9.3 50% PEG-3350

Two-hundred and fifty grams of polyethylene glycol-3350 were made up to a total volume of 500 ml with dH_2O, mixed until dissolved and autoclaved.

3.9.4 1x TE/LiOAc/H_2O

Just before use, 1 part 10x TE (Section 3.9.1), 1 part 10x LiOAc (Section 3.9.2) and 8 parts dH_2O were mixed together.

3.9.5 1x TE/LiOAc/PEG-3350

Just before use, 1 part 10x TE (Section 3.9.1), 1 part 10x LiOAc (Section 3.9.2) and 8 parts 50% PEG-3350 (Section 3.9.3) were mixed together.

3.9.6 Glucose/galactose/raffinose

To obtain 20% (w/v) glucose, 10 g of glucose was dissolved in 50 ml dH_2O.

To obtain 20% (w/v) galactose, 10 g of galactose was dissolved in 50 ml dH_2O.

To obtain 10% (w/v) raffinose, 5 g of raffinose was dissolved in 50 ml dH_2O.

All solutions were mixed in 50 ml Falcon tubes by warming (not boiling) in a microwave at medium power, followed by shaking at 260 rpm for few minutes. Once all ingredients were dissolved, the solution was filter sterilized and stored at 4°C.

3.9.7 Amino acid (and pyrimidine) solutions

Fifty-millilitre (4 mg/ml) stock solutions of tryptophan, uracil, leucine and histidine were prepared by filter sterilizing and stored at 4°C. If a precipitate formed (especially uracil), the tubes were heated briefly in a microwave oven to aid dissolution before use.

3.9.8 YPD broth/agar plates

Twenty-five grams of YPD powder (Sigma-Aldrich) were weighed into 500 ml dH_2O and autoclaved. For YPD agar plates, 10 g agar powder (Invitrogen) was added prior autoclaving.

3.9.9 YNB broth/agar plates

To prepare YNB broth, 3.35 g yeast nitrogen base without amino acids but including ammonium sulphate (MP/Anachem) and 0.3 g $his^-/ura^-/trp^-/leu^-$ dropout mix (MP/Anachem) were weighed into 500 ml dH_2O and autoclaved. For YNB agar plates 10 g agar powder (Invitrogen) was added prior autoclaving. 20% (w/v) glucose (Sigma-Aldrich) or 20% (w/v) galactose (Fisher) and 10% (w/v) raffinose (Alfa Aesar), respectively were added when autoclaved media reached ~50°C to avoid caramelisation.

3.9.10 YNB selective liquid cultures

To prepare 10 ml selective liquid YNB-Broth, the following ingredients were pipetted per universal tube:

1 ml, 20% (w/v) glucose stock **or**

1 ml, 20% (w/v) galactose + 1 ml, 10% (w/v) raffinose

50 µl, 4 mg/ml histidine solution (0.02 mg/ml final conc.)

50 µl, 4 mg/ml uracil solution (0.02 mg/ml final conc.)

150 µl, 4 mg/ml leucine solution (0.06 mg/ml final conc.)

100 µl, 4 mg/ml tryptophan solution (0.04 mg/ml final conc.)

Appropriate amino acids were left out for selection and the volume made up to 10 ml with YNB-Broth. Subsequently, the prepared liquid media were inoculated with one colony from a plate or with 100 µl from another liquid culture. Usually, the liquid cultures were incubated at 30°C in a table top shaker at 220 rpm overnight.
Sixty millilitres (required for small scale transformation) and 300 ml (required for large scale transformation) liquid cultures were prepared with the same ratio of ingredients as described above.

3.9.11 YNB selective plate preparation

To prepare selective YNB-Agar plates, the following amounts of ingredients (as required) were pipetted into 50 ml Falcon tubes (25 ml per plate) and YNB-Agar (~ 50°C) added to a volume of 50 ml:

5 ml, 20% (w/v) glucose stock **or** 5 ml, 20% (w/v) galactose + 5 ml, 10% (w/v) raffinose

The medium was mixed by inversion and ~25 ml poured into each petri dish.

3.9.12 LB-medium

Ten grams of LB-Broth (Sigma-Aldrich) were dissolved in 500 ml of dH_2O by autoclaving. In order to prepare plates, 7.5 g of agar (Invitrogen) was added before autoclaving.

3.9.13 LB-(ampicillin)-medium (LBA)

The LB-medium (500 ml) prepared in Section 3.9.12 was allowed to cool to around 50°C and 1 ml of 50 mg/ml carbenicillin (prepared in dH_2O and filter sterilised) was added prior to pouring the plates or inoculation of liquid cultures.

3.9.14 LB-(kanamycin)-medium (LBK)

The LB-medium (500 ml) prepared in Section 3.9.12 was allowed to cool to 50°C and 500 µl of 50 mg/ml kanamycin sulphate (prepared in dH_2O and filter sterilised) was added prior to pouring the plates or inoculation of liquid cultures.

3.9.15 Trp^- bacterial minimum medium for electroporation

In order to prepare a trp^- bacterial minimum medium, 5.25 g K_2HPO_4 (potassium phosphate, dibasic), 2.25 g KH_2PO_4 (potassium phosphate, monobasic), 0.5 g ammonium sulphate and 0.25 g sodium citrate were dissolved in 80 ml dH_2O and autoclaved along with 7.5 g agar in 400 ml dH_2O. After autoclaving, the two solutions were mixed together and when the solution cooled to ~50°C, 0.5 ml of 20% (w/v) $MgSO_4$, 5 ml of 4 mg/ml uracil, 5 ml of 4 mg/ml histidine, 5 ml of 4 mg/ml leucine, 5 ml of 20% glucose, 0.5 ml of 50 mg/ml kanamycin sulphate and 0.5 ml of 1% thiamine HCl (all filter sterilized) were added.

3.9.16 X-Gal plates for blue/white screening

For blue white selection, X-Gal plates were prepared by adding 50 ml phosphate buffer (4.40 g sodium phosphate ($2xH_2O$; dibasic) and 1.95 g sodium phosphate ($2xH_2O$; monobasic) in 50 ml dH_2O, mixed and autoclaved just before use, no pH adjustment was necessary) and 0.4 ml of 100 mg/ml X-gal to autoclaved 450 ml YNB-Agar at ~50°C.

3.10 Buffers and solutions for overexpression in *P. pastoris*

3.10.1 YPD(S) broth/agar plates (Zeocin selection)

Twenty-five grams of YPD powder (Sigma-Aldrich) were weighed into 500 ml dH_2O and autoclaved. For YPD agar plates, 10 g agar powder (Invitrogen) was added prior autoclaving. For Zeocin selection 0.5 ml of 100 mg/ml Zeocin was added and stored at 4°C. For YPDS broth/agar plates containing 1 M sorbitol, 91.1 g sorbitol was added prior to autoclaving.

4 Methods

4.1 Transformation into NovaBlue cells

Transformation of the two plasmid vectors, pEG202-NLS and pEG202 (OriGene; a generous gift of Dr. Ian Hampson, University of Manchester) as well as the other vectors pGEM-T (Promega) and pJET1.2/blunt (Fermentas), was carried out as described in the NovaBlue manual (Novagen). All these plasmids contain an ampicillin-resistance gene. For the transformation of pEG202(-NLS), 1µl (~10 ng) of the DNA was added to 20 µl NovaBlue-cells and incubated on ice for 5 min followed by a heat-shock at 42°C for 30 s and incubation on ice for 2 min. The bacteria were then plated out onto LB-Agar plates with 50 µg/ml carbenicillin (LB-Carb). Two plates were prepared for each transformed plasmid, one with 10 µl and the other with 40 µl of the transformation mixture. To make sure the plates were sterile, a control with no bacteria was also incubated overnight at 37°C. This confirmed the competent *E. coli* must have been transformed correctly.

4.2 -80°C stock preparation of yeast and bacterial cultures

4.2.1 Yeast -80°C stocks

All yeast culture stocks were prepared by adding 400 µl glycerol to 600 µl of a fresh overnight liquid culture and stored at -80°C.

4.2.2 Bacterial -80°C stocks

All bacterial culture stocks were prepared by adding 80 µl DMSO to 920 µl of a fresh overnight liquid culture and stored at -80°C.

4.2.3 KC8 -80°C stock preparation

The bacterial *E. coli* strain KC8 was used in the Y2H method to recover library plasmid DNA. The library plasmid (pJG4-5) contains a tryptophan gene that allows cells to produce tryptophan and to survive on media lacking this amino acid. To prepare electroporation-ready KC8 cells, some of the purchased cells were streaked onto an LB agar plate (Section 3.1) containing 50 µg/ml kanamycin sulphate and incubated at 37°C overnight. The next day a single colony was picked to inoculate 5 mL of LB-Broth (Section 3.1) containing 50 µg/ml kanamycin sulphate. This liquid culture was incubated at 37°C overnight with shaking at 260 rpm. All of the 5 mL were used to inoculate 500 ml LB-Broth containing 50 µg/ml kanamycin sulphate. This liquid culture was grown at 37°C, 260 rpm until the OD_{600} reached 0.5. The culture was put on ice for 30 min followed by a centrifugation at 5,000 rpm (3,500 x *g*) for 10 min at 4°C. The supernatant was poured off and the pellet resuspended in 300 ml of ice-cold 10% (v/v) glycerol. Then the culture was centrifuged again as above, the supernatant poured off and the pellet resuspended in 150 ml of ice-cold 10% (v/v) glycerol. Centrifugation was repeated as above, the supernatant poured off, the pellet resuspended in 10 ml of ice-cold 10% (v/v) glycerol, centrifuged again and the supernatant aspirated carefully. The pellet was resuspended in 2 ml of ice-cold 10% (v/v) glycerol. Working aliquots of 75 µl per tube were prepared and stored at -80°C.

4.3 Plasmid DNA extraction

The plasmid DNA extraction (miniprep) was carried out as described in the QIAprep Miniprep (Qiagen) or the Pureyield Plasmid Miniprep Kit Handbook (Promega At least two colonies were picked to inoculate 5 ml of LB-broth containing 50 µg/ml carbenicillin or kanamycin sulphate. After overnight incubation in a shaker at 37°C

(220 rpm), 1.5 ml (3 ml for Pureyield Plasmid Miniprep Kit) of the liquid cultures was used for plasmid DNA extraction. After analysing the quantity and purity of the DNA obtained, it was stored at -20°C. To obtain large quantities of plasmid DNA the Qiagen Plasmid Maxi Kit was used according to the manufacturer's instructions.

4.4 Quantification of DNA

The DNA life science analyser (Jenway-Genova) in combination with a TrayCell cuvette (Hellma) and subsequently the Nanodrop 2000 system (Thermo scientific) were used to quantify the conc. and determine the quality of plasmid DNA obtained.

4.5 Digestion with restriction endonucleases

All digestions were carried out by incubating the DNA with experiment dependent restriction endonucleases under the conditions recommended by the supplier (New England Biolabs Ltd, UK).

4.6 Agarose gel electrophoresis

One per cent and 0.8% agarose (Bioline) gels were prepared in 0.5x TBE electrophoresis buffer (Section 3.5) by heating the mixture in a microwave oven. After the agarose had dissolved and the solution cooled to around 50°C, GelRed was added (2 µl per 100 ml). Two microlitres of loading buffer were added to the DNA samples before loading the gel. The DNA was subjected to electrophoresis at 80 - 100 V for 45 to 90 min. The DNA bands were imaged and recorded using the G:BOX gel documentation system and GeneSnap software (Syngene). The molecular size marker, HyperLadder I (Bioline) was included to gauge the size of bands obtained.

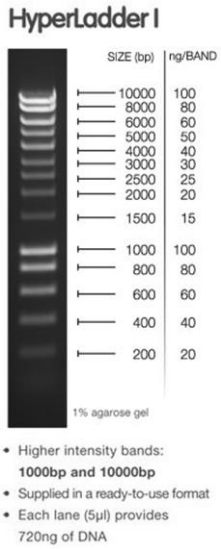

Figure 35: HyperLadder I (Bioline).

4.7 Polymerase chain reaction

Several different DNA polymerases (Taq, Dream Taq (Fermentas), Phusion (NEB), BioXAct-short and MyTaq (Bioline)) were used for the polymerase chain reaction (PCR) throughout the project and the manufacturer's instructions were followed where appropriate. Individual reaction conditions were determined empirically as required.

4.8 DNA Ligation

4.8.1 Insert:Vector molar ratio calculation

In most cases a 3:1 (insert:vector) ratio was used. The amount of insert DNA required was calculated using the following formula:

$$\textbf{ng of insert} = \frac{\text{ng of vector} * \text{kb size of insert}}{\text{kb size of vector}} * \text{insert: vector molar ratio}$$

4.8.2 Ligation of hNEIL3 into pGEM-T vector (Promega)

After hNEIL3 was obtained by PCR with BioXAct-short, it was ligated into the pGEM-T vector following the manufacturer's instructions.

4.8.3 Ligation of hNEIL3 into pJET1.2/blunt vector (Fermentas)

Phusion DNA polymerase generates blunt end products. Therefore, the CloneJET PCR Cloning Kit (Fermentas) was used and carried out as according to the manufacturer's instructions.

4.9 DNA sequencing

For DNA sequencing, BigDye v1.1 (Applied Biosystems) together with the provided 5x buffer (obtained from the DNA sequencing Facility at the University of Manchester) was used in the reaction mix. Table 2 and

Table 3 show the amounts of each constituent and the conditions used for DNA sequencing reactions of plasmid DNA.

Table 2: Reaction mix used for the DNA sequencing reaction.

Primer	1.0 µl	*(4-10 pmol/µl)*
Template DNA	1.0 µl	*(300 – 500 ng DNA)*
BigDye v1.1	1.0 µl	
5 X Buffer	3.5 µl	
H_2O	13.5 µl	
Total	***20.0 µl***	

Temp.	***Time***	
96°C	5 min	
96°C	10 s	
50°C	5 s	35 Cycles
60°C	4 min	
4°C	hold	

Table 3: Reaction mix used for the DNA sequencing reaction.

Primer	1.0 µl	*(4-10 pmol/µl)*
Template DNA	1.0 µl	*(300 – 500 ng DNA)*
BigDye v1.1	1.0 µl	
5 X Buffer	3.5 µl	
H_2O	13.5 µl	
Total	***20.0 µl***	

Temp.	***Time***	
96°C	5 min	
96°C	10 s	
50°C	5 s	35 Cycles
60°C	4 min	
4°C	hold	

After the DNA sequencing reaction was finished an ethanol precipitation was carried out (protocol provided by sequencing facility, Manchester University).

Ethanol Precipitation Protocol:

Twenty microlitres of the sequencing reaction were transferred to a 1.5 ml microcentrifuge tube. Then, 2 µl of 3 M sodium acetate pH 4.5, 44 µl 100% ethanol and 1 µl of BlueDye (GlycoBlue) were added followed by incubation at room temperature for 10-30 min. After centrifugation at 17,000 x *g* for 10 min the supernatant was aspirated and 100 µl of 80% (v/v) ethanol was added and the mixture incubated at room temperature for 2 min. Subsequently, the tubes were centrifuged briefly, the supernatant aspirated and the lid left open for evaporation of the ethanol (>20 min). A little blue point was visible at the bottom of the tube which indicated the position of the DNA pellet. After ethanol precipitation the tubes were taken for sequencing at the DNA sequencing Facility at the University of Manchester.

4.10 Bradford assay

4.10.1 Protein extraction for Bradford assay

Yeast colonies (one per extraction) were used to inoculate 10 ml YNB (Glu) ura^-/his^- medium and the culture placed in a shaking incubator at 30°C and 250 rpm overnight. Subsequently, 1.5 ml of each liquid culture was transferred to sterile 1.5 ml centrifuge tubes and centrifuged at maximum speed (17,000 x *g*) for 2 min. The supernatant was discarded, each pellet resuspended in 1.5 ml dH_2O and spun at maximum speed for a further 2 min. The supernatant was again discarded and each pellet resuspended in 100 µl TBS(T) buffer (Section 3.8.3) followed by sonication on ice at full power (highest amplitude and frequency possible) for 15-30 s to break open the yeast cell walls. After sonication the suspension was centrifuged at maximum speed for 2 min, the supernatant transferred to fresh 1.5 ml centrifuge tube and stored at -20°C.

4.10.2 BSA standard dilutions

Five milligrams per millilitre of BSA stock solution (5 mg BSA in 1 ml TBS(T)-buffer) was prepared and stored at -20°C until needed. To obtain a standard curve for the Bradford reagent, the stock solution was diluted 1:2 with TBS(T) (250 µl stock solution + 250 µl TBS(T) buffer) to obtain 2.5 mg/ml BSA solution (considered Dilution 1). Dilution 1 was diluted five more times (Dilution 2-6, Table 4). Dilution 7 contained 500 µl of TBS(T) buffer only without BSA added and was used to blank the spectrophotometer.

Table 4: Final concentrations of BSA protein standards.

BSA (Final conc.)	**Dilution number**
5 mg/ml	Undiluted
2.5 mg/ml	Dilution 1
1.25 mg/ml	Dilution 2
0.625 mg/ml	Dilution 3
0.3125 mg/ml	Dilution 4
0.15625 mg/ml	Dilution 5
0.078125 mg/ml	Dilution 6
0 mg/ml	Dilution 7 (blank)

4.10.3 Bradford reagent assay method

The Bradford reagent was mixed in the bottle prior to use and brought to room temperature. The BSA standards were prepared as described in Section 4.10.2 and 50 µl of each standard dilution was pipetted into a disposable plastic cuvette and 1.5 ml of Bradford reagent added. Each sample was incubated at room temperature for approximately 5 min (max. 45 min) prior to measuring. The absorbance of each sample was measured at 595 nm within 10 min of each other. From the data obtained a standard curve was plotted. Then, 10 µl of unknown protein solution was combined with 1.5 ml of Bradford reagent and the OD_{595} measured. Two more different dilutions of unknown protein were measured to decrease failure and the mean, considering the dilution factor, was calculated.

4.11 SDS-PAGE

4.11.1 Protein extraction from yeast for direct SDS gel loading

To extract proteins from yeast a modified method described by Kushnirov (2000) was performed. Therefore, 1.5 ml of a fresh overnight liquid culture was transferred to a sterile 1.5 ml centrifuge tube and spun at maximum speed (17,000 x *g*) for 1 min. The supernatant was discarded and the pellet resuspended in 100 µl of dH_2O and 100 µl 0.2 M NaOH. The mixture was incubated at room temperature for 5 min and then centrifuged at maximum speed for 1 min. The supernatant was discarded, the pellet resuspended in 50 µl (1x) SDS-PAGE sample buffer (Section 3.7.8) and heated at 95°C in a heating block for 3 min. The tube was centrifuged at maximum speed for 1 min and supernatant transferred to a sterile 1.5 ml centrifuge tube. 20 µl of the soluble protein mixture was loaded directly into a well of an SDS-PAGE gel (Section 4.11.3).

4.11.2 Casting of SDS-PAGE gels

The gel plates were assembled, a comb placed in position and a mark made approximately 1 cm below the bottom of the comb after which the comb was removed. The separating gel mixture (Section 3.7.4) was poured and carefully overlaid with 200 µl of water saturated 2-propanol. After the gel had polymerised (10 to 30 min) the 2-propanol was rinsed off and the plates dried by passing Whatman filter paper between them. The stacking gel mixture (Section 3.7.5) was then poured directly onto the separating gel. After polymerisation (5 to 10 minutes) the gel was transferred to the electrophoresis tank (Labnet). The inner chamber was filled with 1x SDS-running buffer (Section 3.7.7) to the top and the outer chamber only until 1 cm over lower edge of the gel glass plate. Then the combs were removed and the wells loaded with the denatured protein samples.

4.11.3 SDS gel loading

Protein samples were prepared as described in Table 5. After mixing the samples were heated at 95°C for 5 min and 20 µl (~15-30 µg) loaded in each well. If the wells were blocked by gel fragments a syringe needle was used to empty the wells. SDS-PAGE was carried out at 200 V for 45 min or until the tracking dye reached the bottom of the gel. The protein ladder used was a Full-range Rainbow Marker (GE Healthcare, Figure 36).

Table 5: Sample preparation scheme for SDS gel loading.

Cell-Lysate/ Protein mixture	x µl (30-60 µg)
TE-buffer	x µl (up to 40 µl)
Sample buffer (4x)	10 µl
Total	40 µl

← *Calculated by Bradford assay (Section 4.10)*

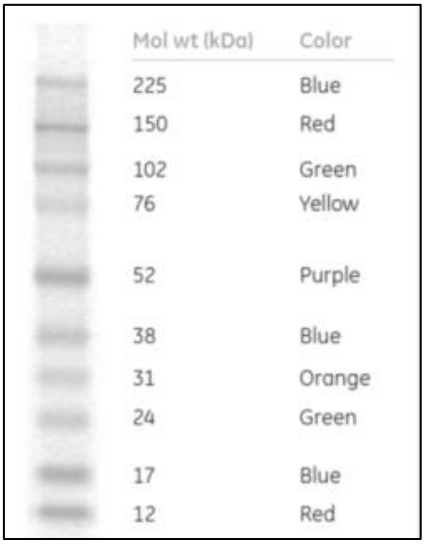

Figure 36: Full-range Rainbow Marker (GE Healthcare, Image taken from: http://bit.ly/wVQsay).

4.11.4 Coomassie blue staining dye

Because SDS-PAGE was performed in duplicate it was possible to stain one gel with Coomassie blue while the other was used for western blotting. The gel was stained in Coomassie blue dye (Section 3.7.9) with gentle agitation for 20 - 60 min. Then the gel was destained in destain solution (Section 3.7.10) for 3 x 15 min followed by incubation overnight.

4.12 Western blot

Proteins separated by SDS-PAGE were transferred to a nitrocellulose membrane (Hybond ECL, GE Healthcare) using a Mini Trans-Blot Electrophoretic Transfer Cell (Bio-Rad).

4.12.1 Blotting

The transfer buffer was prepared as described in Section 3.8.1 and stored at 4°C. Two hours before use the bottles were chilled at -20°C to ensure as cold conditions during blotting are provided as possible. The fibre pad, filter paper (two per gel), SDS gel and membrane were pre-wetted in western blot transfer buffer and the gel sandwich assembled as shown in Figure 37.

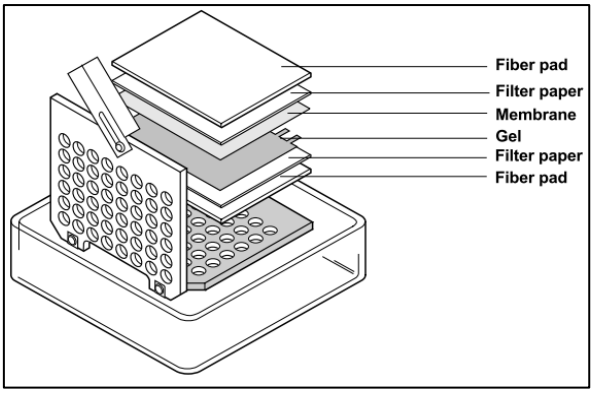

Figure 37: Gel sandwich assembling (Image taken from: Mini Trans-Blot Electrophoretic Transfer Cell instruction manual, Bio-Rad).

The cassette was closed and slotted into a module. The module then was placed in a tank (black side to negative cathode) along with a frozen cooling unit and filled with Western Blot transfer buffer (Section 3.8.1). A magnetic stirring bar was added and the tank put onto a magnetic stirrer. Electrophoretic transfer was carried out for one hour at 100 V.

4.12.2 Western blotting

After transfer, the membrane was transferred to a plastic container and blocking buffer (Section 3.8.2) was added until the membrane was fully covered. Blocking was performed at room temperature for one hour or overnight. Afterwards, the blocking buffer was discarded, the membrane transferred into a polythene bag made from a piece of autoclave bag heat sealed on three sites. Five millilitres of primary antibody (1/10000 to 1/25000 rabbit monoclonal anti LexA ,Abcam) diluted in 0.5% blocking buffer, was added and the bag heat sealed. The membrane was incubated at room temperature on a rocking table for about 1.5 hours. The membrane was then transferred to a plastic container, washed 3 x 10 min in TBS(T), transferred to a fresh polythene bag and incubated with 5 ml of 1/3000 horseradish peroxidase (HRP) conjugated secondary antibody (diluted with TBS(T)) on a rocking table at room

temperature for about 45 minutes. Following this, the membrane was again washed 3 x 10 min with TBS(T). After the last wash the TBS(T) was drained off by dipping one side of the membrane onto a paper tissue. Subsequently, the membrane was transferred to cling film (protein side up) and 5 ml of enhanced chemiluminescence (ECL) reagent, prepared according to the manufacturer's instructions, poured on the membrane and incubated at room temperature for 1 min. Excess ECL reagent was drained off and the membrane wrapped in cling film. The wrapped membrane was placed in the G:BOX and continuous pictures with 30 s, 1 min and 2 min exposure times were taken. Depending on the results of the initial pictures taken, the exposure time was increased or decreased, as appropriate.

4.13 Yeast two-hybrid

4.13.1 Small scale transformation

Prior to transformation, a 60 ml liquid culture was inoculated with the appropriate amount of an overnight 10 ml liquid culture to obtain an OD_{600} of 0.15 *(calculation used: OD_{600} wanted / OD_{600} got x final volume = volume to inoculate)*. The 60 ml liquid culture was incubated at 30°C and 220 rpm until the OD_{600} reached 0.7-1.0 (after 5-7 h). Then the culture was transferred into two 50 ml Falcon tubes (30 ml each). The tubes were centrifuged at 3000 rpm (1500 x *g*) for 5 min, the supernatant was discarded and the pellet resuspended in 30 ml (15 ml each tube) of sdH_2O. The suspensions were brought together into one tube, centrifuged at 3000 rpm (1500 x *g*) for 5 min and as much supernatant as possible was aspirated and the pellets stored on ice (for up to 2 hours). 1 ml of 1xTE/LiOAc/dH_2O and 2 ml of 1xTE/LiOAc/PEG-3350 were freshly prepared (Sections 3.9.4 and 3.9.5) and 50 µg of carrier DNA (from salmon sperm) was added to sterile 1.5 ml centrifuge tubes. Afterwards, the

pellets were resuspended in 0.3 ml 1xTE/LiOAc/dH_2O and 100 µl of this mixture, 100 ng of the appropriate plasmid and 300 µl of 1xTE/LiOAc/PEG-3350 were added to the 1.5 ml tube containing the carrier DNA. The tubes were mixed by inversion and placed in a petri dish at 30°C in a table top shaker at 63 rpm for 30 min. After incubation, 70 µl of DMSO was added to each tube and mixed by inversion followed by a heat shock. For this, the tubes were placed in a preheated water bath at 42°C for 5 min, then immediately centrifuged at 1,000 rpm (65 x *g*) for 1 min. The supernatant was discarded and each pellet resuspended in 500 µl sdH_2O. One hundred microliters of each transformation mixture was carefully spread onto appropriate plates and transferred to an incubator at 30°C for a 30 min incubation with the plates not inverted. Finally, the plates were inverted and left in the incubator at 30°C overnight.

4.13.2 Large scale transformation of library cDNA

The large scale transformations were carried out with cDNA libraries obtained from placental tissue (generous gift from Dr. Ian Hampson, University of Manchester) and Jurkat T-Cells (OriGene) as followed.

Day1

For the large scale transformation of a cDNA library, 10 ml YNB (Glu) ura^-/his^- medium was inoculated with one colony of EGY48 yeast carrying pEG202-N3 and pRB1840 plasmids and incubated at 30°C and 250 rpm for 7 hours. Next, this culture was transferred into 50 ml YNB (Glu) ura^-/his^- medium and incubated at 30°C and 250 rpm overnight.

Day2

The next day, the OD_{600} of the 60 ml culture was measured and, depending on the results, 300 ml of YNB (Glu) ura^-/his^- medium was inoculated with a volume of culture to obtain an OD_{600} of 0.2. The culture was incubated at 30°C and 250 rpm until an OD_{600} of 1 was reached (approx. 4 hours). Meanwhile, 31 x 1.5 ml sterile centrifuge tubes were put into a bag and stored at -20°C (one tube was labelled as control). Once the 300 ml culture reached OD_{600} of 1, it was transferred into 6 x 50 ml Falcon tubes and the cells were harvested by centrifugation at 3,000 rpm (1,500 x *g*) for 5 min. The supernatant was poured off and the pellet resuspended in 5 ml sterile dH_2O. All six solutions were poured together into one 50 ml Falcon tube and the cells harvested again by centrifugation at 3,000 rpm (1,500 x *g*) for 5 min. The supernatant was poured off and the pellets put on ice (up to 2 h). The 31 x 1.5 ml centrifuge tubes were taken out of the freezer and 50 µg of (pre-boiled) salmon sperm carrier DNA was pipetted into each tube and fresh 5 ml and 10 ml aliquots of 1xTE/LiOAc/H_2O and 1xTE/LiOAc/PEG-3350 respectively were prepared (Sections 3.9.4 and 3.9.5).

The cell pellet was resuspended in 1.5 ml of 1xTE/LiOAc/H_2O and 50 µl aliquots were pipetted into the 30 pre-chilled sterile 1.5 ml microcentrifuge tubes. To ensure each yeast cell obtained just one copy of the plasmid a maximum of 1 µg of pJG4-5-based library plasmid DNA was aliquotted into each of the thirty microcentrifuge tubes, followed by 300 µl of 1 x TE/LiOAc/PEG-3350, mixed by inversion and incubated at 30°C and 63 rpm for 30 min. Subsequently, 40 µl of DMSO was pipetted into each tube and mixed by inversion followed by a heat shock at 42-45°C for 5 min. To estimate the transformation efficiency a control plate was prepared: 10 µl of one transformant was diluted 1:10 with 990 µl of sdH_2O into a fresh 1.5 ml centrifuge tube and 100 µl of the dilution was spread onto a YNB (Glu) $ura^-/his^-/trp^-$ plate followed by incubation at 30°C overnight (this plate was for estimation of total transformants

described in Section 4.13.3). In addition, 100 µl of the same transformant was used to inoculate 10 ml of YNB (Glu) $ura^-/his^-/trp^-$ liquid medium and incubated at 30°C and 220 rpm overnight. A plate and liquid culture was also prepared for the control tube that lacked the library vector. Finally, the remaining transformants were poured into 3 x 300 ml YNB (Glu) $ura^-/his^-/trp^-$ medium (10 transformants per 300 ml culture) and incubated at 30°C and 280 rpm overnight.

Day3

After it was confirmed that the controls did not show any growth, neither on plates nor in liquid cultures, and that the 300 ml cultures only contained yeast (checked via microscope for bacterial contamination) the 3 x 300 ml YNB (Glu) $ura^-/his^-/trp^-$ cultures were poured in equal amounts into 50 ml Falcon tubes, centrifuged at 2500 rpm (1000 x *g*) for 10 min and the supernatant decanted. Next, all pellets were resuspended in a total volume of 200 ml sdH_2O. Then the suspensions were split among four Falcon tubes followed by centrifugation at 2,500 rpm (1000 x *g*) for 5 min. The supernatant was decanted, the pellets resuspended in equal volumes of sdH_2O (~2.5 ml) and brought together into one 50 ml Falcon tube. The total volume was estimated and an amount of sterile 50% (v/v) glycerol equalling half that volume was added. The suspension was split into 1 ml aliquots and stored at -80°C.

4.13.3 Library cDNA screening (placental cDNA library)

The number of colony forming units (cfu) in the frozen 1 ml aliquots prepared on Day 3 in Section 4.13.2 was estimated (2.8×10^8 cfu/ml) by incubating 100 µl of this aliquot on YNB (Gal,Raf) $ura^-/his^-/trp^-$ plates at 30°C for three days and the number of total transformants (1.47×10^7) was estimated (therefore the plate for examination of total transformants prepared in Section 4.13.2 (Day 2) was used).

A YNB (Gal,Raf) ura$^-$/his$^-$/trp$^-$/leu$^-$ liquid culture containing 1x10^7 cfu/ml of viable transformants was incubated at 30°C and 150 rpm for 4 hours to induce prey protein production. Next, 100 µl of culture was spread onto YNB (Gal,Raf) ura$^-$/his$^-$/trp$^-$/leu$^-$ plates (~1x10^6 cfu/plate). After colonies appeared they were transferred onto separate YNB (Gal,Raf) ura$^-$/his$^-$/trp$^-$/leu$^-$ master plates and incubated at 30°C overnight. Each colony from these master plates was resuspended in 100 µl sdH_2O and then (2 µl) spotted onto each plate as shown in Table 6.

Table 6: Media used for testing colonies during Y2-H screening.

Plate	Selection	Positives
YNB (Glu)	ura$^-$/his$^-$/trp$^-$/leu$^-$	No growth
YNB (Gal,Raf)	ura$^-$/his$^-$/trp$^-$/leu$^-$	Growth
YNB (Glu)	ura$^-$/his$^-$/trp$^-$ + X-gal	No blue colonies
YNB (Gal,Raf)	ura$^-$/his$^-$/trp$^-$ + X-gal	Blue colonies

After incubation at 30°C for 1-2 days all positives estimated were picked from the YNB (Gal,Raf) ura$^-$/his$^-$/trp$^-$/leu$^-$ plate to inoculate 5 ml YNB-(Glu) trp$^-$ liquid cultures followed by incubation at 30°C at 250 rpm overnight. Finally, 600 µl of each overnight culture was transferred into 2 ml tubes containing 400 µl of 80% glycerol and stored at -80°C until needed for subsequent plasmid extraction.

4.13.4 Library plasmid DNA extraction of potential positives

Initially, the standard method described in the DupLEX-A application guide (OriGene) was used to extract pJG4-5 plasmids, carrying a library cDNA insert, from the EGY48 yeast strain. However, after low efficiency was experienced a new PCR method was developed that allowed a highly specific and much faster analysis of inserts in potential positive pJG4-5 plasmids.

4.13.4.1 "Modified" standard method

Plasmid extraction from yeast

In this method, potential positive clones were grown in 3 ml YNB (Glu) trp^- liquid medium at 30°C and 250 rpm overnight. If growth was observed the next day, 10 ml of fresh YNB (Glu) trp^- liquid medium was inoculated with 100 µl of the 3 ml overnight culture and incubated at 30°C and 250 rpm overnight. On day three, 2 ml of each culture was transferred into 2 ml centrifuge tubes and spun at 17,000 x *g* for 30 s. The supernatant was discarded and a further 2 ml of the 10 ml overnight culture added, spun again at 17,000 x *g* for 30 s and the supernatant discarded. This was repeated until all of the 10 ml overnight culture was used. Each pellet was then resuspended in 600 µl TE-buffer and sonicated on ice at maximum amplitude and frequency for 30 s. Plasmid DNAs were extracted using a miniprep kit (Pureyield Plasmid Miniprep System, Promega) and the concentration and purity of the DNA was measured in the Nanodrop.

Electroporation of extracted plasmid DNA into KC8 *E. coli*

Following the testing of different electroporation conditions, the parameters listed in Table 7 resulted in the highest transformation efficiency of *E. coli* KC8 cells using a Micro Pulser (Bio-Rad) instrument.

Table 7: Electroporation conditions used to transform *E. coli* KC8 cells.

Volume competent cells (KC8)	40 µl
Yeast plasmid DNA	10 µl (>20 ng)
Voltage	2.5 kV
Time constant	~5 ms
SOC medium for recovery	1 ml

After electroporation and recovery in super optimal broth with added glucose (SOC) the cultures were spread onto trp^- bacterial minimum plates (Section 3.9.15) and incubated at 37°C overnight. The next day, at least one colony from each plate was transferred into 5 ml LB-Broth containing 50 µg/ml kanamycin and incubated in a shaking incubator at 37°C and 250 rpm overnight. Following incubation, plasmid DNA was extracted and the concentration/purity of the DNA was measured.

4.13.4.2 "PCR Method"

Because the use of the "modified" as well as the unmodified standard method described in the DupLEX-A application guide (OriGene) had given unsatisfactory results (Section 5), a new method was developed to allow a much faster and more specific analysis of library cDNA carried by potential yeast clones. The initial extraction of the plasmid DNA from yeast was performed as described in Section 4.13.4.1. However, instead of transforming the obtained plasmid DNA into KC8 cells by electroporation a PCR with *Taq* DNA polymerase was performed followed by direct sequencing. Therefore, PCR conditions as shown in Table 8 and the following primers were used:

pJG4-5 forward primer: 5′-CTG AGT GGA GAT GCC TCC-3′

pJG4-5 reverse primer: 5′-GCC GAC AAC CTT GAT TG-3′

Table 8: PCR conditions for library cDNA inserts with Taq DNA polymerase.

	Temperature	Time
Pre-Denaturation	94°C	1 min
Denaturation	94°C	30 s
Annealing	55°C	30 s
Extension	72°C	2 min
Final-Extension	72°C	5 min
30 Cycles		

4.13.5 Mating assay to confirm potential interaction partners for hNEIL3

The mating assay was used to confirm the potential positive findings of the placental cDNA library screen by transforming pEG202-N3 and the reporter pRB1840 (or pSH18-34) into yeast strain RFY206 and the isolated potential positive library vector pJG4-5 back into EGY48. These two clones were then cross streaked onto YPD plates for mating (Figure 38).

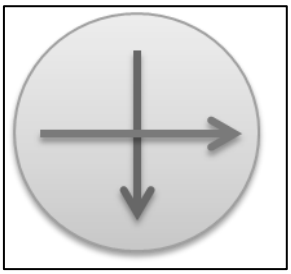

Figure 38: Cross streak method for transformed mating strains RFY206 (horizontal arrow) and EGY48 (vertical arrow)

The plate was incubated at 30°C overnight and three parts (start of horizontal arrow, start of vertical arrow and the crossed part in Figure 38) were transferred onto selective media (YNB (Glu,X-Gal), ura$^-$, his$^-$, trp$^-$ and YNB (Gal,X-Gal), ura$^-$, his$^-$, trp$^-$) for *LacZ* selection.

4.13.6 Interaction studies with LigIIIα and Polβ

To estimate if the interacting protein partners LigIIIα and Polβ found for NEIL1 and NEIL2 (Das *et al.,* 2006; Wiederhold *et al,* 2004) are also interacting with NEIL3 the CDS cDNA of both proteins where cloned into the library vector pJG4-5 to make Y2H studies. The only restriction sites available in the multiple cloning site of pJG4-5 were *Eco*RI and *Xho*I. However, as both restriction sites were also present in LigIIIα and Polβ it was not possible to use the pGEM-T method as described in Section 4.8.2.

Therefore, a workaround was established that made it possible to clone the cDNA directly into the pJG4-5 vector. Firstly, the pJG4-5 vector was linearized with *Eco*RI and *Xho*I and then the sticky overhangs were blunted by the blunting enzyme mung bean nuclease (NEB). After blunting the linearized vector it was possible to ligate the PCR product of either LigIIIα or Polβ into pJG4-5. At this point it was important, that the primers used for amplification were designed in a way that the 3′ G on the *EcoRI* and the 5′ G on the *XhoI* site of the vector were excluded. This way, only if the insert is ligated the right way around the final restriction sites for *Eco*RI and *Xho*I in the insert stay intact and can be targeted and digested by *Eco*RI and *Xho*I. If the insert was ligated the wrong way around the restriction sites were destroyed and therefore restriction digest with *Eco*RI and *Xho*I failed (Figure 39).

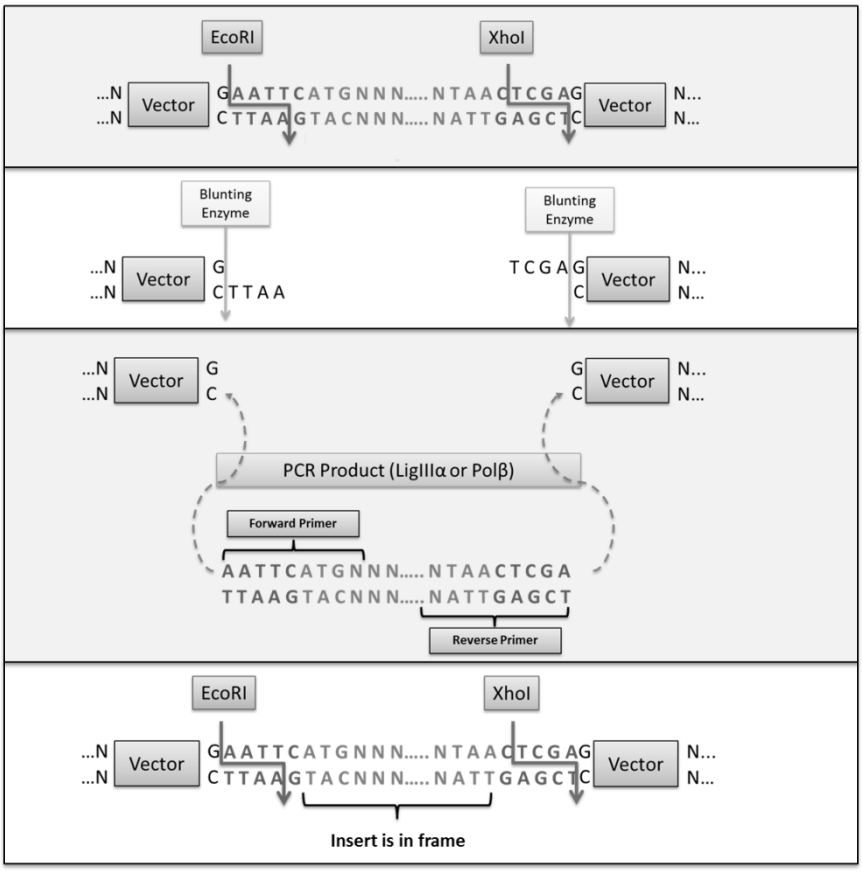

Figure 39: Cloning method used for insertion of either LigIIIα or Polβ into the library vector pJG4-5. For more details see text.

4.14 Overexpression in *Pichia pastoris*

The *P. pastoris* strain X-33 used in this project was a generous gift of Dr Natalie Ferry. The pGAPZαA vectors containing either full length mNEIL1 or hNEIL3 cDNA, or truncated versions of hNEIL3 with amino acid length 1-394 or 1-502 (hN3-394 or hN3-502) were generated by Mengxin Yin and Constantina Stylianou (2010). Primers used to construct the hNEIL3 clones are shown in Table 9 (Yin, 2010).

Table 9: Primers used for hNEIL3, hN3-394 and hN3-502 generation (Yin, 2010).

hNEIL3 Forward	5′-CTC GAG AAA AGA ATG GTG GAA GGA CCA GGC TG-3′
hNEIL3 Reverse	5′-GC GGC CGC GCA TCC AGG AAT AAT TTT TAT TCC TGG C-3′
hN3-394 Reverse	5′-GC GGC CGC ATC AGT CAA GAC AAG AGT TGT AGT TCC-3′
hN3-502 Reverse	5′-GC GGC CGC AGG ATT TAA GGT ACG AGG GCC ATC-3′

4.14.1 Electroporation of pGAPZαA constructs into P. pastoris

Electroporation was used to transfect *P. pastoris* with linearized pGAPZαA constructs. Therefore, 5 ml of YPD was inoculated with *P. pastoris* and incubated at 30°C at 250 rpm overnight in a 50 ml conical flask. Next day, 500 ml YPD broth was inoculated with 0.1 ml of the overnight culture and incubated at 30°C and 250 rpm until the OD_{600} reached 0.8 - 1.1. Then the culture was centrifuged in a cooled centrifuge at 3,000 rpm (1,500 x *g*) for 5 min and the pellet resuspended in 500 ml of ice-cold sdH_2O. The suspension was centrifuged again at 3,000 rpm (1,500 x *g*) for 5 min, the supernatant discarded and the pellet resuspended in 250 ml of ice-cold (<4°C) sdH_2O. Centrifugation was repeated as before and the pellet was resuspended in 20 ml of ice-cold (<4°C) 1 M sorbitol solution. Then, following another centrifugation step, the pellet was resuspended in 1 ml of ice-cold (<4°C) 1 M sorbitol solution to obtain a final volume of approximately 1.5 ml (if the pellet was large more

1 M sorbitol was used). About 10 µg (dissolved in nuclease free sdH_2O) of linearized pGAPZαA DNA construct was pipetted into 80 µl of the cell solution prepared before and transferred to an ice-cold (<4°C) 2 mm electroporation cuvette. The mixture was incubated on ice for 5 min and then pulsed in accordance with the manufacturer's instructions (Micro Pulser, Bio-Rad). For *P. pastoris*, the programme chosen was *pic* and the resulting conditions observed after pulsing were always around 1.98 kV for 5.1 ms. Directly after pulsing 1 ml of 1 M ice-cold (<4°C) sorbitol was added and the sample transferred to a 15 ml sterile tube and incubated at 30°C without shaking for 1 h. After incubation, 10, 20, 50, 100, 200 and 500 µl were spread onto YPDS plates containing 100 µg/ml Zeocin and incubated at 30°C for three days. Once colonies appeared, two clones were picked and restreaked onto fresh YPD plates containing 100 µg/ml Zeocin.

4.14.2 Extraction of chromosomal DNA from P. pastoris using LiOAc-SDS

In preparation for PCR analysis of homologous recombined constructs in *P. pastoris* clones, the chromosomal DNA was first extracted. Therefore, 4 ml of a 10 ml YPD culture that had been incubated at 30°C and 250 rpm for two days was centrifuged at maximum speed (~13,000 x *g*) for 30 s. Then the supernatant was discarded and the pellet resuspended in 300 µl of LiOAc-SDS solution (200 mM LiOAc and 1% SDS). This mixture was incubated for 10 min at 70°C with mixing every 2.5 min, after which 900 µl of 96-100% ethanol was added, the sample mixed vigorously and centrifuged at 13,000 x *g* for 3 min. The supernatant was discarded and 70% ethanol was added to wash the pellet (twice) followed by centrifugation at 13,000 x *g* for 15 s. After the supernatant was discarded, the pellet containing precipitated proteins, cell debris and chromosomal DNA was dissolved in 100 µl dH_2O. Insoluble cell components and debris were spun down by centrifugation at 13,000 x *g* for 15 s. Finally, the

supernatant which contained dissolved chromosomal DNA was transferred to a fresh 1.5 ml centrifuge tube and the DNA concentration was measured prior to use as template DNA in the subsequent PCR.

4.14.3 PCR of incorporated pGAPZαA inserts extracted from P. pastoris

To confirm correct integration of the linearized pGAPZαA plasmid DNA into the chromosomal DNA of *P. pastoris,* PCR was carried out with primers shown in Table 10. Reaction components shown in Table 11 and PCR conditions in

Table 12. For this method, MyTaq Red Mix (Bioline) was used. This mix contains a Taq DNA polymerase, dNTPs and buffer and only the DNA template, primers and water had to be added in order to perform the PCR. 1000, 500, 250 and 125 ng of template DNA were used for PCR and although all worked, 500 ng seemed to give the best visual result in terms of band thickness.

Table 10: Primer sequences for PCR of pGAPZαA insert.

pGAP-Forward	5´-GCAAATGGCATTCTGACATCC-3´
3′ *AOX1*	5´-GTCCCTATTTCAATCAATTGAA-3´

Table 11: Components for the PCR of pGAPZαA inserts from extracted chromosomal DNA.

DNA template	x µl	~500 ng
3′ *AOX1* primer	2 µl	
pGAP Forward primer	2 µl	
dH_2O	x µl	
MyTaq Red Mix (Bioline)	25 µl	
Total	**50 µl**	

Table 12: Conditions for PCR of pGAPZαA inserts from extracted chromosomal DNA.

	Temperature	Time	
Initial denaturation	*95°C*	*3 min*	
Denaturation	95°C	15 s	30 cycles
Annealing	55°C	15 s	
Extension	72°C	1 min	
Final Extension	*72°C*	*5 min*	
Soak while end	*4°C*	--	

4.14.4 Overexpression conditions

For the overexpression of mNEIL1, full length hNEIL3 and its truncated versions 394 and 502 different conditions were used for incubation to estimate the best parameters for optimal expression:

Table 13: Overexpression conditions in *P. pastoris*

Condition No.	Temp.	Time	Volume
Condition 1	28°C	Up to 120 h	10 ml, 50 ml, 250 ml
Condition 2	29°C	Up to 120 h	10 ml, 50 ml, 250 ml
Condition 3	30°C	Up to 120 h	10 ml, 50 ml, 250 ml

In addition all three conditions were repeated with baffled flasks for the 250 ml volume which showed a slightly faster growth confirmed via OD. The shaker speed used for incubation was 180 rpm. Every 24 h of incubation 1 ml samples were transferred from each flask to sterile 1.5 ml centrifuge tubes and centrifuged at 17,000 x *g*. The supernatant was then transferred to a fresh sterile 1.5 ml centrifuge tube. Subsequently, the pellet and the supernatants were shock frozen in liquid nitrogen and stored at -80°C. This way it was possible to load all different stages of incubation times onto the same SDS-PAGE gel at once.

5 Results

5.1 Y2H Summary

The bait vectors, pEG202 and pEG202-NLS, containing hNEIL3-cDNA were generated and autoactivation tests to check if hNEIL3 autoactivates the reporter gene transcription on its own were carried out. Once the results of these preliminary tests were confirmed to be negative, the pEG202-hNEIL3 bait vector was used in Y2H studies to screen cDNA libraries obtained from placental tissue and Jurkat T-Cells. Subsequently, 60 potential positive clones obtained from the placental and 27 potential positive clones from the Jurkat T-cell cDNA library screen were sequenced and subjected to bioinformatic analysis.

5.2 Y2H bait vector preparation

5.2.1 Preparation of hNEIL3 cDNA insert

5.2.1.1 Designing primers for PCR of hNEIL3-cDNA

For the PCR of the hNEIL3-cDNA (full length) it was necessary to design specific oligonucleotide primers. This was achieved by comparing the hNEIL3 cDNA sequence with the restriction-sites in the multiple cloning sites of pEG202 and pEG202-NLS (Appendix 8.2, Figure 98 and Figure 99). To make it possible to use one sort of primers for both vectors, the restriction-sequences for *EcoR*I and *Bam*HI were chosen and added to the 5′ end of each primer. This is necessary to clone the hNEIL3 cDNA after amplification into the plasmids pEG202 (Figure 98) and pEG202-NLS (Figure 99). Both vectors have restriction-sites for *Eco*RI and *Bam*HI in their multiple-cloning-region. As the full length hNEIL3 cDNA contains a stop codon, it was not necessary to add one to the hNEIL3_stop_*Bam*HI primer. However, if primers for

amplification of truncated versions of hNEIL3 are needed a stop codon must be included.

Partial reverse Primer: **hNEIL3_1538_Reverse (T_m= 63.33ºC)**

5′ - CAC AAC TCG GAG AAT GCA GA – 3′

Full Primer$_1$: **hNEIL3_stop_*Bam*HI (T_m= 69.79ºC)**

5′ - GGA TCC TTA GCA TCC AGG AAT AAT TTT TAT TCC TGG C – 3′

Full Primer$_2$: **hNEIL3_start_*EcoR*I (T_m= 68.41°C)**

5′ - GAA TTC ATG GTG GAA GGA CCA GGC TGT AC – 3′

T_m-calculator provided by Finnzyme was used to calculate the annealing temperatures (can be found at http://www.finnzymes.com/tm_determination.html).

5.2.1.2 PCR of pCMV6-AC/hNEIL3 with BioXAct-short

Initially, the BioXAct-short DNA polymerase from Bioline was used for the amplification of the full length coding sequence (CDS) of hNEIL3. However, no bands were obtained (not shown). Taq polymerase was then used as a control and a band of the correct size was obtained (Figure 40). Therefore, it was assumed that the long (31 bases) full length reverse primer (hNEIL3_stop_*Bam*HI, Section 5.2.1.1) could have caused problems and to test this, the PCR was repeated with a shorter reverse primer that annealed to bp 1538 – 1557 in hNEIL3 CDS (hNEIL3_1538_Reverse, Section 5.2.1.1) giving rise to a truncated version of NEIL3. Interestingly BioXAct-short was able to amplify this truncated version of the hNEIL3 cDNA with the full forward (hNEIL3_start_*Eco*RI, Section 5.2.1.1) and the hNEIL3_1538_Reverse primer (Figure 41).

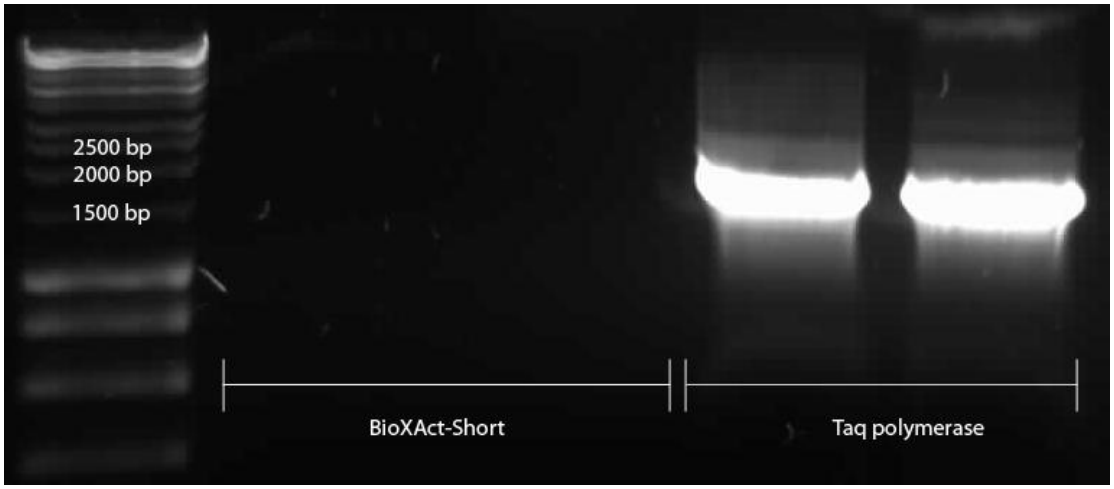

Figure 40: Agarose gel electrophoresis of hNEIL3 PCR products. The PCR of full length hNEIL3 with Taq polymerase did work, but with BioXAct-Short it did not. The lanes were loaded in duplicate.

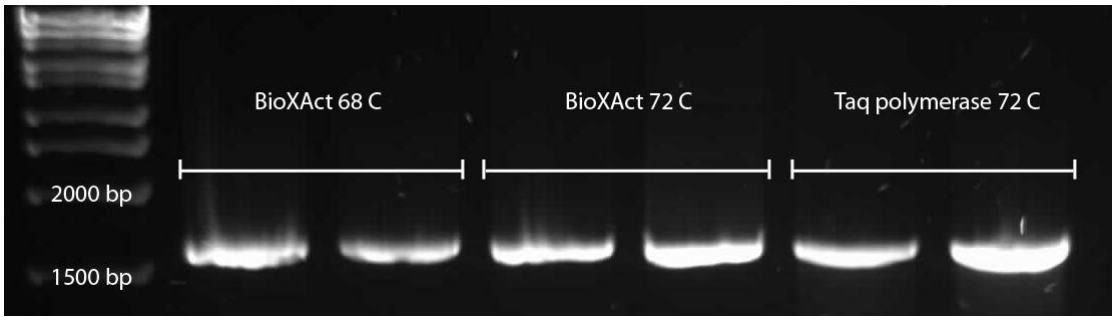

Figure 41: Agarose gel electrophoresis of truncated hNEIL3 (1538 bp) PCR products. The PCR worked for all conditions (68°C and 72°C extension temperature) as well as for both enzymes BioXAct-short and Taq polymerase. The lanes were loaded in duplicate.

The PCR was repeated with the full length primers until the right conditions for the DNA polymerase BioXAct-Short were found to amplify the full length hNEIL3 cDNA (Table 14 and Table 15). This made it possible to obtain PCR products of hNEIL3 shown in Figure 42 and A-NEIL3 and C-NEIL3 were used for further cloning.

Table 14: PCR-Mix and conditions for the first PCR (A_{NEIL3}).

DNA	0.5 µl			
10x Buffer	5 µl			
50 mM $MgCl_2$	2.5 µl			
100 mM dNTPs	1 µl	**Temp.**	**Time**	
10 µM *Full Primer$_1$*	0.5 µl	*95ºC*	*5 min*	
10 µM *Full Primer$_2$*	0.5 µl	**95ºC**	**30 s**	**30 Cycles**
BioXAct (short)	1 µl	**54ºC**	**30 s**	
H_2O	39 µl	**68ºC**	**5 min**	
Total	50 µl	*68ºC*	*10 min*	

Obtained **A_{NEIL3}** *(40 ng/µl)*

Table 15: PCR-Mix and conditions for the second PCR (B_{NEIL3} and C_{NEIL3}).

DNA	1 µl			
10x Buffer	5 µl			
50 mM $MgCl_2$	2 µl			
100 mM dNTPs	0.5 µl	**Temp.**	**Time**	
10 µM *Full Primer$_1$*	0.5 µl	*94ºC*	*1 min*	
10 µM *Full Primer$_2$*	0.5 µl	**94ºC**	**30 s**	**30 Cycles**
BioXAct (short)	0.5 µl	**54ºC**	**45 s**	
H_2O	39 µl	**68ºC**	**2 min**	
Total	50 µl	*68ºC*	*5 min*	

Obtained **B_{NEIL3}** *(10 ng/µl)* and **C_{NEIL3}** *(30 ng/µl)*.

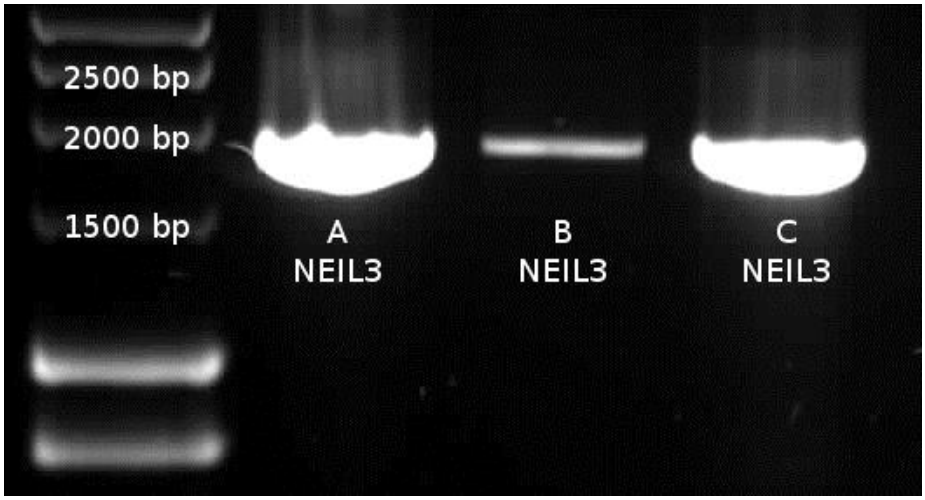

Figure 42: Agarose gel electrophoresis of amplified NEIL3 PCR products. For A-NEIL3 the PCR conditions in Table 14 were used, while for B-NEIL3 and C-NEIL3 those in Table 15 were used but with different amounts of template DNA (10 ng for B-NEIL3 and 30 ng for C-NEIL3)

5.2.1.3 Cloning of hNEIL3 (A-NEIL3 and C-NEIL3) into pGEM-T

After A-NEIL3 and C-NEIL3 were ligated into pGEM-T (Table 16), a transformation with blue/white selection into NovaBlue *E. coli* cells was performed.

Table 16: Scheme for the ligation of hNEIL3 into pGEM-T vector.

2x Rapid Buffer	5 µl	
pGEM-T vector	1 µl	50 ng
PCR product	1 µl	~35 ng
T4 DNA Ligase	1 µl	
Deionized H_2O	2.25 µl	
Total	**10 µl**	

The ligation was carried out at an incubation temperature of 4°C overnight.

White colonies from plates of A_{NEIL3} and C_{NEIL3} were picked and liquid cultures (LB-Carb) were set up at 37ºC overnight. Plasmid purification and digestion with *Eco*RI and *Bam*HI was performed and Figure 43 shows the sizes obtained for pGEM-T and the hNEIL3 insert. In some lanes a third band is visible which is likely to be incompletely digested plasmid DNA. However, the bands are all the expected size and samples A2 and C1 were then gel purified to obtain the hNEIL3 insert with *Eco*RI and *Bam*HI overhangs.

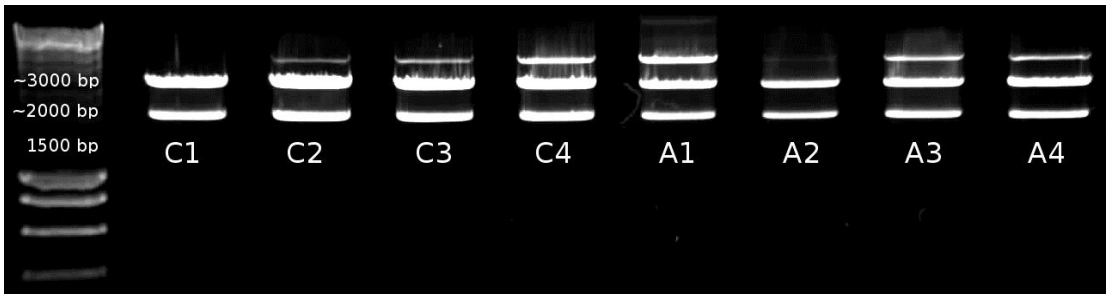

Figure 43: Agarose gel electrophoresis of pGEM-T/NEIL3 digested with *Eco*RI and *Bam*HI. C1 - C4 and A1 - A4 are plasmids obtained from four different liquid cultures each. C1 - C4 indicates that the PCR product C-NEIL3 is contained and A1 - A4 indicates that the PCR product A-NEIL3 is contained in the pGEM-T vector.

5.2.2 Preparation of pEG202 and pEG202-NLS vectors

A large scale double-digestion with *Eco*RI and *Bam*HI and 4 X ~5 µg template DNA in a total volume of 50 µl was performed for pEG202 and pEG202-NLS. The linearized plasmids were purified from an agarose gel and a DNA concentration of ~30 ng/µl was obtained for pEG202 and ~50 ng/µl for pEG202-NLS in a total volume of 300 µl for each vector. Figure 44 shows bands for the linearized plasmids pEG202-NLS and pEG202 at the predicted size (~10.2 kb).

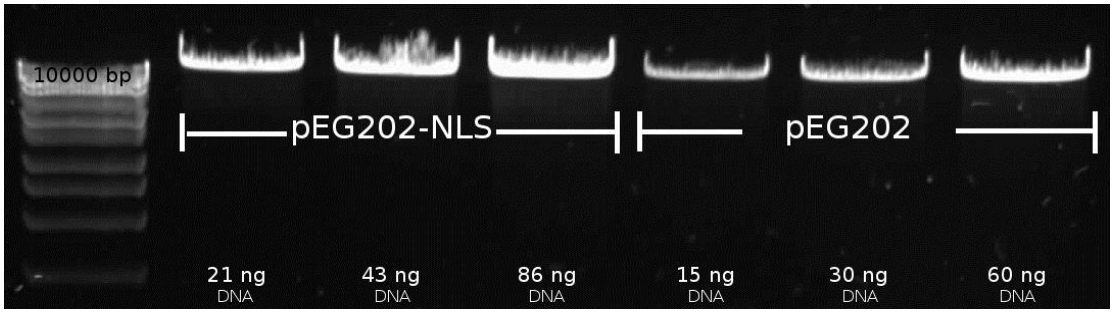

Figure 44: Agarose gel electrophoresis of linearized pEG202 and pEG202-NLS after digestion with *Eco*RI and *Bam*HI and gel purification.

The linearised vectors were stored at -20ºC until they were used for the ligation with hNEIL3 cDNA.

5.2.3 Cloning of hNEIL3 (A_2) into pEG202 and pEG202-NLS

The gel purified hNEIL3 DNA (A_2, Figure 43) with *Eco*RI and *Bam*HI overhangs was used to perform the ligation into both the pEG202 and pEG202-NLS vectors followed by a transformation into NovaBlue competent cells. Six colonies from each of the two plates were picked to inoculate 12 liquid cultures. All the liquid cultures grew and miniprep plasmid purification was performed.

To confirm the insert was cloned into the yeast vectors successfully a digest with *Eco*RI and *Bam*HI was carried out and an agarose gel ran to visualize the results. In Figure 45 it can be seen, that all clones have the correct size and thus were used for DNA sequencing.

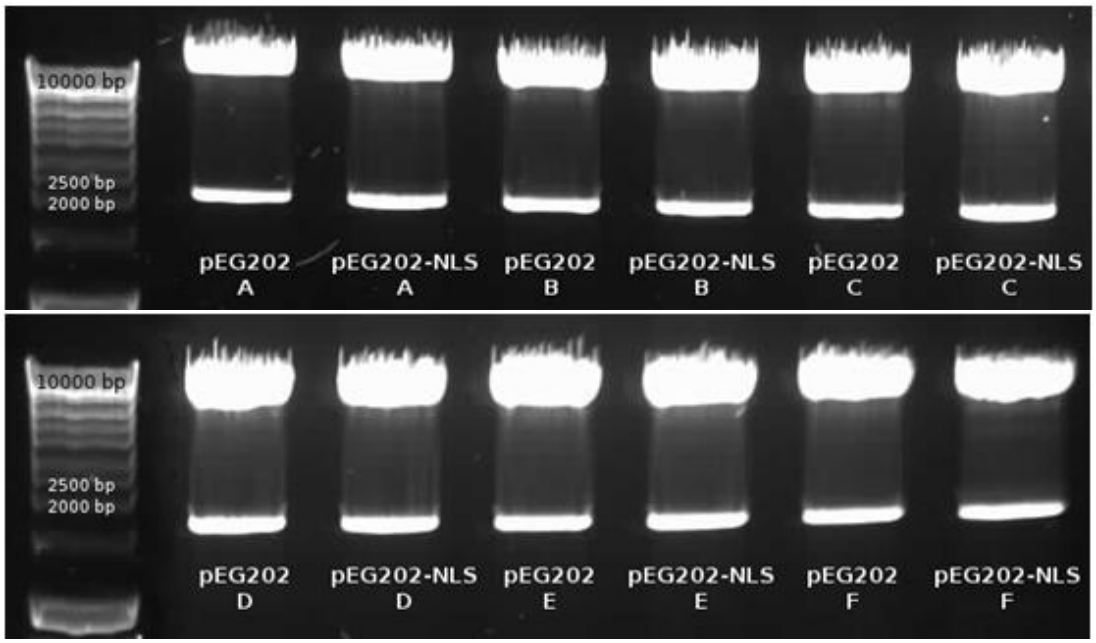

Figure 45: Agarose gel electrophoresis of pEG202-N3 and pEG202-NLS-N3 double-digested with *Eco*RI and *Bam*HI.

5.2.4 DNA sequencing

Because the DNA sequence of hNEIL3 in the pCMV6-AC vector from OriGene is different to the hNEIL3 cDNA sequence found on NCBI (http://www.ncbi.nlm.nih.gov/nuccore/NM_018248.2), the DNA sequences were analysed for known single nucleotide polymorphisms (SNPs) using the SNP search tool available at http://www.ncbi.nlm.nih.gov/projects/SNP/. Several SNPs were found and are shown in Appendix 8.4.

5.2.4.1 Primers used for DNA sequencing reactions:

N3_641 (Tm=60.6°C): 5′ - CAG ATG AAC AGA TCC ATC ACC TC - 3′
N3_793r (Tm=62.4°C): 5′ - GGC ACA CAG TTA TTC TGC AGT GG - 3′
N3_1249 (Tm=60.3°C): 5′ - CAA AAC TCT CCT CCT GCT AGT G - 3′
hNEIL3_1538 Reverse (T_m= 57.3ºC): 5′- CAC AAC TCG GAG AAT GCA GA - 3′

- To sequence the hNEIL3 insert in the pGEM-T vector the standard primers T7 and Sp6 were used as well as N3_641.

- To sequence the hNEIL3 insert in the pJET1.2/blunt vector standard primer T7, a reverse primer supported in the CloneJET kit, the N3_641 and the N3_1249 primers were used.

5.2.4.2 DNA sequencing of pEG202(-NLS)-N3-(A_2) (BioXAct-short)

pEG202-N3 (A_2) and pEG202-NLS-N3 (A_2) shown in Figure 45 were used for sequencing. Unfortunately, as it is shown in Table 17, point-mutations developed during the cloning process. All of these point-mutations were confirmed by comparing the amplified hNEIL3 DNA with the DNA sequence provided by OriGene (see Appendix 8.2). To check if the observed mutations had arisen during the amplification and cloning process, the hNEIL3 DNA in pCMV6-AC was sequenced and showed no variation to the DNA sequence provided by the supplier (Appendix 8.2). Therefore, these mutations must have occurred during amplification of the hNEIL3 cDNA from pCMV6-AC by the BioXAct-short DNA polymerase. The same mutations were found in both vectors used (pEG202 and pEG202-NLS).

Table 17: Point-mutations (not SNPs in hNEIL3) in the pEG202/N3 (A_2) and pEG202-NLS/N3 (A_2) DNA sequence.

Codon-Position *(bp)*	***426***	***1014***	***1219***	***1639***	***1787***
OriGenSequence	GAA (Glu)	GAT (Asp)	AAG (Lys)	GCA (Ala)	GGG (Gly)
DNA sequencingResult	GAG (Glu)	GGC (Asp)	GAG (Glu)	GTA (Val)	GAG (Glu)

(grey: no change in resulting amino acid; **black:** change in resulting amino acid)

5.2.4.3 DNA sequencing of pEG202(-NLS)-N3(-C_1) (BioXAct-short)

Because, the hNEIL3 cDNA C_1 shown in Figure 43 (obtained from another PCR) was also ligated into pEG202 and pEG202-NLS, DNA sequencing was performed to check if point mutations were also present in this sequence. However, like A_2, many point mutations appeared (data not shown) and the constructs could not be used for further studies.

5.2.4.4 DNA sequencing of pGEM-T-hNEIL3 (BioXAct-short)

From the DNA sequencing results of pEG202(-NLS)-N3 (A_2 and C_1) it was likely the base pair changes occurred during the initial PCR. Therefore, the PCR was repeated with BioXAct-short and the PCR products have been cloned into pGEM-T. To avoid loss of time, this construct was directly DNA sequenced. However, the hNEIL3 cDNA sequence again showed various point mutations, despite the presence of a proofreading activity on the DNA polymerase (data not shown).

5.2.4.5 DNA sequencing of pGEM-T-partial-hNEIL3 (BioXAct-short)

The three DNA sequencing results showed that the BioXAct-short from Bioline, designated as a proofreading polymerase mixture, was not able to amplify hNEIL3 cDNA without causing base changes. However, given the initial inability of this enzyme mixture to amplify full length NEIL3, (Section 5.2.1.2) it was decided to check if a truncated version of hNEIL3 (1000-1818bp) amplified with BioXAct-short and cloned into pGEM-T, also contained a significant number of base changes. However, analysis of this truncated NEIL3 clone again showed point mutations (data not shown). Interestingly, when all the DNA sequencing results were compared, apart from the random point mutations in the sequence, there was always one point

mutation which appeared in all four constructs, where guanine was changed to adenine at base pair position 1787 in the hNEIL3 sequence resulting in an altered amino acid (Figure 48). The significance of this is not known.

5.2.5 PCR of pCMV6-AC/hNEIL3 (Phusion)

To carry on with Y2H it was essential to obtain the hNEIL3 sequence without any base changes. Therefore, a new proofreading DNA polymerase called Phusion from Finnzymes was purchased (NEB). However, this DNA polymerase produces DNA fragments with blunt ends. Therefore, in place of pGEM-T, which has single T-overhangs to aid the ligation of Taq-generated amplicons, the CloneJET PCR Cloning Kit (Fermentas) was chosen for Phusion – generated ligation products. The conditions for the recommended two step PCR used for amplification of full length hNEIL3 are shown in Table 18.

Table 18: Conditions for PCR of full length hNEIL3 with Phusion DNA polymerase.

DNA	1.0 µl (10 ng)			
5x Buffer	10.0 µl			
100 mM dNTPs	0.4 µl (200 µM)	**Temp.**	**Time**	
10 µM *Full Primer*$_1$	1.0 µl (0.2 µM)	*98ºC*	*30 s*	
10 µM *Full Primer*$_2$	1.0 µl (0.2 µM)	**98ºC**	**10 s**	**30 Cycles**
Phusion	0.5 µl	**72ºC**	**1 min**	
H_2O	36.1 µl	*72ºC*	*10 min*	
Total	50.0 µl	*4ºC*	*Hold*	

The PCR product was then ligated into the pJET1.2/blunt vector (for vector map, see Appendix 8.1, Figure 97) using the conditions shown in Table 19 at a 3:1 insert to vector ratio.

Table 19: Scheme for the ligation of NEIL3 into pJET1.2/blunt vector.

2x Reaction mix	10 µl	
pJET1.2/blunt vector	1 µl	50 ng
PCR product	5 µl	~100 ng
T4 DNA Ligase	1 µl	
Deionized H_2O	3 µl	
Total	**20 µl**	

The ligation was carried out at an incubation temperature of 22.5 °C for 30 min.

The pJET1.2/blunt vector has a size of 2974 bp and hNEIL3, including *Eco*RI and *Bam*HI overhangs, 1830 bp. Figure 46 shows a digestion with *Eco*RI and *Bam*HI of the miniprep of pJET1.2/blunt containing the hNEIL3 insert and the bands are of the expected sizes.

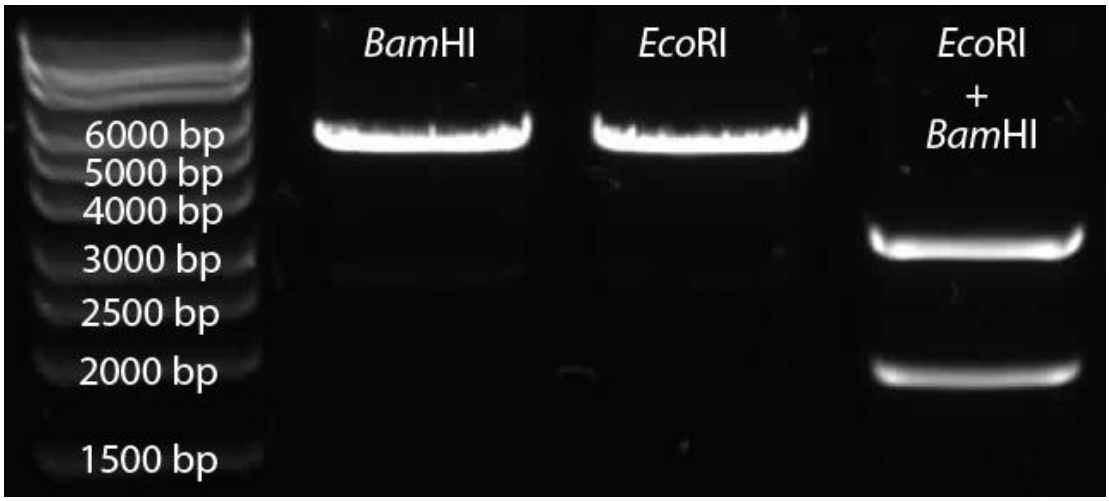

Figure 46: Agarose gel electrophoresis of single- and double-digests with *Bam*HI and *Eco*RI of pJET1.2/blunt vector containing NEIL3.

A large scale digestion was performed and gel purified to obtain the pure hNEIL3 fragment (data not shown) followed by ligation into pEG202 and pEG202-NLS. Figure 47 shows that hNEIL3 was cloned correctly into pEG202 and pEG202-NLS and the hNEIL3 insert was then subjected to DNA sequencing.

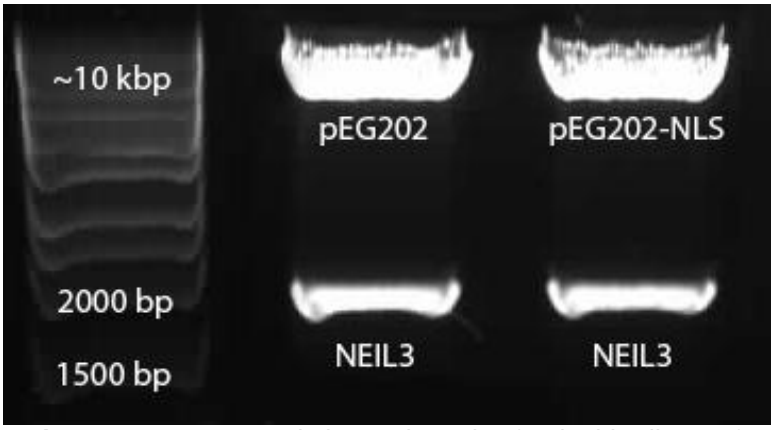

Figure 47: Agarose gel electrophoresis of a double-digest of pEG202(-NLS)-NEIL3 with *Eco*RI and *Bam*HI.

5.2.6 DNA sequencing of pEG202(-NLS)-N3 (Phusion)

The DNA sequencing results showed no point mutations in the hNEIL3 DNA (data not shown). Now it was possible to perform a large scale plasmid extraction (Maxiprep) of pEG202-N3 and pEG202-NLS-N3 and to prepare for the Y2H screening.

To sequence the whole of the hNEIL3 cDNA insert in pEG202 and pEG202-NLS and to ensure no mutation is present, the primers N3_641, N3_1538r, N3_793r and N3_1249 were used to perform the four sequencing reactions required. No base changes were obtained and as indicated in Figure 48 the point mutation that was induced when BioXAct Short was used (Section 5.2.4.5) was not obtained with Phusion DNA polymerase.

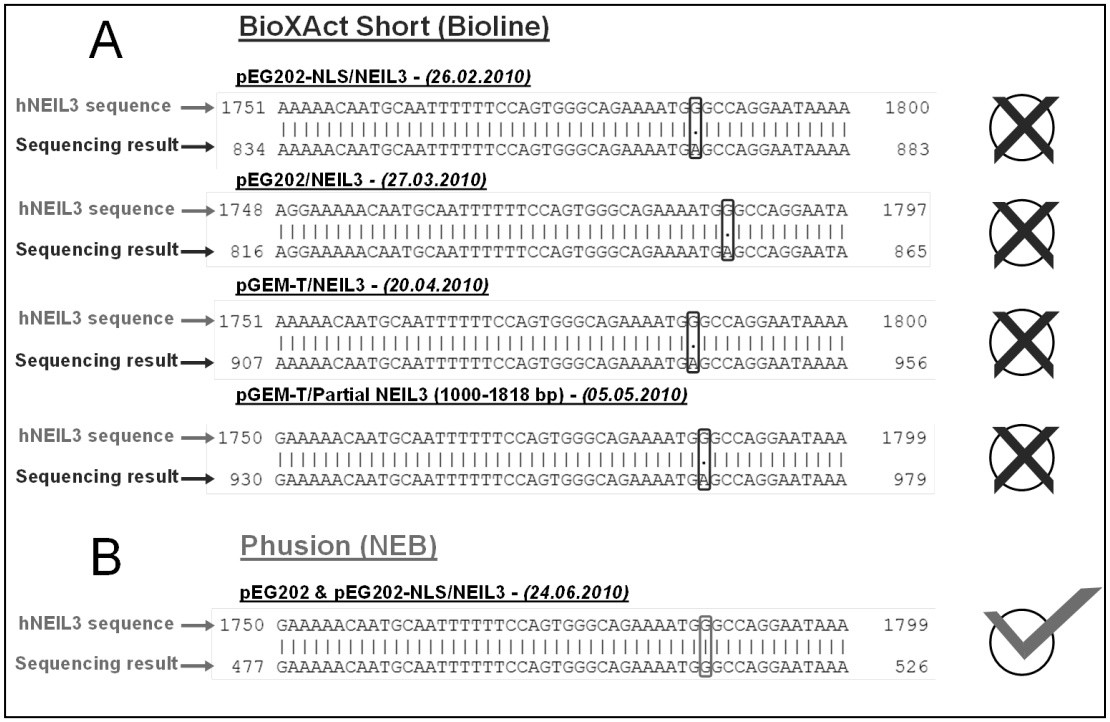

Figure 48: Summary of sequencing results. (Only the part is shown which represents the significant point mutation at bp 1787.)

5.3 Small scale transformation of pEG202(-NLS)-N3 into EGY48

The bait vectors pEG202-N3 and pEG202-NLS-N3 along with the other reporter plasmids (pRHFM1, pJK101, pSH17-4, and pEG202-Max) needed for the autoactivation tests and the repression assays were used to transform the yeast strain EGY48 (Figure 49). For more details on the vectors see Section 5.4 and Table 20.

Table 20: Summary of vectors used in Y2H.

Vector name	Genotype	Description
pEG202-NLS-N3	HIS3, Amp^r	Bait vector containing hNEIL3 CDS fused to LexA and an additional NLS
pEG202-N3	HIS3, Amp^r	Bait vector containing hNEIL3 CDS fused to LexA only
pEG202-Max	HIS3, Amp^r	Bait vector containing Lex A fusion protein sequence. Used as positive control in the repression assay and western blot.
pJG4-5	TRP1, Amp^r	Prey vector containing a random protein cDNA
pRHFM1	HIS3, Amp^r	Bait protein used as a negative control in LacZ autoactivation test along with pJK101
pSH17-4	HIS3, Amp^r	Bait protein used as a positive control in LacZ autoactivation test along with pJK101
pJK101	URA3, Amp^r, GAL1-2 ops.-LacZ	LacZ reporter plasmid used in repression assay
pRB1840	URA3, Amp^r, 1 op.-LacZ	Low sensitivity LacZ reporter plasmid used in cDNA library screen
pSH18-34	URA3, Amp^r, 8 ops.-LacZ	High sensitivity LacZ reporter plasmid used in cDNA library screen
pBait	HIS3, Amp^r	Used as positive control in mating assay in combination with pTarget.
pTarget	TRP1, Amp^r	Used as positive control in mating assay in combination with pBait.

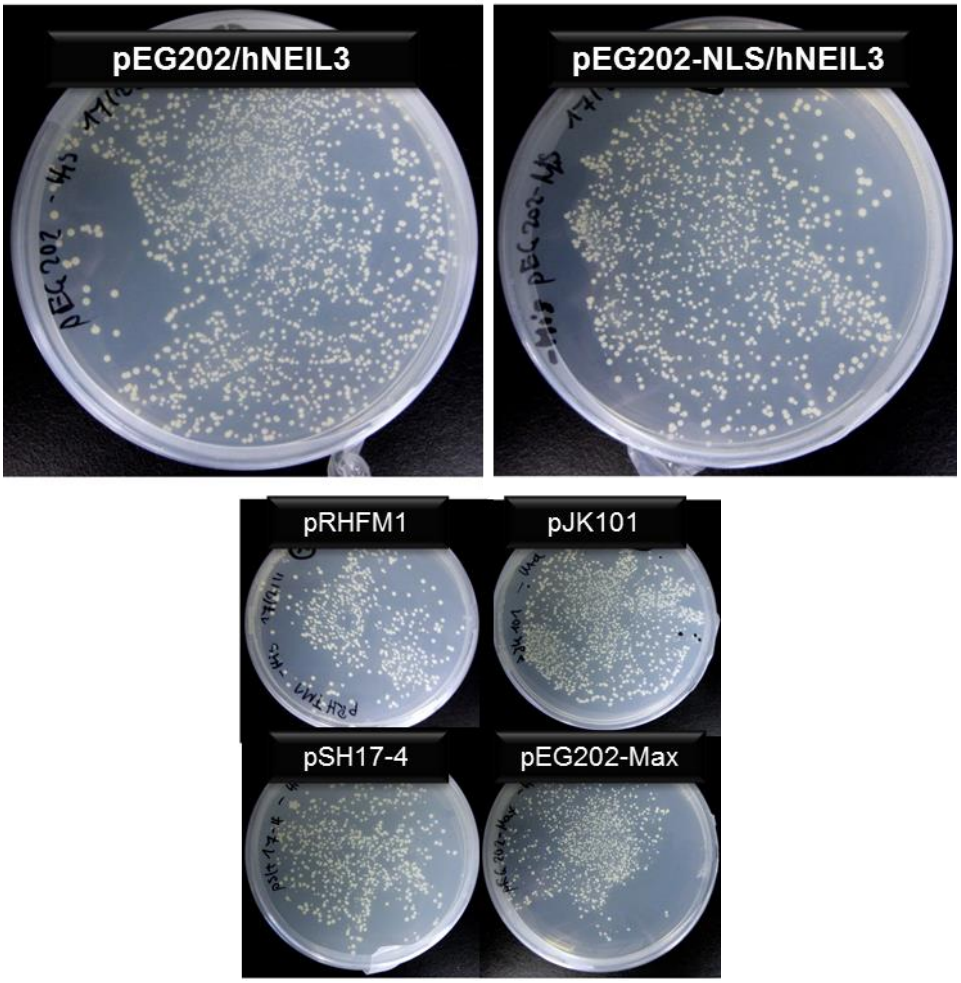

Figure 49: YNB (Glu) ura$^-$ (pJK101) and YNB (Glu) his$^-$ plates (all other vectors) with high colony number, showing high transformation efficiency of all necessary plasmids. pEG202-N3 and pEG202-NLS-N3 = Bait vectors; pRHFM1 and pSH17-4 were used for the *LacZ* autoactivation test; pJK101 and pEG202-Max were used for the LexA repression assay.

5.4 Autoactivation tests and repression assay

To test that the full length hNEIL3 fused with LexA (hNEIL3-LexA) protein is not autoactivating the leucine coding gene (*Leu2*) and *LacZ* expression on its own, autoactivation assays were carried out. If hNEIL3-LexA is able to interact with the activation domain of the transcription factor on its own and in absence of the prey fusion protein that contains the actual activating domain B42, it would cause false positive results. In addition, a repression assay was performed to show that, after translation, the hNEIL3-LexA fusion protein is able to enter the nucleus and bind to LexA operators in the genomic DNA of EGY48 or the reporter vectors used in this project, respectively.

The following combinations of plasmids were transformed into yeast strain EGY48 as described in Section 4.13.1:

For the *Leu2* expression autoactivation test:

- pEG202-N3
- pEG202-NLS-N3

For the *LacZ* expression autoactivation test:

- pEG202-N3 or pEG202-NLS-N3 and pRB1840 (test)
- pSH17-4 and pRB1840 (positive control)
- pRFHM1 and pRB1840 (negative control)

For the repression assay:

- pEG202-N3 or pEG202-NLS-N3 and pJK101 (test)
- pEG202-Max and pJK101 (positive control)
- pJK101 only (negative control)

The results of each of these tests and details about the function of each vector will be described in the following sections.

5.4.1 Autoactivation test of Leu2 expression by hNEIL3-LexA

Before carrying out a large scale transformation with the cDNA library plasmids, the plasmid vectors pEG202-N3 and pEG202-NLS-N3 were tested for autoactivation of the leucine coding gene (*Leu2*). Therefore, clones containing either pEG202-N3 or pEG202-NLS-N3 where plated onto YNB (Glu) his^-/leu^-, or YNB (Glu) his^- agar plates, respectively. No growth on YNB (Glu) his^-/leu^-, but on YNB (Glu) his^- was observed which indicates full length hNEIL3-LexA did not activate *Leu2* expression on its own (Figure 50).

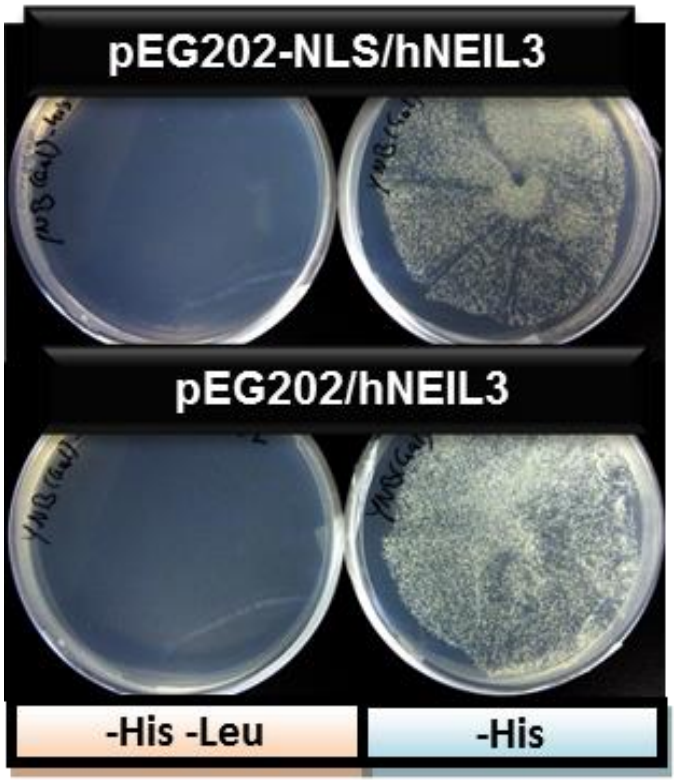

Figure 50: Plating EGY48 containing either pEG202-NLS/hNEIL3 or pEG202/hNEIL3 onto YNB (Glu) his^-/leu^- or YNB (Glu) his^- agar respectively showed that full length hNEIL3 does not activate leucine expression on its own.

5.4.2 Autoactivation test of LacZ expression by hNEIL3-LexA

In addition to *Leu2*, the potential of the hNEIL3-LexA fusion protein to autoactivate *LacZ* gene expression had also to be tested, in order for a correct interpretation of the results obtained by the subsequent cDNA library screening. The ADH promoter in pRFHM1 expresses a LexA-Bicoid homeodomain fusion that is not able to activate *LacZ* gene expression on its own, whereas the ADH promoter in pSH17-4 expresses a LexA-GAL4 activation domain fusion that activates *LacZ* gene expression. Hence, pRFHM1 clones were used as a negative and pSH17-4 clones as a positive control in the *LacZ* autoactivation test (Section 5.4.2).

Figure 51 shows that neither pEG202-N3 (Figure 51, 2) nor pEG202-NLS-N3 (Figure 51, 1) results in autoactivation of *LacZ* gene expression, indicated by the yellowish colour of the colonies that is the same as for the negative control (Figure 51, 3). The negative controls are EGY48 yeast cells that contain the pRFHM1 plasmid, and the positive controls are EGY48 cells containing the pSH17-4 plasmid (Figure 51, 4).

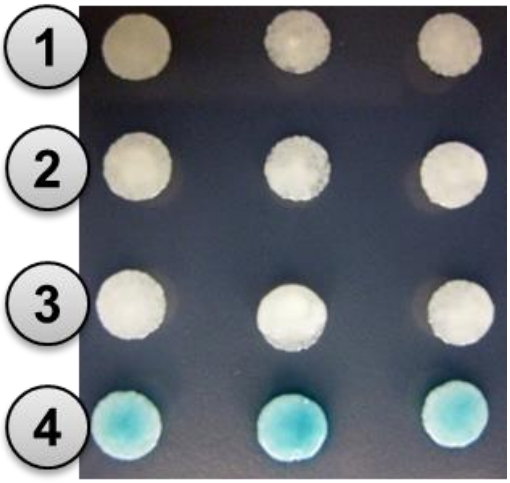

Figure 51: Testing the *LacZ* gene autoactivation potential of pEG202-NLS-N3 (1) and pEG202-N3 (2). No autoactivation of the *LacZ* gene occurred. (3) pRFHM1 as negative control and (4) pSH17-4 as positive control.

5.4.3 Repression assay

To test if the bait vectors pEG202-N3 (Figure 52, 2) and pEG202-NLS-NEIL3 (Figure 52, 3) were able to enter the nucleus and bind LexA operators, repression assays using the pJK101 reporter plasmid were performed (Figure 101). pJK101 contains a LexA operator between its upstream activation sequence (UAS) and the TATA box of the GAL1-10 promoter. pEG202-Max is a vector that expresses a LexA fusion protein known to tightly bind to LexA operators in pJK101 and therefore was used as a positive control in this repression assay that results in white colonies, while clones that contain pJK101 alone will not be repressed in the production of β-galactosidase and thus colonies turn blue on X-Gal containing plates. Hence, if hNEIL3-LexA fusion protein binds to the LexA operators it will reduce or abolish *LacZ* gene expression by disrupting the UAS-TATA box signalling in pJK101.

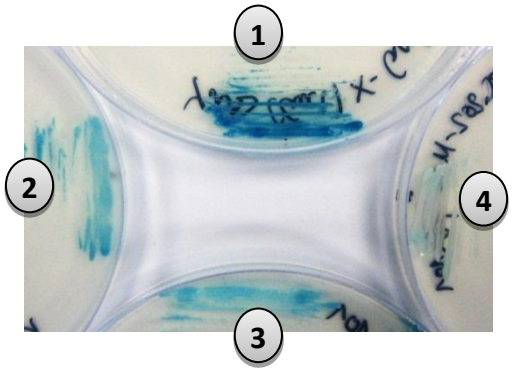

Figure 52: Result of the repression assay. pEG202-N3 (2); pEG202-NLS-N3 (3); negative (1) and positive (4) control.

Compared with the negative (Figure 52, 1) and positive (Figure 52, 4) controls, same levels of repression of *LacZ* expression was observed for both pEG202-N3 and pEG202-NLS-N3. This result indicated that NEIL3-LexA was able to enter the nucleus and therefore an additional NLS was not needed in this Y2H assay.

5.5 Western blot of hNEIL3-LexA expression

To further check that the autoactivation tests were genuine, a western blot was performed to confirm hNEIL3-LexA expression in EGY48. Therefore, actual screening conditions where prepared, *i.e.* the clones were transformed with the bait vectors along with the *LacZ* reporter plasmid pRB1840 that was needed for subsequent blue/white screening once potential positive clones were identified via leucine selection (Section 5.6.3). Therefore, three 10 ml cultures were prepared, the first, (YNB (Glu) his^-/ura^-) was inoculated with an EGY48 colony containing pEG202-N3 and pRB1840 reporter plasmid, the second (YNB (Glu) his^-/ura^-) with an EGY48 colony containing pEG202-Max and pRB1840 plasmids (positive control) and finally (YNB (Glu) ura^-) with EGY48 containing pRB1840 only (negative control) and incubated at 30°C and 250 rpm overnight or until OD_{600}= ~3.0. The proteins were extracted as described in Section 4.11.1 and then separated by SDS-PAGE. The subsequent western blot was probed with a polyclonal anti-LexA antibody and the results showed a band at 91 kDa (61 kDa hNEIL3 + 30 kDa LexA, Figure 53, 1) as predicted for pEG202-N3. Lower molecular mass bands were also visible, probably representing different degradation states of the hNEIL3-LexA fusion protein. The negative control (Figure 53, 2) showed no band at 91 kDa and pEG202-Max, used as a positive control (Figure 53, 3), showed expression of a LexA fusion protein at ~45 kDa.

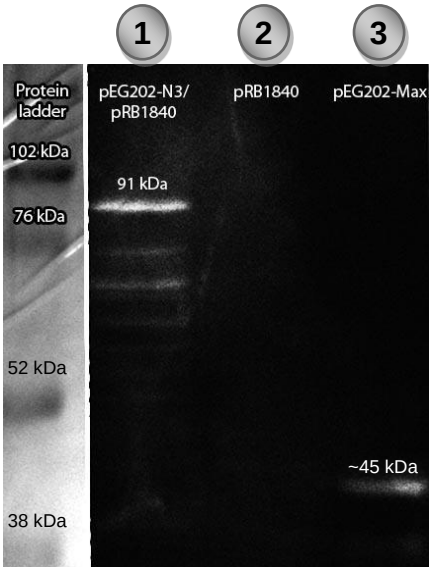

Figure 53: Western blot of hNEIL3-LexA fusion protein expressed from pEG202-N3 (1), a negative (2) and a positive control (3).

5.6 Y2H screening with a human placental cDNA library

5.6.1 Large scale transformation of library cDNA

As the autoactivation tests, the repression assay and the western blot showed encouraging results, it was likely that full length hNEIL3 could be used to screen a cDNA library by Y2H. Therefore, a large scale transformation of a placental cDNA library into EGY48 containing pEG202-N3 was performed as described in Section 4.13.2. To estimate the transformation efficiency the control plate (made out of one of the 30 transformations and used in a 1:1000 dilution, Section 4.13.2) was examined after two days of incubation and 70 colonies were counted. Using the formula "colonies counted (70) x dilution factor (1000) x number of transformation tubes (30)" a total number of 2.1 x 10^6 transformants were calculated. To perform a successful screening 1.47 x 10^7 (= 7 x 2.1 x 10^6) transformants were needed to ensure full coverage of the cDNA library for the subsequent screening. Due to the fact that each of the 1 ml aliquots contained 2.8 x 10^8 cfu (estimated by plating and colony counting one 1 ml aliquot) a 52.5 µl volume (~1.47 x 10^7 cfu) was used to inoculate ~1.42 ml

YNB (Gal,Raf) ura$^-$/his$^-$/trp$^-$/leu$^-$ liquid media to obtain a 1 x 10^7 cfu/ml culture. After incubation at 30°C and 150 rpm for 4 h, to induce prey production by the presence of galactose, 100 µl aliquots were spread onto YNB (Gal,Raf) ura$^-$/his$^-$/trp$^-$/leu$^-$ plates (~1 x 10^6 cfu/plate) and left at 30°C for more than 7 days.

5.6.2 Screening of transformants for potential positive interactors

The cDNA library screening was carried out in duplicate to ensure that as many potential interacting protein partners for hNEIL3 as possible would be found. Although the growth of first colonies started after five instead the expected two days, the results were assumed to be genuine as it was still within the timeframe indicated in the DupLEX-A application guide (OriGene, Figure 54), especially as negative control plates (clones containing either prey or bait and reporter vector only) showed no growth over ten days incubation at 30°C. Therefore, 216 colonies were picked on day seven and spotted onto YNB (Gal,Raf) ura$^-$/his$^-$/trp$^-$/leu$^-$ master plates followed by incubation at 30°C for two days. On these plates, 190 colonies grew (see in Appendix, Figure 106) and were used for further tests.

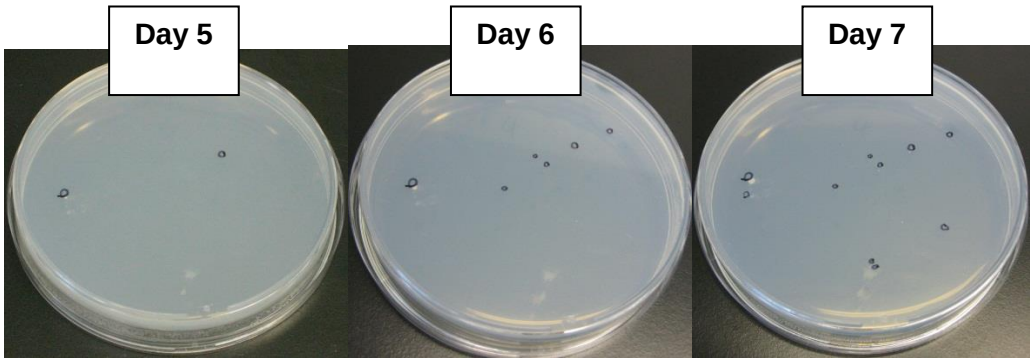

Figure 54: One out of 28 YNB (Gal,Raf) ura$^-$/his$^-$/trp$^-$/leu$^-$ plates as example for showing growth of 100 µl of induced transformants (~1 x 10^6 colony forming units) per plate over a 72 h period.

5.6.3 Galactose/Glucose tests with potential positive clones

In the pJG4-5 vector, library fusion protein expression is induced by a Gal1 promoter (for more details see Appendix - Figure 100). Therefore, yeast carrying potential protein partners for hNEIL3 should only be able to grow on Gal^+ but not on Gal^-/Glu^+ plates and the 190 potential positive colonies were spotted onto YNB (Gal,Raf) $ura^-/his^-/trp^-/leu^-$ and YNB (Glu) $ura^-/his^-/trp^-/leu^-$ plates and grown over night at 30°C. Unfortunately, growth for all 190 colonies occurred on both selective media. It was assumed the use of the most sensitive yeast strain, EGY48, that contained six LexA operators had resulted in autoactivation of leucine expression by hNEIL3, even although autoactivation tests were negative (Section 5.4.1). To double check this result, 190 x 2 ml tubes containing 1 ml Glu^+ liquid media were prepared and inoculated with all 190 colonies from the Gal^+ master plates. After overnight incubation at 30°C and 200 rpm, 20% of the cultures grew. On the second day 40% had grown and on the third day >80% had grown (data not shown). Because the DupLEX-A application guide (OriGene) for the Y2H assay suggested that growth on plates should be checked after 1-2 days, a final test was performed. All 190 colonies were picked again from Gal^+ master plates, inoculated into 600 µl YNB (Gal,Raf) $ura^-/his^-/trp^-/leu^-$ liquid medium and grown at 30°C and 200 rpm for 2 days. Then 2 µl of each culture was spotted onto both Gal^+ and Glu^+ plates. This method ensured the same concentration of colony forming units on both plates. These plates were then incubated at 30°C. After 24 hours the first examination showed equal growth on both, Gal^+ and Glu^+ plates (some spots even grew faster on Glu^+ plates, Figure 55).

Galactose plates Glucose plates

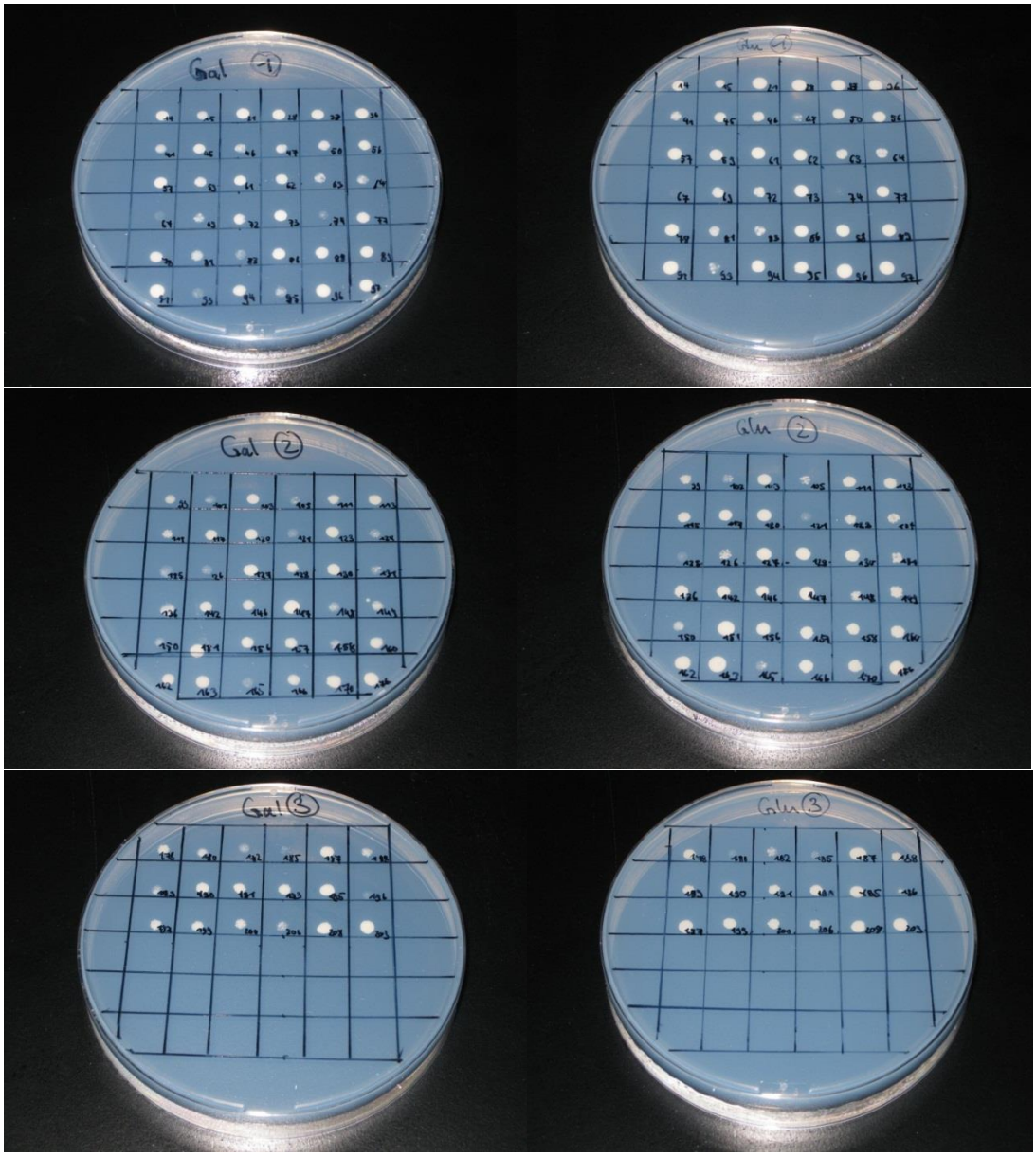

Figure 55: Galactose/Glucose test of potential positive interactors on leucine lacking YNB medium.

5.6.4 X-Gal test of potential positive interactors

Although, results from the Galactose/Glucose test (Section 5.6.3) indicated that non-specific activation of *Leu2* expression had occurred in these clones, the X-Gal screening was performed to confirm this. This assay is to check if the potential positive clones obtained from the initial *Leu2* screen show the same behaviour in an alternative reporter gene assay that uses *LacZ* gene expression instead of *Leu2*. This test was performed on YNB (Gal, Raf, X-Gal) $ura^-/his^-/trp^-$ and YNB (Glu, X-Gal) $ura^-/his^-/trp^-$ plates as indicated in the manual (Figure 56) but additionally on YNB (Gal, Raf, X-Gal) $ura^-/his^-/trp^-/leu^-$ and YNB (Glu, X-Gal) $ura^-/his^-/trp^-/leu^-$ plates to determine if the lack of leucine affected the ability of the clones to metabolise X-Gal (Figure 57).

Following incubation at 30°C overnight, growth was observed on both Glu^+ and Gal^+ plates lacking leucine, which is the same result as obtained for the initial Galactose/Glucose test (Section 5.6.3). If growth on glucose plates was due to a non-specific interaction, it would be expected that all colonies would turn blue in the presence of either glucose or galactose. However contrary to this, and unexpectedly, a differential response was observed with 60 colonies turning blue and the remainder (30 colonies) remaining colourless on galactose containing medium. Encouragingly, very few colonies turned blue on glucose plates (5 out of 65 colonies; red circles in Figure 57) and similar results were obtained independent of the presence of leucine in the media (Figure 56, Figure 57). Therefore, this result suggested that the protein-protein interactions might be genuine in this screen and the isolation of the library plasmids from colonies that turned blue on Gal^+ but remained white on Glu^+ plates for DNA sequencing was carried out.

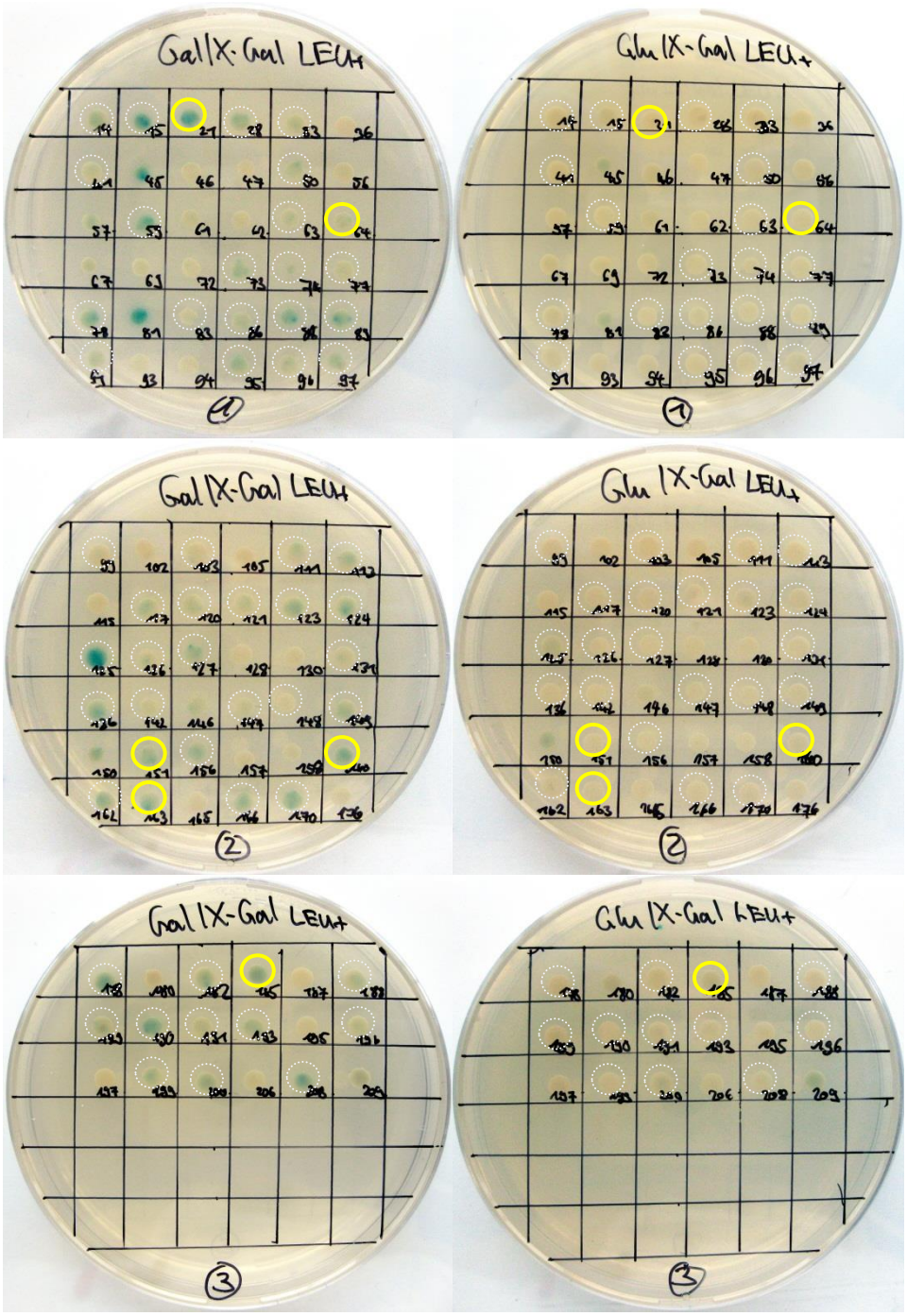

Figure 56: Potential positve clones spoted onto YNB (Gal,Raf,X-Gal) $his^-/ura^-/trp^-$ (left) and YNB (Glu,X-Gal) $his^-/ura^-/trp^-$ (right). Grey doted circles indicate clones were chosen for further experiments, yellow circles indicate clones that showed to be potential genuine clones after plasmid extraction (Section 5.6.7).

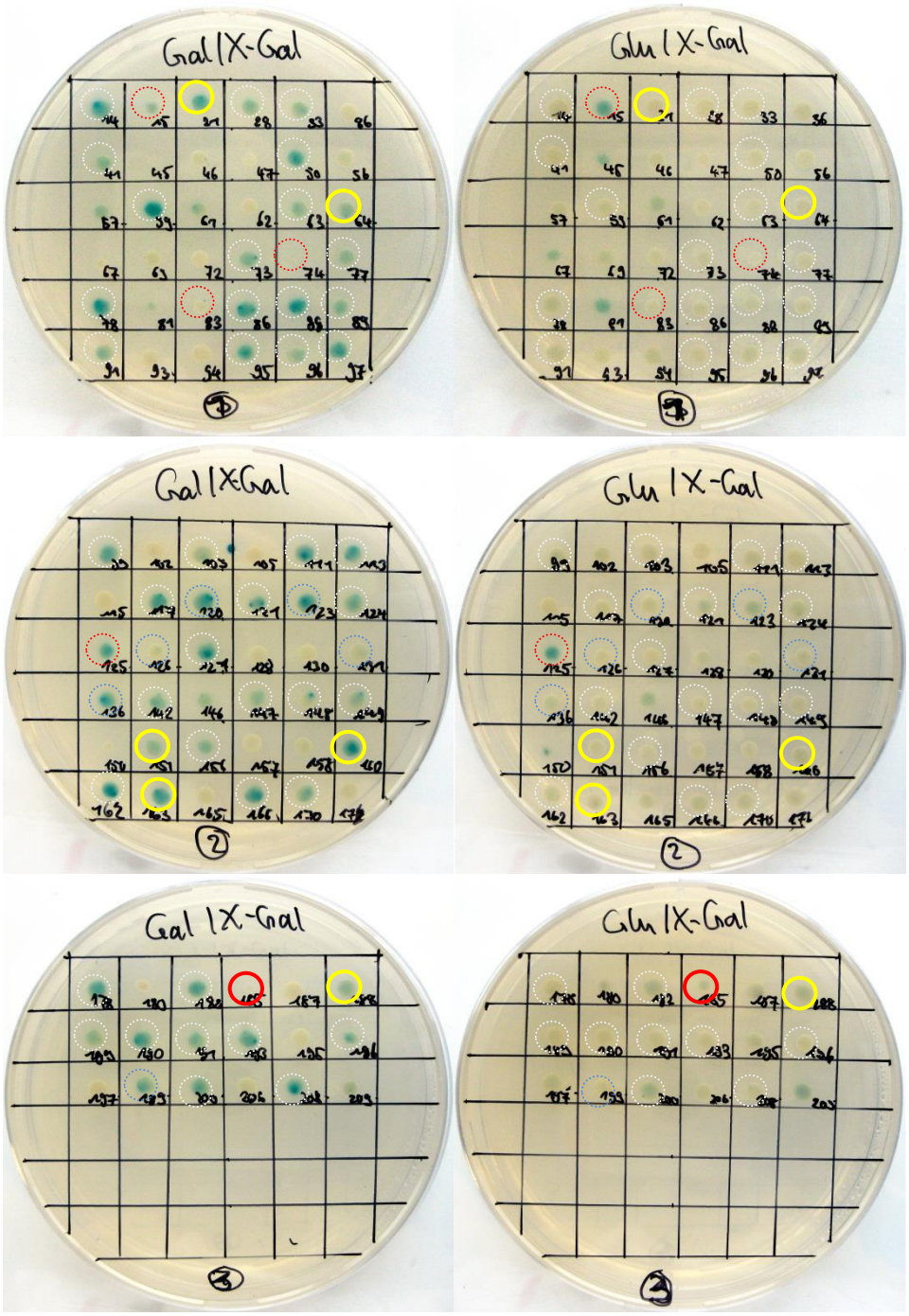

Figure 57: Potential positve clones spotted onto YNB (Gal,Raf,X-Gal) $his^-/ura^-/trp^-/leu^-$ (left) and YNB (Glu,X-Gal) $his^-/ura^-/trp^-/leu^-$ (right). Grey doted circles indicate clones were chosen for further experiments, yellow circles indicate clones that showed to be potential genuine clones after plasmid extraction (Section 5.6.7), red circles indicate clones where X-Gal degradation was higher on Glu^+ plates than on Gal/Raf^+ plates, an indicator for false positives.

5.6.5 *Library plasmid DNA identification – "modified" standard method*

In this method the library plasmid pJG4-5 (Figure 100) was extracted from yeast as described in Section 4.13.4.1. Although, plasmid DNA was obtained from all clones, a digestion with *Eco*RI and *Xho*I of these vectors revealed that some vectors contained a band around 2000 bp (Figure 58). DNA sequencing of these vector inserts confirmed, the bands were hNEIL3 inserts and the band around 10,000 bp was the pEG202 vector (sequencing data not shown). Only the clones 14, 41, 59, 63 and 200 were pJG4-5 vectors carrying a random cDNA insert from the library (see BLAST results in Appendix 8.6.1).

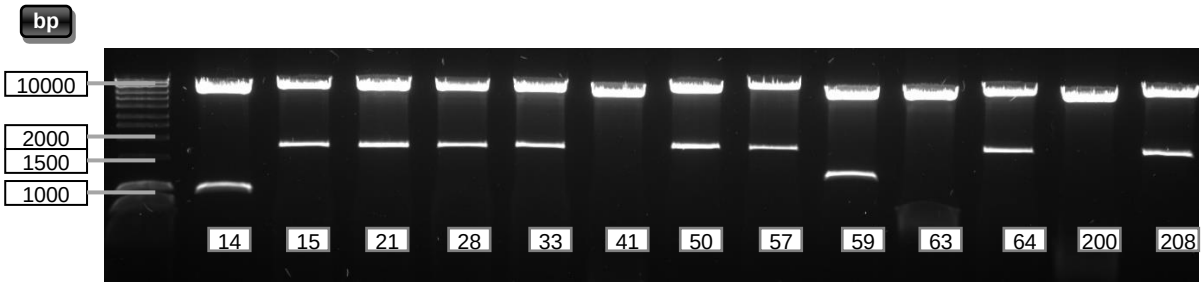

Figure 58: Agarose gel electrophoresis of potential positive clone plasmid extractions. Clones 15, 21, 28, 33, 50, 57, 64 and 208 were pEG202 plasmids carrying a hNEIL3 cDNA insert. Clones 14, 41, 59, 63, 200 show different sizes of inserts and were potential positives.

This result was unexpected, as the bacterial KC8 strain used for electroporation is *trp*$^-$ and as pJG4-5 enables tryptophan production only clones carrying this plasmid should grow on media lacking tryptophan. This shows that pEG202-N3 was also electroporated into the bacterial *trp*$^-$ KC8 strain instead of, or along with, the library plasmid pJG4-5 and that tryptophan selection did not work as was intended. Therefore, the experiment was repeated with the original method described in the DupLexA manual (OriGene) but the efficiency was even lower. Out of 22 clones used for extraction and electroporation into KC8 cells only 6 were transformed successfully and subsequent restriction enzyme digest with *Eco*RI and *Xho*I revealed that only three contained the library vector (clones 28, 89 and 99 in Figure 59).

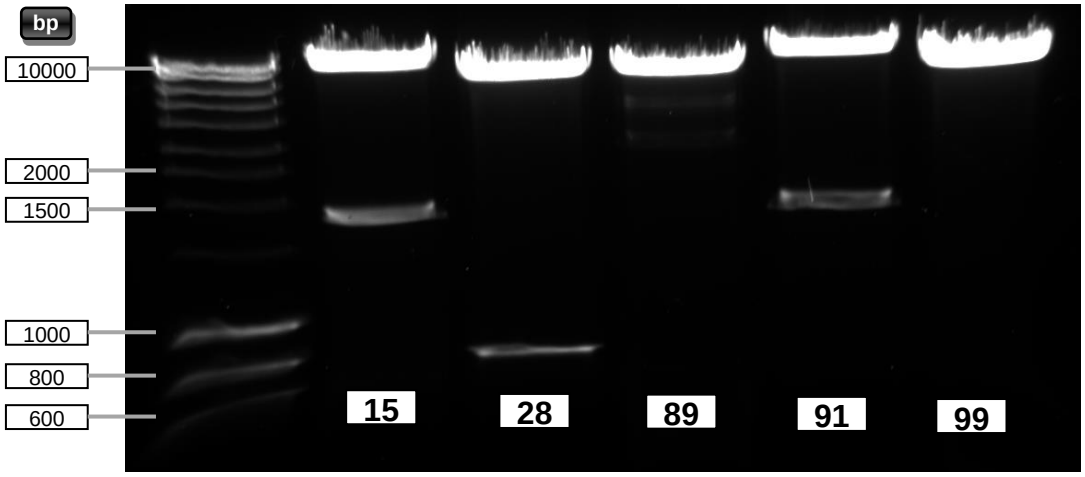

Figure 59: Agarose gel electrophoresis of potential positive clones 15, 28, 89, 91, 99 obtained by the standard plasmid extraction method described in the DupLexA application guide (OriGene).

Therefore, a more specific method was designed (Section 4.13.4.2) that allowed direct DNA sequencing of PCR products obtained from the cDNA library inserts without the need for separation of the extracted plasmid mixture (pEG202-N3, pJG45 and pRB1840) from yeast.

5.6.6 Library plasmid DNA identification – "PCR Method"

An initial test of the alternative method using direct PCR from yeast plasmid extractions on four clones, confirmed that the same insert sequences were obtained by PCR by both methods. DNA fragments obtained by the PCR method from clone 15 (negative control) and clones 14, 28 and 63 showed the same size (Figure 60) as previously obtained by using the standard method (Figure 58, Figure 59). Furthermore, DNA sequencing of these PCR products revealed that they had the same sequence as obtained from the products in Section 5.6.5. In addition, it was even possible to sequence the cDNA of clone 28 for the first time. Hence, it was confirmed that the alternative method was highly specific and with a higher efficiency that made it possible to sequence the cDNA of all potential positive clones quickly.

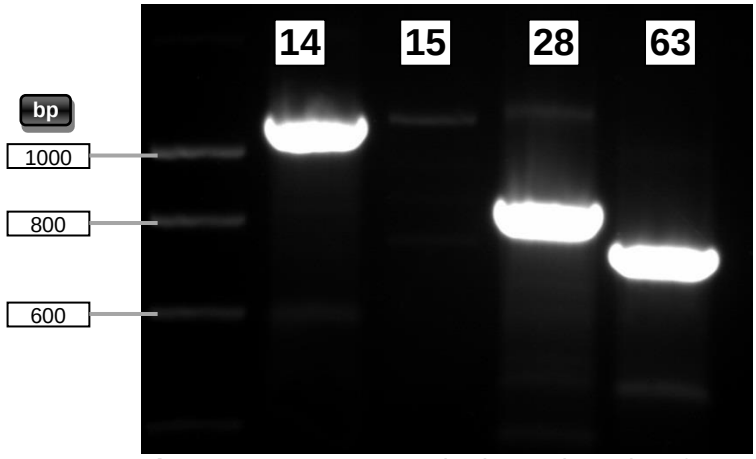

Figure 60: Agarose gel electrophoresis of PCR products (cDNA inserts from clones 14, 15, 28, 63) amplified from pJG4-5 library plasmids extracted from potential positive clones.

As the functionality of the PCR method was successfully validated it was now possible to extract library plasmid DNA from the 60 potential positive yeast clones and to directly amplify the cDNA sequences with Taq polymerase for subsequent DNA sequencing. The quality of all PCR products, after purification was good enough to proceed with DNA sequencing without the need of further processing (Appendix 8.5, Table 25). Figure 60 to Figure 66 show PCR products of all clones chosen through evaluation of the X-Gal test (Section 5.6.4) for the DNA sequencing step. Figure 61 shows that all PCR reactions worked except for clone 50.

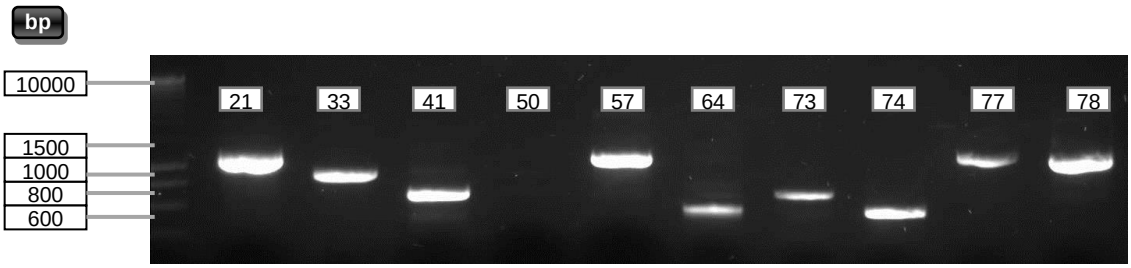

Figure 61: Agarose gel electrophoresis of PCR products (cDNA inserts from clones 21, 33, 41, 50, 57, 64, 73, 74, 77, 78) amplified from pJG4-5 library plasmids and extracted from yeast strain EGY48.

Figure 62 shows that PCR worked for all clones. However, clones 89 and 91 showed several bands and subsequent DNA sequencing gave no results (Appendix 8.6.1). Furthermore, subsequent DNA sequencing revealed that clone 83, 86, 95 and 96 were also not genuine PCR products.

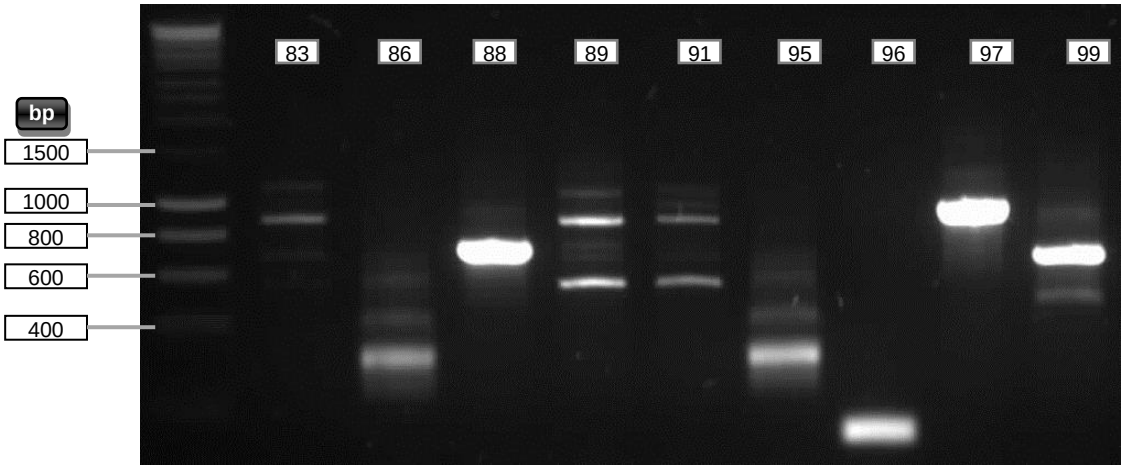

Figure 62: Agarose gel electrophoresis of PCR products (cDNA inserts from clones 83, 86, 88, 89, 91, 95, 96, 97, 99) amplified from pJG4-5 library plasmids and extracted from yeast strain EGY48.

Figure 63 shows PCR products for all clones tested. However, clone 121 did not give any result in subsequent DNA sequencing (Appendix 8.6.1).

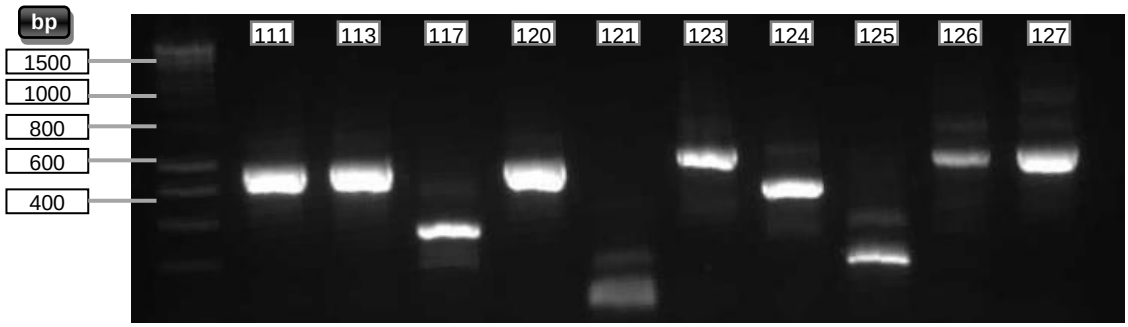

Figure 63: Agarose gel electrophoresis of PCR products (cDNA inserts from clones 111, 113, 117, 120, 121, 123, 124, 125, 126, 127) amplified from pJG4-5 library plasmids and extracted from yeast strain EGY48.

Figure 64 shows that PCR products were obtained for all clones used except for clone 156.

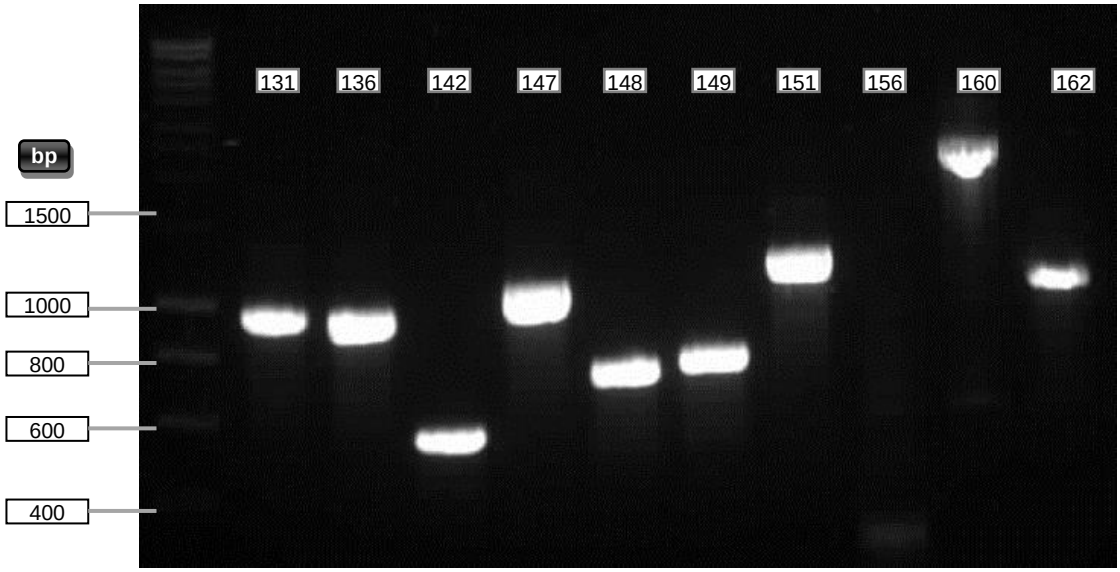

Figure 64: Agarose gel electrophoresis of PCR products (cDNA inserts from clones 131, 136, 142, 147, 148, 149, 151, 156, 160, 162) amplified from pJG4-5 library plasmids and extracted from yeast strain EGY48.

Figure 65 reveals that PCR products from clones 178 and 190 were apparently not amplified properly. However, while this was confirmed by DNA sequencing for clone 190 it was not for 178 which showed to be correctly amplified by PCR with Taq polymerase indicating that the band around 500 bp was genuine (Appendix 8.6.1).

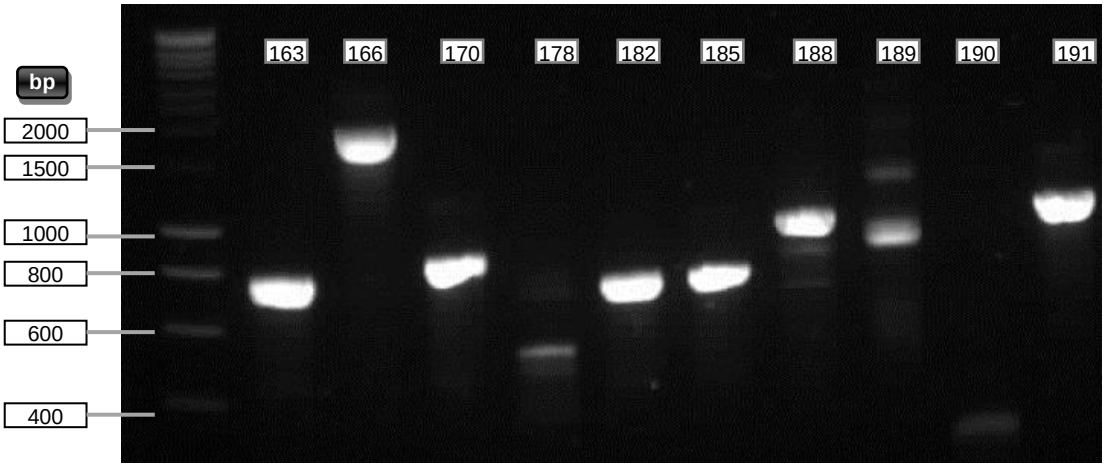

Figure 65: Agarose gel electrophoresis of PCR products (cDNA inserts from clones 163, 166, 170, 178, 182, 185, 188, 189, 190, 191) amplified from pJG4-5 library plasmids and extracted from yeast strain EGY48.

Figure 66 shows that PCR products were obtained for all clones. However, the band for clone 196 was blurred and although subsequent DNA sequencing revealed a sequence for that clone, it could not be identified by BLAST (Appendix 8.6.1).

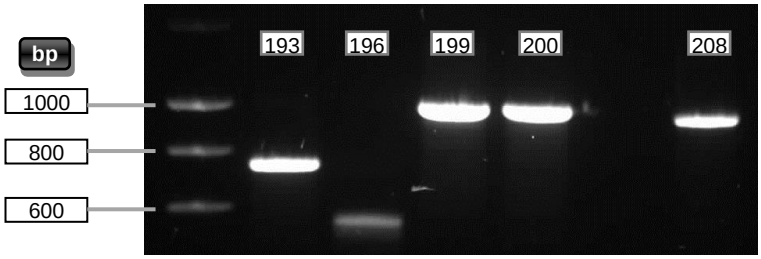

Figure 66: Agarose gel electrophoresis of PCR products (cDNA inserts from clones 193, 196, 199, 200, 208) amplified from pJG4-5 library plasmids and extracted from yeast strain EGY48.

5.6.7 DNA sequencing of potential clones

DNA sequencing and subsequent BLAST analysis of the 60 PCR products obtained from potential positive plasmid extractions revealed several potential genuine interactors (*i.e.* they were considered genuine if the library sequences contained a coding sequence in the correct reading frame in the library vector). The growth hormones chorionic somatomammotropin hormone 1 (placental lactogen; CSH1),

chorionic somatomammotropin hormone 2 (CSH2) and chorionic gonadotropin, beta polypeptide 8 (CGB8) were found in more than one clone. In addition, a number of unique clones were discovered that coded for, proteoglycan decorin, the metallopeptidase inhibitor TIMP2, a homeobox protein domain (HOPX), the RNA-binding protein ELAV1 (HuR), haemoglobin (gamma G, HBG2 and beta, HBB) and the translational-controlled tumour protein TPT1 (Appendix 8.6.1).

5.6.8 Mating Assay

After DNA sequencing of the potential positive clones was completed, a mating assay was performed to further confirm their ability to interact with hNEIL3. Therefore, all three plasmids present in each of the clones (the library, bait and reporter plasmid) were isolated and the mixture used to transform the yeast strain EGY48. In order to ensure that EGY48 cells contained only library plasmids, the transformants were streaked onto YNB (Glu) trp^- plates ensuring that tryptophan would be the only selective factor (as required for the library vector pJG4-5). However, as the plasmid extractions used for this transformation also contained pEG202-N3 (enables histidine production) and pRB1840 (enables uracil production) it was necessary to further identify the transformants obtained via tryptophan selection and containing pJG4-5. Therefore, colonies were re-streaked onto YNB (Glu) $his^-/ura^-/trp^-$, YNB (Glu) ura^-/trp^-, YNB (Glu) his^-/trp^- and YNB (Glu) trp^- plates. This way it was possible to pick colonies only growing on YNB (Glu) trp^- but not on one of the others, which confirmed that those clones only carry the cDNA library vector (pJG4-5). Transformants obtained this way contained library plasmids carrying cDNA inserts of either HOPX, SMC6, Phosphorylase 1, CSH1, CGB8, CSH2, TPT1, ELAV1, Decorin or Haemoglobin. These clones were then picked from the trp^- plates and restreaked onto YPD plates with a vertical orientation (Figure 67). In addition, the

vector pEG202-N3 was transformed along with the reporter plasmid pRB1840 into the yeast mating strain RFY206. These transformants were streaked in a horizontal orientation onto YPD that crossed the vertical streak containing EGY48 transformants carrying the cDNA library vector pJG4-5 (Figure 67). If mating occurs between the RFY206 and EGY48 strains in the middle of the cross, clones at this position should contain all three plasmids (pEG202-N3, pRB1840 and pJG4-5) while cells on the outside of the cross should remain in their initial state. Therefore, clones picked from the middle should be able to produce histidine, uracil and tryptophan. Only these clones were able to grow on YNB (Glu) $ura^-/his^-/trp^-$ plates (Figure 68). In addition a positive control was generated. The vector pBait expresses a LexA fusion protein that is known to interact with the B42 fusion protein that is expressed by pTarget. Therefore, this vector combination was used as a positive control in the mating assay and was generated the same way as described before.

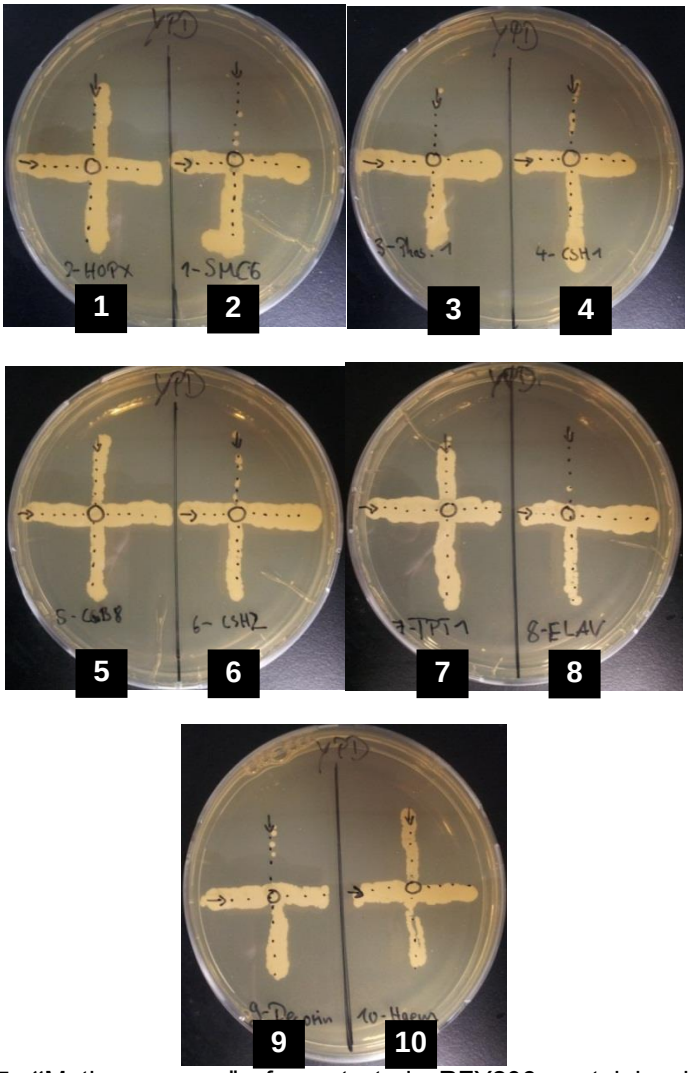

Figure 67: "Mating crosses" of yeast strain RFY206 containing hNEIL3 and reporter plasmid (lane from left to right containing bait plasmid pEG202-N3 + reporter plasmid pRB1840) and strain EGY48 containing potential positive findings (library plasmids containing cDNA of HOPX (1); SMC6 (2); Phosphorylase 1 (3); CSH1 (4); CGB8 (5); CSH2 (6); TPT1 (7); ELAV1 (8); Decorin (9); Haemoglobin beta (10)) after two days of growth.

In Figure 68 it can be seen that clones transferred from the junction of the "mating cross" grew on YNB (Glu,X-Gal) $ura^-/his^-/trp^-$ plates while clones picked from the outsides of the cross did not. This was as expected and was found for all mated clones.

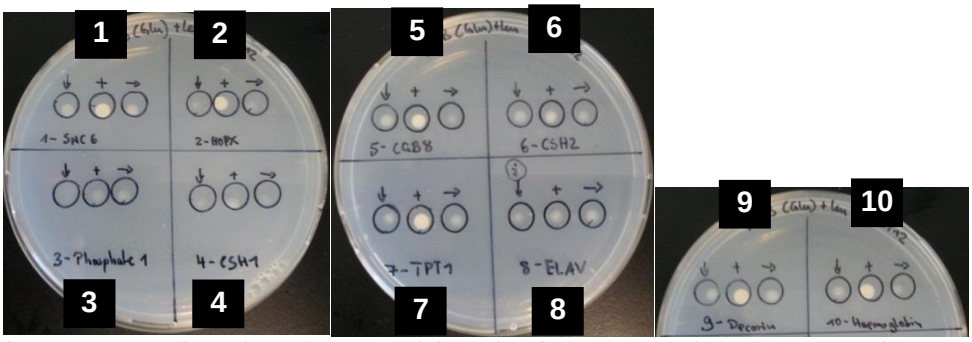

Figure 68: Confirmation of successful mating between strains RFY206 and EGY48. Cells picked from top of "mating cross" were spotted onto down arrow in picture (↓), cells picked from left of "mating cross" were spotted onto right arrow location (→), cells picked from the centre of the "mating cross" were spotted onto +.

The clones that grew (+ circle in Figure 68) were transferred onto YNB (Glu,X-Gal) ura$^-$/his$^-$/trp$^-$ and YNB (Gal,Raf,X-Gal) ura$^-$/his$^-$/trp$^-$ plates and incubated at 30°C for 5 days in order to confirm *LacZ* gene expression that was observed in the initial screening (Section 5.6.4). However, only the mated clone containing CGB8 cDNA protein turned pale blue, all other clones remained white (Figure 69). This is a contradictory result (except for CGB8) to that obtained in Section 5.6.4, indicating that the initial results were most likely false positives. The positive control with pBait and pTarget show strong expression of the *LacZ* gene showing that the method itself works.

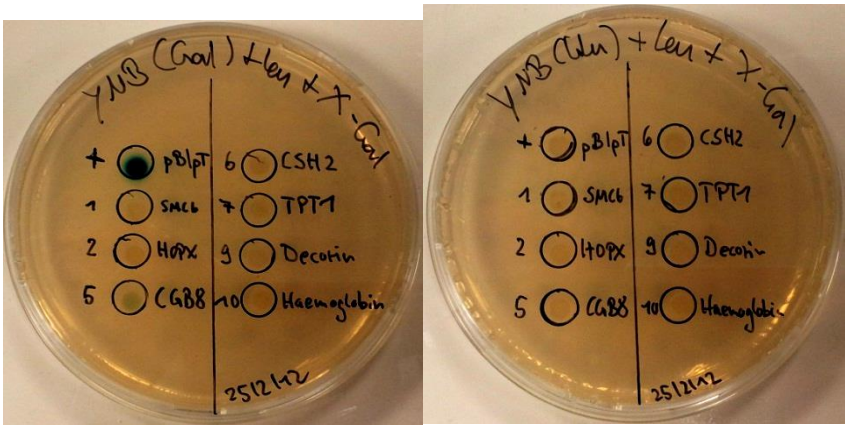

Figure 69: Mating assay showed colour change of pBait/pTarget (+) and CGB8/pEG202-N3/pRB1840 (5) after 5 days of incubation at 37°C.

The next step would have been to repeat the mating assay without pEG202-N3 but with a bait vector such as pLexA-Max, pBait or pRHFM1 that should not interact with the prey proteins and therefore the clones should remain white. However, as the phenotype seen during the initial blue/white screening (Section 5.6.4) could not be repeated no further mating tests were performed.

5.7 Y2H screening with a Jurkat T-Cell cDNA library

Following the placental cDNA library screening, a second screening with a cDNA library obtained from a Jurkat T-Cell line (OriGene) was performed as this cell line was known to have different gene expression patterns for hNEIL3 compared to placental tissue. Therefore, EGY48 yeast cells were generated that carry the *LacZ* reporter plasmid pSH18-34 that has 8 LexA operators in front of the *LacZ* gene instead of 1 operator in the pRB1840 plasmid used in the first screening. This was expected to increase sensitivity in the X-Gal test. The large scale transformation efficiency was 1.38 x 10^5 cfu per µg library plasmid DNA and 4.14 x 10^6 total transformants were calculated. This was two fold higher total transformants than had been obtained for the placental library transformation (Section 5.6.1). The calculation and preparation of the plates was carried out as described before (Section 5.6.1).

After three days of incubation at 30°C, the first colonies became visible (data not shown). This was two days earlier than for the placental cDNA library screening (Section 5.6.2). After the fifth day of incubation a total of 56 colonies were picked from YNB (Gal,Raf) $ura^-/his^-/trp^-/leu^-$ screening plates and diluted in 50 µl YNB while 4 µl of this solution was spotted onto YNB (Gal,Raf) $ura^-/his^-/trp^-/leu^-$, YNB (Glu) $ura^-/his^-/trp^-/leu^-$, YNB (Gal,Raf,X-Gal) $ura^-/his^-/trp^-$ and YNB (Glu,X-Gal) $ura^-/his^-/trp^-$ plates for further analysis.

5.7.1 *Galactose/Glucose test of potential positive interactors*

After 24 h, growth occurred on all plates. However, no or less growth was expected on the YNB (Glu) ura$^-$/his$^-$/trp$^-$/leu$^-$ plate compared to the YNB (Gal,Raf) ura$^-$/his$^-$/trp$^-$ /leu$^-$ plate (Figure 70) as there is no prey protein expression induced due to the lack of galactose, *i.e.* no interaction with hNEIL3-LexA should occur that enables the cells to express *Leu2* and thus they should not grow on plates lacking leucine. This result is similar to that obtained from the first screening when using the placental cDNA library (Section 5.6.3).

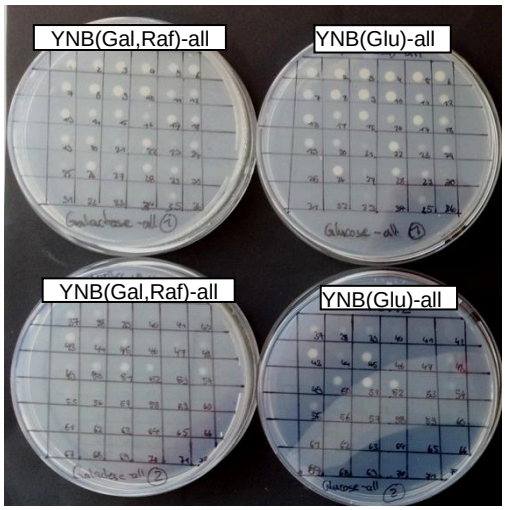

Figure 70: Fifty-six potential positive clones picked from screening plates and spotted onto YNB (Gal,Raf) ura$^-$/his$^-$ /trp$^-$/leu$^-$ (left) and YNB (Glu) ura$^-$/his$^-$/trp$^-$/leu$^-$ (right) plates.

5.7.2 *X-Gal test of potential positive interactors*

Although there was strong growth of all 56 clones on the YNB (Glu) ura$^-$/his$^-$/trp$^-$/leu$^-$ plates (Figure 70, right), the blue/white screening on X-Gal media and identification of the cDNA library insert by sequencing was still carried out. After two days of incubation on YNB (Glu,X-Gal) ura$^-$/his$^-$/trp$^-$ and YNB (Gal,Raf,X-Gal) ura$^-$/his$^-$/trp$^-$ a

colour change to blue of some colonies became visible. However, only clones 1, 2, 3, 4, 5, 6, and 43 (green circles in Figure 71 to Figure 73) seemed to be genuine as they became blue on YNB (Gal,Raf,X-Gal) ura$^-$/his$^-$/trp$^-$ but remained white on YNB (Glu,X-Gal) ura$^-$/his$^-$/trp$^-$ plates. Colonies 16, 20, 28, 29, 38, 39 and 48 (red circles in Figure 71 to Figure 73) seemed to be false positives as the colour change only occurred on YNB (Glu,X-Gal) ura$^-$/his$^-$/trp$^-$ or on both YNB (Gal,Raf,X-Gal) ura$^-$/his$^-$/trp$^-$ and YNB (Glu,X-Gal) ura$^-$/his$^-$/trp$^-$ plates.

It must be mentioned that some colonies seemed not to grow properly in general. The reason could be that these colonies were very small compared to others when picked from screening plates and after dilution in the 50 µl YNB prior spotting only a low concentration of cfu remained in the 5 µl that was finally spotted. However, even after longer incubation these colonies did not seem to grow in size and therefore they were assumed to be false positive clones.

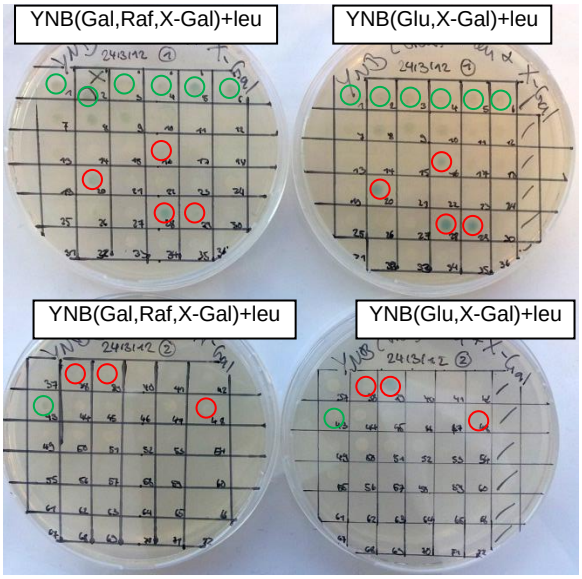

Figure 71: On day 3 the colour change became more distinguishable. Green circled clones were used in further tests. Red circled clones were not used is in further tests.

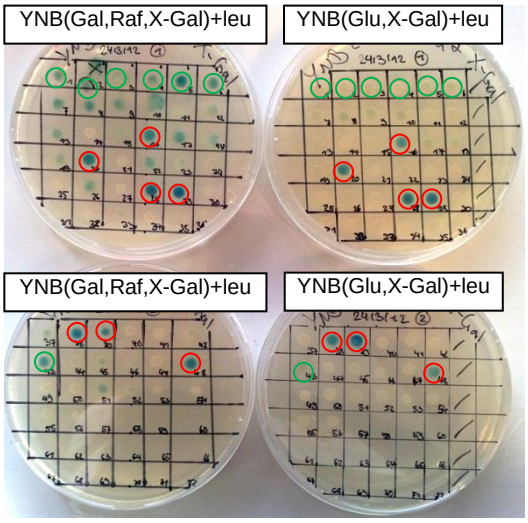

Figure 72: On day 4 more colonies changed the colour from white to blue on Gal/Raf plates. Green circled clones were used in further tests. Red circled clones were not used is in further tests.

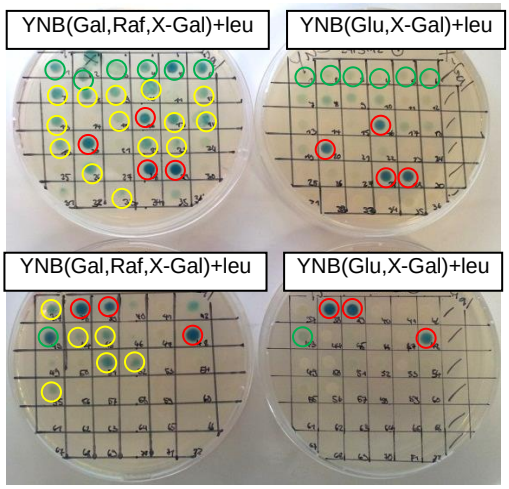

Figure 73: On day 5 the colour change became more distinguishable. Green and yellow circled clones were used in further tests. Red circled clones were not used is in further tests.

Since after five days incubation more clones (yellow circles in Figure 73) turned blue on YNB (Gal,Raf,X-Gal) ura$^-$/his$^-$/trp$^-$ and remained white on YNB (Glu,X-Gal) ura$^-$/his$^-$ /trp$^-$, than was initially observed on day 3, those clones were also considered as potential positive. Hence, clones 1 - 10, 12, 13, 15, 17 - 19, 22, 23, 26, 33, 37, 43 - 45, 51, 52 and 55 were picked to sequence their cDNA library inserts.

To confirm if the potential positive clones that changed colour on YNB medium containing X-Gal + galactose but not on medium containing X-Gal + glucose expressed NEIL3 interacting polypeptides (Figure 71 to Figure 73), 10 ml YNB liquid cultures containing glucose or galactose respectively but lacking leucine were inoculated and incubated for 48 h at 260 rpm and 30°C. The liquid cultures containing glucose grew even faster than the ones that contained galactose/raffinose (Figure 74) and this phenotype was the same for all selected clones and is similar to the tests carried out in Section 5.7.1 and 5.6.3. This is the opposite of what was expected. However, as for the placental cDNA library screening, sequencing was still performed.

1) After 24 h incubation at 30°C and 260 rpm.

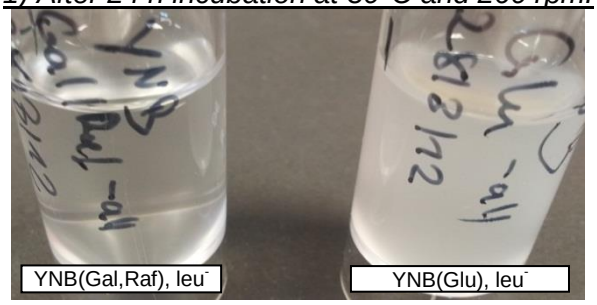

2) After 48 h incubation at 30°C and 260 rpm.

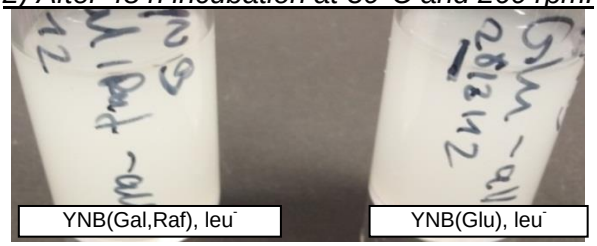

Figure 74: Incubation of potential positive clones in YNB (Gal,Raf), leu$^-$ or YNB (Glu), leu$^-$ respectively after 24 h (1) and 48 h (2) of incubation at 260 rpm and 30°C.

5.7.3 DNA sequencing of potential positive clones

DNA sequencing of the potential positive clones obtained after screening the Jurkat T-Cell cDNA library revealed that all the clones tested were false positive as their

cDNA library sequences were either not protein coding sequences or the DNA sequence was out of frame (Appendix 8.6.2). Therefore, further tests such as the mating assay were not carried out.

5.8 Interaction studies of human LigIIIα and Polβ with hNEIL3-LexA

As EGY48 clones containing pEG202-N3 and the *LacZ* reporter plasmid pSH18-34 were already available, it was of interest to test proteins that were already known to physically interact with NEIL1 and NEIL2 (Section 2.3.6). Therefore, the BER downstream proteins LigIIIα and Polβ were chosen for this experiment and their cDNAs were transformed into the Y2H library plasmid pJG4-5 that had previously been used for the screening experiments. However, as only the restriction sites for *Xho*I and *Eco*RI were available in the multiple cloning site of the vector (Appendix Figure 100) and the fact that both, LigIIIα and Polβ, contain *Xho*I and *Eco*RI restriction sites in their CDS sequences it was necessary to perform an alternative method of cloning (for more details see Section 4.13.6).

5.8.1 Preparation of library vectors containing either LigIIIα or Polβ

The cDNAs of LigIIIα and Polβ were readily cloned into the vector pCMV-XL5 (OriGene, Appendix Figure 95) and were ready to use in PCR.

5.8.1.1 Designing primers for PCR of LigIIIα and Polβ cDNA

As the multiple cloning site in the Y2H library vector pJG4-5 (Appendix Figure 100) only offers one pair of restriction sites for cloning (*Eco*RI and *Xho*I) the primers were designed accordingly. However, as discussed before, this resulted in a problem as

LigIIIα as well as Polβ contain both an *Eco*RI and a *Xho*I site in their CDS. Therefore, it was not possible to simply clone the PCR products into a pGEM-T vector and cut it out again with restriction enzymes to obtain an insert with cohesive ends that can be used to clone into pJG4-5. Therefore, a protocol was designed and carried out using mung bean nuclease to clone the PCR products directly into pJG4-5 (for more details see Section 4.13.6). To make this method work the 5′ base of each restriction site used in each primer was left out (Table 21). Furthermore, it was important to use a proofreading DNA polymerase that produces blunt end products.

Table 21: Primers used for amplification of LigIIIα and Polβ cDNA.

hLig3aEcoRI-5′G: *Tm: 72.98°C (Finnzyme Tm)-- nt: 34 -- GC ratio: 35.92%*
5`- AA TTC ATG TCT TTG GCT TTC AAG ATC TTC TTT CC-3`
hLig3aXhoI-5′C: *Tm: 71.93 °C (Finnzyme Tm) -- nt: 26 -- GC ratio: 57.69%*
5`- TC GAG CTA GCA GGG AGC TAC CAG TCT -3`
hPOLB-EcoRI-5′G: *Tm: 76.29 °C (Finnzyme Tm)-- nt: 25 -- GC ratio: 52.00%*
5`- AA TTC ATG AGC AAA CGG AAG GCG CC-3`
hPOLB-XhoI-5′C: *Tm: 75.91 °C (Finnzyme Tm) -- nt: 24 -- GC ratio: 58.33%*
5`- TC GAG TCATTCGCTCCGGTCCTTG -3`

Figure 75 shows the results of a PCR with the designed primers and that the expected band sizes were achieved (3030 bp for LigIIIα and 1008 bp for Polβ).

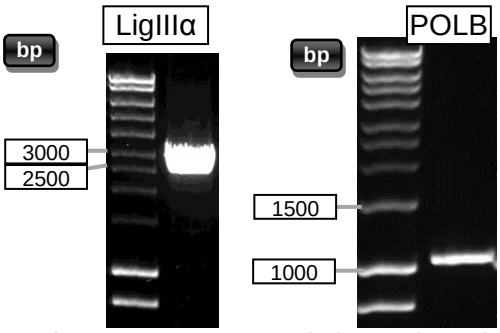

Figure 75: Agarose gel electrophoresis of PCR of LigIIIα (left) and Polβ (right).

5.8.2 *Preparation of library vector pJG4-5 for blunt end cloning*

The size of the Y2H library vector pJG4-5 was checked by restriction enzyme digest using *Eco*RI and *Xho*I and separated on an agarose gel along with undigested plasmid DNA (Figure 76).

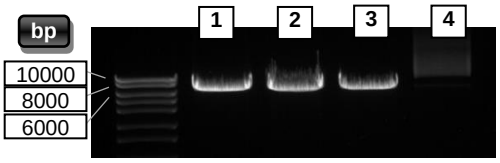

Figure 76: Agarose gel electrophoresis of digested pJG4-5 (1, 2, 3) and undigested pJG4-5 (4)

After it was confirmed that the linearized pJG4-5 DNA was the correct size (6449 bp), a large scale double-digest with *EcoR*I and *Xho*I was performed, separated by agarose gel electrophoresis and gel purified. The resulting DNA concentration of the linearized plasmid DNA was ~100 ng/µl in a total volume of 50 µl.

5.8.3 *Ligation of LigIIIα and Polβ into linearized pJG4-5*

As described in Section 4.13.6, prior to ligation it was necessary to blunt-end the pJG4-5 vector to allow the inserts to be integrated in frame. Therefore, mung bean nuclease was used under the conditions shown in Table 22.

Table 22: Conditions for Mung Bean Nuclease blunting reaction

Components	Amount
DNA (100 ng/µl)	26.5 µl
10X mung bean nuclease Buffer	3.0 µl
5 units of mung bean nuclease	0.5 µl
Total	**30.0 µl**

The mixture was incubated at 30°C for 30 minutes followed by enzyme deactivation with 0.01% SDS. After blunting, the DNA was purified using the Wizard SV Gel and PCR clean up kit (Promega). The final concentration of linearised, blunt-ended pJG4-5 was 90 ng/µl in a total volume of 30 µl. It was possible to ligate LigIIIα or Polβ cDNA into the pJG4-5 vector using the conditions shown in Table 23.

Table 23: Conditions for ligation of LigIIIα or Polβ cDNA, respectively, into pJG4-5.

LigIIIα → pJG4-5		**Polβ → pJG4-5**	
Components	Amount	Components	Amount
10X T4 DNA Ligase Buffer	2.0 µl	10X T4 DNA Ligase Buffer	2.0 µl
pJG4-5 vector (90 ng/µl)	2.4 µl	pJG4-5 vector (90 ng/µl)	2.4 µl
LigIIIα cDNA	3.8 µl	Polβ cDNA	1.3 µl
Nuclease-free water	10.8 µl	Nuclease-free water	13.3 µl
T4 DNA Ligase	1.0 µl	T4 DNA Ligase	1.0 µl
Total	20.0 µl	Total	20.0 µl

After the mixtures were incubated overnight at 16°C, transformation of the ligation mixtures into Novablue competent cells was performed as described in Section 4.1. After incubation of the transformations on LB-Agar containing 50 µg/ml carbenicillin at 30°C overnight >200 colonies per plate were obtained for further investigations.

5.8.4 Confirmation of correct integration of LigIIIα and Polβ into pJG4-5

As the ligation of LigIIIα or Polβ cDNA, into pGJ4-5 was performed with blunt end fragments, the integration could have occurred in two ways. Therefore, it was necessary to screen for a clone that contains pJG4-5 carrying LigIIIα or Polβ in the correct orientation for protein expression in later experiments. As pJG4-5, LigIIIα and Polβ each contain a *Xho*I restriction site, it was possible to perform single restriction digestions to obtain two fragments of known size for each plasmid if the insert was in the correct orientation. However, if the insert is ligated into pJG4-5 in the wrong direction the 5′ *Xho*I restriction site is destroyed and thus *Xho*I cuts only once which

results in only a single band on the agarose gel. Therefore, if the ligation was correct the resulting band sizes for pJG4-5 containing LigIIIα should be 7157 bp and 2310 bp and for pJG4-5 containing Polβ 6739 bp and 706 bp.

For constructs, pJG4-5-LigIIIα and pJG4-5-Polβ, 30 clones were picked from each transformation plate to inoculate LB liquid cultures in preparation for plasmid DNA isolation. After plasmid DNA was recovered from each clone, 60 restriction digests with *Xho*I were performed in order to find a clone carrying the correct insert (Figure 77 to Figure 82). Interestingly, for each construct, pJG4-5-LigIIIα and pJG4-5-Polβ, only one out of 30 picked clones was carrying the correct plasmid (clone L28 in Figure 80 and P21 in Figure 82).

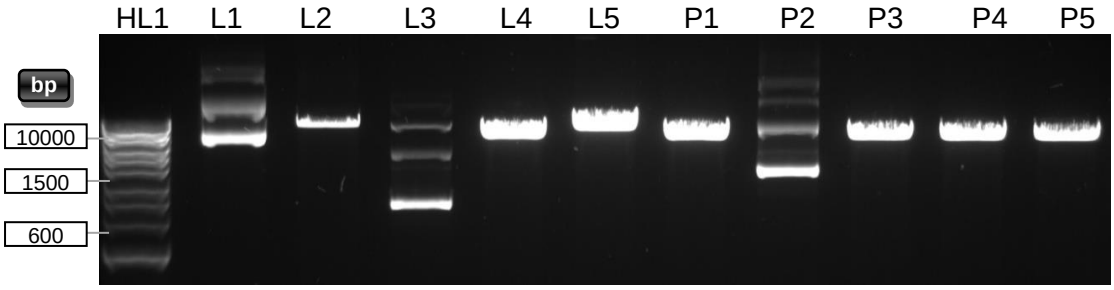

Figure 77: Agarose gel electrophoresis of restriction digest with *Xho*I of extracted pJG4-5 plasmid DNA from clones L1-L5 containing LigIIIα and P1-P5 containing Polβ cDNA.

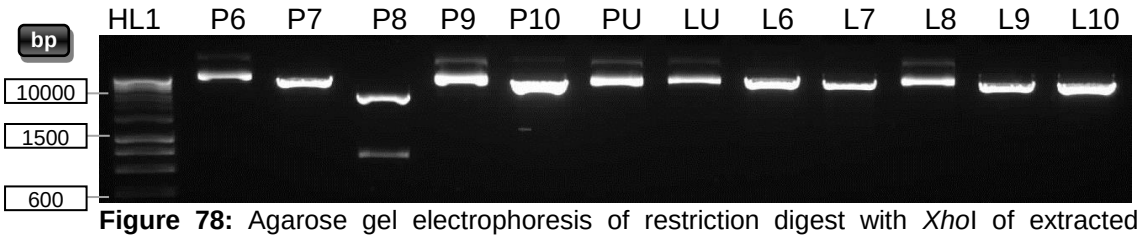

Figure 78: Agarose gel electrophoresis of restriction digest with *Xho*I of extracted pJG4-5 plasmid DNA from clones P6-P10 containing Polβ and L6-L10 containing LigIIIα cDNA. PU and LU are undigested P6 and L6 respectively.

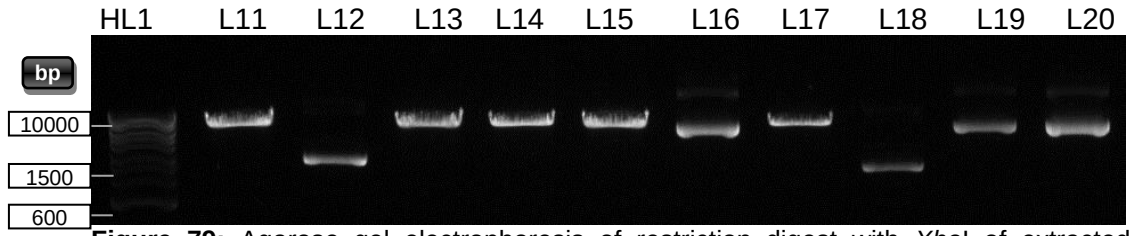

Figure 79: Agarose gel electrophoresis of restriction digest with *Xho*I of extracted pJG4-5 plasmid DNA from clones L11-L20 containing LigIIIα cDNA.

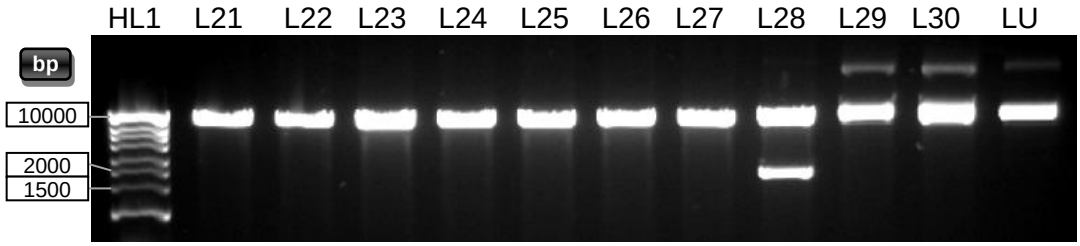

Figure 80: Agarose gel electrophoresis of restriction digest with *Xho*I of extracted pJG4-5 plasmid DNA from clones L21-L30 containing LigIIIα cDNA. LU is undigested L21. L28 is a positive clone that was picked for further experiments.

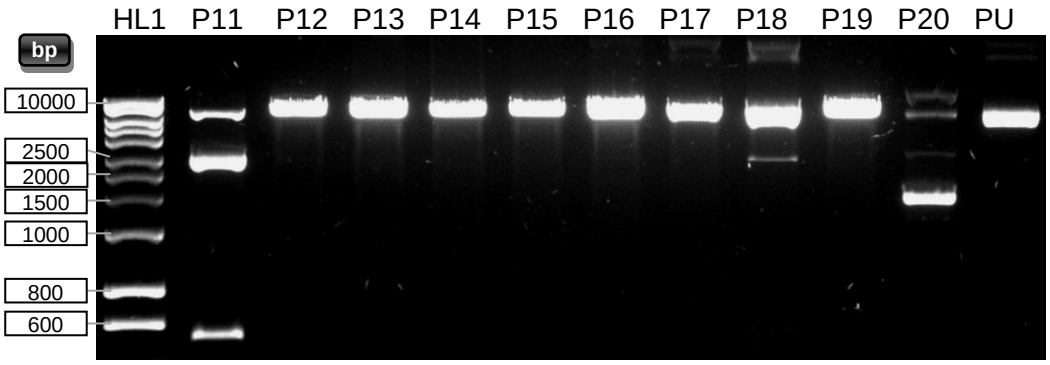

Figure 81: Agarose gel electrophoresis of restriction digest with *Xho*I of extracted pJG4-5 plasmid DNA from clones P11-P20 containing Polβ cDNA. PU is undigested P11.

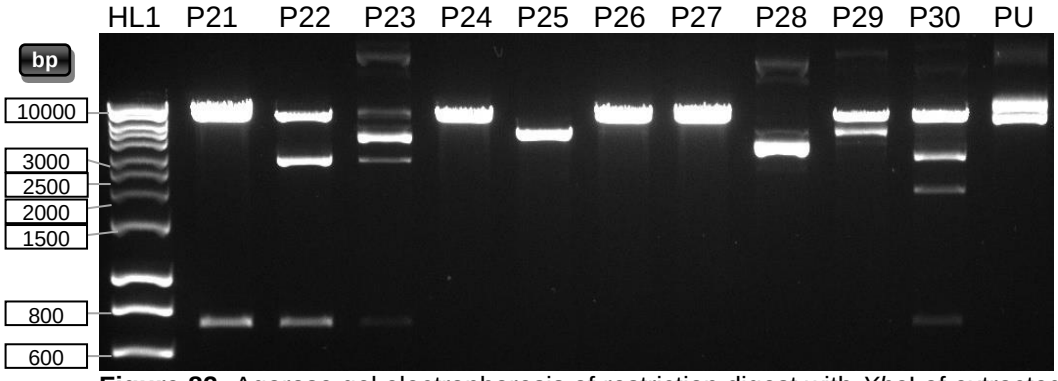

Figure 82: Agarose gel electrophoresis of restriction digest with *Xho*I of extracted pJG4-5 plasmid DNA from clones P21-P30 containing Polβ cDNA. PU is undigested P21.

In order to confirm the integrity of these two clones, further restriction digests with *Eco*RI and *Xho*I (either single- or double-digests) were performed. Agarose gel electrophoresis revealed the expected band sizes for these clones and therefore confirmed that the integration of LigIIIα and Polβ into pJG4-5 had been successful. The calculated band sizes for the restriction digest with *Xho*I for pJG4-5 containing LigIIIα were 7169 bp and 2310 bp (LX in Figure 83) and for pJG4-5 containing Polβ 6751 bp and 706 bp (PX in Figure 83). The result of the restriction digest with *Eco*RI showed the expected band sizes 7117 bp and 2362 bp for pJG4-5 containing LigIIIα (LE in Figure 83) and 7011 bp and 446 bp for pJG4-5 containing Polβ (PE in Figure 83). Finally, the double-digest with *Eco*RI and *Xho*I also resulted in the expected band sizes 668 bp, 720 bp, 1642 bp and 6449 bp for pJG4-5 containing LigIIIα (LDD in Figure 83) and 144 bp, 302 bp, 562 bp and 6449 bp for pJG4-5 containing Polβ (PDD in Figure 83) while the 144 bp band was not visible due to the resolution of the gel used.

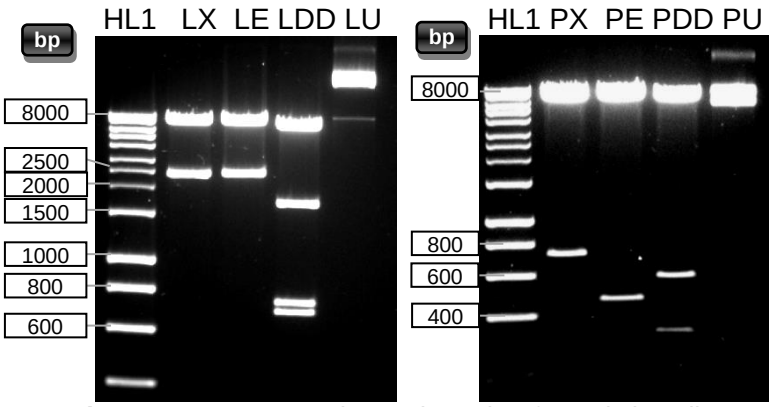

Figure 83: Agarose electrophoresis of restriction digest of L28 (left) and P21 (right) with *Xho*I (LX and PX), *Eco*RI (LE and PE) and *Xho*I and *Eco*RI (LDD and PDD). LU and PU was undigested DNA.

5.8.5 *Small scale transformation of pJG4-5-LigIIIα and pJG4-5-Polβ into EGY48*

The constructs pJG4-5-LigIIIα and pJG4-5-Polβ generated in Section 5.8.1 to 5.8.4 were transformed into EGY48 already containing pEG202-N3 and the *LacZ* reporter plasmid pSH18-34 using the small scale transformation protocol described in Section 4.13.1. However, no transformants were obtained for the Polβ clone and only three colonies for pJG4-5-LigIIIα. Due to time limitations the transformation was not repeated, instead the interaction studies using X-Gal plates for blue/white selection and leucine lacking plates for *Leu2* selection were performed.

5.8.6 *Testing LacZ and Leu2 gene expression for LigIIIα/hNEIL3 clone*

The three colonies obtained through transformation along with a negative control (EGY48 containing pEG202-N3, pSH18-34 and empty pJG4-5) were picked, added to 50 µl YNB, then 5 µl spotted onto either, YNB (Gal,Raf,X-Gal) $ura^-/his^-/trp^-$, YNB (Glu,X-Gal) $ura^-/his^-/trp^-$, YNB (Gal,Raf) $ura^-/his^-/trp^-/leu^-$, or YNB (Glu) $ura^-/his^-/trp^-/leu^-$ plates and incubated at 30°C for more than four days. After four days a strong colour change became visible for pJG4-5-LigIIIα on YNB plates containing X-Gal and galactose but remained white on YNB plates containing X-Gal and glucose. This would indicate a positive interaction result as the prey protein expression in this case of LigIIIα is only induced on X-Gal plates containing galactose and therefore should only interact here with NEIL3 that then can induce *LacZ* expression. However, the negative control carrying empty pJG4-5 showed a similar colour change indicating the results could be false positives (Figure 84). On YNB plates lacking the amio acid leucine, no growth was detected, which shows that there was no interaction between hNEIL3 and LigIIIα as this would have resulted in *Leu2* gene expression and therefore in growth on the YNB plate containing galactose (bottom right in Figure 84).

Figure 84: YNB (Gal,Raf,X-Gal) ura$^-$/his$^-$/trp$^-$ (top right), YNB (Glu,X-Gal) ura$^-$/his$^-$/trp$^-$ (top left), YNB (Gal,Raf) ura$^-$/his$^-$/trp$^-$ /leu$^-$ (bottom right), YNB (Glu) ura$^-$/his$^-$/trp$^-$/leu$^-$ (bottom left) plates spotted with three different pJG4-5-LigIIIα clones and a negative control.

When the experiment was repeated, the LigIIIα/hNEIL3 clone 2 seemed to have a potential positive interaction as the colour change occurred earlier then for the negative control (Figure 85).

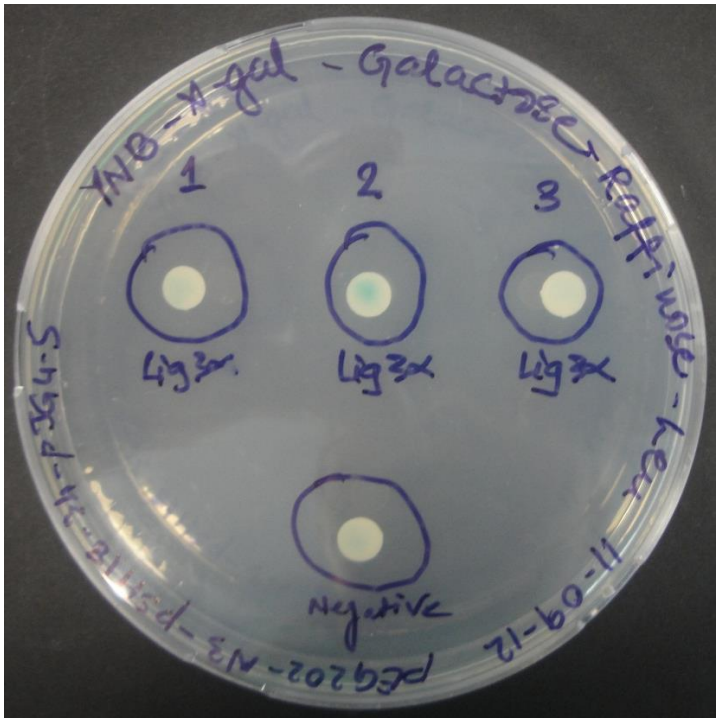

Figure 85: Repetition of interaction experiment showed in Figure 84.

However, more evidence that there is an interaction between hNEIL3 and LigIIIα is required and a repeat of the small scale transformation with a higher efficiency (Section 5.8.5) must be achieved in the first place.

5.9 Overexpression of hNEIL3 and mNEIL1 in *Pichia pastoris*

It is of great interest to obtain purified and active hNEIL3 protein in order to perform assays that allow investigations of its DNA repair capabilities as well as protein-protein or DNA-protein interactions *in vitro*. Therefore, it was decided to use a eukaryotic expression system based on the yeast *P. pastoris and the constitutive expression vector* pGAPZαA in order to express full-length and truncated versions of hNEIL3.

5.9.1 *Confirmation of pGAPZαA clones obtained from bacterial stocks*

pGAPZαA vectors containing either full length mNEIL1 cDNA (CDS) constructed by Constantina Stylianou (2010) or full length hNEIL3 cDNA (CDS) and truncated versions of hNEIL3 (394 and 502 amino acids) constructed by Mengxin Yin (2010) were used for protein overexpression in *P. pastoris*.

To confirm that the pGAPZαA clones carried the correct inserts a single and double-digest with *Eco*RI and *Xho*I was performed (Figure 86).

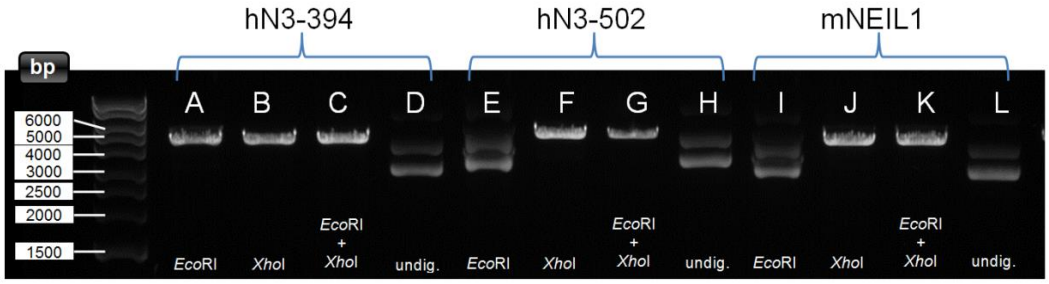

Figure 86: Agarose gel electrophoresis picture showing single and double-digests of pGAPZαA containing either hN3-394 (A, B, C, D), hN3-502 (E, F, G, H) or mNEIL1 (I, J, K, L) inserts. *Eco*RI single digest is shown in lanes A, E and I. *Xho*I digest is shown in lanes B, F, J. *Xho*I and *Eco*RI double-digest is shown in lanes C, G, K. The lanes D, H and L contained undigested plasmid DNA.

There are two *Xho*I restriction sites in the multiple cloning site of pGAPZαA and an *Eco*RI site in between these two sites. It was expected that *Eco*RI would not cut any of the plasmids as this restriction site was deleted during the cloning process. However, this was not the case for hN3-394 but for hN3-502 and mNEIL1 (A, E and I in Figure 86). Because *Eco*RI seemed to cut the used clone of hN3-394 (hN3-394-Clone-3), four more clones obtained from frozen stocks of hN3-394 and full length hNEIL3 were digested with *Eco*RI and *Avr*II. As expected for hN3-394-Clone-3 two bands appeared after digestion. However, all the other clones (hN3-394-Clone- 1, 2, 4, 5 and full length hNEIL3) seemed to be genuine as the plasmid was linearized and

not cut twice (Figure 87). Therefore, clone 1 of hN3-394 (1 in Figure 87) was used for electroporation into *P. pastoris*.

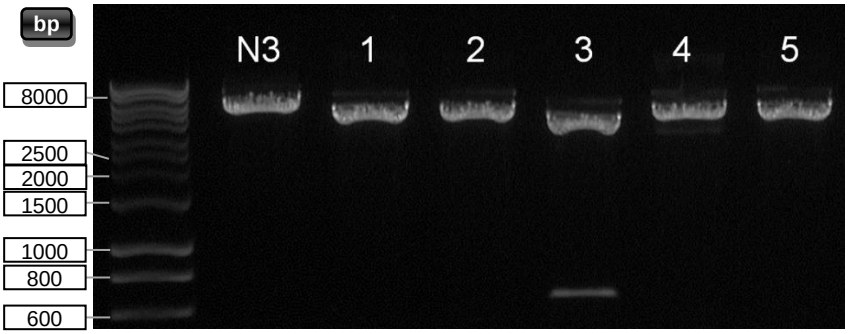

Figure 87: Agarose gel electrophoresis of double-digest with *EcoR*I and *Avr*II. Full length hNEIL3 (N3), hN3-394-Clone1, (1) hN3-394-Clone2 (2), hN3-394-Clone3 (3), hN3-394-Clone4 (4), hN3-394-Clone5 (5).

5.9.2 Linearization of pGAPZαA clones hN3-394, hN3-502 and mNEIL1

After the correct insert integration was confirmed, three separate plasmid DNA extractions were performed for each clone and the three eluates combined and purified with the Wizard Gel and PCR purification kit (Promega) to increase final DNA concentration in a total volume of 150 µl (Table 24). This was necessary to perform electroporation at a high efficiency.

Table 24: DNA concentration in 150 µl total volume after purification

Clone	Concentration
hN3-394	725.9 ng/ul
hN3-502	943.1 ng/ul
mNEIL1	738 ng/ul

To allow integration of each pGAPZαA clone into the chromosomal DNA of *P. pastoris* via homologous recombination, the plasmids had to be linearized. Therefore, each vector was digested with *Avr*II and linearization was confirmed on an agarose gel (Figure 88). Although shadow bands appeared on the agarose gel the

products were considered genuine as later PCR of genomic extracts will confirm (Section 5.9.4).

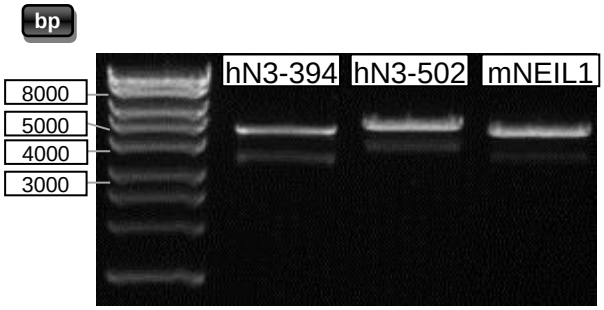

Figure 88: Agarose gel electrophoresis of linearized pGAPZαA vectors containing hN3-394, hN3-502 or mNEIL1.

5.9.3 Electroporation of pGAPZαA clones into P. pastoris

P. pastoris cells were electroporated with pGAPZαA containing either, hNEIL3, hN3-394, hN3-502 or mNEIL1 as described in Section 4.14.1. After electroporation the clones were spread onto YPD containing 100 mg/ml Zeocin in six different volumes (10 µl, 20 µl, 50 µl, 100 µl, 200 µl and 500 µl). In addition *P. pastoris* only (also electroporated but without DNA) was also plated in these volumes as a negative control. After three days of incubation at 30°C colonies appeared for hN3-394, hN3-502 and mNEIL1 on each plate except the 10 µl plates. The electroporation with hNEIL3 resulted in one colony only on the plate with 200 µl of sample. However, this construct was prepared in a separate electroporation which might have caused different conditions which led to a low electroporation efficiency. For the negative control, plates that contained 10 µl – 200 µl sample showed no growth but the plate that contained 500 µl of electroporated sample of *P. pastoris* only (negative without DNA) showed strong growth. However, this can be explained by the high concentration of cfu plated that most likely caused a neutralization of Zeocin over time resulting in the survival of some cells. But as the other negative plates showed no growth colonies that grew on plates with 200 µl or less were used for subsequent manipulations. Two single colonies from two different plates from each

electroporation were picked re-plated on YPD plates containing 100 mg/ml Zeocin. The plates the colonies were picked from are shown in Figure 89.

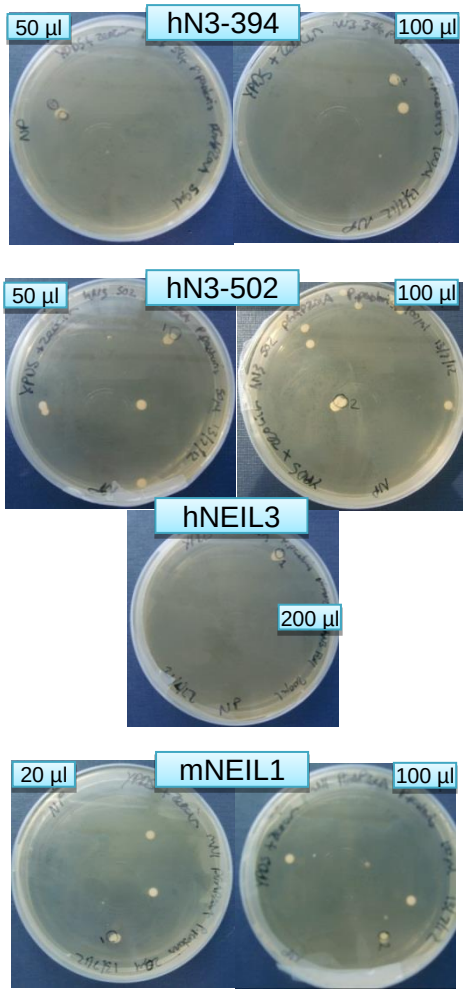

Figure 89: YPDS plates containing electroporated clones after four days of incubation at 30°C. Colonies picked for further experiments are marked with a black circle.

After colonies appeared, one from each plate was used to inoculate 10 ml of YPD broth and grown overnight at 30°C at 250 rpm and frozen stocks (-80°C) were prepared as described in Section 4.2.1.

5.9.4 PCR of chromosomal DNA extractions from P. pastoris

To confirm correct integration of pGAPZαA carrying either, hNEIL3, hN3-394, hN3-502 or mNEIL1, PCR using the primers pGAP-Forward and 3′ *AOX1* was carried out

(for more details on primers see Section 4.14.3). In Figure 90 it can be seen that all clones picked from electroporation plates contain inserts that correlate to the expected sizes (including 540 bp the primers add to the insert, 1722 bp for hN3-394, 2046 bp for hN3-502, 1710 bp for full length mNEIL1 and 2358 bp for full length hNEIL3 band size was expected; Figure 90).

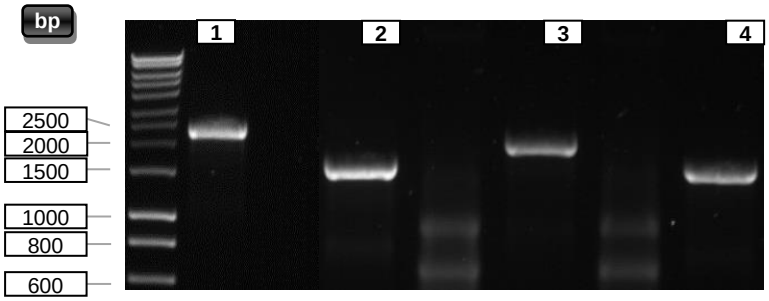

Figure 90: Agarose gel electrophoresis of PCR products amplified from *P. pastoris* clones carrying full length (1) and truncated versions of hNEIL3 (hN3-394 (2) and hN3-502 (3)) and full length mNEIL1 (4) cDNA.

5.9.5 SDS-PAGE of cell lysates

After *P. pastoris* with integrated pGAPZαA carrying full length hNEIL3 CDS cDNA and untransformed *P. pastoris* were incubated in 50 ml YPD for 96 h, a total protein extraction was performed using sonication as described in Section 4.10.1. Subsequently, protein quantification using the Bradford assay (Section 4.10.3), 15 to 30 µg of total protein were separated through a 12% SDS-PAGE at 200 V for 1 h (Figure 91).

No distinguishable band was detected indicating that overexpression of NEIL3 within the cell had not occurred. As the pGAPZαA vector carries a protein secretion sequence that is fused to the expressed protein, another SDS-PAGE using the culture medium/supernatant of the liquid culture. After 48 h incubation there was no band for hNEIL3 overexpression visible on the gel. However the control, mNEIL1,

showed a band at the predicted size (~63 kDa) after 48 h (Figure 92). Thus, although further experiments are required to confirm the identity of the observed band, these preliminary results indicate that the *P. pastoris* overexpression system with pGAPZαA vector could be used to express the NEIL proteins.

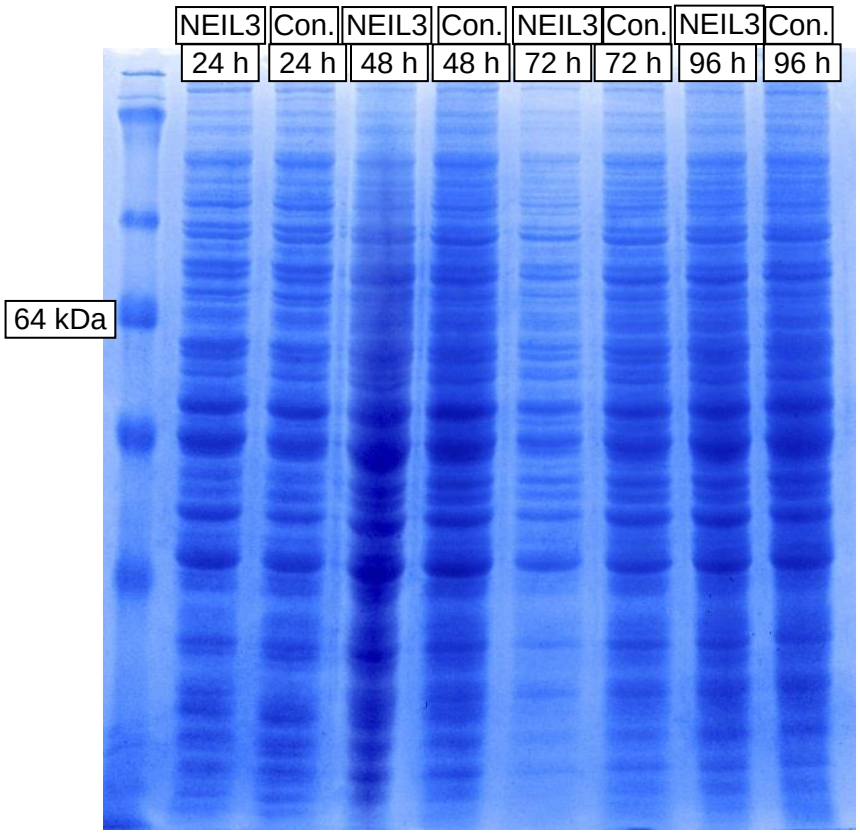

Figure 91: Coomassie blue staining of an SDS-PAGE gel of hNEIL3 (NEIL3) and untransformed *P. pastoris* (Con.) after different incubation times.

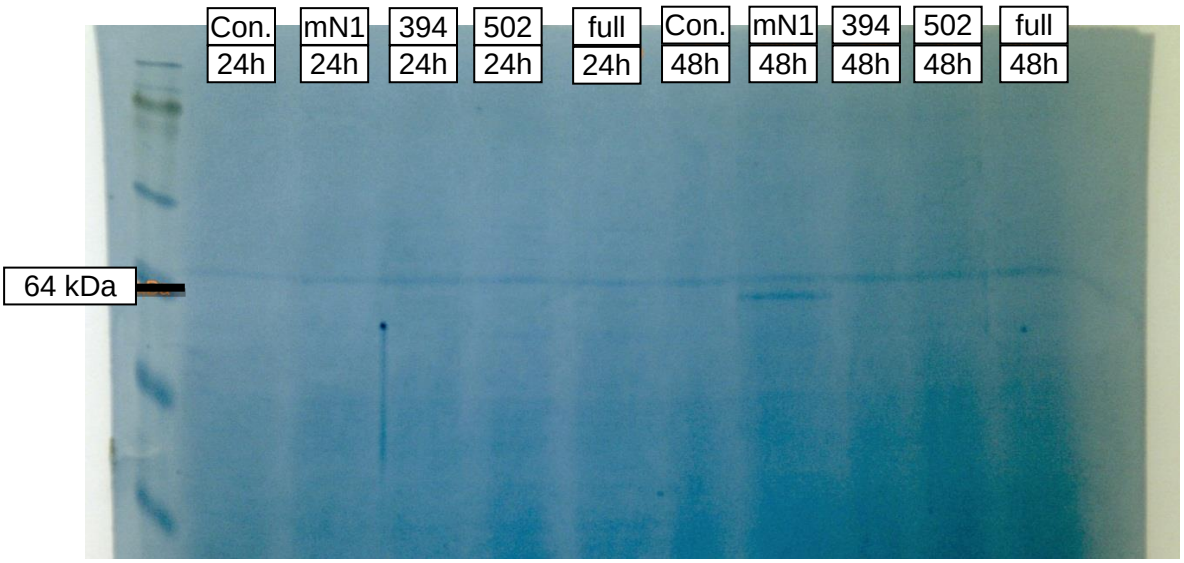

Figure 92: Coomassie blue staining of an SDS-PAGE gel of secreted proteins from mNEIL1 (mN1) and full length and truncated versions (394, 502 and full) of hNEIL3 after 24 h and 48 h incubation.

6 Discussion

6.1 Yeast two-hybrid results

The vectors pEG202 and pEG202-NLS containing the hNEIL3 cDNA sequence were successfully generated in preparation for the Y2H assay (Section 5.1). Expression of hNEIL3 fused to LexA (hNEIL3-LexA) was confirmed by western blot analysis (Section 5.5). Furthermore, autoactivation tests were performed and showed that full length hNEIL3 did not autoactivate any of the reporter genes used in this assay. hNEIL3 was also able to enter the nucleus after translation as shown by the repression assay results (Section 5.4). Therefore, based on these control experiments hNEIL3 seemed to be a suitable candidate for use as a bait protein in the Y2H assay.

As proteins larger than ~60 kDa (NEIL3 = 68 kDa [Krokeide *et al.,* 2009]) have been suggested to be expressed at low levels in yeast cells (Fashena *et al*., 2000), this might explain the delayed growth observed in the screening with the placental cDNA library. This is because, only if NEIL3 interacts with another protein leucine will be expressed and cells are able to grow on media lacking leucine as is the case in the large scale screening. Thus, if NEIL3 expression occurs only at a low level, the production of leucine, and therefore growth of yeast colonies during screening will be delayed (Section 5.6.1; Fashena *et al.*, 2000). However, complicating the issue, the colonies that were obtained from the placental, as well as from the Jurkat T-Cell cDNA library screening, showed growth on medium lacking leucine, but containing glucose and because prey protein expression is only induced if galactose is present, this is suggestive of a false positive result. Contrary to this, however, the Y2H system

that was used in this project includes a second selection method, the *LacZ* selection allowing a blue/white screening. This second screening system uses a different selection method where positive interactions lead to expression of β-galactosidase from a reporter plasmid rather than leucine which is expressed from the genomic DNA. Hence, interactions that were negative in the first instance during leucine selection might be positive in the blue/white screening assay due to the different DNA substrate NEIL3-LexA is binding to (plasmid DNA). Using this assay, all potential positive clones from the initial screen also grew on plates lacking leucine but containing either glucose or galactose as before (Section 5.6.3). However, using blue/white screening on plates containing X-Gal different phenotypes were observed (Section 5.6.4), which led to the assumption that interaction between NEIL3 and those prey proteins might still be genuine.

The following Sections discuss the results of potential positive protein partners for hNEIL3. However, as the Jurkat T-Cell screening revealed only out of frame or non-coding prey cDNA sequences (Section 5.7.3) this screening will not be included in the discussion.

6.1.1 Potential positive interactors

The most promising finding was the homeobox protein (HOPX), because as for NEIL3, higher expression levels have been found in MOLT4 cell lines. In addition, HOPX is thought to be a tumour suppressor protein, which gives rise to the hypothesis that NEIL3 might play a role in its regulation and ability to bind to DNA (European Bioinformatics Institute, 2012e). Furthermore, this protein contains a conserved homeodomain that is known to be “involved in transcriptional regulation of key eukaryotic developmental processes” (NCBI, 2011). Although, the *LacZ*

phenotype could not be confirmed by the mating assay and the fact that it appeared only once during screening, this protein could still be worth investigating further, as it makes functional sense that it might interact with NEIL3. As explained later for CGB8, the recovered mRNA sequence encompassed the whole CDS and also large parts of the 5′ and 3′ UTR. Therefore, the CDS on its own could either be cloned into the library vector pJG4-5 and retested in Y2H, or it could be used in a pull-down assay for immunological interaction studies. Because of its small size (222 bp) it is not as expensive as many other protein coding DNA sequences to purchase (CDS sequence can be found here http://1.usa.gov/P5obYb).

The chorionic somatomammotropin hormone 1 (placental lactogen, CSH1, European Bioinformatics Institute, 2012a), chorionic somatomammotropin hormone 2 (CSH2, European Bioinformatics Institute, 2012b) and chorionic gonadotropin, beta polypeptide 8 (CGB8, European Bioinformatics Institute, 2012c) were found several times, lending support to the idea that they might be genuine interactors. However, on performing mating assays (Section 5.6.8) only CGB8 showed the same phenotype as during blue/white screening (Section 5.6.4). Evidence of interaction could not be confirmed for any of the other clones. One possible reason for this could be that the yeast spontaneously mutated during growth and gained a *LacZ* expression phenotype independently of the prey protein.

As a first step to confirm that the interaction between CGB8 and NEIL3 was genuine a further mating assay could be performed using bait proteins other than NEIL3 that are unlikely to interact with CGB8, such as those expressed by the Y2H bait vectors pLexA-Max, pBait or pRHFM1. If the resulting colonies remain white compared to the clones expressing NEIL3, a pull-down system using the CDS DNA of CGB8 should be performed for further confirmation that the interaction is genuine. It is crucial to make further tests as the DNA of the isolated library insert also covers parts of the

5′ and 3′ UTR of CGB8 in addition to the CDS, as mentioned previously. Furthermore, as the pJG4-5 library vector that CGB8 was expressed from carries an ATG start codon upstream relative to the insert, the 5′-UTR sequence will have been translated as well. This might have led to a random peptide that interacted with NEIL3, or bound to the LexA binding side on the reporter plasmid.

As mentioned before, the protein hormones CSH1, CSH2 and CGB8 appeared more often than other proteins in the placental cDNA library screen. Although this could be a sign of genuine protein partners it also has to be considered that the number of these interactions could be due to the fact that the cDNA library used was not normalized and therefore that some cDNAs obtained by reverse transcription were present statistically more often than others. Giving credence to this, the protein hormones CSH1 and CSH2 are mainly expressed during pregnancy in placental tissue and are involved in lactation and foetal growth, while expression patterns for CGB8 are unknown.

Other putative interactors found from the placental library Y2H screen included decorin, TIMP2, ELAVL1, haemoglobin subunit beta and the tumour protein TPT1. However, none of these proteins appears to be linked to NEIL3, given what we know about its cellular location and possible molecular function. The negative results in the mating assay and the fact that these proteins were found only once during screening increase the chance they are false positives.

6.1.2 Reasons for false positive results

Common false positive protein interaction partners found in most Y2H screens are ribosomal and proteasome specific proteins and these were also identified via DNA

sequencing during this Y2H screening with placental cDNA library. Golemis *et al.* (1999) suggest that if only individual cDNAs were found during sequencing of putative positive clones this might be due non-specific binding of the bait protein with false positives. On the other hand if several putative clones contained several cDNA of the same protein it is very likely that this clone is genuinely positive.

Krokeide *et al.* (2009) found that when NEIL3 is overexpressed in mammalian cells, it results in extreme cytotoxicity. This might also be a problem when full length hNEIL3 is expressed in yeast during Y2H. It is known that when bait proteins poison yeast, it almost always results in a high frequency of false positive clones in screens (Duttweiler, 1996; Serebriiskii *et al*., 2000). One indicator that shows this might have happened here is the delay in the start of colony growth during the screening. Instead of two days it took five days until growth of colonies was first detected (Section 5.6.2). Therefore, during this time, the yeast may have evolved mutations in the host strain due to selective pressure by the leucine lacking media and the toxicity of NEIL3, allowing the cells to grow on selective media without interaction of bait and prey. Further evidence that the host yeast strain had mutated can be inferred from the fact that potential positive colonies, picked from the screening plates, grew on glucose medium lacking leucine (Section 5.6.3; MacDonald *et al.,* 2001). That would also explain why the initial autoactivation test (Section 5.4.1) showed no autoactivation of *Leu2* expression by full-length hNEIL3, because at that stage of the project, the yeast strain contained no mutations.

In addition, the fact that for the Jurkat T-Cell library screen the colonies appeared after only three days but with the same phenotype as described above leads to the conclusion that the expression of the *Leu* gene caused by mutation happened only due to toxicity of overexpressed NEIL3 rather than selective pressure.

In contrast to this theory the phenotype of a negative control clone which expressed the bait, NEIL3-LexA, and the activation domain B42 on its own (without the prey) did not show any growth on plates lacking leucine suggesting that the hypothesis that a mutation led to leucine production and therefore growth of random cells was not correct. However, interestingly a colour change was observed for the same clones on the blue/white screening plates ('negative' in Figure 84). This was contradictory to the results from both Y2H library screenings. In these screenings some clones remained white on both plates which indicated that no interaction had occured. As clones expressing NEIL3-LexA on its own do not show this phenotype it leads to the conclusion that NEIL3-LexA might interact with B42 itself resulting in the observed colour change of the colonies to blue. In addition, if B42 is fused to another protein, the final product might fold in a way that hinders NEIL3-LexA binding to the B42 domain and therefore does not allow *LacZ* gene expression. This would explain why the colonies remained white on X-Gal plates. The extended C-terminus of NEIL3 might play a crucial role in this interaction as its function remains unknown. Therefore, it may be important to use truncated versions of NEIL3 for the negative control to confirm this hypothesis. On the other hand, the fact that no growth of negative control clones on plates lacking leucine was observed might indicate that NEIL3-LexA, or the prey fusion protein, was not able to enter the nucleus in the first place, whereas some prey was able to and activated leucine expression on their own. However, if the repression assay (used to confirm localization of bait NEIL3-LexA into the nucleus after expression) performed in Section 5.4.3 is compared with the repression assay performed by Dr. Manal Shalaby (2009) the same grade of colour change can be observed (Figure 52 and Figure 93). Because of these contradictory results, it remains unclear if hNEIL3 was able to enter the nucleus or not.

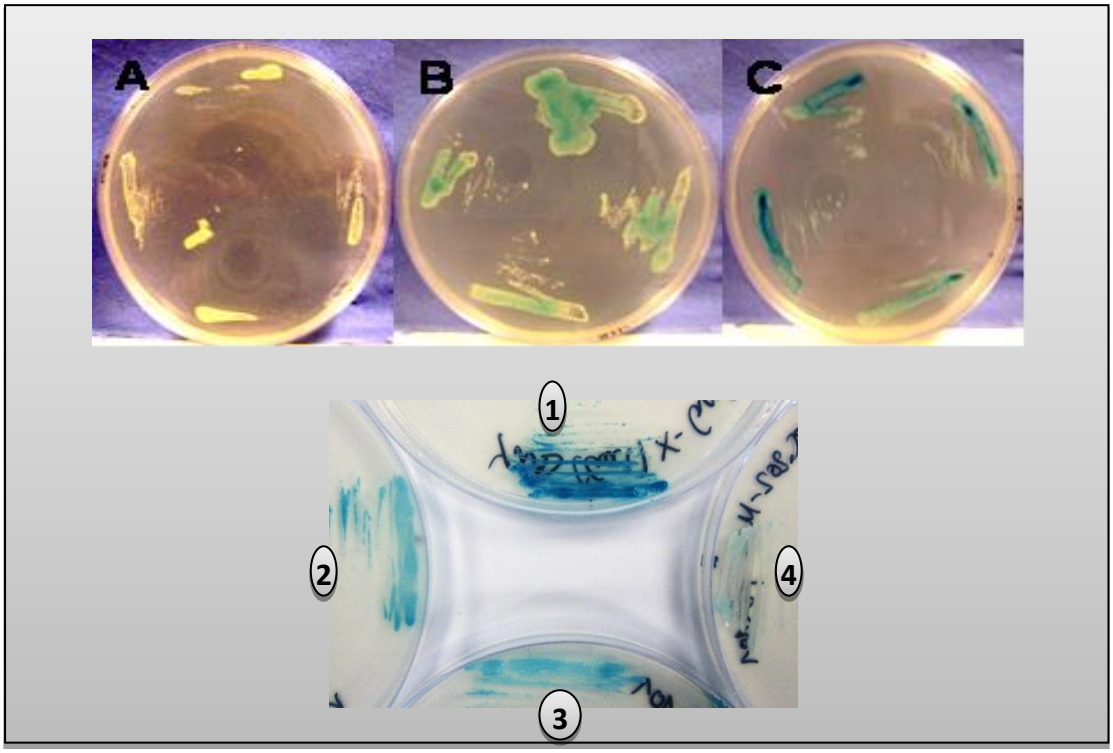

Figure 93: Comparison between repression assay results. Top = Result of a repression assay performed by Manal Shalaby (2009); positive control (A); pEG202-Tip-1 (B); negative control (C). Bottom = result of repression assay from Section 5.4.3; negative (1); pEG202-N3 (2); pEG202-NLS-N3 (3); and positive (4) control.

As Liu *et al.* (2013) stated "Full-length mNeil3 is … prone to aggregation." it might be possible that NEIL3 protein accumulated in the yeast and therefore allowed some proteins to bind depending on what structure was formed and what motifs were presented to the surrounding area.

According to Serebriiskii *et al.* (2000), transcription of the *LacZ* gene can be activated by the expressed prey protein itself or if co-expressed with the bait protein. This would result in a colour change on media where the expression of the prey protein is induced by the galactose, while colonies on plates that contain glucose, where the prey protein is not expressed, would remain white, as observed in this project. This would also explain why not all clones showed this phenotype during screening and why autoactivation tests carried out with hNEIL3 did not show any activation of *LacZ* gene expression on its own (Section 5.4.2).

Degradation of hNEIL3 after expression cannot be ruled out as the western blot that was carried out in Section 5.5 was performed with a 24 h culture. This does not represent the conditions during a screening that took more than five days for the yeast to grow. Additional faint bands were observed when the western blot was performed after 24 h that might indicate degraded hNEIL3-LexA. If hNEIL3-LexA is degraded over time, perhaps one or more of the proteolytic products are able to interact with proteins expressed from the cDNA library and hence activating leucine expression.

Regarding this project, the autoactivation tests appear to be correct, as autoactivation of leucine expression by hNEIL3 would have led to early growth (or high background growth) during screening on plates lacking leucine rather than a delay of growth. Furthermore, a more evenly distributed colour change during the blue/white screening would have been expected as NEIL3 should also autoactivate *LacZ* gene expression than was observed for both Y2H screenings performed.

6.2 Overexpression in *P. pastoris*

Before starting these experiments, a band of the expected size was obtained following western blotting with an anti-LexA antibody on lysates obtained from *S. cerevisae* strain EGY48 that expresses a hNEIL3-LexA fusion protein for use in Y2H (Figure 53). Therefore, having shown that expression of full length hNEIL3 was possible in yeast, it was decided to try to overexpress hNEIL3 using a *P. pastoris* system optimized for recombinant protein expression.

Thus, several clones of *P. pastoris* each carrying either full length CDS cDNA of hNEIL3, full length CDS cDNA of mNEIL1 or truncated versions of hNEIL3 (amino

acid length 394 or 502) were successfully generated, correct DNA integration was confirmed by PCR and clones were stored at -80°C for further experiments.

Coomassie blue stained SDS-PAGE gels of samples of culture medium that should contain secreted protein showed a band for mNEIL1 at the predicted size, whereas no band was visible for hNEIL3 (Figure 92). Although different temperatures (28°C and 30°C), incubation times (24 h to 120 h) and culture volumes (10 ml and 50 ml) were used to increase the likelihood of hNEIL3 protein expression, no recombinant protein was detected. However, western blotting with a monoclonal anti-His-Tag antibody did not recognize either protein indicating that the observed band was not his-tagged NEIL1 and the antibody was not binding as expected or was denatured. Unfortunately, no positive control was available to check the latter possibility. Similarly, a rabbit polyclonal anti-hNEIL3 antibody used in western blotting with cell lysates and liquid culture medium did not reveal the existence of any hNEIL3 protein. Further experiments would be needed to clarify the situation, but unfortunately time did not permit this.

In addition, it has previously been reported that in *E. coli*, overexpressed full length hNEIL3 protein is very unstable and difficult to recover from cells in detectable quantities (Krokeide *et al.,* 2009; Takao *et al.,* 2009; Liu *et al.,* 2010, 2012). Hence, hNEIL3 might be rapidly degraded after its expression and/or secretion into the medium from *P. pastoris*. However, since it was possible to isolate a full length hNEIL3-LexA fusion protein expressed in *S. cerevisiae* EGY48 cells, clearly hNEIL3 was not completely degraded when expressed as a fusion protein. Therefore, either hNEIL3 was protected from degradation because it was part of a fusion protein, or the

S. cerevisiae strain EGY48 has different cellular conditions than the *P. pastoris* strain, or the fact that hNEIL3 was not secreted in the *S. cerevisae* system might

explain the successful recovery. To confirm this latter hypothesis, further experiments would have to be carried out, *e.g.* expression of hNEIL3 in *P. pastoris* without the secretion signal to see if it is secreted in the first place and to determine if it stays intact if not secreted.

Difficulty in expressing active full length NEIL3 could be related to the extended C-terminal domain and its tandem GRF-zinc finger motifs as, interestingly, both APE2 and TopoIIIα, which have this domain, have also been reported to be difficult to express and purify (Hanai *et al.*, 1996; Hadi & Wilson, 2000). This was confirmed by Krokeide *et al.,* (2009) who made truncated versions of mouse NEIL3 without the GRF-zinc finger motifs that showed a much more efficient expression of active protein, leading to the conclusion that GRF-zinc finger motifs probably hinder the correct expression and folding of NEIL3. In addition, recent studies show that processing of the N-terminal methionine in NEIL3 is crucial for its activity and underscores the importance of posttranslational modifications (Liu *et al.*, 2012). This group co-expressed an *E. coli* methionine aminopeptidase Y168A variant with mouse and human NEIL3 to improve the N-terminal methionine processing. This way they were able to obtain a higher percentage of active full length and truncated mouse and truncated human NEIL3. Interestingly, 85% of the full length mouse NEIL3 protein remained inactive and no active full length human NEIL3 protein was obtained. This indicates the difficulty encountered in expression of full length NEIL3 and that the problem lies principally in its C-terminal region where amino acid residues 400 to 500 are predicted to be structurally disordered. This region of the NEIL3 polypeptide contains only a putative NLS domain (amino acid residues 465-468). Based on this information, truncated versions of NEIL3 generated in prior studies (Krokeide *et al.* 2009; Liu *et al.*, 2012) should also be used in future studies of hNEIL3 in comparison with the full length version, should this be achievable.

6.3 Future outlook

It must be considered if it is useful to use a Y2H assay to search for NEIL3-interacting proteins. NEIL3 is only expressed in vertebrate cells, which has led to the suggestion, that the biological function of NEIL3 is specific to higher eukaryotes (Takao *et al.,* 2009). Therefore, this leads to the conclusion that NEIL3 may require mammalian cell - like conditions including specific posttranslational modifications, which may not be identical or appropriately controlled in yeast cells, to be fully functional.

Mammalian two-hybrid as alternative to Y2H

Although mammalian two-hybrid (M2H) systems have been used less than Y2H systems, the fact that yeast do not provide the full range, or correct control of posttranslational modifications as mammalian cells, gives the system an advantage. The functionality of the M2H system was verified by Luo *et al*. (1997), who confirmed the interaction of the mouse p53 tumour suppressor protein with the simian virus 40 large T antigen. Furthermore, they showed that assay results can be obtained within 48 h of transfection and also made the point that studying protein interactions in mammalian cells may be closer to the actual *in vivo* interactions in the cell of origin (Luo *et al.,* 1997). The reason why Y2H is more commonly used is that M2H is not suitable to screen large numbers of prey proteins due its format and it is more likely to give false negative results, which means that potential protein partners for NEIL3 may stay undiscovered (Dr. A.W. Oliver personal communication; Anon, 2007). Therefore, while Y2H is much more sensitive, results obtained should be confirmed in a M2H assay. However, as discussed in Section 6.1.2, it is important to consider that overexpression of hNEIL3 might be toxic to primary eukaryotic cells in general.

Co-immunoprecipitation

Co-immunoprecipitation is commonly used to confirm potential protein-protein interactions *in vivo*. Because the protein of interest is expressed in its natural environment, post-translational modifications that may be necessary for interaction will occur and the proteins will be available in their native conformation. To this end, it would be interesting to use the MOLT4 lymphoblastic leukaemia cell line in these investigations, since recent studies have shown high gene expression levels for hNEIL3 in this cell line (Figure 104; Genomics Institute of the Novartis Research Foundation, 2009). Another system that may hold promise for future studies makes use of the HaloTag technology developed by Promega. This could be used to investigate the cellular localization of NEIL3 and possible protein interactions in pull-down studies. The HaloTag system is a mammalian expression vector system that uses a tag that codes for a monomeric 33 kDa protein that is fused during expression to either the N-terminal or C-terminal end of the protein of interest. As NEIL3 showed extreme cytotoxic effects when overexpressed in mammalian cells, it is of special interest to express NEIL3 at low levels and with HaloTag it might still be possible to visualize or recover it within or from the cell (Krokeide *et al*., 2008).

FRET/BRET

The problem with co-immunoprecipitation is that the cell-content has to be extracted, which may cause an alteration in the conformation of the protein complex of interest. This may lead to a loss of interaction with a potential protein partner. To observe protein-protein interactions *in situ*, immunofluorescence methods such as fluorescence resonance energy transfer (FRET) and bioluminescence resonance energy transfer (BRET) can be used. However, these techniques are only suitable to confirm an interaction observed by another method and thus it is not useful for

screening large numbers of prey proteins. However, they maybe useful for confirming potential protein-protein interactions determined by *in vitro* assays in a mammalian cell environment and to reveal their location within the cell (Anon, 2007).

6.4 Overall discussion

Recent studies investigating DNA glycosylase and AP lyase activities of NEIL3 suggest that this protein plays a role in BER (Krokeide *et al.,* 2009; Takao *et al.,* 2009; Liu *et al.,* 2010, 2012, 2013). Therefore, NEIL3 would contribute to the defence against ROS in a cell and in the maintenance of genomic stability. However, recent research also suggests that overexpressed BER enzymes play a vital role in the survival of tumour cells treated with genotoxic agents. For example, a high level of APE1 expression was linked to tumour cell resistance to chemo- and radiotherapy by several groups (Bobola *et al.*, 2005; Freitas *et al.*, 2003; Robertson *et al.*, 2001). On the other hand, if APE1 was downregulated it sensitized these cells to anticancer drugs and induced apoptosis (Izumi *et al.*, 2005; Robertson *et al.,* 1997; Wang *et al.*, 2004).

Although the common DNA oxidation product 8-oxoG has not been identified as a preferred substrate for NEIL3, other types of oxidized guanine, such as FapyG and the hydantoin lesions Sp and Gh (oxidised forms of 8-oxoG), were found to be released by the N-terminal DNA glycosylase domain of NEIL3 (Liu *et al.,* 2012). In addition, studies on gene expression patterns in neoplastic cells revealed that expression of the *NEIL3* gene is dramatically increased in metastatic cancer cells compared to that of other BER genes such as *hOGG1* (Kauffmann *et al.,* 2008). The fact that proteins that are linked to DNA repair and also to DNA replication are overexpressed in melanoma cells could partly explain the resistance of these

malignant cells to genotoxic chemotherapy agents. Compounds that inhibit specific proteins involved in DNA repair such as PARP-1 have already been developed and their use in combination with other chemotherapy agents shows some benefit in the clinic (O'Shaughnessy *et al.,* 2009; Kummar *et al*., 2012). The latest clinical trials show that PARP-1 inhibitors are especially effective for the treatment of breast cancer where the cells have a mutation in the tumour suppressor genes BRCA 1 or 2 resulting in a decreased rate of DSB repair, so called synthetic lethality (O'Shaughnessy *et al.,* 2009; Tutt *et al*., 2010).

One reason why PARP-1 was used as a target for inhibition in the first place is that it plays a role in BER and its inhibition was known to delay strand rejoining (Hooten *et al.*, 2012; Mansour *et al.*, 2010). As NEIL3 expression is so much higher in malignant cells compared to normal cells it might play a crucial role in combating DNA damage and therefore securing cancer cell survival. Therefore, it is of great interest to investigate the effects on viability of a NEIL3 knockout (or double knockout with PARP) cancer cell line treated with a genotoxic agent.

However, the problem in inhibiting proteins that are involved in DNA repair is that it affects the whole organism and results in collateral toxicities (Drew & Plummer, 2009). Furthermore, each metastasis will be resistant to different drugs, which makes treatment of metastatic cancer difficult. However, as NEIL3 is highly expressed in malignant cells, inhibiting it might preferentially target the tumour cells and on the other hand have less effect on normal cells. In addition, NEIL3 might play a crucial role in genomic maintenance to secure cell survival and increased resistance of the cell against DNA targeted anticancer drugs (Hildrestrand *et al.,* 2009). Although the inhibition of DNA glycosylases may be inefficient due to back up functions of other DNA glycosylases, or make cells even more resistant to genotoxic agents, as shown for knockout mouse models, respectively (Rinne *et al.*, 2004; Roth & Samson, 2002)

NEIL3 could still be an interesting target for protein inhibiting anticancer drugs because of its spatially and temporally restricted expression pattern (Hegde *et al*. 2008b). Tumour cell targeted NEIL3 knockdown by siRNAs is another treatment possibility that is the subject of much recent research (Pecot *et al*., 2011).

The first evidence that a DNA glycosylase is involved in regulation of the cell cycle was given for the DNA glycosylase MPG which inhibits p53-mediated cell cycle arrest (Song *et al.* 2012). Like NEIL3, MPG expression is cell cycle dependent with levels highest during G_1 phase (Bouziane, 2000). Since it is known that NEIL3 gene expression is upregulated in cells leaving the G_0 phase and entering G_1 phase (Neurauter *et al.*, 2012), it might be of interest to investigate possible interactions of NEIL3 with p53 or other cell cycle regulatory proteins.

Another indicator that NEIL3 is active during DNA replication is the similarity of its C-terminal end with that of TopoIIIα. TopoIIIα is expressed mainly in testes and is active during DNA recombination on the double Holliday junction dissolvasome complex (Chen *et al.*, 2012). Interestingly, the function of TopoIIIα relies on its C-terminal tandem GRF zinc finger domain (Chen *et al.,* 2012), which is also present in the C-terminal domain of NEIL3. Further evidence that this domain is involved in recombination is that the other type IA topoisomerase, TopoIIIβ which is not able to dissolve the double Holliday junction, has a shorter C-terminus that lacks the GRF zinc fingers (Chen *et al.,* 2012). This group also showed that these GRF zinc fingers are responsible for the interaction with the first 133 N-terminal amino acids and the 150 C-terminal amino acids of the Bloom Syndrome protein (BLM helicase; Hu *et al*., 2001). In addition, BLM helicase is considered to be a major protein interaction partner for p53 and therefore indirectly regulates transcription and cell growth but on the other hand p53 indirectly regulates the processing of Holliday junctions by its inhibitory interaction with BLM (Wang *et al.*, 2001; Yang *et al*., 2002). Interestingly,

overexpression of BLM helicase showed an inhibition of proliferation which might also affect the expression of NEIL3 as the expression levels of NEIL3 are high in proliferating cells (Garkavtsev *et al.*, 2001). Therefore, the GRF Znf at the C-terminal region of NEIL3 might also be able to interact with the BLM helicase. Furthermore, FEN1 also was shown to interact with BLM helicase (Sharma *et al.*, 2004). This is interesting, because FEN1 shows similar expression patterns to that of NEIL3 (Neurauter *et al.,* 2012). Therefore, with increased knowledge about these protein domains, it might be possible to find other potential binding partners that have conserved BLM helicase motifs.

Furthermore, TopoIIIα together with BLM helicase are known to play an important role in the alternative pathway of telomere lengthening in the absence of telomerase. In fact, an absence of TopoIIIα led to an increase in overall DNA damage on telomeres in cells lacking telomerase (Temime-Smaali *et al.,* 2008). This indicates that TopoIIIα might be an essential telomere-associated factor and as expression levels of NEIL3 are high in testes, where telomeres are maintained at their maximum length, it might be worth focusing studies for NEIL3 on telomere maintenance pathways. The fact that no change in phenotype of NEIL3$^{-/-}$ mice was observed might be due to the short period of time the tests were made and no generational studies have been reported (Torisu *et al.*, 2005). As telomeres are known to play an important role in aging, a change in telomeres, either by their shortening or mutation, might affect an organism only in later stages of life (Cherif *et al.*, 2002). On the other hand, first attempts to link high expression levels of NEIL3 in tumour cells to telomere shortening were not successful (Frias *et al.*, 2008). However, these studies were carried out in non-small cell lung cancer cells which have not been reported to have high levels of active NEIL3 (Section 2.3.5.2.3). Hence, it is important to consider that NEIL3 has very tissue specific expression patterns which might acutely affect the phenotype only of certain tissues, but not the whole organism.

The fact that the expression level of NEIL3 is elevated in certain oxidatively stressed cells and during G_1-S phase and the similarity of its C-terminal structure with that of TopoIIIα leads to the conclusion that NEIL3 might play a role in counteracting the effects of oxidative stress on telomeres via its DNA glycosylase activity and maybe in cooperation with BLM helicase. As it was found that stressed animals have shorter telomeres on average, which might be related to increased levels of oxidative stress, it might be worth repeating these tests in NEIL3 knockout mice with respect to their telomeres (Epel *et al.,* 2004).

There is also evidence that p53 not only interacts with BLM helicase but also with WRN to inhibit their activity (Yang *et al*., 2002). Interestingly WRN is also an interaction partner for NEIL1 that enhances its DNA glycosylase activity on oxidized purines (Das *et al*., 2007a). As the expression of NEIL1, like NEIL3, is cell cycle dependent and is also mainly active on ssDNA substrates, it would be of great interest to determine potential interactions between NEIL3 and WRN.

To date, several groups have reported that an efficient expression and purification of active full length NEIL3 in an eukaryotic cell system in amounts high enough to be used in downstream assays could not be achieved (Krokeide *et al.,* 2009; Liu *et al.,* 2010 and 2012) and although it was possible in this project to express full length NEIL3 as a fusion protein in an eukaryotic cell system (yeast) it was not possible to purify active NEIL3 for further use.

It is known that NEIL1 and NEIL2 interact with other proteins involved in BER such as PNK, Polβ and LigIIIα and thus it is possible that NEIL3 also has to interact with these proteins to fulfil its function in BER (Wiederhold *et al.,* 2004; Das *et al.,* 2006). The first evidence of interaction was found for RPA as it was co-localized with

hNEIL3 in the nucleus and alignment of hNEIL3 protein sequence with sequences from proteins known to bind to PCNA and RPA revealed a putative PCNA- (residues 80-96) and RPA-binding (residues 30-45) site (Morland *et al.* 2002).

BER is known to be a pathway where many different protein complexes are involved depending on the sort of DNA damage. Proteins contained in such complexes can either act as scaffold proteins or as enhancers that increase the activity or turnover rate of other proteins. An example of an enhancer is the YB-1 protein which significantly enhances the base excision activity of NEIL2 via a stable interaction (Das *et al.,* 2007b). However, as YB-1 also interacts with the downstream proteins LigIIIα and Polβ, it is likely that NEIL2 and YB-1 are part of a larger protein complex during DNA repair. Furthermore, YB-1 is also an interacting partner of APE1. If APE1 is posttranslationally acetylated it modulates YB-1-mediated activation of expression of the ABC-transporter P-glycoprotein-1 (Chattopadhyay *et al*., 2008). The membrane protein P-glycoprotein-1 is responsible for multidrug resistance by acting as an efflux pump to remove xenobiotics such as antitumour agents from cells (Kakumoto *et al*., 2005). If NEIL3, with respect to its high expression levels in cancer cells, also indirectly stimulates P-glycoprotein-1 expression through YB-1 modulation, it might explain why these cells show a high degree of drug resistance. On the other hand, it was recently shown that YB-1 and RPA inhibit the AP lyase activity of NEIL1 on ssDNA, presumably due to competition, as YB-1 and RPA both have a high affinity for ssDNA (Pestryakov *et al*., 2012).

Not only proteins such as YB-1 might be an important target for further investigations on the biological role of NEIL3 but also posttranslational modifications, in particular acetylation. For example, for NEIL2 it was found that posttranslational acetylation of the Lys49 residue by the acetyltransferase p300 inhibits its DNA glycosylase and AP lyase activity (Bhakat *et al.*, 2004). Interestingly, Lys49 is a residue that is conserved

within the NEIL family. Acetylation on residues other than Lys49 might affect the ability of NEIL3 to interact with certain protein partners and has to be considered when carrying out protein-protein interaction studies. For example, it was shown that PCNA is also acetylated by p300, however, when it is deacetylated by histone deacetylase-1 (HDAC1) it loses its affinity for Polβ and Polδ (Naryzhny & Lee, 2004). Other proteins that are acetylated by p300 are FEN1, Polβ, OGG1 and thymine DNA glycosylase (TDG) (Bhakat *et al.*, 2006; Hasan *et al.*, 2001, 2002; Tini *et al*., 2002). For example, acetylation of OGG1 at Lys338/Lys341 increases its rate of repair of 8-oxoG by 2.5-fold (Bhakat *et al*., 2006) which leads to the suggestion that p300 might play a crucial role in the regulation of BER proteins.

DNA glycosylases such as OGG1 (Hill *et al.*, 2001), UNG (Parikh *et al*., 1998), TDG (Privezentzev *et al.*, 2001; Waters, Gallinari *et al.*, 1999), single-strand selective monofunctional uracil DNA glycosylase (SMUG1) (Kavli *et al*., 2002) and NTH1 (Marenstein *et al*., 2003) are known to have a higher affinity to the AP-site they create than they had to the original DNA lesion. However, APE1 seems to have more affinity for the AP lesion, replacing the DNA glycosylases and therefore increasing their turnover rate (Hill *et al.*, 2001; Parikh *et al.*, 1998; Privezentzev *et al*., 2001; Kavli *et al*., 2002; Marenstein *et al.*, 2003). It must be considered that these DNA glycosylases are either monofunctional (UNG, TDG, SMUG1) or bifunctional with β-lyase activity (OGG1 and NTH1) but that both result in a substrate for APE1 (either AP-site for monofunctional or unsaturated aldehyde overhangs for bifunctional DNA glycosylases). For the NEIL proteins this is not the case as they have a β,δ-lyase activity resulting in the release of the deoxyribose sugar leaving 5′-P and 3′-P. Therefore, the function of APE1 that increases the turnover rate of other DNA glycosylases may not be applicable to the NEIL proteins, as the 3′-phosphatase activity of APE1 is very weak (Wiederhold *et al.*, 2004). Therefore, APE1 may be unlikely to interact with NEIL3. However, perhaps PNK plays a similar role to APE1

for the NEIL proteins by increasing their turnover rate due to its affinity for 3′-P sites. Recently, it was shown that in the presence of XRCC1, LigIIIα and Polβ, PNK is part of a BER complex with NEIL1 and NEIL2 (Wiederhold *et al*., 2004; Das *et al*., 2006). Similarly, PCNA is known to enhance the activity of NEIL1 on the oxidized base 5-OH-U from ssDNA where it acts as a clamp that helps NEIL1 to load the substrate (Dou *et al.,* 2008). Although, PCNA does not stimulate NEIL2 it might still play a role in the function of NEIL3 as its substrates are more related to those of NEIL1.

While they usually act as DNA glycosylases, NEIL1 and OGG1 also can stimulate the poly(ADP-ribosyl)ation activity of PARP-1 by binding to its C-terminal domain (Hooten *et al.,* 2011, 2012). This is an example of proteins (in this case NEIL1 and OGG1) that can have different functions depending on the kind of interaction. Hence, it is not controversial if it is proposed on one hand that NEIL3 plays a part in BER during DNA replication and in recombination of chromosomes on the other. Another example of a multifunctional protein is XRCC1, a scaffold protein known as a fundamental protein interactor during BER and SSB repair. If NEIL3 acts during BER as suggested, XRCC1 might be a very important target as a protein partner for NEIL3. It might stabilise the DNA binding capability of NEIL3 or it could recruit other proteins essential for the DNA interaction or repair process.

As NEIL3 contains a RanBP zinc finger and a NLS sequence it is likely that NEIL3 also has to interact with specific nucleus transport proteins to be located correctly within the cell after its translation (Section 2.3.5.2.3).

A suppression of HIV integration following RNAi knockdown of proteins involved in BER was first reported by Kameoka *et al.* (2004). NEIL3 also seems to play an important role in this as recent siRNA studies revealed that genomic HIV integration in cells lacking NEIL3 is significantly decreased (Yoder *et al.,* 2011; Espeseth *et al.,*

2011a and Zhou *et al.,* 2008). One hypothesis might be that bifunctional DNA glycosylases such as NEIL3 help the viral integrase protein to fulfil its function. For example, perhaps NEIL3 can interact with the integrase protein transporting it into the nucleus via its NLS where it then binds to DNA. Once NEIL3 has excised an oxidized base and cut the resulting AP site via its AP-lyase activity, the resulting gap could be used by the integrase itself to insert the vDNA in form of a DNA loop. Subsequent DNA replication would then fully integrate the vDNA into the genomic DNA. However, such a DNA loop would be prone to recognition by p53 which would activate repair complexes such as MMR or even induce apoptosis. On the other hand, depending on its final conformation the loop could be resistant to repair mechanisms as was proposed for MMR and short DNA loops (Lang *et al.,* 2011). The fact that HIV cannot replicate within a cell during quiescence (G_0-phase in cell cycle) because this state blocks the reverse transcription process gives further evidence for the involvement of hNEIL3 in vDNA integration as its expression is stimulated by the release from quiescence (Amado & Chen, 1999; Neurauter *et al.,* 2012). The patent submitted by Espeseth *et al.* (2011b) regarding drugs inhibiting hNEIL3 underscores the importance of studying the biological role of hNEIL3 in relation to HIV integration and lentivirus integration in general. This patent also includes MUTYH, LigIIIα, Polβ as potential drug targets to hinder HIV integration. However, the inhibition of LigIIIα and Polβ would affect the whole organism and its DNA metabolism that includes DNA repair, replication and recombination, whereas hNEIL3 might have a significant effect on HIV integration but not on the overall fitness of the organism and this could reduce harmful side-effects.

The fact that there was no obvious change in the phenotype of NEIL3$^{-/-}$ mice does not mean that the organism was not affected at all. As stated before, maybe only specific tissues were affected or the observations were too short in time to see changes that might have only arisen with age. In addition it has to be considered that

perhaps the learning and memory capacity of NEIL3$^{-/-}$ mice is affected which is not necessarily an obvious aspect. Therefore, strategies to test this should be devised as also suggested by other groups (*e.g.* Marin-Burgin & Schinder, 2012). Evidence for the influence of NEIL3 on the brain was given by Regnell *et al.* (2012) who discovered morphologic alterations in the hippocampal network and reduced neurogenesis *in vivo* for NEIL3$^{-/-}$ cells. Neurogenesis is essential for the restoration of brain function after injury and also required for shaping the structural basis for learning and memory in the hippocampal structure (Sejersted *et al*., 2011). Hence, NEIL3 might play a crucial role as the main DNA glycosylase for Sp and Gh lesions in ssDNA in neuronal cells and therefore may be essential for retaining the cognitive behaviour in vertebrates.

Conclusions and future perspectives

The aim of this project was to find potential interacting protein partners for human NEIL3 and thus provide a clue to understanding the biological role of NEIL3. While recent studies have begun to shed light on the different biological processes that NEIL3 is involved in, it is still not clear why mammalian cells require this DNA glycosylase in particular, and what role the unique protein motifs play in its biological activities. It is known that the N-terminal region of NEIL3 includes a DNA glycosylase and H2TH motif conserved among NEIL1, NEIL2 and Fpg/Nei *in E. coli*. The function of these domains in the other proteins leads to the conclusion that NEIL3 plays a role in DNA repair. However, the predominantly C-terminal protein domains have yet to be ascribed a biological function and unfortunately this question remains as relevant now as at the start of this project.

While mouse NEIL3 expression was shown to be upregulated in hematopoietic tissue and testes, during embryonic development and in stem/progenitor rich regions in the

brain the gene expression patterns of human NEIL3 in these tissues remains largely to be determined (Hildrestrand *et al.*, 2009; Kauffmann *et al*., 2008; Morland *et al.*, 2002; Rolseth *et al.*, 2008; Takao *et al.*, 2009; Torisu *et al*., 2005). As all these tissues contain highly proliferating cells, and the fact that NEIL3 is upregulated in early S phase, makes it most likely that its function is to remove lesions from the genome in replicating cells (Neurauter *et al.*, 2012). As it is known that NEIL3 shows higher activity in murine neural stem/progenitor cells compared to differentiated cells (Rolseth *et al.*, 2008; Hildrestand *et al.*, 2009), and that NEIL3$^{-/-}$ mice show a decreased repair capacity in damaged areas of the brain, it leads to the conclusion that NEIL3 gene expression is stimulated by transcription factors that are regulated by the differentiation and proliferation state of vertebrate neural progenitor cells.

To date, the potential interacting protein partners found in this project remain to be confirmed. However, although there seems to be no link between a protein such as CGB8 and NEIL3, it does not necessarily mean that it is a false positive result. NEIL3 was shown and is suggested, as discussed before, to play an important role in several independent processes within a cell. Therefore it is still important to undertake further efforts to find potential protein partners. Such proteins might be responsible for posttranslational modifications of NEIL3 or help NEIL3 to bind to DNA or other proteins. Such results would help to develop hypotheses or to confirm assumptions already made about the biological role of NEIL3. To confirm its place within BER, further investigations have to be carried out which focus on interaction with downstream and scaffold proteins involved in BER. The focus herein should be on *in vivo* investigations as only this way can the correct folding and posttranslational modification be ensured.

The recently identified DNA substrates that NEIL3 can release from DNA comprise oxidized guanines (Liu *et al.*, 2012), which are likely to be formed more frequently by

ROS in cells that have an increased metabolic rate (Beckman & Ames, 1998). If the latest results regarding gene expression levels and the DNA repair capability of NEIL3 are brought together with the fact that ROS generation is especially increased in cancer cells (Pelicano *et al*., 2004), it makes good sense that rapidly dividing cells need NEIL3 to secure their genomic integrity during DNA replication and therefore stimulate its expression. Thus, further studies should be focused on a restricted assortment of cell types where high expression of NEIL3 has been determined, such as cancer cell lines. Clarifying the significance of increased expression levels of NEIL3 in tumour cells might also explain its potential function within the normal cell and maybe NEIL3 can even be used as a new biological marker for diagnostic purposes or as a target for next generation cancer drugs. In addition, as evidence was found that NEIL3 reduces reverse transcription up to or including integration of HIV (Espeseth *et al.*, 2011a; Yoder *et al.,* 2011; Zhou *et al.,* 2008), another benefit of NEIL3 inhibiting drugs could be their use in the prevention of HIV pathogenesis.

In summary this work has demonstrated the following:

- Design, construction and validation of new DNA vectors for Y2H and LexA fusion protein expression
- Successful expression of hNEIL3-LexA in yeast
- Identification of potential interacting clones and DNA sequences
- Establishment of a Y2H system for DNA glycosylases
- Possible interaction between LigIII and hNEIL3
- Use of *P. pastoris* as an expression system

7 References

Alanazi, M., Leadon, S.A. & Mellon, I. (2002). Global genome removal of thymine glycol in *Escherichia coli* requires endonuclease III but the persistence of processed repair intermediates rather than thymine glycol correlates with cellular sensitivity to high doses of hydrogen peroxide. *Nucleic Acids Res., 30*, 4583-4591.

Amado, R.G. & Chen, Y.I.S. (1999). Lentiviral vectors – the promise of gene therapy within reach? *Science, 285*, 674-676.

Anon (2007). Promega - protein interaction guide [Online] Available at: http://www.promega.com/guides/protein.interactions_guide/protein.interactions_gde.pdf [Accessed 02 December 2010].

Anon (2009). OriGene – TrueClone human full-length cDNA clones application guide [Online] Available at: http://www.origene.com/assets/Documents/catalog_manual/AppGuideTruecloAp10ug.pdf [Accessed 07 December 2010].

Asagoshi, K., Terato, H., Ohyama, Y. & Ide, H. (2002). Effects of a guanine-derived formamidopyrimidine lesion on DNA replication - translesion DNA synthesis, nucleotide insertion, and extension kinetics. *J. Biol. Chem., 277*, 14589-14597.

Bambara, R.A., Murante, R.S. & Henricksen, L.A. (1997). Enzymes and reactions at the eukaryotic DNA replication fork. *J. Biol. Chem., 272*, 4647-4650.

Bandaru, V., Sunkara, S., Wallace, S.S. & Bond, J.P. (2002). A novel human DNA glycosylase that removes oxidative DNA damage and is homologous to *Escherichia coli* endonuclease VIII. *DNA Repair, 1*, 517-529.

Bandaru, V., Zhao, X., Newton, M.R., Burrows, C.J. & Wallace, S.S. (2007). Human endonuclease VIII-like (NEIL) proteins in the giant DNA mimivirus. *DNA Repair, 6*, 1629-1641.

Beckman, K.B. & Ames, B.N. (1998). Radical Theory of Aging Matures. *Physiol. Rev., 78*(2), 547-581.

Bernstein, C., Bernstein, H., Payne, C.M. & Garewal, H. (2002). DNA repair/proapoptotic dual-role proteins in five major DNA repair pathways: fail-safe protection against carcinogenesis. *Mutat. Res., 511*(2), 145-178.

Bhakat, K.K., Hazra, T.K. & Mitra, S. (2004). Acetylation of the human DNA glycosylase NEIL2 and inhibition of its activity. *Nucleic Acids Res., 32*(10), 3033-3039.

Bhakat, K.K., Mokkapati, S.K., Boldogh, I., Hazra, T.K. & Mitra, S. (2006). Acetylation of human 8-oxoguanine-DNA glycosylase by p300 and its role in 8-oxoguanine repair *in vivo*. *Mol. Cell. Biol., 26*(5), 1654-1665.

Bobola, M.S., Finn, L.S., Ellenbogen, R.G., Geyer, J.R., Berger, M.S., Braga, J.M., Meade, E.H., Gross, M.E. & Silber, J.R. (2005). Apurinic/apyrimidinic endonuclease activity is associated with response to radiation and chemotherapy in medulloblastoma and primitive neuroectodermal tumours. *Clin. Cancer Res., 11*, 7405-7414.

Bouziane, M., Miao, F., Bates, S.E., Somsouk, L, Sang, B.C., Denissenko, M. & O'Connor, T.R. (2000). Promoter structure and cell cycle dependent expression of the human methylpurine-DNA glycosylase gene. *Mutat. Res., 461*, 15-29.

Breen, A.P. & Murphy, J.A. (1995). Reactions of oxyl radicals with DNA. *Free Radical Bio. Med., 18*(6), 1033-1077.

Brown, E.J. & Baltimore, D. (2003). Essential and dispensable roles of ATR in cell cycle arrest and genome maintenance. *Gene Dev., 17*, 615-628.

Brown, T.A. (1998) *Genetics - A molecular approach* (3rd ed.). Cheltenham: Stanley Thornes (Publishers) Ltd.

Brown, T.A. (2002) *Genomes* (3rd ed.). Oxford: BIOS Scientific Publishers Ltd.

Bruner, S.D., Nash, H.M., Lane, W.S. & Verdine, G.L. (1998). Repair of oxidatively damaged guanine in *Saccharomyces cerevisiae* by an alternative pathway. *Curr. Biol., 8*, 393-403.

Burgess, S., Jaruga, P., Dodson, M.L., Dizdaroglu, M. & Lloyd, R.S. (2002). Determination of active site residues in *Escherichia coli* endonuclease VIII. *J. Biol. Chem., 277*, 2938-2944.

Cadet, J., Sage, E. & Douki, T. (2005). Ultraviolett radiation-mediated damage to cellular DNA. *Mutat. Res., 571*, 3-17.

Caldecott, K.W., Tucker, J.D., Stanker, L.H. & Thompson, L.H. (1995). Characterization of the XRCC1-DNA ligase III complex *in vitro* and its absence from mutant hamster cells. *Nucleic Acids Res., 23*, 4836-4843.

Caldecott, K.W., Aoufouchi, S., Johnson, P. & Shall, S. (1996). XRCC1 polypeptide interacts with DNA polymerase beta and possibly poly (ADP-ribose) polymerase, and DNA ligase III is a novel molecular 'nick- sensor' *in vitro*. *Nucleic Acids Res., 24*, 4387–4394.

Campalans, A., Marsin, S., Nakabeppu, Y., O'Connor, T.R., Boiteux, S. & Radicella, J.P. (2005). XRCC1 interactions with multiple DNA glycosylases: A model for its recruitment to base excision repair. *DNA Repair, 4*(7), 826-835.

Campalans, A., Amouroux, R., Bravard, A., Epe, B. & Radicella, P. (2007). UVA irradiation induces relocalisation of the DNA repair protein hOGG1 to nuclear speckles. *J. Cell. Sci., 120*, 23-32.

Chattopadhyay, R., Das, S., Maiti, A.K., Boldogh, I., Xie, J., Hazra, T.K., Kohno, K., Mitra, S. & Bhakat, K.K. (2008). Regulatory role of human AP-endonuclease (APE1/Ref-1) in YB-1-mediated activation of the multidrug resistance gene MDR1. *Mol. Cell. Biol., 28*(23), 7066-7080.

Chen, S.H., Wu, C.H., Plank, J.L. & Hsieh, T.S. (2012). Essential functions of C terminus of *Drosophila* topoisomerase IIIα in double holliday junction dissolution. *J. Biol. Chem., 287*, 19346-19353.

Chen, J., Tomkinson, A.E., Ramos, W., Mackey, Z.B., Danehower, S., Walter, C.A., Schultz, R.A., Besterman, J.M. & Husain, I. (1995). Mammalian DNA ligase III: molecular cloning, chromosomal localization, and expression in spermatocytes undergoing meiotic recombination. *Mol. Cell. Biol., 15*, 5412-5422.

Cheng, K.C., Preston, B.D., Cahill, D.S., Dosanjh, M.K., Singer, B. & Loeb, L.A. (1991). The vinyl chloride DNA derivative N^2,3-ethenoguanine produces G → A transitions in *Escherichia coli*. *Proc. Natl. Acad. Sci. USA, 88*, 9974-9978.

Cherif, H., Tarry, J.L., Ozanne, S.E. & Hales, C.N. (2002). Ageing and telomeres: a study into organ- and gender-specific telomere shortening. *Nucleic Acids Res., 31*, 1576-1583.

Clements, P.M., Breslin, C., Deeks, E.D., Byrd, P.J., Ju, L., Bieganowski, P., Brenner, C., Moreira, M.C., Taylor, A.M. & Caldecott, K.W. (2004). The ataxia-oculomotor apraxia 1 gene product has a role distinct from ATM and interacts with the DNA strand break repair proteins XRCC1 and XRCC4. *DNA Repair, 3*, 1493-1502.

Cooke, M.S., Evans, M.D., Dizdaroglu, M. & Lunec, J. (2003). Oxidative DNA damage: mechanisms, mutation, and disease. *FASEB J., 17*, 1195-1214.

Daniel, R., Greger, J.G., Katz, A., Taganov, K.D., Wu, X., Kappes, J.C. & Skalka, M. (2004). Evidence that stable retroviral transduction and cell survival following DNA integration depend on components of the nonhomologous end joining repair pathway. *J. Virol., 78*, 8573-8581.

Dantzer, F., Luna, L., Bjøras, M. & Seeberg, E. (2002). Human OGG1 undergoes serine phosphorylation and associates with the nuclear matrix and mitotic chromatin in vivo. *Nucleic Acids Res., 30*, 2349-2357.

Daly, R. & Hearn, M.T. (2005). Expression of heterologous proteins in *Pichia pastoris*: a useful experimental tool in protein engineering and production. *J. Mol. Recognit., 18*(2), 119-138.

Das, A., Rajagopalan, L., Mathura, V.S., Rigby, S.J., Mitra, S. & Hazra, T.K. (2004). Identification of a zinc finger domain in the human NEIL2 (Nei-like-2) protein. *J. Biol. Chem., 279*, 47132-47138.

Das, A., Wiederhold, L., Leppard, J.B., Kedar, P., Prasad, R., Wang, H., Boldogh, I., Karimi-Busheri, F., Weinfeld, M., Tomkinson, A.E., Wilson, S.H., Mitra, S. & Hazra, T.K. (2006). NEIL2-initiated, APE1-independent repair of oxidized bases in DNA: Evidence for a repair complex in human cells. *DNA repair, 5*, 1439-1448.

Das, A., Boldogh, I, Lee, J.W., Harrigan, J.A., Hegde, M.L., Piotrowski, J., de Souza Pinto, N., Ramos, W., Greenberg, M.M., Hazra, T.K., Mitra, S. & Bohr, V.A. (2007a). The human Werner syndrome protein stimulates repair of oxidative DNA base damage by the DNA glycosylase NEIL1. *J. Biol. Chem., 282*, 26591-26602.

Das, S., Chattopadhyay, R., Bhakat, K.K., Boldogh, I., Kohno, K., Prasad, R., Willson, S.H. & Hazra, T.K. (2007b). Stimulation of NEIL2-mediated oxidized base excision repair via YB-1 interaction during oxidative stress. *J. Biol. Chem., 282*, 28474-28484.

Date, T., Tanihara, K., Yamamoto, S., Nomura, N. & Matsukage, A. (1992). Two regions in human DNA polymerase *β* mRNA suppress translation in *Escherichia coli*. *Nucleic Acids Res., 20*, 4859-4864.

David, S.S. & Williams, S.D. (1998). Chemistry of glycosylases and endonucleases involved in base-excision repair. *Chem. Rev., 98*, 1221-1261.

Debaisieux, S., Rayne, F., Yezid, H. & Beaumelle, B. (2012). The ins and outs of HIV-1 Tat. *Traffic, 13*, 355-363.

DeMott, M.S., Zigman, S. & Bambara, R.A. (1998). Replication protein A stimulates long patch DNA base excision repair. *J. Biol. Chem., 273*(42), 27492-27498.

Demple, B. & DeMott, M.S. (2002). Dynamics and diversions in base excision DNA repair of oxidized abasic lesions. *Oncogene, 21*(58), 8926-8934.

Devasagayam, T.P.A., Tilak, J.C., Boloor, K.K., Sane, K.S., Ghaskadbi, S.S. & Lele, R.D. (2004). Free radicals and antioxidants in human health: Current status and future prospects. *JAPI, 52*, 794 – 804.

Dhenaut, A., Boiteux, S. & Radicella, J.P. (2000). Characterization of the *hOGG1* promoter and its expression during the cell cycle. *Mutat. Res., 461*, 109-118.

Dou, H., Mitra, S. & Hazra, T.K. (2003). Repair of oxidized bases in DNA bubble structures by human DNA glycosylases NEIL1 and NEIL2. *J. Biol. Chem., 278*, 49679-49684.

Dou, H., Theriot, C.A., Das, A., Hegde, M.L. Matsumoto, Y., Boldogh, I., Hazra, T.K., Bhakat, K.K. & Mitra, S. (2008). Interaction of the human DNA glycosylase NEIL1 with proliferating cell nuclear antigen. *J. Biol. Chem., 283*, 3130-3140.

Doublié, S., Bandaru, V., Bond, J.P. & Wallace, S.S. (2004). The crystal structure of human endonuclease VIII-like 1 (NEIL1) reveals a zincless finger motif required for glycosylase activity. *Proc. Natl. Acad. Sci. USA, 101*, 10284-9.

Drablos, F., Feyzi, E., Aas, P.A., Vaagbo, C.B., Kavli, B., Bratlie, M.S., Pena-Diay, J., Otterlei, M., Slupphaug, G. & Krokan, H.E. (2004). Alkylation damage in DNA and RNA repair mechanisms and medical significance. *DNA Repair, 3*(11), 1389-1407.

Drew, Y. & Plummer, R. (2009). Parp inhibitors in cancer therapy: two modes of attack on the cancer cell widening the clinical applications. *Drug Resist. Update, 12*, 153-156.

Duttweiler, H.M. (1996). A highly sensitive and non-lethal beta-galactosidase plate assay for yeast. *Trends Genet., 12*, 340-341.

Epel, E.S., Blackburn, E.H., Lin, J., Dhabhar, F.S., Adler, N.E., Morrow, J.D. & Cawthon, R.M. (2004). Accelerated telomere shortening in response to life stress. *Proc. Natl. Acad. Sci. USA, 101*, 17312-17315.

Espejel, S., Franco, S., Rodriguez-Perales, S., Bouffler, S.D., Cigudosa, J.C. & Blasco, M.A. (2002). Mammalian Ku86 mediates chromosomal fusions and apoptosis caused by critically short telomeres. *EMBO J., 21*(9), 2207-2219.

Espeseth, A.S., Fishel, R., Hazuda, D., Huang, Q., Xu, M., Yoder, K. & Zhou, H. (2011a). siRNA Screening of a targeted library of DNA repair factors in HIV infection reveals a role for base excision repair in HIV integration. *PLoS ONE, 6*, e17612.

Espeseth, A.S., Hazuda, D.J., Xu, M. & Zhou, H. (2011b). *Novel HIV targets*. US Patent No. US 2011/0065087 A1.
Retrieved from http://www.freepatentsonline.com/20110065087.pdf.

European Bioinformatics Institute. (2012a). Gene & Protein Summary - Chorionic somatomammotropin hormone 1.
Retrieved 03 January, 2012, from http://bit.ly/yuqOjT

European Bioinformatics Institute (2012b). Gene & Protein Summary - Chorionic somatomammotropin hormone 2. Retrieved 03 January, 2012, from http://bit.ly/xpIDwE

European Bioinformatics Institute (2012c). Gene & Protein Summary - chorionic gonadotropin, beta polypeptide 8. Retrieved 03 January, 2012, from http://bit.ly/AeaJwc

European Bioinformatics Institute (2012d). Gene & Protein Summary - Decorin Retrieved 03 January, 2012, from http://bit.ly/zTTYWT

European Bioinformatics Institute (2012e). Gene & Protein Summary - Homeobox (HOPX). Retrieved 03 January, 2012, from http://bit.ly/wFllXM

Fan, J., Otterlei, M., Wong, H.K., Tomkinson, A.E. & Wilson, D.M. (2004). Third XRCC1 co-localizes and physically interacts with PCNA. *Nucleic Acids Res., 32*, 2193–2201.

Fashena, S.J., Serebriiskii, I.G. & Golemis, E.A. (2000). LexA-based two-hybrid systems. *Methods Enzymol., 328***,** 14-26.

Freitas, S., Moore, D.H., Michael, H. & Kelley, M.R. (2003). Studies of apurinic/apyrimidinic endonuclease/ref-1 expression in epithelial ovarian cancer: correlations with tumour progression and platinum resistance. *Clin. Cancer Res., 9*, 4689-4694.

Frias, C., Garcia-Aranda, C., Juan, C.D., Moran, A., Ortega, P., Gomez, A., Hernando, F., Lopez-Asenjo, J.A., Torres, A.J., Benito, M. & Inesta, P. (2008). Telomere shortening is associated with poor prognosis and telomerase activity correlates with DNA repair impairment in non-small cell lung cancer. *Lung Cancer, 60*, 416-425.

Friedberg, E.C. (2001). How nucleotide excision repair protects against cancer. *Nat. Rev. Cancer, 1*, 22-33.

Fromme, J.C., Banerjee, A. & Verdine, G.L. (2004). DNA glycosylase recognition and catalysis. *Curr. Opin. Struc. Biol., 14*, 43-49.

Garkavtsev, I.V., Kley, N., Grigorian, I.A. & Gudkov, A.V. (2001). The Bloom syndrome protein interacts and cooperates with p53 in regulation of transcription and cell growth control. *Oncogene, 20*(57), 8276-8280.

GeneCards – The Human Gene Compendium (2012) – Weizmann Institute of Science [Online] Available at: http://www.genecards.org/ [Accessed 06 September 2012]

GeneNote – Gene Normal Tissue Expression (2011) – Weizmann Institute of Science [Online] Available at: http://bioinfo2.weizmann.ac.il/cgi-bin/genenote/home_page.pl [Accessed 06 September 2012]

GNF – Genomics Institue of the Novartis Research Foundation (2009) BioGPS – The Gene Portal Hub [Online] Available at: http://biogps.gnf.org/#goto=genereport&id=55247 [Accessed 01 December 2010]

Golemis, E.A., Serebriiskii, I. & Law, S.F. (1999). The Yeast two-hybrid system: criteria for detecting physiologically significant protein-protein interactions. *Curr. Issues Mol. Biol., 1*, 31-46.

Graziewicz, M.A., Zastawny, T.H., Olinski, R., Speina, E., Siedlecki J. & Tudek, B. (2000). Fapyadenine is a moderately efficient chain terminator for prokaryotic DNA polymerases. *Free Radical Bio. Med., 28*, 75-83.

Guschlbauer, W., Duplaa, A.M., Téoule, R. & Fazakerley, G.V. (1991). Structure and *in vitro* replication of DNA templates containing 7,8-dihydro-8-oxoadenine. *Nucleic Acids Res., 19*, 1753-1758.

Hanai, R., Caron, P.R. & Wang, J.C. (1996). Human TOP3: a single-copy gene encoding DNA topoisomerase III. *Proc. Natl. Acad. Sci. USA, 93*, 3653-3657.

Hadi, M.Z. & Wilson, D.M. (2000). Second human protein with homology to the *Escherichia coli* abasic endonuclease exonuclease III. *Environ. Mol. Mutagen., 36*, 312-324.

Hall, T.M.T. (2005) Multiple modes of RNA recognition by zinc finger proteins. *Curr. Opin. Struc. Biol., 15*, 367-373.

Hakem, R. (2008). DNA-damage repair; the good, the bad, and the ugly. *EMBO J., 27,* 589-605.

Harris, S.L. & Levine, A.J. (2005). The p53 pathway: positive and negative feedback loops. *Oncogene, 27*, 2899-2908.

Hasan, S., Stucki, M., Hassa, P.O., Imhof, R., Gehrig, P., Hunziker, P., Hubscher, U. & Hottiger, M.O. (2001). Regulation of human flap endonuclease-1 activity by acetylation through the transcriptional coactivator p300. *Mol. Cell., 7*, 1221-1231.

Hasan, S., El-Andaloussi, N., Hardeland, U., Hassa, P.O., Burki, C., Imhof, R., Schar, P. & Hottiger, M.O. (2002). Acetylation regulates the DNA end-trimming activity of DNA polymerase beta. *Mol. Cell., 10*, 1213-1222.

Hazra, T.K., Izumi, T., Boldogh, I., Imhoff, B., Kow, Y.W., Jaruga, P., Dizdaroglu, M. & Mitra, S. (2002a). Identification and characterization of a human DNA glycosylase for repair of modified bases in oxidatively damaged DNA. *Proc. Natl. Acad. Sci. USA, 99*, 3523-3528.

Hazra, T.K., Kow, Y.W., Hatahet, Z., Imhoff, B., Boldogh, I., Mokkapati, S.K., Mitra, S. & Izumi, T. (2002b). Identification and characterization of a novel human DNA glycosylase for repair of cytosine-derived lesions. *J. Biol. Chem., 277*, 30417-30420.

Hazra, T.K., Izumi, T., Kow, Y.W. & Mitra, S. (2003). The discovery of a new family of mammalian enzymes for repair of oxidatively damaged DNA, and its physiological implications. *Carcinogenesis, 24*, 155-157.

Hecht, S.S. (1999). DNA adduct formation from tobacco-specific N-nitrosamines. *Mutat. Res., 424*(1-2), 127-142.

Hegde, M.L., Theriot, C.A., Das, A., Hegde, P.M., Guo, Z., Gary, R.K., Hazra, T.K., Shen, B. & Mitra, S. (2008a). Physical and functional interaction between human oxidized base-specific DNA glycosylase NEIL1 and flap endonuclease 1. *J. Biol. Chem., 283*, 27028-27037.

Hegde, M.L., Hazra, T.K. & Mitra, S. (2008b). Earl steps in the DNA base excision/single-strand interruption repair pathway in mammalian cells. *Cell Res., 18*, 27-47.

Hildrestrand, G.A., Neurauter, C.G., Diep, D.B., Castellanos, C.G., Krauss, S., Bjøras M. & Luna, L. (2009). Expression patterns of *Neil3* during embryonic brain development and neoplasia. *BMC Neurosci., 10*. 45 – 53.

Hill, J.W., Hazra, T.K., Izumi, T. & Mitra, S. (2001). Stimulation of human 8-oxoguanine-DNA glycosylase by AP-endonuclease: potential coordination of the initial steps in base excision repair. *Nucleic Acids Res., 29*, 430-438.

Hitomi, K., Iwai, S. & Tainer, J.A. (2007). The intricate structural chemistry of base excision repair machinery: Implications for DNA damage recognition, removal, and repair. *DNA Repair, 6*, 410-428.

Hoeijmakers, J.H., Eker, A.P., Wood, R.D. & Robins, P. (1990). Use of in vivo and in vitro assays for the characterization of mammalian excision repair and isolation of repair proteins. *Mutat. Res., 236*, 223-238.

Hooten, N.N., Kompaniez, K., Barnes, J., Lohani, A. & Evans, M.K. (2011). Poly(ADP-ribose) polymerase 1 (PARP-1) binds to 8-oxoguanine-DNA glycosylase (OGG1). *J. Biol. Chem., 286*, 44679-44690.

Hooten, N.N., Fitzpatrick, M., Kompaniez, K., Jacob, K.D., Moore, B.R., Nagle, J., Barnes, J., Lohani, A. & Evans, M.K. (2012). Coordination of DNA repair by NEIL1 and PARP-1: a possible link to aging. *Aging, 4*, 674-685.

Hori, M., Yonekura, S.I., Nohmi, T., Gruz, P., Sugiyama, H., Yonei, S. & Zhang-Akiyama, Q.M. (2010). Error-prone translesion DNA synthesis by *Escherichia coli* DNA polymerase IV (DinB) on templates containing 1,2-dihydro-2-oxoadenine. *J. Nuc. Acids, 2010*, 1-10.

Hsieh, P. & Yamane, K. (2008). DNA mismatch repair: Molecular mechanism, cancer, and ageing. *Mech. Ageing Dev., 129*, 391-407.

Hu, J., de Souza-Pinto, N.C., Haraguchi, K., Hogue, B.A., Jaruga, P., Greenberg, M.M., Dizdaroglu, M. & Bohr, V.A. (2005). Repair of formamidopyrimidines in DNA involves different glycosylases - Role of the OGG1, NTH1, and NEIL1 enzymes. *J. Biol. Chem., 280*, 40544-40551.

Huffman, J.L., Sundheim, O. & Tainer, J.A. (2005). DNA base damage recognition and removal: New twists and grooves. *Mutat. Res., 577*, 55-76.

Imai, K., Nakata, K., Kawai, K., Hamano, T., Mei, N., Kasai, H. & Okamoto, T. (2005). Induction of *OGG1* gene expression by HIV-1 Tat. *J. Biol. Chem., 280*, 26701-26713.

Inoue, M., Kamiya, H., Fujikawa, K., Ootsuyama, Y., Murata-Kamiya, N., Osaki, T., Yasumoto, K. & Kasai, H. (1998). Induction of chromosomal gene mutations in *Escherichia coli* by direct incorporation of oxidatively damaged nucleotides: new evaluation method for mutagenesis by damaged DNA precursors in vivo. *J. Biol. Chem., 273*, 11069-11074.

Iyer, R.R., Pluciennik, A., Burdett, V. & Modrich, P.L. (2006). DNA mismatch repair: Functions and mechanisms. *Chem. Rev., 160*, 302-323.

Izumi, T., Wiederhold, L.R., Roy, G., Roy, R., Jaiswal, A., Bhakat, K.K., Mitra, S. & Hazra, T.K. (2003). Mammalian DNA base excision repair proteins: their interactions and role in repair of oxidative DNA damage. *Toxicology, 193*, 43-65.

Izumi, T., Brown, D.B., Naidu, C.V., Bhakat, K.K., Macinnes, M.A., Saito, H., Chen, D.J. & Mitra, S. (2005). Two essential but distinct functions of the mammalian abasic endonuclease. *Proc. Natl. Acad. Sci. USA, 102*, 5739-5743.

Jair, K.W., Bachman, K.E., Suzuki, H., Ting, A.H., Rhee, I., Yen, R.W.C., Baylin, S.B. & Schuebel, K.E. (2013). *De novo* CpG island methylation in human cancer cells. *Cancer Res., 66(2)*, 682-692.

Jaruga, P., Xiao, Y., Vartanian, V., Lloyd, R.S. & Dizdaroglu, M. (2010). Evidence for the involvement of DNA repair enzyme NEIL1 in nucleotide excision repair of (5′R)- and (5′S)-8,5′-cyclo-2′-deoxyadenosines. *Biochemistry, 49*, 1053-1055.

Jena, N.R. & Mishra, P.C. (2012). Formation of ring-opened and rearranged products of guanine: Mechanisms and biological significance. *Free Radical Bio. Med., 53*, 81-94.

Jiricny, J. (2006). The multifaceted mismatch-repair system. *Nat. Rev. Mol. Cell. Biol., 7*, 335-346.

Kaina, B. (2003). DNA damage-triggered apoptosis: critical role of DNA repair, double-strand breaks, cell proliferation and signalling. *Biochem. Pharmacol., 66*(8), 1547-1554.

Kakumoto, M., Sakaeda, T., Takara, K., Nakamura, T., Kita, T., Yagami, T., Kobayashi, H., Okamura, N. & Okumura, K. (2005). Effects of carvedilol on MDR1-mediated multidrug resistance: comparison with verapamil. *Cancer Sci., 94*, 81-86.

Kameoka, M., Nukuzuma, S., Itaya, A., Tanaka, Y., Ota, K., Inada, Y., Ikuta, K. & Yoshihara, K. (2005). Poly(ADP-ribose)polymerase-1 is required for integration of the human immunodeficiency virus type 1 genome near centromeric alphoid DNA in human and murine cells. *Biochem. Biophys. Res. Comm., 334*, 412-417.

Kamiya, H., Miura, H., Murata-Kamiya, N., Ishikawa, H., Sakaguchi, T., Inoue, H., Sasaki, T., Masutani, C., Hanaoka, F., Nishimura, S. & Ohtsuka, E. (1995a). 8-Hydroxyadenine (7,8-dihydro-8-Oxoadenine) induces misincorporation in *in vitro* DNA synthesis and mutations in NIH 3T3 cells. *Nucleic Acids Res., 23*, 2893-2899.

Kamiya, H. & Kasai, H. (1995b). Formation of 2-hydroxydeoxyadenosine triphosphate, an oxidatively damaged nucleotide, and its incorporation by DNA polymerases. *J. Biol. Chem., 270*, 19446-19450.

Kanvah, S., Joseph, J., Schuster, G.B., Barnett, R.N., Cleveland, C.L. & Landman, U. (2010). Oxidation of DNA: damage to nucleobases. *Accounts Chem. Res., 43*(2), 280-287.

Kauffmann, A., Rosselli, F., Lazar, Winnepenninckx, V., Mansuet-Lupo, A., Dessen, P., van den Oord, J.J., Spatz, A. & Sarasin, A. (2008). High expression of DNA repair pathways is associated with metastasis in melanoma patients. *Oncogene, 27*, 565-573.

Kavli, B., Sundheim, O., Akbari, M., Otterlei, M., Nilsen, H., Skorpen, F., Aas, P.A., Hagen, L., Krokan, H.E. & Slupphaug, G. (2002). hUNG2 is the major repair enzyme for removal of uracil from U : A matches, U:G mismatches, and U in single-stranded DNA, with hSMUG1 as a broad specificity backup. *J. Biol. Chem., 277*, 39926-39936.

Keyer, K. & Imlay, J.A. (1996). Superoxide accelerates DNA damage by elevating free-iron levels. *Proc. Natl. Acad. Sci. USA, 93,* 13635-13640.

Kilzer, J.M., Stracker, T., Beitzel, B., Meek, K., Weitzman, M. & Bushman, F.D. (2003). Roles of host cell factors in circularization of retroviral DNA. *Virology, 314*, 460-467.

Klungland, A. & Lindahl, T. (1997). Second pathway for completion of human DNA base excision-repair: reconstitution with purified proteins and requirement for DNase IV (FEN1). *EMBO J., 16*, 3341-3348.

Kreutzer, D.A. & Essigmann, J.M. (1998). Oxidized, deaminated cytosines are a source of C → T transitions *in vivo*. *Proc. Natl. Acad. Sci. USA, 95*, 3578-3582.

Krishnamurthy, N., Zhao, X., Burrows, C.J. & David S.S. (2008). Superior removal of hydantoin lesions relative to other oxidized bases by the human DNA glycosylase hNEIL1. *Biochemistry, 47*, 7137-7146.

Krokan, H.E., Standal, R. & Slupphaug, G. (1997). DNA glycosylases in the base excision repair of DNA. *Biochemistry, 325*, 1-16.

Krokeide, S.Z., Bolstad, N., Laerdahl, J.K., Bjøras, M. & Luna, L. (2009). Expression and purification of NEIL3, a human DNA glycosylase homolog. *Protein Expres. Purif., 65*, 160-164.

Krwawicz, J., Arczewska, K.D., Speina, E., Maciejewska, A. & Grzesiuk, E. (2007). Bacterial DNA repair genes and their eukaryotic homologues: 1. Mutations in genes involved in base excision repair (BER) and DNA-end processors and their implication in mutagenesis and human disease. *Acta Biochim. Pol., 54*, 413-434.

Kummar, S., Chen, A., Parchment, R.E., Kinders, R.J., Ji, J., Tomaszewski, J.E. & Doroshow, J.H. (2012). Advances in using PARP inhibitors to treat cancer. *BMC Med., 10*(25), 1-5.

Kushnirov, V.V. (2000). Rapid and reliable protein extraction from yeast. *Yeast, 16*, 857-860.

Kusumoto, R., Masutani, C., Iwai, S. & Hanaoka, F. (2002). Translesion synthesis by human DNA polymerase eta across thymine glycol lesions. *Biochemistry, 41*(19), 6090-6099.

Lang, W.H., Coats, J.E., Majka, J., Hura, G.L., Lin, Y., Rasnik, I. & McMurray, C.T. (2011). Conformational trapping of mismatch recognition complex MSH2/MSH3 on repair-resistant DNA loops. *Proc. Natl. Acad. Sci. USA, 108*, E837-E844.

Langouet, S., Muller, M. & Guengerich F.P. (1997). Misincorporation of dNTPs opposite 1,N2-ethenoguanine and 5,6,7,9-tetrahydro-7-hydroxy-9-oxoimidazo[1,2-a]purine in oligonucleotides by *Escherichia coli* polymerase I exo- and II exo-, T7 polymerase exo-, human immunodeficiency virus-1 reverse transcriptase, and Rat polymerase. *Biochemistry, 36*, 6069-6079.

Laity, J.H., Lee, B.M. & Wright, P.E. (2001). Zinc finger proteins: new insights into structural and functional diversity. *Curr. Opin. Struc. Biol., 11*, 39-46.

Larrea, A.A., Lujan, S.A. & Kunkel, T.A. (2010). SnapShot: DNA mismatch repair. *Cell, 141*, 730.

Lavrukhin, O.V. & Lloyd, S. (2000). Involvement of phylogenetically conserved acidic amino acid residues in catalysis by an oxidative DNA damage enzyme formamidopyrimidine glycosylase. *Biochemistry, 39*, 15266-15271.

Lehman, I.R. (1974). DNA ligase: structure, mechanism, and function. *Science, 186*, 790–797.

Leppard, J.B., Dong, Z., Mackey, Z.B. & Tomkinson, A.E. (2003). Physical and functional interaction between DNA ligase III alpha and poly(ADP-Ribose) polymerase 1 in DNA single-strand break repair. *Mol. Cell. Biol., 23*, 5919-5927.

Lewis, L.K., Harlow, G.R., Gregg-Jolly, L.A. & Mount, D.W. (1994). Identification of high affinity binding sites for LexA which define new DNA damage-inducible genes in *Escherichia coli*. *J. Mol. Biol., 241*, 507-523.

Li, L., Olvera, J.M., Yoder, K.E., Mitchell, R.S., Butler, S.L., Lieber, M. Martin, S.L. & Bushman, F.D. (2001). Role of the non-homologous DNA end joining pathway in the early steps of retroviral infection. *EMBO J., 20*, 3272-3281.

Li, L. & Zou, L. (2005). Sensing, signaling, and responding to DNA damage: organization of the checkpoint pathways in mammalian cells. *J. Cell. Biochem., 94*, 298-306.

Lijinsky, W. (1999). N-Nitroso compounds in the diet. *Mutat. Res., 443*(1-2), 129-138.

Lindahl, T. (1993). Instability and decay of the primary structure of DNA. *Nature, 362*, 709-715.

Liu, M., Bandaru, V., Bond, J.P., Jaruga, P., Zhao, X., Christov, P.P., Burrows, C.J., Rizzo, C.J., Dizdaroglu, M. & Wallace, S.S. (2010). The mouse ortholog of NEIL3 is a functional DNA glycosylase in vitro and in vivo. *Proc. Natl. Acad. Sci. USA, 107*, 4925-4930.

Liu, M., Bandaru, V., Holmes, A., Averill, A.M., Cannan, W. & Wallace, S.S. (2012). Expression and purification of active mouse and human NEIL3 proteins. *Protein Expres. Purif., 84*, 130-139.

Liu, M., Imamura, K., Averill, A.M., Wallace, S.S. & Doublie, S. (2013). Structural characterization of a mouse ortholog of human NEIL3 with a marked preference for single-stranded DNA. *Structure, 21*, 247-256.

Luo, Y., Batalao, A., Zhou, H. & Zhu, L. (1997). Mammalian two-hybrid system: A complementary approach to the yeast two-hybrid system. *BioTechniques, 22*, 350-352.

MacDonald, P.N. (2001). *Methods in Molecular Biology - Two-Hybrid Systems - Methods and Protocols.* New Jersey: Humana Press-Totowa Inc.

Mansour, W.Y., Rhein, T. & Dahm-Daphi, J. (2010). The alternative end-joining pathway for repair of DNA double-strand breaks requires PARP1 but is not dependent upon microhomologies. *Nucleic Acids Res., 38*(18), 6065-6077.

Marenstein, D.R., Ocampo, M.T.A., Chan, M.K., Altamirano, A., Basu, A.K., Boorstein, R.J., Cunningham, R.P. & Teebor, G.W. (2001). Stimulation of human endonuclease III by Y Box-binding protein 1 (DNA-binding Protein B). *J. Biol. Chem., 276*, 21242-21249.

Marenstein, D.R., Chan, M.K., Altamirano, A., Basu, A.K., Boorstein, R.J., Cunningham, R.P. & Teebor, G.W. (2003). Substrate specificity of human endonuclease III (hNTH1). Effect of human APE1 on hNTH1 activity. *J. Biol. Chem., 278*, 9005-9012.

Marin-Burgin, A. & Schinder, A.F. (2012). Requirement of adult-born neurons for hippocampus dependent learning. *Behav. Brain Res., 227*, 391-399.

Marsin, S., Vidal, A.E., Sossou, M., de Murcia, J.M., Page, F.L., Boiteux, S., de Murcia, G. & Radicella, J.P. (2003). Role of XRCC1 in the coordination and stimulation of oxidative DNA damage repair initiated by the DNA glycosylase hOGG1. *J. Biol. Chem., 278*, 44068-44074.

Matthews, J.M. & Sunde, M. (2002). Zinc fingers-folds for many occasions. *IUBMB Life, 54*, 351-355.

McConnell, L.N.M., Tan, C.K., Downey, K.M. & Fisher, P.A. (1993). Interaction of DNA polymerase delta, proliferating cell nuclear antigen, and synthetic oligonucleotide template-primers. Analysis by polyacrylamide gel electrophoresis-band mobility shift assay. *J. Biol. Chem., 268*, 13571-13576.

Muelhardt, C. (2009). *Der Experimentator Molekularbiologie/Genomics*. 6th ed. Heidelberg: Spektrum Akademischer Verlag.

Muftuoglu, M., de Souza-Pinto, N.C., Dogan, A., Aamann, M., Stevnsner, T., Rybanska, I., Kirkali, G.I., Dizdaroglu, M. & Bohr, V.A. (2009). Cockayne Syndrome Group B Protein Stimulates Repair of Formamidopyrimidines by NEIL1 DNA Glycosylase. *J. Biol. Chem., 284*, 9270-9279.

Mokkapati, S.K., Wiederhold, L., Hazra, T.K. & Mitra, S. (2004). Stimulation of DNA glycosylase activity of OGG1 by NEIL1: Functional collaboration between two human DNA glycosylases. *Biochemistry, 43*, 11596-11604.

Moore, J.K. & Haber, J.E. (1996). Cell cycle and genetic requirements of two pathways of nonhomologous end-joining repair of double-strand breaks in Saccharomyces cerevisiae. *Mol. Cell. Biol., 16*(5), 2164-2173.

Moriya, M., Zhang, W., Johnson, F. & Grollman, A.P. (1994). Mutagenic potency of exocyclic DNA adducts: marked differences between *Escherichia coli* and simian kidney cells. *Proc. Natl. Acad. Sci. USA, 91*(25), 11899-11903.

Morland, I., Rolseth, V., Luna, L., Rognes, T., Bjøras, M. & Seeberg, E. (2002). Human DNA glycosylases of the bacterial Fpg/MutM superfamily: an alternative pathway for the repair of 8-oxoguanine and other oxidation products in DNA. *Nucleic Acids Res., 30*, 4926-4936.

Moynahan, M.E. & Jasin, M. (2010). Mitotic homologous recombination maintains genomic stability and suppresses tumourigenesis. *Nat. Rev. Mol. Cell. Biol., 11*, 196-207.

Nakabeppu, Y., Tsuchimoto, D., Furuichi, M. & Sakumi, K. (2004). The defense mechanisms in mammalian cells against oxidative damage in nucleic acids and their involvement in the suppression of mutagenesis and cell death. *Free Radical Res., 38*, 423-429.

Nam, E.A., Cortez, D. (2011). ATR signalling: more than meeting at the fork. *Biochem. J., 436*, 527-536.

Naryzhny, S.N. & Lee, H. (2004). The post-translational modifications of proliferating cell nuclear antigen. *J. Biol. Chem., 279*(19), 20194-20199.

National Centre for Biotechnology Information – NCBI, 2010. Conserved Domains [Online] Available at: for OGG1 http://www.ncbi.nlm.nih.gov/Structure/cdd/wrpsb.cgi?seqinput=NP_002533.1; for NEIL3 http://www.ncbi.nlm.nih.gov/Structure/cdd/wrpsb.cgi?seqinput=NP_060718.2 [Accessed 30 December 2010]

National Centre for Biotechnology Information – NCBI, 2011. Conserved Domains [Online] Available at: for HOPX http://www.ncbi.nlm.nih.gov/Structure/cdd/wrpsb.cgi?seqinput=NP_001138932.1 [Accessed 05 September 2012]

Neurauter, C.G., Luna, L. & Bjøras, M. (2012). Release from quiescence stimulates the expression of human NEIL3 under the control of the Ras dependent ERK-MAP kinase pathway. *DNA Repair, 11*, 401-409.

Niles, J., Wishnok, J.S. & Tannenbaum, S.R. (2004). Spiroiminodihydantoin and guanidinohydantoin are the dominant products of 8-oxoguanosine oxidation at low fluxes of peroxynitrite: Mechanistic studies with ^{18}O. *Chem. Res. Toxicol., 17*, 1510-1519.

Nilsen, H. & Krokan, H.E. (2001). Base excision repair in a network of defense and tolerance. *Carcinogenesis, 22*, 978-998.

Nishioka, K., Ohtsubo, T., Oda, H., Fujiwara, T., Kang, D., Sugimachi, K. & Nakabeppu, Y. (1999). Expression and differentail intracellular localization of two major forms of human 8-oxoguanine DNA glycosylase encoded by alternatively spliced OGG1 mRNAs. *Mol. Biol. Cell, 10*, 1637-1652.

O′Shaughnessy, J., Osborne, C., Pippen, J., Yoffe, M., Patt, D. Monaghan, G., Rocha, C., Ossovskaya, V., Sherman, B. & Bradley, C. (2009). Efficacy of BSI-201, a poly (ADP-ribose) polymerase-1 (PARP-1) inhibitor, in combination with gemcitabine/carboplatin (G/C) in patients with metastatic triple-negative breast cancer (TNBC): Results of a randomized phase II trial. *J. Clin. Oncol. (Meeting Abstract), 27*:18S.

Ohtsubo, T., Nishioka, K., Imaiso, Y., Iwai, S., Shimokawa, H., Oda, H., Fujiwara, T. & Nakabeppu, Y. (2000). Identification of human MutY homolog (hMYH) as a repair enzyme for 2-hydroxyadenine in DNA and detection of multiple forms of hMYH located in nuclei and mitochondria. *Nucleic Acids Res., 28*, 1355-1364.

OriGene Technologies, Inc. – DupLEX-A – Yeast Two-Hybrid System – Application Guide. *Revision 06.05*. [Online] Available at: http://www.origene.com/assets/Documents/catalog_manual/OTIProductManual-DupLEX-AYeastTwoHybrid.pdf [Accessed 18 April 2013]

Otterlei, M., Warbrick, E., Nagelhus, T.A., Haug, T., Slupphaug, G., Akbari, M., Aas, P.A., Steinsbekk, K., Bakke, G. & Krokan, H.E. (1999). Post-replicative base excision repair in replication foci. *EMBO J., 18*, 3834-3844.

Pandya, G.A. & Moriya, M. (1996). 1,N^6-Ethenodeoxyadenosine, a DNA adduct highly mutagenic in mammalian cells. *Biochemistry, 35*, 11478-11492.

Parikh, S.S., Mol, C.D., Slupphaug, G., Bharati, S., Krokan, H.E. & Tainer, J.A. (1998). Base excision repair initiation revealed by crystal structures and binding kinetics of human uracil-DNA glycosylase with DNA. *EMBO J., 17*, 5214-5226.

Parker, A., Gu, Y., Mahoney, W., Lee, S.H., Singh, K.K. & Lu, A.L. (2001). Human homolog of the MutY repair protein (hMYH) physically interacts with proteins involved in long patch DNA base excision repair. *J. Biol. Chem., 276*, 5547-5555.

Parsons, J.L., Dianova, I.I., Allinson, S.L. & Dianov, G.L. (2005). Poly(ADP-ribose) polymerase-1 protects excessive DNA strand breaks from deterioration during repair in human cell extracts. *FEBS J., 272*, 2012-2021.

Pecot, C.V., Calin, G.A., Coleman, R.L., Lopez-Berestein, G. & Sood, A.K. (2011). RNA interference in the clinic: challenges and future directions. *Nat. Rev. Cancer, 11*, 59-67.

Pelicano, H., Carney, D. & Huang, P. (2004). ROS stress in cancer cells and therapeutic implications. *Drug Resist. Update, 7*, 97-110.

Pestryakov, P., Zharkov, D.O., Grin, I., Fomina, E.E., Kim, E.R., Hamon, Loic, Eliseeva, I.A., Petruseva, I.O., Curmi, P.A., Ovchinnikov, L.P. & Lavrik, O.I. (2012). Effect of themultifunctional proteins RPA, YB-1, and XPC repair factor on AP site cleavage by DNA glycosylase NEIL1. *J. Mol. Recognit., 25*, 224-233.

Peter, H., Löffler, G. & Petrides, P.E. (2006). *Biochemie und Pathobiochemie* (German ed.). Berlin: Springer.

Pierce, B.A. (2012). *Genetics – A Conceptual Approach* (4th ed.). Basingstoke: W. H. Freeman and Company.

Pluciennik, A., Dzantiev, L., Iyer, R.R., Constantin, N., Kadyrov, F.A. & Modrich, P. (2010). PCNA function in the activation and strand direction of MutLα endonuclease in mismatch repair. *Proc. Natl. Acad. Sci. USA, 107*, 16066-16071.

Privezentzev, C.V., Saparbaev, M. & Laval, J. (2001). The HAP1 protein stimulates the turnover of human mismatch-specific thymine-DNA-glycosylase to process 3,N(4)-ethenocytosine residues. *Mutat. Res., 480-481*, 277-284.

Regnell, C.E., Hildestrand, G.A., Sejersted, Y., Medin, T., Moldestad, O., Rolseth, V., Krokeide, S.Z., Suganthan, R., Luna, L., Bjøras, M. & Bergersen, L.H. (2012). Hippocampal adult neurogenesis is maintained by Neil3-dependent repair of oxidative DNA lesions in neural progenitor cells. *Cell Reports, 2*, 503-510.

Rinne, M., Caldwell, D. & Kelley, M.R. (2004). Transient adenoviral *N*-methylpurine DNA glycosylase overexpression imparts chemotherapeutic sensitivity to human breast cancer cells. *Mol. Cancer Ther., 3*(8), 955-967.

Robertson, K.A., Hill, D.P., Xu, Y., Liu, L, Van Epps, S., Hockenbery, D.M., Park, J.R., Wilson, T.M. & Kelley, M.R. (1997). Down-regulation of apurinic/apyrimidinic endonuclease expression is associated with the induction of apoptosis in differentiating myeloid leukemia cells. *Cell Growth Differ., 8*, 443-449.

Robertson, K.A., Bullock, H.A., Xu, Y., Tritt, R., Zimmermann, E., Ulbright, T.M., Foster, R.S., Einhorn, L.H. & Kelley, M.R. (2001). Altered expression of Ape1/ref-1 in germ cell tumours and overexpression in NT2 cells confers resistance to bleomycin and radiation. *Cancer Res., 61*, 2220-2225.

Rojo, F., Garcia-Parra, J., Zazo, S., Tusquets, I., Ferrer-Lozano, J., Menendez, S., Eroles, P., Chamizo, C., Servitja, S., Ramirez-Merino, N., Lobo, F., Bellosillo, B., Corominas, J.M., Yelamos, J., Serrano, S., Lluch, A., Rovira, A. & Albanell, J. (2011). Nuclear PARP-1 protein overexpression is associated with poor overall survival in early breast cancer. *Ann. Oncol., 23*(5), 1156-1164.

Rolseth, V., Rundèn-Pran, E., Luna, L., McMurray, C., Bjøras, M. & Ottersen, O.P. (2008). Widespread distribution of DNA glycosylases removing oxidative DNA lesions in human and rodent brains. *DNA Repair,* 7, 1578-1588.

Rolseth, V., Krokeide, S.Z., Kunke, D., Neurauter, C.G., Suganthan, R., Sejersted, Y., Hildestrand, G.A., Bjøras, M. & Luna, L. (2013). Loss of Neil3, the major DNA glycosylase activity for removal of hydantoins in single stranded DNA, reduces cellular proliferation and sensitizes cells to genotoxic stress. *Biochim. Biophys. Acta, 1833*(5), 1157-1164.

Rosenquist, T.A., Zaika, E., Fernandes, A.S., Zharkov, D.O., Miller, H. & Grollman, A.P. (2003). The novel glycosylase, NEIL1, protects mammalian cells from radiation-mediated cell death. *DNA Repair, 2*, 581-591.

Roth, R.B. & Samson, L.D. (2002). 3-Methyladenine DNA glycosylase-deficient Aag null mice display unexpected bone marrow alkylation resistance. *Cancer Res., 62*, 656-660.

Sancar, A. (2003). Structure and Function of DNA Photolyase and Cryptochrome Blue-Light Photoreceptors. *Chem. Rev., 103*, 2203-2237.

Sandigursky, M. & Franklin, W.A. (1992). DNA deoxyribophosphodiesterase of *Escherichia coli* is associated with exonuclease I. *Nucleic Acids Res., 20*, 4699-4703.

Saparbaev, M., Sidorkina, O.M., Jurado, J., Privezentzev, C.V., Greenberg, M.M. & Laval, J. (2002). Repair of oxidized purines and damaged pyrimidines by *E. coli* Fpg protein: Different roles of proline 2 and lysine 57 residues. *Environ. Mol. Mutagen.*, *39*, 10-17.

Sattler, S.E., Mene-Saffrane, L., Farmer, E.E., Krischke, M., Mueller, M.J. & DellaPenna, D. (2006). Nonenzymatic lipid peroxidation reprograms gene expression and activates defense markers in *Arabidopsis* tocopherol-deficient mutants. *Plant Cell, 18*, 3706-3720.

Shalaby, M. (2009). PhD Thesis - Interaction studies on the transforming virus target Tip-1.

Shiotani, B. & Zou, L. (2009). Single-stranded DNA orchestrates an ATM-to-ATR switch at DNA breaks. *Mol. Cell., 33*, 547-558.

Shrivastav, M., De Haro, L.P. & Nickoloff, J.A. (2008). Regulation of DNA double-strand break repair pathway choice. *Cell Res., 18*, 134-147.

Seewald, M.J., Kraemer, A., Farkasovsky, M., Koerner, C., Wittinghofer, A. & Vetter, I.R. (2003). Biochemical characterization of the Ran-RanBP1-RanGAP system: are RanBP proteins and the acidic tail of RanGAP required for the Ran-RanGAP GTPase reaction?. *Mol. Cell. Biol., 23*, 8124-8136.

Sejersted, Y., Hildrestrand, G.A., Kunke, D., Rolseth, V., Krokeide, S.Z., Neurauter, C.G., Suganthan, R., Atneosen-Asegg, M., Fleming, A.M., Saugstad, O.D., Burrows, C.J., Luna, L. & Bjøras, M. (2011). Endonuclease VIII-like 3 (Neil3) DNA glycosylase promotes neurogenesis induced by hypoxia-ischemia. *Proc. Natl. Acad. Sci. USA, 107*, 18802-18807.

Selby, C.P. & Sancar, A. (2006). A cryptochrome/photolyase class of enzymes with single-stranded DNA-specific photolyase activity. *Proc. Natl. Acad. Sci. USA, 103*, 17696-17700.

Serebriiskii, I., Estojak, J., Bermann, M. & Golemis, E.A. (2000). Approaches to detecting false positives in yeast two-hybrid systems. *BioTechniques, 28*, 328-336.

Sharma, S., Sommers, J.A., Bohr, V.A., Hickson, I.D. & Brosh, R.M. (2004). Stimulation of flap endonuclease-1 by the Bloom's syndrome protein. *J. Biol. Chem., 279*, 9847-9856.

Sidorenkoa, V.S., Nevinskya, G.A. & Zharkova, D.O. (2008). Specificity of stimulation of human 8-oxoguanine–DNA glycosylase by AP endonuclease. *Biochem. Bioph. Res. Co., 368*, 175-179.

Sinha, R.P. & Häder, D.P. (2002). UV-induced DNA damage and repair: a review. *Photochem. Photobiol., 1*, 225-236.

Song, S., Xing, G., Yuan, L, Wang, J., Wang, S., Yin, Y., Tian, C., He, F. & Zhang, L. (2012). *N*-methylpurine DNA glycosylase inhibits p53-mediated cell cycle arrest and coordinates with p53 to determine sensitivity to alkylating agents. *Cell Res., 22*, 1285-1303.

Srivastava, D.K., Tendler, C.L., Milani, D., English, M.A., Licht, J.D. & Wilson, S.H. (2001). The HIV-1 transactivator protein Tat is a potent inducer of the human DNA repair enzyme [beta]-polymerase. *AIDS, 15*, 433-440.

Stetler, A., Gao, Y., Zukin, R.S., Vosler, R.S., Zhang, L., Zhang, F., Cao, G., Bennett, M.V.L. & Chen, J. (2010). Apurinic/apyrimidinic endonuclease APE1 is required for PACAP-induced neuroprotection against global cerebral ischemia. *Proc. Natl. Acad. Sci. USA, 107*, 3204-3209.

Stylianou, C. (2010). MSc Thesis - Construction of a vector for overexpression of mouse NEIL1 in *Pichia pastoris*. University of Salford.

Takao, M., Aburatani, H., Kobayashi, K. & Yasui, A. (1998). Mitochondrial targeting of human DNA glycosylases for repair of oxidative DNA damage. *Nucleic Acids Res., 26*, 2917-2922.

Takao, M., Kanno, S., Shiromoto, T. Hasegawa, H., Ide, H., Ikeda, S., Sarker, A.H., Seki, S., Xing, J.Z., Le, X.C., Weinfeld, M., Kobayashi, K., Miyazaki, J., Muijtjens, M., Hoeijmakers, J.H., van der Horst, G. & Yasui, A. (2002a). Novel nuclear and mitochondrial glycosylases revealed by disruption of the mouse *Nth1* gene encoding an endonuclease III homolog for repair of thymine glycols. *EMBO J., 21*, 3486-3493.

Takao, M., Kanno, S., Kobayashi, K., Zhang, Q.M., Yonei, S., van der Horst, G.T.J. & Yasui, A. (2002b). A back-up glycosylase in *Nth1* Knock-out mice is a functional Nei (endonuclease VIII) homologue. *J. Biol. Chem., 277*, 42205-42213.

Takao, M., Oohata, Y., Kitadokoro, K., Kobayashi, K., Iwai, S., Yasui, A., Yonei, S. & Zhang, Q.M. (2009). Human Nei-like protein NEIL3 has AP lyase activity specific for single-stranded DNA and confers oxidative stress resistance in *Escherichia coli* mutant. *Genes Cells, 14*, 261-270.

Tan, X., Grollman, A.P. & Shibutani, S. (1999). Comparison of the mutagenic properties of 8-oxo-7,8-dihzdro-2′-8-oxo-7,8-dihydro-2′-deoxyguanosine DNA lesions in mammalian cells. *Carcinogenesis, 20*(12), 2287-2292.

Tchou, J., Michaels, M.L., Miller, J.H. & Grollman, A.P. (1993). Function of the zinc finger in *Escherichia coli* Fpg protein. *J. Biol. Chem., 268*, 26738-26744.

Tchou, J., Bodepudi, V., Shibutani, S., Antoshechkin, I., Miller, J., Grollman, A.P. & Johnson, F. (1994). Substrate specificity of Fpg protein. *J. Biol. Chem., 269*, 15318-15324.

Tell, G., Damante, G., Caldwell, D. & Kelley, M.R. (2005). The Intracellular Localization of APE1/Ref-1: More than a passive phenomenon? *Antioxid. Redox. Sign., 7*, 367-384.

Temime-Smaali, N., Guittat, L., Wenner, T., Bayart, E., Douarre, C., Gomez, D., Giraud-Panis, M.J., Londono-Vallejo, A., Gilson, E., Amor-Gueret, M. & Riou, J.F. (2008). Topoisomerase IIIα is required for normal proliferation and telomere stability in alternative lengthening of telomeres. *EMBO J., 27*, 1513-1524.

Tini, M., Benecke, A., Um, S.J., Torchia, J., Evans, R.M. & Chambon, P. (2002). Association of CBP/p300 acetylase and thymine DNA glycosylase links DNA repair and transcription. *Mol. Cell., 9*, 265-277.

Torisu, K., Tsuchimoto, D., Ohnishi, Y. & Nakabeppu, Y. (2005). Hematopoietic tissue-specific expression of mouse Neil3 for endonuclease VIII-Like protein. *J. Biochem., 138*, 763-772.

Toueille, M., El-Andaloussi, N., Frouin, I., Freire, R., Funk, D., Shevelev, I., Friedrich-Heineken, E., Villani, G., Hottiger, M.O. & Hübscher, U. (2004). The human Rad9/Rad1/Hus1 damage sensor clamp interacts with DNA polymerase β and increases its DNA substrate utilisation efficiency: implications for DNA repair. *Nucleic. Acids. Res., 32*(11), 3316-3324.

Tsuchimoto, D., Sakai, Y., Sakumi, K., Nishioka, K., Sasaki, M., Fujiwara, T. & Nakabeppu, Y. (2001). Human APE2 protein is mostly localized in the nuclei and to some extent in the mitochondria, while nuclear APE2 is partly associated with proliferating cell nuclear antigen. *Nucleic Acids Res., 29*, 2349-2360.

Turchi, J.J., Huang, L., Murante, R.S., Kim, Y. & Bambara, R.A. (1994). Enzymatic completion of mammalian lagging-strand DNA replication. *Proc. Natl. Acad. Sci. USA, 91*, 9803-9807.

Tutt, A., Robson, M., Garber, J.E., Domcheck, S.M., Audeh, M.W., Weitzel, J.N., Friedlander, M., Arun, B., Loman, N., Schmutzler, R.K., Wardley, A., Mitchell, G., Earl, H., Wickens, M. & Carmichael, J. (2010). Oral poly(ADP-ribose) polymerase inhibitor olaparib in patients with BRCA1 or BRCA2 mutations and advanced breast cancer: a proof-of-concept trial. *Lancet, 376*, 235-244.

Uchida, K. (2003). 4-Hydroxy-2nonenal: a product and mediator of oxidative stress. *Prog. Lipid Res., 42*, 318-343.

Ushijima, Y., Tominaga, Y., Miura, T., Tsuchimoto, D., Sakumi, K. & Nakabeppu, Y. (2005). A functional analysis of the DNA glycosylase activity of mouse MUTYH protein excising 2-hydroxyadenine opposite guanine in DNA. *Nucleic Acids Res., 33*, 672-682.

Valko, M., Rhodes, C.J., Moncol, J., Izakovic, M. & Mazur, M. (2006). Free radicals, metals and antioxidants in oxidative stress-induced cancer. *Chem-Biol Interact., 160*, 1-40.

Vidal, A.E., Hickson, I.D., Boiteux, S. & Radicella, J.P. (2001a). Mechanism of stimulation of the DNA glycosylase activity of hOGG1 by the major human AP endonuclease: bypass of the AP lyase activity step. *Nucleic Acids Res., 29,* 1285-1292.

Vidal, A.E., Boiteux, S., Hickson, I.D. & Radicella, J.P. (2001b). XRCC1 coordinates the initial and late stages of DNA abasic site repair through protein-protein interactions. *EMBO J., 20*, 6530-6539.

Wallace, S.S. (2002). Biological consequences of free radical-damaged DNA bases. *Free Radical Bio. Med., 33*, 1-14.

Wallace, S.S., Bandaru, V., Kathe, S.D. & Bond, J.P. (2003). The enigma of endonuclease VIII. *DNA repair, 2*, 441-453.

Wang, X.W., Tseng, A., Ellis, N.A., Spillare, E.A., Linke, S.P., Robles, A.I., Seker, H., Yang, Q., Hu, P., Beresten, S., Bemmels, N.A., Garfield, S. & Harris, C.C. (2001). Functional Interaction of p53 and BLM DNA Helicase in Apoptosis. *J. Biol. Chem., 276*, 32948-32955.

Wang, D., Luo, M. & Kelley, M.R. (2004). Human apurinic endonuclease 1 (APE1) expression and prognostic significance in osteosarcoma: enhanced sensitivity of osteosarcoma to DNA damaging agents using silencing RNA APE1 expression inhibition. *Mol. Cancer Ther., 3*, 679-686.

Waters, T.R., Gallinari, P., Jiricny, J. & Swann, P.F. 1999. Human thymine DNA glycosylase binds to apurinic sites in DNA but is displaced by human apurinic endonuclease 1. *J. Biol. Chem., 274*, 67-74.

Whitehouse, C.J., Taylor, R.M., Thistlethwaite, A., Zhang, H., Karimi-Busheri, F., Lasko, D.D., Weinfeld, M. & Caldecott, K.W. (2001). XRCC1 stimulates human polynucleotide kinase activity at damaged DNA termini and accelerates DNA single-strand break repair. *Cell, 104*, 107-117.

Wiederhold, L., Leppard, J.B., Kedar, P., Karimi-Busheri, F., Rasouli-Nia, A., Weinfeld, M., Tomkinson, A.E., Izumi, T., Prasad, R., Wilson, S.H., Mitra, S. & Hazra, T.K. (2004). AP endonuclease-independent DNA base excision repair in human cells. *Mol. Cell., 15*, 209-220.

Wiederholt, C.J., Delaney, M.O. & Greenberg, M.M. (2002). Interaction of DNA containing Fapy dA or its C-nucleoside analogues with base excision repair enzymes. Implications for Mutagenesis and Enzyme Inhibition. *Biochemistry, 41*, 15838-15844.

Wiederholt, C.J., Delaney, M.O., Pope, M.A., David, S.S. & Greenberg, M.M. (2003). Repair of DNA containing Fapy dG and Its β-C-Nucleoside analogue by formamidopyrimidine DNA glycosylase and MutY. *Biochemistry, 42*, 9755-9760.

Winczura, A., Zdzalik, D. & Tudek, B. (2012). Damage of DNA and proteins by major lipid peroxidation products in genome stability. *Free Radical Res., 46*(4), 442-459.

Williams, S.D. & David, S.S. (1998). Evidence that MutY is a monofunctional glycosylase capable of forming a covalent Schiff base intermediate with substrate DNA. *Nucleic Acids Res., 26*, 5123-5133.

Woodhouse, B.C., Dianova, L.I., Parsons, J.L. & Dianov, G.L. (2008). Poly(ADP-ribose) polymerase-1 modulates DNA repair capacity and prevents formation of DNA double strand breaks. *DNA Repair, 7*, 932-940.

Xia, L., Zheng, L., Lee, H.W., Bates, S.E., Federico, L., Shen, B. & O'Connor, T.R. (2005). Human 3-methyladenine-DNA glycosylase: effect of sequence context on excision, association with PCNA, and stimulation by AP endonuclease. *J. Mol. Biol., 346*, 1259-1274.

Yang, H., Clendenin, W.M., Wong, D., Demple, B., Slupska, M.M., Chiang, J.H. & Miller, J.H. (2001). Enhanced activity of adenine-DNA glycosylase (Myh) by apurinic/apyrimidinic endonuclease (Ape1) in mammalian base excision repair of an A/GO mismatch. *Nucleic Acids Res, 29*, 743-752.

Yang, Q., Zhang, R., Wang, X.W., Spillare, E.A., Linke, S.P., Subramanian, D., Griffith, J.D., Li, J.L., Hickson, I.D., Chen, J.C., Loeb, L.A., Mazur, S.J., Appella, E., Brosh Jr., R.M., Karmakar, P., Bohr, V.A. & Harris, C.C. (2002). The processing of Holliday junctions by BLM and WRN helicases is regulated by p53. *J. Biol. Chem., 277*, 31980-31987.

Yin, M. (2010). MSc Thesis - Generation of plasmid vectors for overexpression of human NEIL3 in *Pichia pastoris*. University of Salford.

Yoon, J.H., Iwai, S., O'Connor, T.R. & Pfeifer, G.P. (2003). Human thymine DNA glycosylase (TDG) and methyl-CpG-binding protein 4 (MBD4) excise thymine glycol (Tg) from a Tg:G mispair. *Nucleic Acids Res., 31*, 5399-5404.

Yu, X., Chini, C.C., He, M., Mer, G. & Chen, J. (2003). The BRCT domain is a phospho-protein binding domain. *Science, 302*, 639-642.

Zhang, X., Morera, S., Bates, P.A., Whitehead, P.C., Coffer, A.I., Hainbucher, K., Nash, R.A., Sternberg, M.J.E., Lindahl, T. & Freemont, P.S. (1998). Structure of an XRCC1 BRCT domain: a new protein-protein interaction module. *EMBO J., 17,* 6404-6411.

Zharkov, D.O. & Grollman, A.P. (2002). Combining structural and bioinformatics methods for the analysis of functionally important residues in DNA glycosylases. *Free Radical Bio. Med., 32*, 1254-1263.

Zharkov, D.O., Shoham, G. & Grollman, A.P. (2003). Structural characterization of the Fpg family of DNA glycosylases. *DNA Repair, 2,* 839-862.

Zhou, H. Xu, M., Huang, Q., Gates, A.T., Zhang, X.D., Castle, J.C., Stec, E., Ferrer, M., Strulovici, B., Hazuda, D.J. & Espeseth, A.S. (2008). Genome-Scale RNAi screen for host factors required for HIV replication. *Cell Host Microbe, 4*, 495-504.

Zumstein, L. & Wang, J.C. (1986). Probing the structural domains and function *in vivo* of *Escherichia coli* DNA topoisomerase I by mutagenesis. *J. Mol. Biol., 191*, 333-340.

8 Appendix

8.1 Vector maps

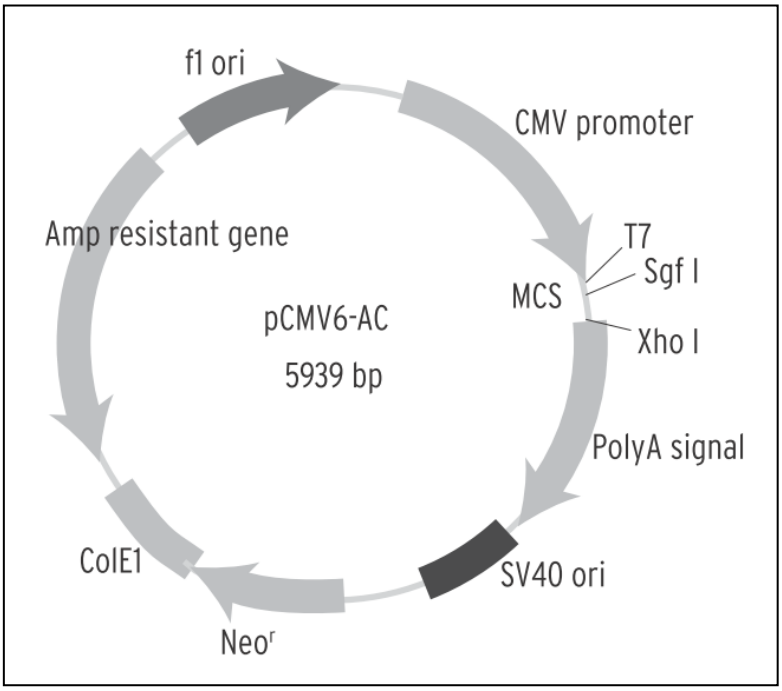

Kozac

EcoRI BamH I Kpn I RBS Sgf I Asc I

CTATAGGGCGGCCGGGAATTCGTCGACTGGATCCGGTACCGAGGAGATCTGCCGCCGCGATCGCCGGCGCGCCAGATCT

Hind III Nhe I Rsr II Mlu I Not I Xho I Pme I Fse I

CAAGCTTAACTAGCTAGCGGACCG ACG CGT TAA GCGGCCGCACTCGAGGTTTAAACGGCCGGCCGCGGAGCT

Figure 94: Vector map from the pCMV6-AC vector from OriGene and its multiple cloning site (MCS).

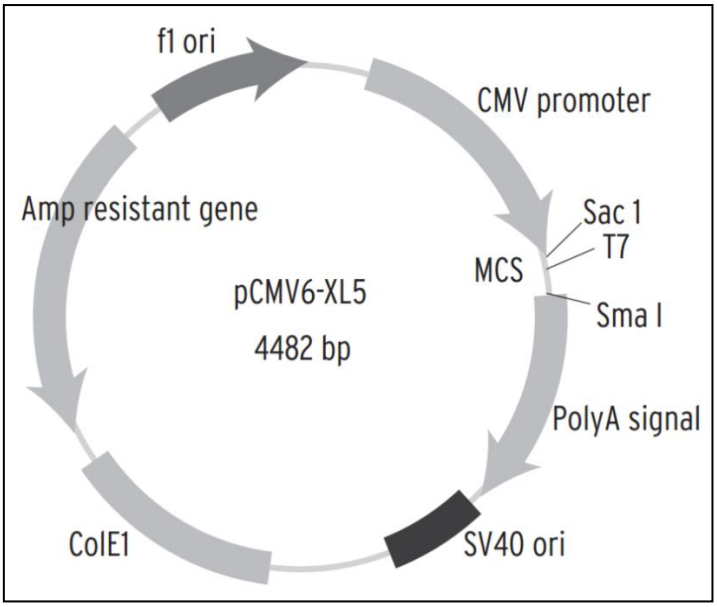

Figure 95: Vector map from the pCMV6-AC vector from OriGene and its multiple cloning site (MCS).

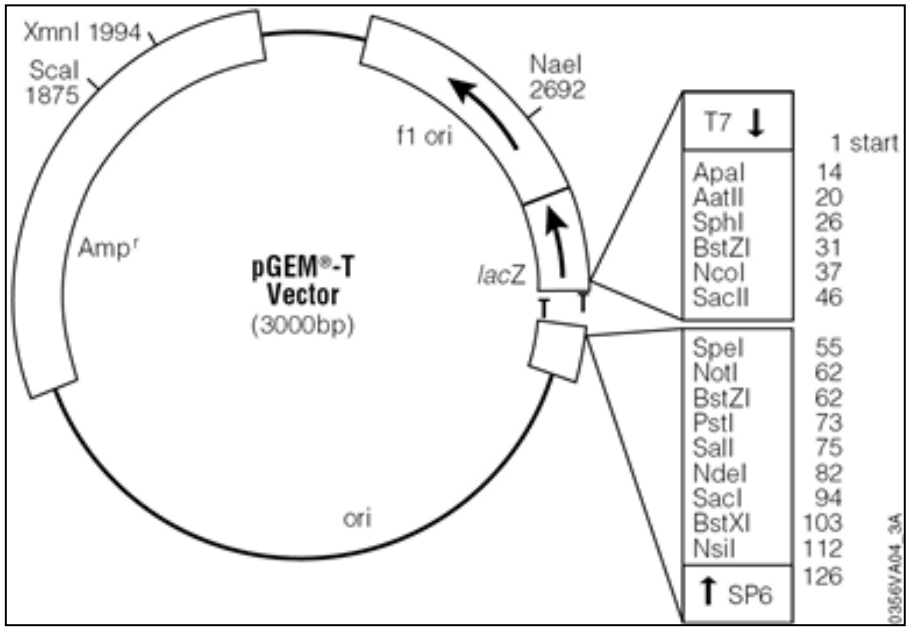

Figure 96: Vector map of the pGEM-T vector from Promega.

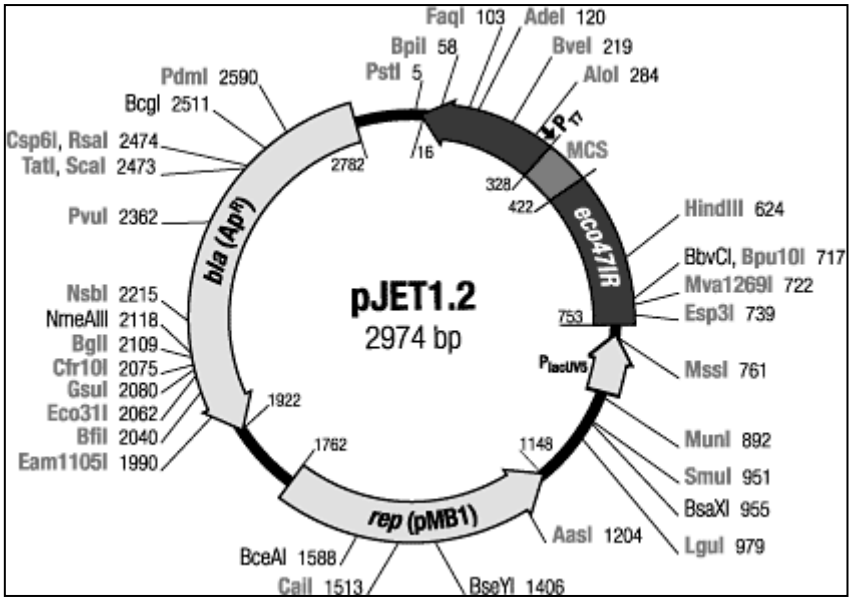

Figure 97: Vector map of the blunt end cloning vector pJET1.2/blunt from the CloneJet PCR Cloning Kit.

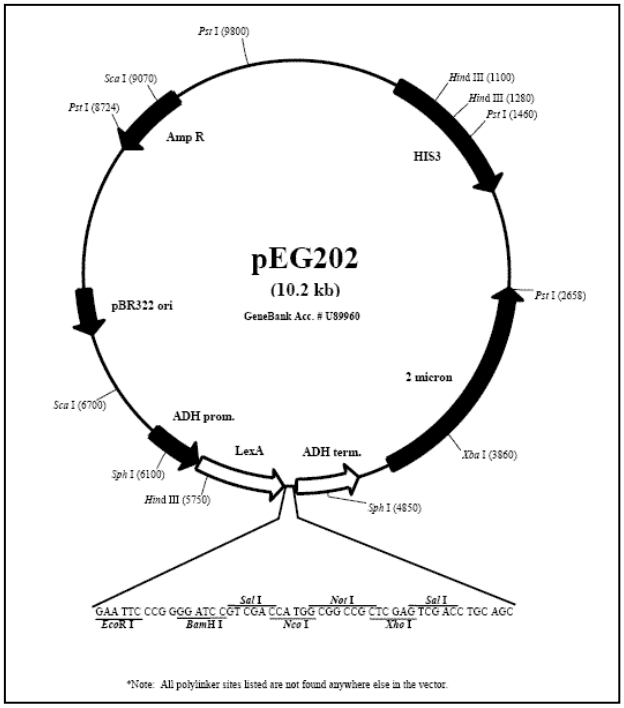

Figure 98: Vector map of the bait vector pEG202 used in Y2H

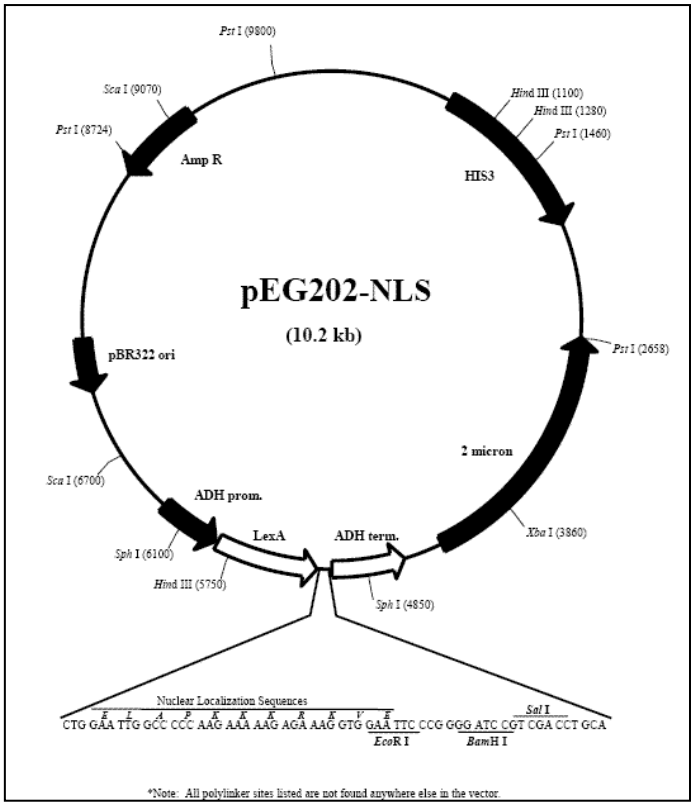

Figure 99: Vector map of the bait vector pEG202-NLS used in Y2H.

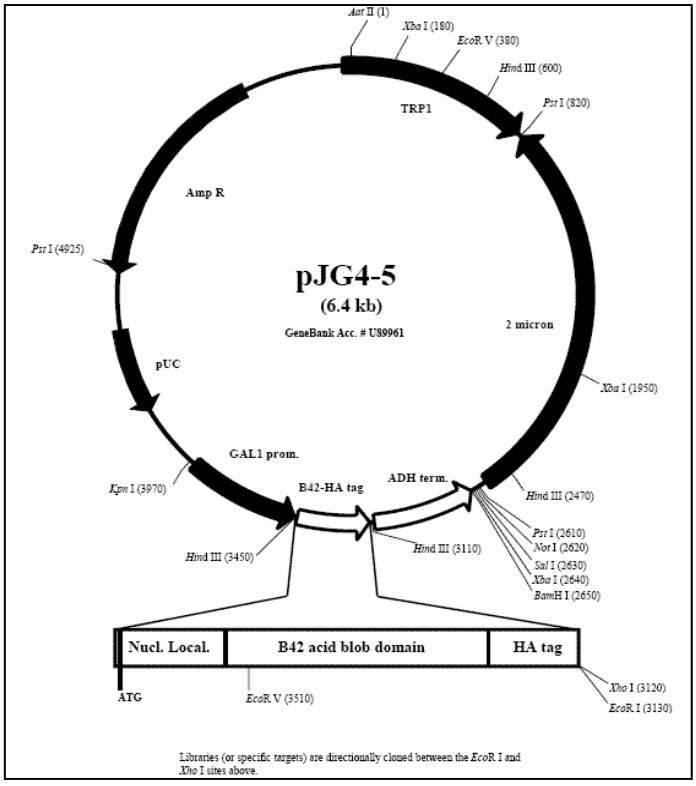

Figure 100: Vector map of the library plasmid pJG4-5 used in Y2H. Expression of fusion protein is induced by a GAL1 promoter.

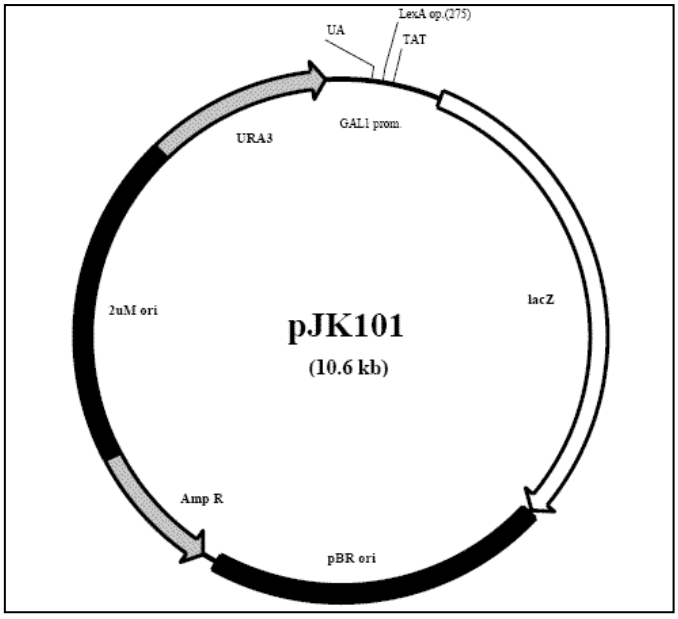

Figure 101: Vector map of the reporter plasmid pJK101 used in the repression assay in Y2H.

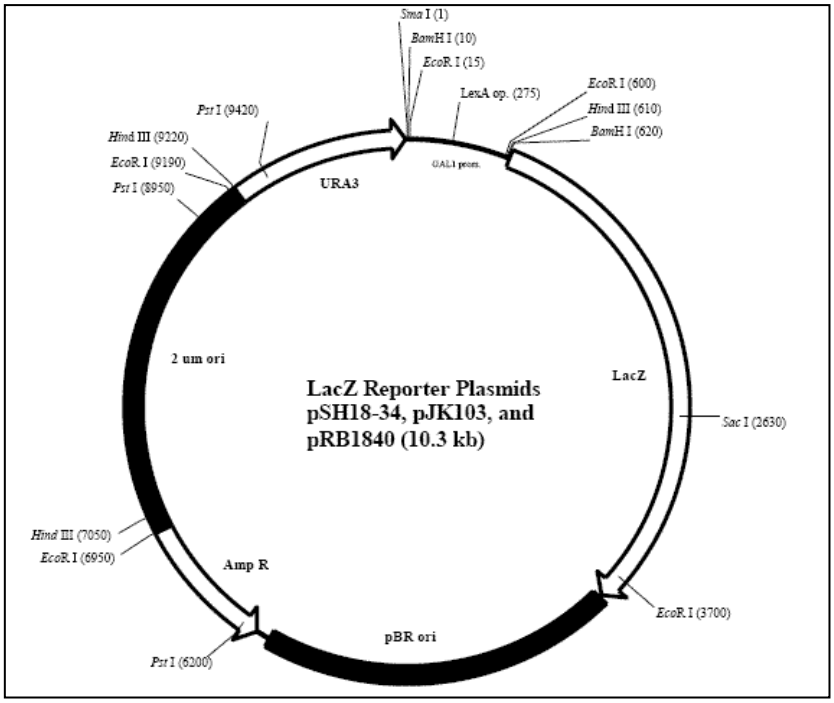

Figure 102: Vector map of the LacZ reporter plasmids pSH18-34 (high sensitivity), pJK103 (medium sensitivity) and pRB1840 (low sensitivity).

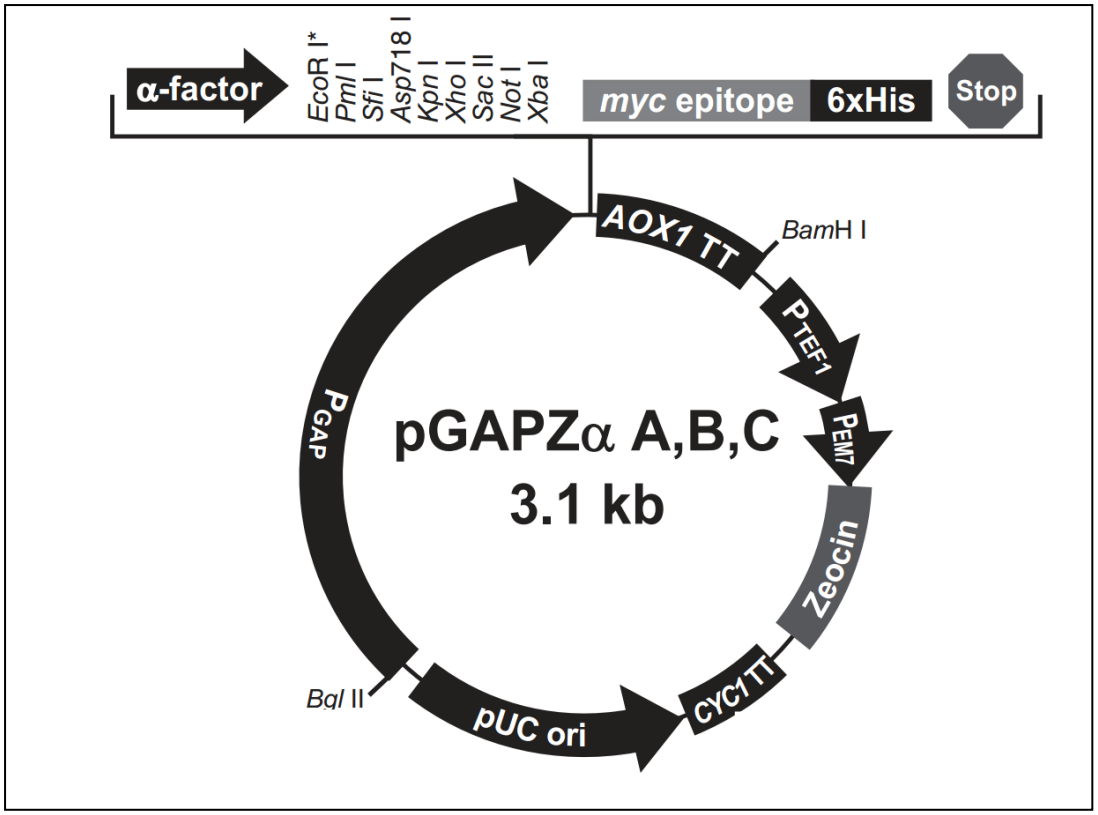

Figure 103: Vector map of *P. pastoris* overexpression vector pGAPZαA(B,C).

8.2 NEIL3 origin sequence included in the pCMV6-AC vector from OriGene

grey = coding sequence

GCGCAGCGTTGAGTTGCACAGCGGTATTCTCACCAGGCCCTGCAATCGGTGGGCCACAGTGCCGGCCAC
AGAG
ATGGTGGAAGGACCAGGCTGTACTCTGAATGGAGAGAAGATTCGAGCGCGGGTGCTCCCGGGCCAGGCG
GTGACCGGCGTGCGGGGAAGCGCTCTGCGGAGTCTGCAGGGCCGCGCCTTGCGGCTCGCAGCCTCCACG
GTTGTGGTCTCCCCGCAGGCTGCTGCACTGAATAATGATTCCAGCCAGAATGTCTTGAGCCTGTTTAAT
GGATATGTTTACAGTGGCGTGGAAACTTTGGGGAAGGAGCTCTTTATGTACTTTGGACCAAAAGCTTTA
CGGATTCATTTCGGAATGAAAGGCTTCATCATGATTAATCCACTTGAGTATAAATATAAAAATGGAGCT
TCTCGTGTTTTGGAAGTGCAGCTCACCAAAGATTTGATTTGTTTCTTTGACTCATCAGTAGAACTCAGA
AACTCAATGGAAAGCCAACAGAGAATAAGAATGATGAAAGAATTAGATGTATGTTCACCTGAATTTAGT
TTCTTGAGAGCAGAAAGTGAAGTTAAAAAACAGAAAGGCCGGATGCTAGGTGATGTGCTAATGGATCAG
AACGTATTGCCTGGAGTAGGGAACATCATCAAAAATGAAGCTCTCTTTGACAGTGGTCTCCACCCAGCT
GTTAAAGTTTGTCAATTAACAGATGAACAGATCCATCACCTCATGAAAATGATACGTGATTTCAGCATT
CTCTTTTACAGGTGCCGTAAAGCAGGACTTGCTCTCTCTAAACACTATAAGGTTTACAAGCGTCCCAAT
TGTGGTCAGTGCCACTGCAGAATAACTGTGTGCCGCTTTGGGGACAATAACAGAATGACATATTTCTGT
CCTCACTGTCAAAAAGAAAATCCTCAACATGTTGACATATGCAAGCTACCGACTAGAAATACTATAATC
AGTTGGACATCTAGCAGGGTGGATCATGTTATGGACTCCGTGGCTCGGAAGTCGGAAGAGCACTGGACC
TGTGTGGTGTGTACTTTAATCAATAAGCCCTCTTCTAAGGCATGTGATGCTTGCTTGACCTCAAGGCCT
ATTGATTCAGTGCTCAAGAGTGAAGAAAATTCTACTGTCTTTAGCCACTTAATGAAGTACCCGTGTAAT
ACTTTTGGAAAACCTCATACAGAAGTCAAGATCAACAGGAAAACTGCATTTGGAACTACAACTCTTGTC
TTGACTGATTTTAGCAATAAATCCAGTACTTTGGAAAGAAAAACAAAGCAAAACCAGATACTAGATGAG
GAGTTTCAAAACTCTCCTCCTGCTAGTGTGTGTTTGAATGATATACAGCACCCCTCCAAGAAGACAACA
AACGATATAACTCAACTATCCAGCAAAGTAAACATATCACCTACAATCAGTTCAGAATCTAAATTATTT
AGTCCAGCACATAAAAAACCGAAAACAGCCCACTACTCATCACCAGAGCTTAAAAGCTGCAACCCTGGA
TATTCTAACAGTGAACTTCAAATTAATATGACAGATGGCCCTCGTACCTTAAATCCTGACAGCCCTCGC
TGCAGTAAACACAACCGCCTCTGCATTCTCCGAGTTGTGAGGAAGGATGGGGAAAACAAGGGCAGGCAG
TTTTATGCCTGTCCTCTACCTAGAGAAGCACAATGTGGATTTTTTGAATGGGCAGATTTGTCCTTCCCA
TTCTGCAACCATGGCAAGCGTTCCACCATGAAAACAGTATTGAAGATTGGACCTAACAATGGAAAGAAT
TTTTTTGTGTGTCCTCTTGGGAAGGAAAAACAATGCAATTTTTTCCAGTGGGCAGAAAATGGGCCAGGA
ATAAAAATTATTCCTGGATGCTAA
TATCTGTAGATTCTCTGGCATTTAGTCTCTTCAAACTGTGTATAATGTTTGGTCCTCCTCTGTTTCATA
GAAAAGTCATAGAATATGATACATTGAAAAGTTACTGCAAAAAAAAAAAAAAAAAAA

8.3 Motif sequences in hNEIL3 (OriGene)

GCGCAGCGTTGAGTTGCACAGCGGTATTCTCACCAGGCCCTGCAATCGGTGGGCCACAGTGC
CGGCCACAGAG

One line is 1-19 aa or 1-57 bp. Sequences in bold are motifs.

N-terminal domain of NEIL 3 (1-151 aa)

ATGGTGGAAGGACCAGGCTGTACTCTGAATGGAGAGAAGATTCGAGCGCGGGTGCTCCCGGG
CCAGGCGGTGACCGGCGTGCGGGGAAGCGCTCTGCGGAGTCTGCAGGGCCGCGCCTTGCGGC
TCGCAGCCTCCACGGTTGTGGTCTCCCCGCAGGCTGCTGCACTGAATAATGATTCCAGCCAG
AATGTCTTGAGCCTGTTTAATGGATATGTTTACAGTGGCGTGGAAACTTTGGGGAAGGAGCT
CTTTATGTACTTTGGACCAAAAGCTTTACGGATTCATTTCGGAATGAAAGGCTTCATCATGA
TTAATCCACTTGAGTATAAATATAAAAATGGAGCTTCTCGTGTTTTGGAAGTGCAGCTCACC
AAAGATTTGATTTGTTTCTTTGACTCATCAGTAGAACTCAGAAACTCAATGGAAAGCCAACA
GAGAATAAGAATGATG

H2TH motif (151-244 aa)

AAAGAATTAGATGTATGTTCACCTGAATTTAGTTTCTTGAGAGCAGAAAGTGAAGTTAAAAA
ACAGAAAGGCCGGATGCTAGGTGATGTGCTAATGGATCAGAACGTATTGCCTGGAGTAGGGA
ACATCATCAAAAATGAAGCTCTCTTTGACAGTGGTCTCCACCCAGCTGTTAAAGTTTGTCAA
TTAACAGATGAACAGATCCATCACCTCATGAAAATGATACGTGATTTCAGCATTCTCTTTTA
CAGGTGCCGTAAAGCAGGACTTGCTCTCTCTAAA

CACTATAAGGTTTACAAGCGTCCCAATTGTGGTCAGTGCCACTGCAGAATAACTGTGTGCCG
CTTTGGGGACAATAACAGAATGACATATTTCTGTCCTCACTGTCAAAAAGAAAATCCTCAAC
ATGTTGACATATGCAAGCTACCGACTAGAAATACTATAATCAGTTGGACATCTAGCAGGGTG
GATCATGTTATGGACTCCGTGGCTCGGAAGTCGGAA

Zf-RanBP (319-343 aa)

GAGCACTGGACCTGTGTGGTGTGTACTTTAATCAATAAGCCCTCTTCTAAGGCATGTGATGC
TTGCTTGACCTCA

AGGCCTATTGATTCAGTGCTCAAGAGTGAAGAAAATTCTACTGTCTTTAGCCAC

NEIL3 unique motif (362-402 aa)

TTAATGAAGTACCCGTGTAATACTTTTGGAAAACCTCATACAGAAGTCAAGATCAACAGGAA
AACTGCATTTGGAACTACAACTCTTGTCTTGACTGATTTTAGCAATAAATCCAGTACTTTG

GAAAGAAAAACAAAGCAAAACCAGATACTAGATGAGGAGTTTCAAAACTCTCCTCCTGCTAG
TGTGTGTTTGAATGATATACAGCACCCCTCCAAGAAGACAACAAACGATATAACTCAACTAT
CCAGCAAAGTAAACATATCACCTACAATCAGTTCAGAATCTAAATTATTTAGTCCAGCACAT
AAAAAACCGAAAACAGCCCACTACTCATCACCAGAGCTTAAAAGCTGCAACCCTGGATATTC
TAACAGTGAACTTCAAATTAATATGACAGATGGCCCTCGTACCTTAAATCCTGACAGC

Zf-GRF 1 (505-550 aa)

CCTCGCTGCAGTAAACACAACCGCCTCTGCATTCTCCGAGTTGTGAGGAAGGATGGGGAAAA CAAGGGCAGGCAGTTTTATGCCTGTCCTCTACCTAGAGAAGCACAATGTGGATTTTTTGAAT GGGCAGATTTGTCC

TTC

Zf-GRF 2 (552-596 aa)

CCATTCTGCAACCATGGCAAGCGTTCCACCATGAAAACAGTATTGAAGATTGGACCTAACAA TGGAAAGAATTTTTTTGTGTGTCCTCTTGGGAAGGAAAAACAATGCAATTTTTTCCAGTGGG CAGAAAATGGG

CCAGGAATAAAAATTATTCCTGGATGC**TAA**

TATCTGTAGATTCTCTGGCATTTAGTCTCTTCAAACTGTGTATAATGTTTGGTCCTCCTCTG TTTCATAGAAAAGTCATAGAATATGATACATTGAAAAGTTACTGCAAAAAAAAAAAAAAAAA AA

8.4 SNPs in hNEIL3 DNA

SNPs in hNEIL3 cDNA (from OriGene) compared to hNEIL3 cDNA (from NCBI).

hNEIL3 cDNA insert in pCMV6-AC vector from OriGene:

GCGCAGCGTTGAGTTGCACAGCGGTATTCTCACCAGGCCCTGCAATCGGTGGGCCAC
AGTGCCGGCCACAGAG

ATGGTGGAAGGACCAGGCTGTACTCTGAATGGAGAGAAGATT

CGA (AA pos.: 15 ; Codon NCBI: CGC ; *Syn.:* Arg)
GCGCGGGTGCTCCCGGGCCAGGCGGTGACCGGCGTGCGGGGAAGCGCTCTGCGGAGT
CTGCAGGGCCGCGCCTTGCGGCTCGCAGCCTCCACGGTTGTGGTCTCCCCGCAGGCT
GCTGCACTGAATAATGATTCCAGCCAGAATGTCTTGAGCCTGTTTAATGGATATGTT
TACAGTGGCGTGGAAACTTTGGGGAAGGAGCTCTTTATGTACTTTGGACCAAAAGCT
TTACGGATTCATTTCGGAATGAAAGGCTTCATCATGATTAATCCACTTGAGTATAAA
TATAAAAATGGAGCTTCT

CGT (AA pos.: 117 ; Codon NCBI: CCT ; *Missense:* G=Arg, C=Pro)
GTTTTGGAAGTGCAGCTCACCAAAGATTTGATTTGTTTCTTTGACTCATCAGTAGAA
CTCAGAAACTCAATGGAAAGCCAACAGAGAATAAGAATGATGAAAGAATTAGATGTA
TGTTCACCTGAATTTAGTTTCTTGAGAGCAGAAAGTGAAGTTAAAAAACAGAAAGGC
CGGATGCTAGGTGATGTGCTAATGGATCAGAACGTATTGCCTGGAGTAGGGAACATC
ATCAAAAATGAAGCTCTCTTTGACAGTGGTCTCCACCCAGCTGTTAAAGTTTGTCAA
TTAACAGATGAACAGATCCATCACCTCATGAAAATGATACGTGATTTCAGCATTCTC
TTTTACAGGTGCCGTAAAGCAGGACTTGCTCTCTCTAAACACTATAAGGTTTACAAG
CGT

CCC (AA pos.: 252 ; Codon NCBI: CCT ; *Syn.:* Pro)
AATTGTGGTCAGTGCCACTGCAGAATAACTGTGTGCCGCTTTGGGGACAATAACAGA
ATGACATATTTCTGTCCTCACTGTCAAAAAGAAAATCCTCAACATGTTGACATATGC
AAGCTACCGACTAGAAATACTATAATCAGTTGGACATCTAGCAGGGTGGATCATGTT
ATGGACTCCGTGGCTCGGAAGTCGGAAGAGCACTGGACCTGTGTGGTGTGTACTTTA
ATCAATAAGCCCTCTTCTAAGGCATGTGATGCTTGCTTGACCTCAAGGCCTATTGAT
TCAGTGCTCAAGAGTGAAGAAAATTCTACTGTCTTTAGCCACTTAATGAAGTACCCG
TGTAATACTTTTGGAAAACCTCATACAGAAGTCAAGATCAAC

AGG (AA pos.: 381 ; Codon NCBI: AGA ; *Syn.:* Arg)
AAAACTGCATTTGGAACTACAACTCTTGTCTTGACTGATTTTAGCAATAAATCCAGT
ACTTTGGAAAGAAAAACAAAGCAAAACCAGATACTAGATGAGGAGTTTCAAAACTCT
CCTCCTGCTAGT

GTG (AA pos.: 424 ; Codon NCBI: GTT ; *Syn.:* Val)
TGTTTGAATGATATACAGCACCCCTCCAAGAAGACAACAAACGATATAACTCAA

CTA (AA pos.: 443 ; Codon NCBI: CCA ; *Missense:* T=Leu, C=Pro)
TCCAGCAAAGTAAACATATCACCTACAATCAGTTCAGAATCTAAATTATTTAGTCCA
GCACATAAAAAACCGAAAACAGCC

CAC (AA pos.: 471 ; Codon NCBI: CAA ; *Missense:* C=His, A=Gln)
TACTCATCACCAGAGCTTAAAAGCTGCAACCCTGGATATTCTAACAGTGAACTTCAA
ATTAATATGACAGATGGCCCTCGTACCTTAAATCCTGACAGCCCTCGCTGCAGTAAA
CACAACCGCCTCTGCATTCTCCGAGTTGTGAGGAAGGATGGGGAAAACAAGGGCAGG
CAGTTTTATGCCTGTCCTCTACCTAGAGAAGCACAATGTGGATTTTTTGAATGGGCA
GATTTGTCCTTCCCATTCTGCAACCATGGCAAGCGTTCCACCATGAAAACAGTATTG
AAGATTGGACCTAACAATGGAAAGAATTTTTTTGTGTGTCCTCTTGGGAAGGAAAAA
CAATGCAATTTTTTCCAGTGGGCAGAAAATGGGCCAGGAATAAAAATTATTCCTGGA
TGC**TAA**

TATCTGTAGATTCTCTGGCATTTAGTCTCTTCAAACTGTGTATAATGTTTGGTCCTC
CTCTGTTTCATAGAAAAGTCATAGAATATGATACATTGAAAAGTTACTGCAAAAAAA
AAAAAAAAAAAA

Explanations:

CDS [Coding Sequence (e.g. ATGGTGGAA…)]

Origin Sequence [Addition to CDS (e.g. GCGCAGCGTT…)]

(e.g.) CGA...: SNPs (Single Nucleotide Polymorphisms)

AA pos.: Amino Acid Position (Codon Position) of SNP

Codon NCBI: Codon at same AA pos. but found altered in cDNA sequence on NCBI.

Syn.: Synonymous – different codon but same resulting amino acid

Missense: Different codon as well as different resulting amino acid

ATG: Start codon

TAA: Stop codon

Source for SNP findings:

http://www.ncbi.nlm.nih.gov/projects/SNP/ → **Gene ID for NEIL3 = 55247**

8.5 PCR product quality from EGY48 yeast extractions

Table 25: PCR product quality, obtained from potential positive EGY48 yeast clones from placental cDNA library screening, after purification using sonication method

Yeast Clone Number	Concentration (ng/µl)	260nm/280nm	260nm/230nm
21	74.4	1.80	1.71
33	65.2	1.83	1.52
41	59.4	1.78	1.58
50	54.4	1.81	0.90
57	36.1	1.81	1.75
64	47.2	1.81	1.33
73	45.3	1.81	1.80
74	53.9	1.82	1.70
77	48.2	1.80	0.88
78	59.2	1.84	1.34
83	40.3	1.90	2.41
86	43.2	1.90	2.46
88	51.3	1.86	2.34
89	36.3	1.92	2.34
91	32.5	1.90	0.39
95	39.5	1.89	2.38
96	36.2	1.86	2.13
97	50.9	1.90	2.07
99	45.5	1.87	2.47
103	13.1	1.81	2.05
111	72.3	1.63	0.94
113	37.6	1.83	1.91

Yeast Clone Number	Concentration (ng/µl)	260nm/280nm	260nm/230nm
117	37.2	1.76	1.60
120	46.8	1.84	1.62
121	37.3	1.84	1.65
123	42.4	1.82	1.70
124	42.9	1.82	1.57
125	44.0	1.80	1.50
126	39.1	1.87	1.75
127	34.3	1.79	1.35
131	34.0	1.89	1.27
136	35.0	1.85	0.27
142	32.6	1.84	1.44
147	43.8	1.86	1.67
148	24.5	1.84	1.41
149	26.6	1.82	1.68
151	27.6	1.80	1.74
156	28.0	1.76	1.28
160	35.5	1.82	0.23
162	40.4	1.83	1.42
163	44.9	1.87	2.05
166	36.7	1.82	1.70
170	42.3	1.78	1.67
178	32.1	1.85	1.77
182	37.7	1.80	1.68
185	37.0	1.83	0.52
188	39.8	1.85	1.72
189	40.1	1.78	1.15

Yeast Clone Number	Concentration (ng/µl)	260nm/280nm	260nm/230nm
190 on 23 Nov	28.5	1.80	1.40
190 on 24 Nov	120.4	1.37	0.33
191	36.7	1.82	1.43
193	38.0	1.80	1.06
196	23.3	1.88	1.38
199	39.0	1.90	1.82
200	40.4	1.85	1.77
208	34.6	1.86	1.36

8.6 Complete sequencing (BLAST) results of Y2H screenings

8.6.1 Complete sequencing (BLAST) results of placental cDNA library screen

Clone No.	BLAST Result	Conserved Domains	In frame?	CDS?
14	*Protein phosphatase 1, regulatory (inhibitor) subunit 7*	*LRR_SD22 Leucine Rich repeats*	*?*	YES
15	*No PCR product*			
21	*Decorin (DCN), transcript variant C, mRNA (also Variants B, A2, A1, E, D)*	*LRR_TYP Leucine Rich repeats (Superfamily)*	*YES*	YES
28	*Interleukin 1 receptor accessory protein (IL1RAP), RefSeqGene on chromosome 3*	*----------No domain found----------*	-	
33	*RPL10 ribosomal protein L10*	*Ribosomal_L16_L10e domain*	*NO*	YES

Clone No.	BLAST Result	Conserved Domains	In frame?	CDS?
41	*Homo sapiens shisa homolog 5 (Xenopus laevis) (SHISA5), mRNA*	*----------No domain found----------*	-	YES
50	*No PCR product*		-	
57	*No DNA Sequence found by sequencing*		-	
59	*Homo sapiens chromosome 6 genomic contig, GRCh37.p5 Primary Assembly -- Features of the part of sequence: AN1-type zinc finger protein 3 [Homo sapiens]*		-	NO
63	*Homo sapiens gamma-aminobutyric acid (GABA) A receptor, epsilon (GABRE), mRNA*		-	NO
64	*TIMP metallopeptidase inhibitor 2 (TIMP2), mRNA*	*NTR_like (Superfamily)*	*YES*	YES
73	*Ribosomal protein L30 (RPL30), mRNA*	*Ribosomal_L7Ae (Superfamily)*	*YES*	YES
74	*RNA binding motif protein 8A (RBM8A), mRNA*	*----------No domain found----------*	*YES*	YES
77	*Chorionic gonadotropin, beta polypeptide 8 (CGB8), mRNA (also polypeptide 5, 7, 2, 1 and luteinizing hormone beta polypeptide (LHB) with decreasing E values and Max ident)*	*GHB_like*	*YES*	YES
78	*Chorionic gonadotropin, beta polypeptide 8 (CGB8), mRNA (also polypeptide 5, 7, 2, 1 and luteinizing hormone beta polypeptide (LHB) with decreasing E values and Max ident)*	*GHB_like*	*NO?*	YES
83	*No DNA sequence found by sequencing*			
86	*No DNA Sequence found by sequencing*			

Clone No.	BLAST Result	Conserved Domains	In frame?	CDS?
88	*Hemoglobin, alpha 1 (HBA1), mRNA*	*Globin*	*NO*	YES
89	*No DNA sequence found by sequencing*			
91	*No DNA sequence found by sequencing*			
95	*No DNA Sequence found by sequencing*			
96	*No significant similarity found whith BLAST.*			
97	*Chorionic somatomammotropin hormone 1 (placental lactogen) (CSH1), mRNA*	*Somatotropin_like*	*NO*	YES
99	*Homo sapiens shisa homolog 5 (Xenopus laevis) (SHISA5), mRNA*		-	
103	*No PCR product*			
111	*Chorionic somatomammotropin hormone 1 (placental lactogen) (CSH1), mRNA*	*Somatotropin_like*	*YES*	YES
113	*Proteasome (prosome, macropain) subunit, alpha type, 5 (PSMA5), transcript variant 1, mRNA*	*Proteasome_alpha _type_5*	*NO*	YES
117	*Osteoclast stimulating factor 1 (OSTF1), mRNA*	*--------No domain found----------*	-	NO
120	*Chorionic somatomammotropin hormone 1 (placental lactogen) (CSH1), mRNA*	*Somatotropin_like*	*YES*	YES
121	*No DNA Sequence found by sequencing*			
123	*Chorionic somatomammotropin hormone 1 (placental lactogen) (CSH1), mRNA*	*Somatotropin_like*	*YES*	YES
124	*Pregnancy specific beta-1-glycoprotein 5 (PSG5), transcript variant 1, mRNA*	*--------No domain found----------*	-	NO

Clone No.	BLAST Result	Conserved Domains	In frame?	CDS?
125	*Chorionic somatomammotropin hormone 1 (placental lactogen) (CSH1), mRNA*	*Somatotropin_like*	*YES*	YES
126	*Chorionic somatomammotropin hormone 2 (CSH2), transcript variant 1, mRNA*	*Somatotropin_like*	*YES*	YES
127	*Chorionic gonadotropin, beta polypeptide 8 (CGB8), mRNA*	*GHB_like*	*NO?*	YES
131	*Chorionic somatomammotropin hormone 1 (placental lactogen) (CSH1), mRNA*	*Somatotropin_like*	*YES*	YES
136	*Chorionic somatomammotropin hormone 2 (CSH2), transcript variant 1, mRNA*	*Somatotropin_like*	*YES?*	YES
142	*Chorionic somatomammotropin hormone 2 (CSH2), transcript variant 1, mRNA*	*--------No domain found----------*	-	NO
147	*Ornithine decarboxylase antizyme 1 (OAZ1), mRNA*	*ODC_AZ (Superfamily)*	*?*	YES
148	*No DNA Sequence found by sequencing*		-	
149	*Structural maintenance of chromosomes 6 (SMC6), transcript variant 1, mRNA*	*ABC_SMC6_euk, P-loop_NTPase (Superfamily)*	*YES mRNA/ NO CDS*	YES
151	*HOP homeobox (HOPX), transcript variant 3, mRNA*	*Homeodomain*	*YES*	YES
156	*No PCR product*		-	
160	*ELAV (embryonic lethal, abnormal vision, Drosophila)-like 1 (Hu antigen R) (ELAVL1), mRNA*	*RRM (found two times in same sequence)*	*YES*	YES

Clone No.	BLAST Result	Conserved Domains	In frame?	CDS?
162	*Proteasome (prosome, macropain) subunit, alpha type, 5 (PSMA5), transcript variant 1, mRNA*	*Proteasome_alpha _type_5*	*NO*	YES
163	*Hemoglobin, beta (HBB), mRNA*	*Globin*	*YES*	YES
166	*Transglutaminase 2 (C polypeptide, protein-glutamine-gamma-glutamyltransferase) (TGM2), transcript variant 1, mRNA*	*--------No domain found----------*	-	NO
170	*Ribosomal protein L9 (RPL9), transcript variant 2, mRNA*	*Ribosomal_L6 (Superfamily)*	*?*	YES
178	*CD59 molecule, complement regulatory protein (CD59), transcript variant 5, mRNA*	*--------No domain found----------*	-	NO
182	*Gamma-aminobutyric acid (GABA) A receptor, epsilon (GABRE), mRNA*	*--------No domain found----------*	-	NO
185	*Homo sapiens hemoglobin, gamma G (HBG2), mRNA*	*Globin*	*YES*	YES
188	*Tumour protein, translationally-controlled 1 (TPT1), mRNA*	*TCTP superfamily (No more information on NCBI)*	*YES*	YES
189	*Secreted protein, acidic, cysteine-rich (osteonectin) (SPARC), mRNA*	*--------No domain found----------*	-	NO
190	*No DNA Sequence found by sequencing*		-	
191	*Chorionic somatomammotropin hormone 1 (placental lactogen) (CSH1), mRNA*	*Somatotropin_like*	*YES*	YES
193	*Gamma-aminobutyric acid (GABA) A receptor, epsilon (GABRE), mRNA*	*--------No domain found----------*	-	NO

Clone No.	BLAST Result	Conserved Domains	In frame?	CDS?
196	*No Transcript found by BLAST*		-	
199	*Chorionic somatomammotropin hormone 1 (placental lactogen) (CSH1), mRNA*	*Somatotropin_like*	*YES*	YES
200	*Proteasome (prosome, macropain) subunit, alpha type, 5 (PSMA5), transcript variant 1, mRNA*	*Proteasome_alpha _type_5*	*NO?*	YES
208 (worked only with PCR method)	*Ribosomal RNA processing 9, small subunit (SSU) processome component, homolog (yeast) (RRP9), mRNA*	*WD40 (Superfamily), TP2 Nuclear transition protein 2 (Superfamily), DNA polymerase III subunits gamma and tau (Multi Domain)*	*YES?*	YES

8.6.2 Complete sequencing (BLAST) results of Jurkat T-cell cDNA library screen

Clone No.	BLAST Result	Conserved Domains	In frame?	CDS?
1	Homo sapiens coiled-coil domain containing 88A (CCDC88A), transcript variant 2, mRNA	none	--	NO
2	Homo sapiens coiled-coil domain containing 88A (CCDC88A), transcript variant 2, mRNA	none		NO
3	Homo sapiens coiled-coil domain containing 88A (CCDC88A), transcript variant 2, mRNA	none		NO
4	No similarity found	none		NO
5	Homo sapiens nudix (nucleoside diphosphate linked moiety X)-type motif 4 (NUDT4), transcript variant 2, mRNA	none		NO
6	Homo sapiens coiled-coil domain containing 88A (CCDC88A), transcript variant 2, mRNA	none		NO
7	Homo sapiens coiled-coil domain containing 88A (CCDC88A), transcript variant 2, mRNA	none		NO
8	Homo sapiens coiled-coil domain containing 88A (CCDC88A), transcript variant 2, mRNA	none		NO

9	No similarity found	none		NO
10	Homo sapiens coiled-coil domain containing 88A (CCDC88A), transcript variant 2, mRNA	none		NO
12	Homo sapiens coiled-coil domain containing 88A (CCDC88A), transcript variant 2, mRNA	none		NO
13	Homo sapiens coiled-coil domain containing 88A (CCDC88A), transcript variant 2, mRNA	none		NO
15	Homo sapiens coiled-coil domain containing 88A (CCDC88A), transcript variant 2, mRNA	none		NO
17	Homo sapiens coiled-coil domain containing 88A (CCDC88A), transcript variant 2, mRNA	none		NO
18	Homo sapiens coiled-coil domain containing 88A (CCDC88A), transcript variant 2, mRNA	none		NO
19	Homo sapiens coiled-coil domain containing 88A (CCDC88A), transcript variant 2, mRNA	none		NO
22	Homo sapiens coiled-coil domain containing 88A (CCDC88A), transcript variant 2, mRNA	none		NO
23	Cytochrome c oxidase	none		NO
26	Homo sapiens coiled-coil domain containing 88A (CCDC88A), transcript variant 2, mRNA	none		NO
33	Homo sapiens solute carrier family 25 (mitochondrial carrier; phosphate carrier), member 3 (SLC25A3), nuclear gene encoding mitochondrial protein, transcript variant 2, mRNA	none	NO	YES
37	Homo sapiens ribosomal protein L4 (RPL4), mRNA	none	NO	YES
43	Homo sapiens coiled-coil domain containing 88A (CCDC88A), transcript variant 2, mRNA	none		NO
45	Homo sapiens coiled-coil domain containing 88A (CCDC88A), transcript variant 2, mRNA	none		NO
51	Homo sapiens coiled-coil domain containing 88A (CCDC88A), transcript variant 2, mRNA	none		NO
44	Homo sapiens pyruvate kinase, muscle (PKM2), transcript variant 3, mRNA	Pyruvate kinase (PK)	NO	YES
52	No similarity found	none		NO
55	No similarity found	none		NO

8.7 Additional pictures

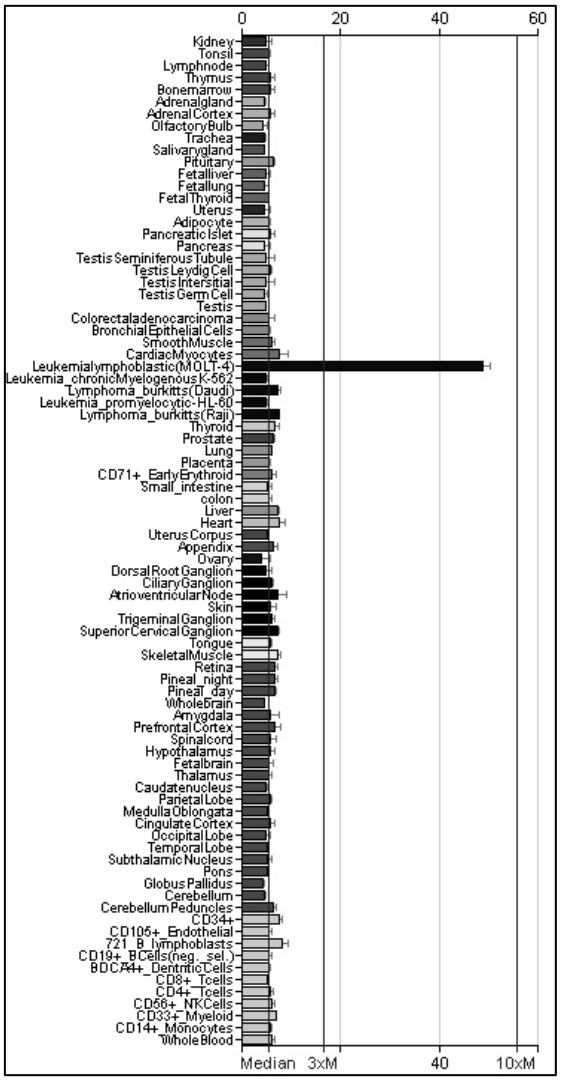

Figure 104: GeneExpression of NEIL3 in different human cell lines. (Image taken from http://biogps.gnf.org/#goto=genereport&id=55247(2010)).

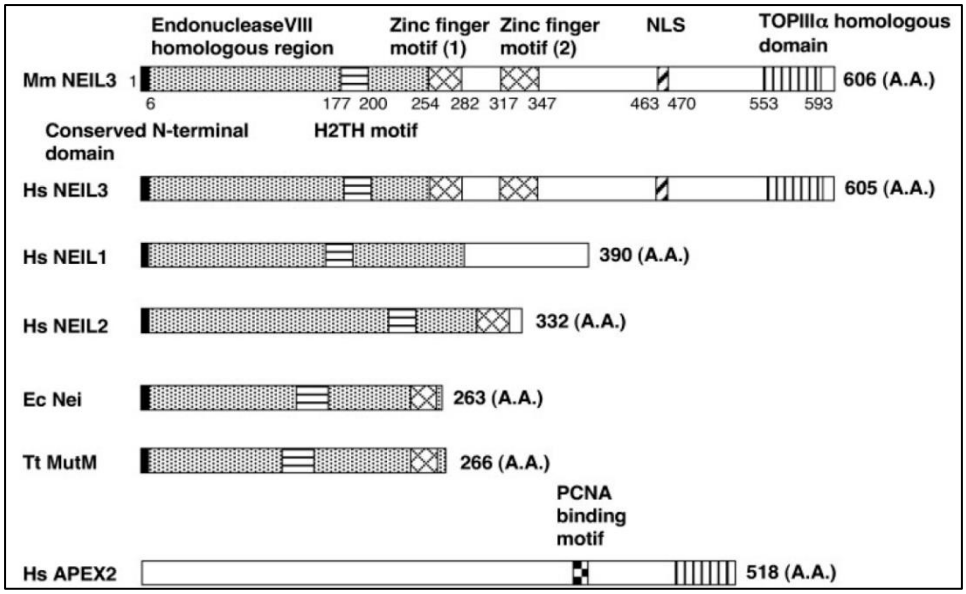

Figure 105: Structures of mouse/human NEIL3, human NEIL1, NEIL2, *E. coli* Nei, *Thermus thermophilus* MutM (Fpg) and human APE2 proteins. Black boxes, the conserved N-terminal domain; horizontally-striped box, H2TH motif; cross-hatched box, zinc finger motifs; hatched box, putative nuclear localization signals; vertically-striped box, topoisomerase IIIα homologous domain; checkered box, PCNA binding motif. (Image taken from Torisu *et al.,* 2005).

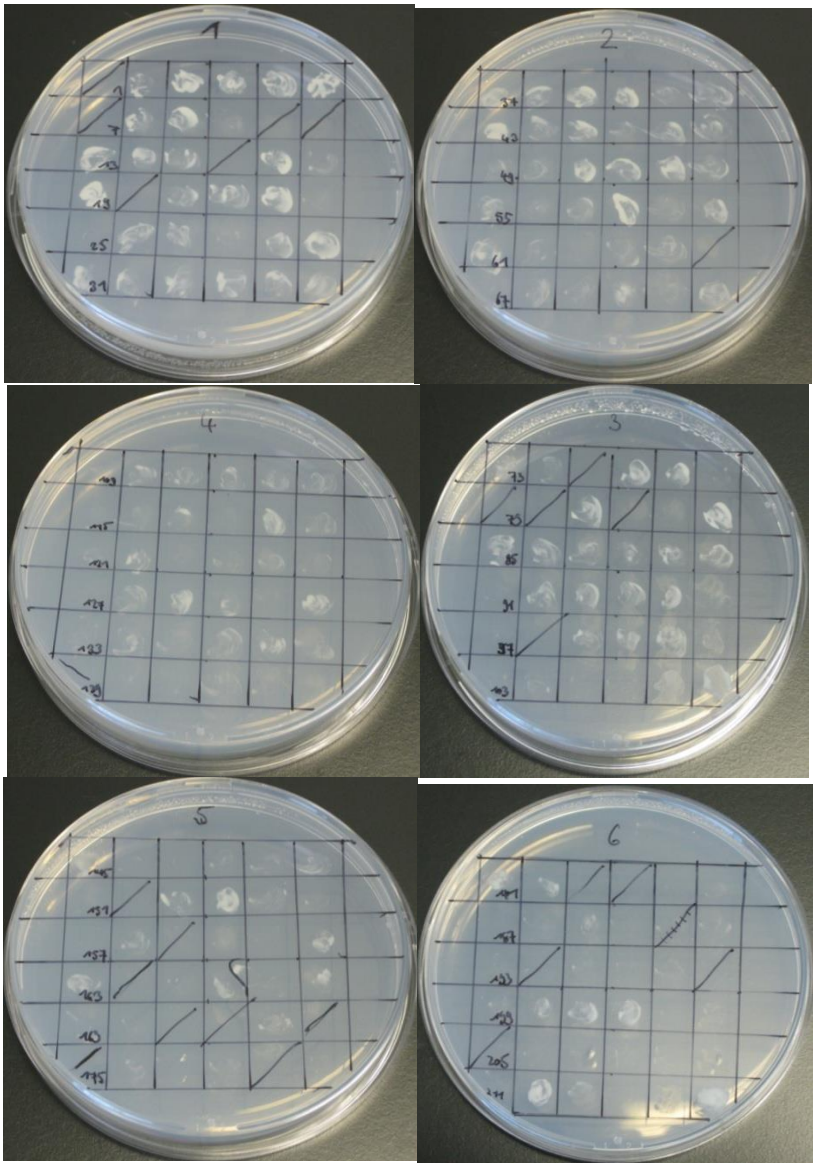

Figure 106: 216 potential genuine clones on YNB (gal) ura$^-$/his$^-$/trp$^-$/leu$^-$ master plates, picked from screening plates after incubation at 30°C for two days.